

194

Topics in Current Chemistry

Editorial Board:

**A. de Meijere • K.N. Houk • J.-M. Lehn • S. V. Ley
J. Thiem • B.M. Trost • F. Vögtle • H. Yamamoto**

Springer

Berlin
Heidelberg
New York
Barcelona
Budapest
Hong Kong
London
Milan
Paris
Santa Clara
Singapore
Tokyo

Microsystem Technology in Chemistry and Life Science

Volume Editors: A. Manz, H. Becker

With contributions by

R. C. Anderson, A. van den Berg, J. Cheng,
C. S. Effenhauser, W. Ehrfeld, G. Fuhr, V. Hessel,
R. J. Jackman, G. Jobst, L. J. Kricka, T. S. J. Lammerink,
H. Lehr, R. J. Lipshutz, G. McGall, J.-U. Meyer, D. Qin,
J. A. Rogers, E. L. Sheldon, S. G. Shirley, S. Shoji,
T. Stieglitz, G. A. Urban, G. M. Whitesides,
P. Wilding, Y. Xia, X.-M. Zhao



Springer

This series presents critical reviews of the present position and future trends in modern chemical research. It is addressed to all research and industrial chemists who wish to keep abreast of advances in the topics covered.

As a rule, contributions are specially commissioned. The editors and publishers will, however, always be pleased to receive suggestions and supplementary information. Papers are accepted for "Topics in Current Chemistry" in English.

In references Topics in Current Chemistry is abbreviated Top. Curr. Chem. and is cited as a journal.

Springer WWW home page: <http://www.springer.de>
Visit the TCC home page at <http://www.springer.de/>

ISSN 0340-1022
ISBN 3-540-63424-X
Springer-Verlag Berlin Heidelberg New York

Library of Congress Catalog Card Number 74-644622

This work is subject to copyright. All rights are reserved, whether the whole or part of the material is concerned, specifically the rights of translation, reprinting, reuse of illustrations, recitation, broadcasting, reproduction on microfilms or in any other ways, and storage in data banks. Duplication of this publication or parts thereof is only permitted under the provisions of the German Copyright Law of September 9, 1965, in its current version, and permission for use must always be obtained from Springer-Verlag. Violations are liable for prosecution under the German Copyright Law.

© Springer-Verlag Berlin Heidelberg 1998
Printed in Germany

The use of general descriptive names, registered names, trademarks, etc. in this publication does not imply, even in the absence of a specific statement, that such names are exempt from the relevant protective laws and regulations and therefore free for general use.

Cover design: Friedhelm Steinen-Broo, Barcelona; MEDIO, Berlin
Typesetting: Fotosatz-Service Köhler OHG, Würzburg

SPIN: 10552156 66/3020 – 5 4 3 2 1 0 – Printed on acid-free paper

Volume Editors

Prof. Andreas Manz

Dr. Holger Becker

Department of Chemistry

Imperial College of Science and Technology

Zeneca/Smithkline Beecham Centre for Analytical Sciences

South Kensington

London SW7 2AY

E-mail: h.becker@ic.ac.uk

a.manz@ic.ac.uk

Editorial Board

Prof. Dr. Armin de Meijere

Institut für Organische Chemie

der Georg-August-Universität

Tammannstraße 2

D-37077 Göttingen, Germany

E-mail: ucoc@uni-goettingen.de

Prof. Jean-Marie Lehn

Institut de Chimie

Université de Strasbourg

1 rue Blaise Pascal, B.P. Z. 296/R8

F-67008 Strasbourg Cedex, France

E-mail: lehn@chimie.u-strasbg.fr

Prof. Dr. Joachim Thiem

Institut für Organische Chemie

Universität Hamburg

Martin-Luther-King-Platz 6

D-20146 Hamburg, Germany

E-mail: thiem@chemie.uni-hamburg.de

Prof. Dr. Fritz Vögtle

Institut für Organische Chemie

und Biochemie der Universität

Gerhard-Domagk-Straße 1

D-53121 Bonn, Germany

E-mail: voegt@chemie1.chemie.uni-bonn.de

Prof. K. N. Houk

Department of Chemistry and Biochemistry

University of California

405 Hilda Avenue

Los Angeles, CA 90024-1589, USA

E-mail: houk@chem.ucla.edu

Prof. Steven V. Ley

University Chemical Laboratory

Lensfield Road

Cambridge CB2 1EW, Great Britain

E-mail: svl1000@cus.cam.ac.uk

Prof. Barry M. Trost

Department of Chemistry

Stanford University

Stanford, CA 94305-5080, USA

E-mail: bmtrost@leland.stanford.edu

Prof. Hisashi Yamamoto

School of Engineering

Nagoya University

Chikusa, Nagoya 464-01, Japan

E-mail: j45988a@nucc.cc.nagoya-u.ac.jp

*Dedicated to the late H. Michael Widmer,
world-renowned analytical chemist,
enthusiastic teacher, and ardent supporter of μ -TAS.
(May 11, 1933 – May 25, 1997)*

Preface

The aim of this book is to cover a novel interdisciplinary research area of high current interest, namely microsystems for use in chemistry and the life sciences, with a set of comprehensive reviews. Since 1975, when Steve Terry and his coauthors at Stanford published an account of their gas chromatograph on a silicon wafer, a large number of publications have appeared in the literature. Particularly after 1990 this field started exploding. For an inexperienced scientist it is a difficult task to obtain a good overview of what has happened during the last few years. Even conferences with the best possible coverage of authors would only feature recent research results.

It seems obvious that the miniaturisation first started in the analytical arena. After a number of conferences on analytical chemistry, the first conference devoted to microsystems, chemistry and life science 'μ-TAS' was organised at Enschede (The Netherlands) in November 1994. In the following years I was asked for a number of review articles about this topic. Last year I found out that almost all my colleagues in the field suffered from a similar problem: an excessive amount of writing! The 'lab on a chip' idea has really taken off in the public interest! That is why we decided to put a comprehensive volume together that could then be referred to instead of continuously publishing review articles here and there.

The book is clearly aimed at the well educated scientist with a biology, biochemistry, chemistry or engineering background. The chapters are easy to read and give a large number of references for further details. Chapters have been chosen to give a good overview of what has been achieved in the last decade. They can by no means be complete in describing every experiment published. We hope, that the authors and ourselves have made a good choice for examples that illustrate the essentials. For an update, we would advise attending international conferences such as Transducers (bi-annual), MEMS (annual), μ-TAS (bi-annual) and selected sessions in all application areas, e.g. the HPCE conference for applications in the electrophoresis area.

This book is dedicated to the late H. Michael Widmer, because he gave great support to my (A.M) μ-TAS project at Ciba-Geigy from 1989 to 1995, and he developed the basic concept of modern analytical monitoring and its miniaturisation.

Finally, it gives me great pleasure to thank all the authors for their contributions and suggestions. Many thanks to the publishing house, which allowed a smooth publication of this volume.

London, May 1997

Andreas Manz
Holger Becker

Contents

Microfabrication, Microstructures and Microsystems	
D. Qin, Y. Xia, J. A. Rogers, R. J. Jackman, X.-M. Zhao, G. M. Whitesides . . .	1
Micro Total Analysis Systems: Microfluidic Aspects, Integration Concept and Applications	
A. van den Berg, T. S. J. Lammerink	21
Integrated Chip-Based Microcolumn Separation Systems	
C. S. Effenhauser	51
Biological Application of Microstructures	
G. Fuhr, S. G. Shirley	83
Polynucleotide Arrays for Genetic Sequence Analysis	
R. C. Anderson, G. McGall, R. J. Lipshutz	117
Microtechnical Interfaces to Neurons	
T. Stieglitz, J.-U. Meyer	131
Fluids for Sensor Systems	
S. Shoji	163
Sensor Systems	
G. A. Urban, G. Jobst	189
Sample Preparation in Microstructured Devices	
J. Cheng, L. J. Kricka, E. L. Sheldon, P. Wilding	215
Microreactors for Chemical Synthesis and Biotechnology – Current Developments and Future Applications	
W. Ehrfeld, V. Hessel, H. Lehr	233
Author Index Volumes 151 – 194	253

Contents of Volume 191

Electronic and Vibronic Spectra of Transition Metal Complexes II

Volume Editor: H. Yersin

Spectroscopy of the Spin Sublevels of Transition Metal Complexes

T. Azumi, H. Miki

Magnetic and Spectroscopic Properties of $\text{Os}_2(\text{O}_2\text{CR})_4\text{Cl}_2$.

Evidence for a $^3(\delta^*\pi^*)$ Ground State

V.M. Miskowski, H. B. Gray

**Luminescence and Absorption Studies of Transition Metal Ions
in Host Crystals, Pure Crystals and Surface Environments**

H. H. Patterson

**Angular Overlap Model Applied to Transition Metal Complexes
and d^N -Ions in Oxide Host Lattices**

T. Schönherr

**Characterization of Excited Electronic and Vibronic States
of Platinum Metal Compounds with Chelate Ligands
by Highly Frequency-Resolved and Time-Resolved Spectra**

H. Yersin, W. Humbs, J. Strasser

Microfabrication, Microstructures and Microsystems

Dong Qin · Younan Xia · John A. Rogers · Rebecca J. Jackman · Xiao-Mei Zhao · George M. Whitesides*

Department of Chemistry and Chemical Biology, Harvard University, Cambridge, MA 02138, USA. E-mail: gwhitesides@gmwgroup.harvard.edu

This review gives a brief introduction to materials and techniques used for microfabrication. Rigid materials have typically been used to fabricate microstructures and systems. Elastomeric materials are becoming attractive, and may have advantages for certain types of applications. Photolithography is the most commonly used technique for the fabrication of structures for microelectronic circuits, microelectromechanical systems, microanalytical devices and micro-optics. Soft lithography represents a set of non-photolithographic techniques: it forms micropatterns of self-assembled monolayers (SAMs) by contact printing and generates microstructures of polymers by contact molding. The aim of this paper is to illustrate how non-traditional materials and methods for fabrication can yield simple, cost-effective routes to microsystems, and now they can expand the capabilities of these systems.

Keywords: Microfabrication, microsystems, microlithographic techniques.

1	Introduction	2
2	Requirements on Materials for Microsystems	3
2.1	Rigid Materials for Microsystems	3
2.2	Elastomeric Materials for Microsystems	4
3	Microlithographic Techniques	5
3.1	Photolithography	5
3.2	Soft Lithography	6
3.2.1	Microcontact Printing	6
3.2.2	Molding of Organic Polymers	10
3.3	Rapid Prototyping	12
3.4	Other Methods for Microfabrication	14
4	Conclusions and Future Directions	16
5	References	17

* Corresponding author.

1 Introduction

Microfabrication is increasingly central to modern science and technology. Many opportunities in technology derive from the ability to fabricate new types of microstructures or to reconstitute existing structures in down-sized versions. The most obvious examples are in microelectronics. Microstructures should also provide the opportunity to study basic scientific phenomena that occur at small dimensions: one example is quantum confinement observed in nanostructures [1]. Although microfabrication has its basis in microelectronics and most research in microfabrication has been focused on microelectronic devices [2], applications in other areas are rapidly emerging. These include systems for microanalysis [3–6], micro-volume reactors [7, 8], combinatorial synthesis [9], microelectromechanical systems (MEMS) [10, 11], and optical components [12–14].

One particularly exciting use for microanalytical devices is in the separation and analysis of chemical and biological substances [3–6]. These devices require only small quantities of reagents, have relatively short analysis times and can show efficiencies in separations that are better than larger counterparts. In the past few years, a number of miniaturized total chemical analysis systems (μ TAS) [15] have been developed that perform all sample-handling steps in an integrated fashion. For example, capillary electrophoresis (CE) devices using microchannels etched into planar glass substrates have attracted attention [16–18] for their use in applied molecular genetics. Systems for free-flow electrophoresis [19], gas chromatography [20], liquid chromatography [21, 22], capillary electrophoresis [23] and micellar electrokinetic capillary chromatography (MECC) [24] have been developed. Rapid and efficient capillary zone electrophoretic separations in micromachined channels (open, gel-filled or polyacrylamide-coated) on quartz substrates have also been demonstrated [3, 25, 26].

Devices for performing not only analysis, but also chemical synthesis in miniaturized systems (or microreactors) are also being developed [7, 27–34]. An array of chemical tools on a chip would make it possible, for example, to synthesize, analyze and characterize extremely small amounts of product ($\sim 10^{-12}$ l) [6]; these systems will be useful for combinatorial synthesis as part of new procedures for the parallel synthesis and screening of large numbers of compounds. Development of several prototypical microreactors suggest that microfabrication will play an important role in biology and chemistry: examples include DNA chips for high-speed DNA sequencing [35–38]; microchips for carrying out the polymerase chain reaction (PCR) [39]; microchip-based apparatus for the synthesis and characterization of libraries of peptides and oligonucleotides [40]; and microchip-based drug discovery using electronic addressing for the investigation of small objects such as single biological cells [41].

In addition to their biological and chemical applications, microstructures used in MEMS have evolved rapidly to integrate electronics with monitoring, actuating, and controlling tools (including chemical, optical, and mechanical sensors) for use in engineering. In the past few years, the scope of fabrication

techniques and the types of devices categorized as MEMS have widened dramatically [10, 11, 42, 43]. Most are fabricated from silicon using standard microlithographic techniques (silicon bulk micromachining and polysilicon surface micromachining) [44–46]. With these methods, thousands of mechanical elements (for example, cantilevered beams, springs, linkages, mass elements and joints) can be batch-fabricated on a single silicon substrate [9, 11]. Micro-actuators, micromotors and microengines [46] have been fabricated for optical switches, fluid pumps [47], systems for drug delivery and microchemical analysis and high-speed rotational gyros for navigation [48–51]. More recently, surface micromachining techniques have been used to fabricate miniaturized optical components [12–14]. A free-space micro-optical system comprising three-dimensional microgratings, micromirrors and microlenses is one example [14, 52]. These and similar miniaturized optical devices are attractive for applications in spectrometers, free-space optical interconnects, display devices, sensors, optoelectronic packages and data storage devices.

These current and potential applications motivate the development of techniques for fabricating and manipulating objects with nanometer and micrometer feature sizes. This review gives a brief introduction to materials and techniques commonly used for microfabrication; its focus is on those currently being explored in our laboratory. Our aim is to illustrate how non-traditional materials and methods for fabrication can yield simple, cost effective routes to microsystems, and how they can expand the capabilities of these systems. In a concluding section we provide brief descriptions of a number of other techniques for fabrication that, like those we are developing, may provide variable alternatives to photolithography.

2 Requirements on Materials for Microsystems

Miniaturized systems for performing chemical/biochemical reactions and analysis require cavities, channels, pumps, valves, storage containers, couplers, electrodes, windows and bridges [53]. The typical dimensions of these components are in the range of a few micrometers to several millimeters in length or width, and between 100 nm and 100 μm in depth and height. An extensive set of techniques for fabricating these microstructures is discussed in Sect. 3.

2.1 Rigid Materials for Microsystems

Microsystems can be built on various substrates with a range of materials: crystalline silicon, amorphous silicon, glass, quartz, metals, and organic polymers. Single-crystal silicon substrates have been used in most areas of microfabrication for a range of excellent reasons:

1. Silicon processing itself can be carried out using thin films of organic photoresists as resists against etching, and this technology is very highly developed.

2. Two- and three-dimensional shapes and patterns can be reproduced in silicon with high precision using bulk and surface micromachining techniques [46, 54]
3. Silicon devices can be batch-fabricated using the technology currently used for fabricating integrated circuits.
4. Silicon/silicon dioxide is stable chemically and thermally.

Crystalline silicon also has several disadvantages: it is expensive, brittle, and opaque in the UV/visible regions, and its surface chemistry is complicated to manipulate. As alternatives to silicon, glass, quartz and some rigid organic polymers (for example, epoxy, polyurethane, polyimide, polystyrene and polymethylmethacrylate) have properties that make them useful as materials for microsystems [55, 56]. In particular, they are transparent in the visible and UV regions and so can be easily adapted to optical detection in microanalytical devices. Microstructures of these materials can be replicated readily using low-cost methods such as replica molding and embossing [55–61]. In addition, the surface properties of these substrates (e.g. wetness ability, adhesion, surface adsorption and surface reactivity) can be modified rationally using a variety of surface chemistries. Techniques involving the formation of self-assembled monolayers (SAMs) [62] and the attachment of complex macromolecules [63] (e.g. immunoglobulins and nucleic acids) provide new routes to tailoring surface properties. Polymers are, however, not stable at high temperatures and their low thermal conductivities may limit their use in applications requiring high local power dissipation (e.g. in CE).

Integration of various components of a miniaturized device requires methods for bonding materials to substrates [64]. The most commonly used technologies for joining glass and silicon components include:

1. Anodic bonding [65], which uses electrostatic attraction to bring a glass wafer into contact with a silicon wafer and to form covalent bonds between them;
2. Silicon fusion bonding [65], which employs a similar mechanism to bond together the surfaces of two slightly-oxidized silicon wafers at high temperatures; and
3. Thermal bonding [66], which joins two glass wafers by locally melting them under controlled conditions.

Bonding technologies for organic polymers will probably be based on adhesives and other ones that are still being developed.

2.2

Elastomeric Materials for Microsystems

Rigid materials have typically been used to fabricate MEMS and optical components (for example, diffraction gratings, lenses and mirrors). These materials have the advantages of structural rigidity and strength. In certain applications, however, rigid materials may not provide the only solution to structural problem: adaptive optics is such an application [67]. Adaptive optics have com-

monly been constructed by assembling smaller, rigid elements that can be moved independently to modify characteristics [68]. Elastomers are well suited as materials for similar systems. We have created a new route for fabricating optical elements and optical systems from elastomeric materials such as poly(dimethylsiloxane), PDMS [69]. These types of optical components and devices have characteristics that can be controlled by changing their shapes with mechanical compression or extension. There are several advantages to using PDMS as a material for adjustable optical elements:

1. It can be deformed reversibly and repeatedly without permanent distortion or relaxation of features [70].
2. It can be molded at a scale suitable for optical applications (with feature sizes in the range of 0.1 – 10 μm) with high fidelity [71].
3. It is optically transparent down to ~ 300 nm [72].
4. It is durable and chemically inert.
5. It is non-toxic, commercially available and inexpensive.

We have demonstrated the concept of elastomeric optics by fabricating elastomeric lenses, corner cubes, mirrors and diffraction gratings [69]. We have used these components as photothermal detectors [73]; devices for measuring displacement, strain, stress, force, torque, and acceleration [70]; optical modulators and display devices [74]. In these devices, the active optical element is a block of PDMS with the relief of a binary diffraction grating on its surface. Mechanical compression/extension controls the relative optical path of light passing through the grating; this change in path causes the patterns of diffraction to be coupled to the compression/extension. Fabrication of elastomeric light valves represents additional examples of elastomeric optical devices [75]. One such example is an array of retroreflective corner cubes [76]. The amount of light transmitted through the valve is controlled by mechanical compression and extension against the surfaces of the PDMS blocks in the out-of-plane direction. These deformable elastomeric light valves may have applications in display devices, energy saving windows, sensors (accelerometers and pressure gauges) and photolithographic systems (such as photomasks) [77].

3 Microlithographic Techniques

In the following sections, we begin with a description of photolithography, then focus on a number of methods developed in our laboratory and conclude with some other non-traditional techniques. More extensive descriptions of traditional approaches are reviewed elsewhere [78].

3.1 Photolithography

Photolithography is the most commonly used microlithographic technique [2, 78]. In photolithography, a substrate, spin-coated with a thin layer of photo-

sensitive polymer (photoresist), is exposed to a UV light source through a photomask. The photomask is typically a quartz plate covered with patterned microstructures of an opaque material (usually chromium). The photoresist exposed to UV light becomes either more (positive resist) or less (negative resist) soluble in a developing solution. In either case, the pattern on the photomask is transferred into the film of photoresist; the patterned photoresist can subsequently be used as the mask in doping or etching the substrate.

In addition to conventional photoresist polymers, Langmuir-Blodgett (LB) films and SAMs [79–81] have been used as resists in photolithography. In such applications, photochemical oxidation, cross-linking, or generation of reactive groups are used to transfer micropatterns from the photomask into the monolayers [82–84].

Photolithography is widely used to fabricate structures for microelectronic circuits, MEMS, microanalytical devices and micro-optics. It has, however, a number of disadvantages. It is a relatively high-cost technology and the investment required to build and maintain photolithographic facilities makes this technique less than accessible to many chemists and biochemists. It can not be applied easily to curved surfaces (the formation of micropatterns and microstructures on non-planar substrates is important in the fabrication of certain types of optical and MEMS devices). It is applicable to only a small set of materials and it gives little control over the properties of the surfaces that are generated. These limitations have motivated the development of alternative, low-cost microlithographic techniques for manufacturing microstructures.

3.2

Soft Lithography

We have developed a set of non-photolithographic techniques for microfabrication that are based on the printing of SAMs and molding of organic polymers; we refer to these techniques, collectively, as soft lithography. Soft lithographic techniques include microcontact printing [80], micromolding in capillaries [85], microtransfer molding [86] and replica molding [60, 71]. Embossing [58], injection molding, and some techniques based on electrochemical deposition and etching might also be included as soft lithographic techniques. The capability and feasibility of soft lithography have been demonstrated by the fabrication of microstructures and systems in polymers and metals on a variety of substrates.

3.2.1

Microcontact Printing

Microcontact printing (μ CP) is a technique that uses an elastomeric stamp with relief on its surface to generate patterned SAMs on the surface of both planar and curved substrates [87, 88]. SAMs are highly ordered molecular assemblies that form spontaneously by chemisorption of functionalized long-chain molecules on the surfaces of appropriate substrates [79, 89]. Well-established systems of SAMs include alkanethiolates on coinage metals (Au, Ag, Cu) [90]; alkylsiloxanes on hydroxyl-terminated surfaces (Si/SiO₂, glass) [91]; carboxylic and

hydroxamic acids on oxide of metals [79, 92]; alkylphosphonates on ZrO_2 [93, 94]; and alkylphosphonic acids on Indium Tin Oxide [95]. The thickness of a SAM is about 2–3 nm, and can be varied with an precision of ~ 0.1 nm by changing the number of methylene groups in the alkane chain. The surface properties of a SAM can be controlled by modifying the tail groups (that is, the functional groups distal to the surface). SAMs have many of the features that are attractive in microfabrication:

1. They are quasi-equilibrium structures that are at, or close to, thermodynamic minima, and that tend, as a consequence, to be self-healing and defect-rejecting [62].
2. SAMs function as ultrathin resists against certain types of etches, and patterned SAMs can also be used as templates to control the nucleation and deposition of other materials (e.g. polymers [96], copper [97] and mammalian cells [98]).
3. They can be handled outside of clean room facilities, and certain types of fabrication involving SAMs are relatively low in cost compared with conventional photolithographic methods.

Figure 1 outlines the procedure used for μCP . This technique is experimentally simple and inherently parallel. The elastomeric stamp is fabricated by casting a prepolymer of PDMS against a master, which can be prepared using photolithography or other related techniques (for example, micromachining or e-beam writing). We have cast more than 50 stamps against a single master. To print hexadecanethiol (HDT) on gold, the “ink” used is a solution of HDT in ethanol (~ 2 mM). After the PDMS stamp is inked, it is brought into contact with a substrate to form patterned SAMs (Fig. 1A). Large area patterning (10 – 100 cm^2) is possible either by using a large flat stamp or by mounting a thin PDMS stamp onto a cylindrical rod and then rolling the stamp across the substrate (Fig. 1B) [99]. μCP also allows generation of micropatterns and microstructures on curved substrates by rolling curved substrates across an inked stamp (Fig. 1C) [87]. Conventional lithography lacks the depth of focus to pattern on curved substrates. We have been able to generate patterned SAMs of alkanethiolates on coinage metals [90, 100–102], patterned SAMs of alkylsiloxanes on hydroxyl-terminated surfaces [103–105]. CP has also been extended for patterning arrays of colloidal particles of Pd on Si/SiO₂ [106]. In μCP , each PDMS stamp can be used more than 100 times without degradation in performance; much higher levels of use may also be possible but have not been explored.

μCP followed by selective wet etching allows the formation of arrays of microstructures of coinage metals with controlled shapes and dimensions [96, 107]. This capability has direct applications in the fabrication of sensors [108], arrays of microelectrodes [109], and diffraction gratings [110]. Moreover, the patterned metallic microstructures can be used as secondary masks in the etching of underlying substrates (for example, Si, SiO₂ and gallium arsenide) to fabricate microchannels and microcavities for microreactors and microanalytical systems [54]. Figure 2 shows several typical examples of microstructures fabricated using the combination of μCP and selective etching. Figure 2A shows

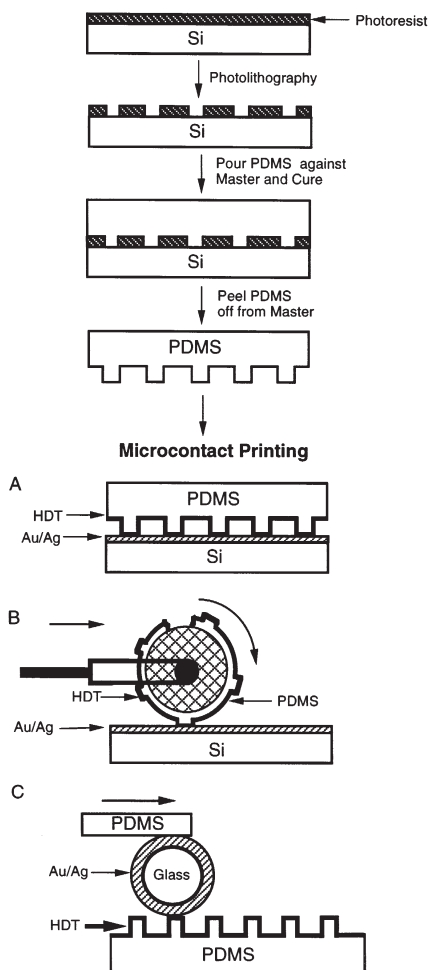


Fig. 1. Schematic procedures for μ CP: (A) printing on a planar substrate with a planar PDMS stamp; (B) printing on a planar substrate with a rolling stamp; and (C) printing on a curved substrate with a planar stamp

a scanning electron micrograph (SEM) of patterned microstructures of Ag on a Si/SiO₂ surface that were generated by μ CP hexadecanethiol with a rolling stamp, followed by selective wet etching in an aqueous ferricyanide solution [107]. We can routinely produce sub- μ m ($>0.3 \mu\text{m}$) features over an area of $\sim 50 \text{ cm}^2$ in a single impression in approximately 30 s [99]. We are beginning to define the registration and distortion of the patterns associated with elastomeric stamps [111]. Figure 2B shows an SEM of patterned microstructures of Ag on Si/SiO₂. Figure 2C shows a cross-sectional SEM of microchannels that were generated in a Si(100) wafer using a combination of μ CP, shadow evaporation and silicon micromachining [54]. Figure 2D shows an SEM of a microtrans-

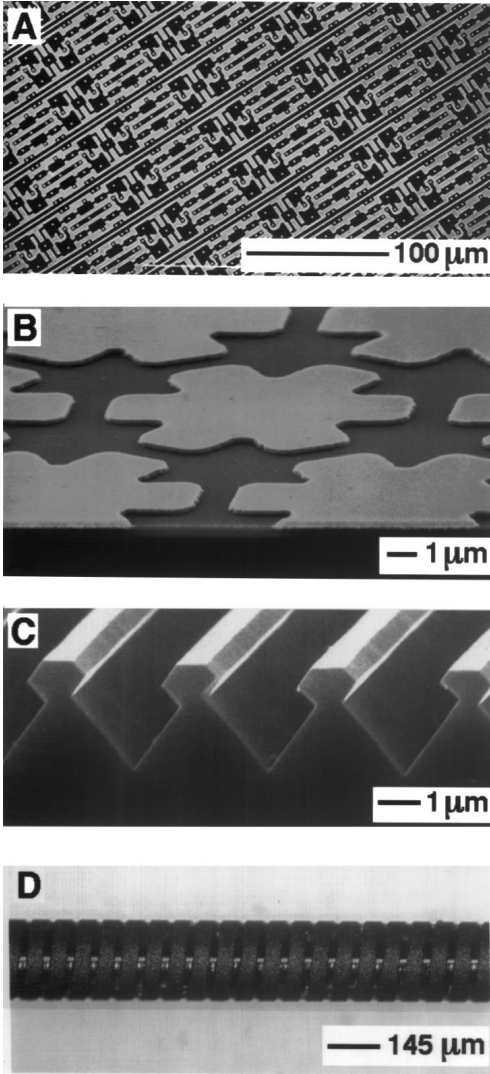


Fig. 2. A, B SEMs of test patterns of silver fabricated using μ CP, followed by selective etching; C cross-sectional SEM of microchannels etched in Si(100); and D optical micrograph of a microtransformer fabricated using μ CP, selective etching and electroplating

former fabricated using a combination of μ CP, selective wet etching and electroplating [112]. Conducting microcoils produced in this way on micro-capillaries have been used for high-resolution proton NMR spectroscopy on nanoliter volumes [113] and as current carriers in micro-inductors [114]. Similar cylindrical structures maybe useful as intravascular stents and micro-springs [114].

3.2.2

Molding of Organic Polymers

Formation of replicas by molding against rigid masters has been widely used to manufacture compact disks (CDs) [115] and diffraction gratings [59]. By extending this procedure to include an elastomer as the material for the mold, we have developed a number of techniques for fabricating microstructures of polymers, including micromolding in capillaries (MIMIC) [85, 116, 117], microtransfer molding (μ TM) [86], and replica molding [60, 71]. An elastomeric (PDMS) stamp with relief on its surface is central to each of these procedures (Fig. 3). In MIMIC, a liquid prepolymer (for example, a UV curable polyurethane or a thermally curable epoxy) wicks spontaneously by capillary action into the network of channels formed by conformal contact between an elastomeric mold and a substrate. In μ TM, the recessed regions of an elastomeric mold are filled

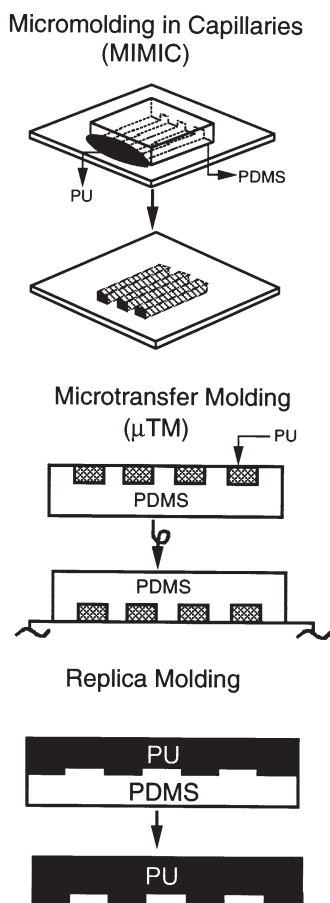


Fig. 3. Schematic procedures for MIMIC, μ TM and replica molding

with a liquid prepolymer, and the filled mold is brought into contact with a substrate. After curing the prepolymer, the mold is removed, leaving a polymer microstructure on the substrate. MIMIC can only be used to fabricate interconnected microstructures. Figure 4A shows an SEM of a free-standing microstructure of polyurethane that was fabricated on an SiO_2 surface using MIMIC, followed by lift-off in an aqueous HF solution [85, 116]. Figure 4B shows polystyrene beads crystallized in microchannels fabricated by MIMIC using an aqueous suspension of the colloidal beads [118]. Arrays of such crystalline microbeads are interesting for potential applications in chromatography and applied optics. μTM can be used to generate both isolated and interconnected microstructures; it can also be used sequentially to fabricate multi-layer structures. The smallest features we have produced using these procedures are parallel lines with cross sections of $\sim 0.1 \times 2 \text{ m}^2$. These dimensions are limited by the PDMS molds used in our work. Figs 4C and 4D show SEMs of two- and three-layer microstructures fabricated using TM [86]. Figs 4E and 4F show SEMs of carbonized polymeric structures (an interdigitated capacitor and an optical deflector) fabricated by μTM [119].

In replica molding, microstructures are directly formed by casting and curing a UV curable polymer against an elastomeric mold. This method is effective for replicating feature sizes ranging from several centimeters to $\sim 30 \text{ nm}$. Figure 4G shows an SEM of a hemispherical object with 100 m corner-cubes on its surface that was fabricated using replica molding against a deformed PDMS mold [60]. Replica molding also provides a convenient route to microstructures with high aspect ratios. Figure 4H shows an SEM of one such structure replicated from a master generated in a thin film of heat-shrinkable polystyrene [120].

Molding against an elastomeric PDMS master has several advantages. First, the elastomer can form conformal contact with a substrate; it can also be released easily, even from complex and fragile structures. Secondly, PDMS provides a surface with low interfacial free energy ($\sim 21.6 \text{ dyn cm}^{-1}$) and low reactivity. As a result, the polymers being molded do not adhere irreversibly to or react with the surface of PDMS. Thirdly, the deformation of PDMS can be controlled easily by mechanical compression, bending and stretching. Taking advantage of this flexibility, we have been able to fabricate microstructures of polymers with controlled shapes on both planar and non-planar surfaces [60].

Microfabrication based on molding is remarkable for its simplicity, for its economy, and for its fidelity in transferring the patterns from the mold to the polymeric structures that it forms. MIMIC, μTM and replica molding have been used to fabricate microstructures of a wide range of materials, including polymers, inorganic and organic salts, sol-gels, polymer beads and precursor polymers to ceramics and carbon. The feasibility of these molding techniques has been demonstrated by the fabrication of chirped, blazed diffraction gratings [60], polymeric waveguides [121], waveguide interferometers/couplers [122], interdigitated carbon capacitors [118], and suspended carbon microresonators [123]. Without steps for transferring patterns, photolithography can only be used to generate microstructures in the classes of polymers that have been developed as photoresists.

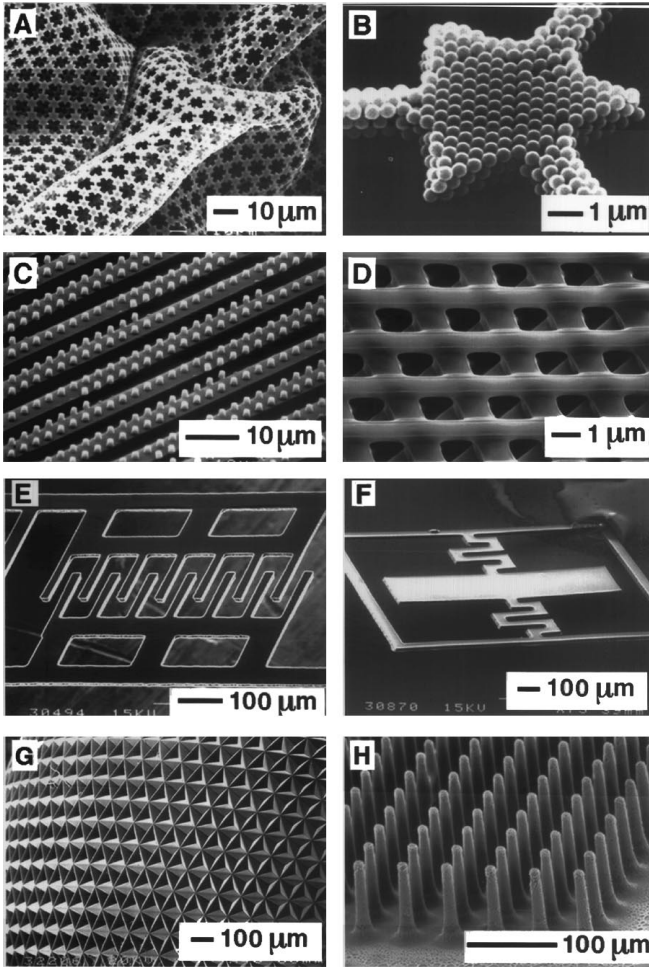


Fig.4. SEMs of microstructures fabricated using A, B MIMIC; C, D, E, F μ TM and G, H replica molding. See text for details

3.3

Rapid Prototyping

An elastomeric stamp or mold with relief structures on its surface is the key to soft lithographic techniques (see Sect. 3.2). As a result, the utility of these techniques is often limited by the availability of appropriate masters. In general, the masters are fabricated using photolithography. Chrome masks are available commercially from custom fabricators, but the time required for vendors to produce a chrome mask from a design presented in a computer aided design (CAD) file can be weeks, and they are expensive ($\sim \$300$ per square inch for features larger than $20\ \mu\text{m}$, and $\sim \$500$ – $\$1000$ per square inch for features between 1 and

20 μm). The time and expense involved in generating chrome masks are barriers to the use of photolithography by chemists and biologists and have limited the use of microfabrication in these fields.

Recently, we [124] and others [125] have developed a system that has enabled us to fabricate masters having feature sizes $\geq 20\ \mu\text{m}$ rapidly and at low cost. In this technique [124], we draw patterns using computer programs such as Macro-media Freehand or AutoCAD and print them directly onto polymer films using a commercial, laser-assisted image-setting system (for example, Herkules PRO, resolution of 3387 dpi, Linotype-Hell Company, Hauppauge, NY). Using this method, photolithographic masks – transparent polymeric films patterned with microstructures of black ink – can be made in a few hours at a cost of $\sim \$1$ per square inch. Although these masks do not have the durability and dimensional stability required for use in the manufacturing of microelectronic devices, they are suitable for the rapid production of limited numbers of prototype microfluidics, sensors, micro-optics, and microanalytical systems. They also have two other attractive features:

1. They are flexible, and can be used to pattern non-planar substrates.
2. They are thin, and can be stacked on top of one another to generate new types of patterns.

After the patterns on these polymer films are transferred into photoresist films coated on silicon substrates using photolithography, the developed photoresist patterns can serve as a master to make the required PDMS stamps. By combining this method of rapid prototyping with soft lithographic techniques, we can fabricate patterned microstructures of polymers and metals within 24 h of the time that the design is completed. Rapid prototyping makes it possible to produce substantial numbers of simple microstructures rapidly and inexpensively.

The rapid prototyping method has been demonstrated by fabricating structures representative of those used in microanalytical systems. Figure 5 shows two examples: a microCE channel and a surface acoustic wave (SAW) device. Figure 5A shows a schematic design of the pattern used in the microCE. Figs. 5B and 5C show optical micrographs of two areas of the pattern that were etched into a glass slide using the patterned film of photoresist as the mask. Figure 5D illustrates the pattern used for a SAW device and Fig. 5E shows an SEM of a portion of this device (made of silver on Si/SiO_2) that was fabricated by selective etching in an aqueous ferricyanide solution.

At present, the smallest features that can be generated directly using this procedure are $\sim 20\ \mu\text{m}$, a size that is limited by the resolution (3387 dpi) of the image-setting system. It should be possible to generate features with smaller sizes by using printers with higher resolution. Even with masks made by the current image-setting system, we are able to generate features significantly smaller than $20\ \mu\text{m}$ by using some of the techniques reported previously (e.g. mechanical compression of an elastomeric stamp) [126]. We believe that rapid prototyping paves the way for expanded use of microfabrication (especially when patterns may be complex but require only modest linewidths) in chemistry and biology.

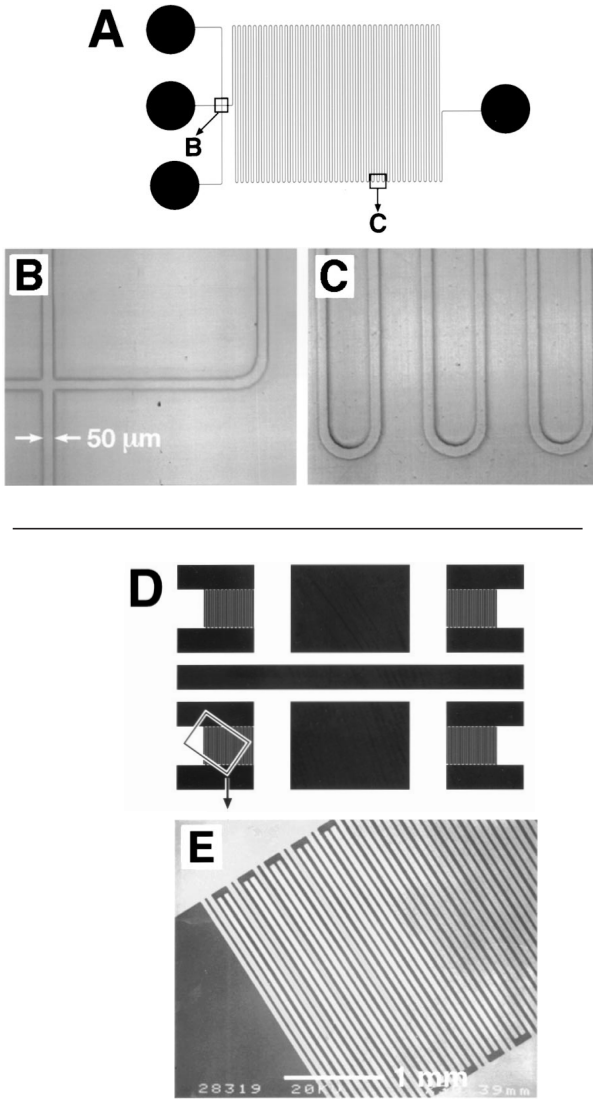


Fig. 5. **A** The designed pattern used in microCE; and **B, C** optical micrographs of two selected areas of the pattern that was transferred into a glass slide. **D** The designed pattern used in SAW device; and **E** an SEM image of a portion of the pattern generated in silver on Si/SiO_2

3.4

Other Methods for Microfabrication

Embossing (or Imprinting) is a low-cost, high-throughput manufacturing technique that imprints microstructures in plastic materials [127]. The manufacture of CDs based on imprinting in polycarbonate is a good example of a large-

volume commercial application of this technique [115]. Until recently, embossing had not been seriously developed as a method for fabricating microstructures of semiconductors, metals and other materials used in semiconductor integrated circuit manufacturing. Work by Chou and coworkers showed that embossing can be used to make features as small as 25 nm and has attracted attention to the potential of this kind of patterning [58, 128]. We have also demonstrated a variant of embossing using an elastomeric master [129]. In this technique, the elastomeric master is wet with an appropriate solvent and is brought into contact with the surface of a polymer. The polymer is softened by the solvent, and the resulting (probably gel-like) polymeric material is molded against the relief structure of the elastomer to form a pattern complementary to that on the surface of the mold.

Injection Molding is an alternative technique used for manufacturing CDs [57]. It has been used to generate microstructures with feature sizes of $>0.5\text{ }\mu\text{m}$. Injection molding combined with sintering technology provides a potential route to complex structures made of nearly every sinterable material or material combination [130]. The capability of this technique has been demonstrated by producing fiber-reinforced metal components and those made of metal-ceramic compounds [130]. Based on the two-component injection molding process, it is possible to produce components with a rigid exterior and a tough core. A low-pressure injection molding technique [131] has been used as a method for fabricating ceramic thread-guide components used in the textile industry. Injection molding has great promise for fabrication on the $<100\text{ nm}$ scale, although the required technology has not yet been developed.

Excimer Laser Micromachining [132, 133] is a technique based on laser ablation. Currently, this process can routinely ablate vias as small as $6\text{ }\mu\text{m}$ in diameter in polymers, glass, ceramics and metals. The minimum size of the features that this method can produce is limited by diffraction and by heat/mass transport. Commercial instruments and services are available from a number of companies (for example, Resonetics, Itek).

Laser Direct Writing is a technique that combines laser-assisted deposition and a high-resolution translational stage to fabricate patterned microstructures from a wide range of materials [134–137]. For example, laser-assisted deposition can be used for generating micropatterns of seeding materials for electroless plating [138]. Laser-assisted polymerization enables the fabrication of patterned microstructures of polymers [139]. Stereolithography, based on laser-assisted processing, can be used to fabricate three-dimensional microstructures [140–142].

LIGA (Lithography, Electroforming, Molding) [143, 144] is a technique that combines X-ray (or synchrotron) lithography, electroplating, and molding for fabricating microstructures with high aspect ratios and relatively large feature sizes ($\sim 10\text{ }\mu\text{m}$). Although the standard equipment for UV exposure can be adapted for this application, special optics and alignment systems are needed for structures thicker than $200\text{ }\mu\text{m}$.

Electrochemical micromachining (EMM) is a technique designed to generate patterned microstructures in metals and alloys [145]. Microfabrication by EMM may involve maskless or through-mask dissolution. Maskless EMM uses the

impingement of a fine electrolytic jet for thin film patterning. Through-mask EMM involves selective metal dissolution from those regions unprotected by a patterned photoresist on the workpiece. The smallest feature that can be achieved using this technique is $\sim 1\text{ }\mu\text{m}$.

Ultrasonic machining, also known as ultrasonic impact grinding, uses ultrasonically induced vibration delivered to a tool to create accurate cavities and channels of many shapes [146]. It can be used to form deep cavities as small as $250\text{ }\mu\text{m}$ in diameter (with an accuracy of $\sim 50\text{ }\mu\text{m}$) in both hard and brittle materials such as glass, quartz, polymers, ceramics and metals. This technique may be useful for fabrication of large masters.

4 Conclusions and Future Directions

Microstructures and systems are typically fabricated from rigid materials, such as crystalline silicon, amorphous silicon, glass, quartz, metals and organic polymers. Elastomeric materials can be used in applications where rigidity is a drawback. We have demonstrated the concepts of elastomeric systems by fabrication of photothermal detectors, optical modulators and light valves. We believe that elastomeric materials will find additional applications in the areas of optical systems, microanalytical systems, biomaterials and biosensors.

Microfabrication is growing in importance in a wide range of areas outside of microelectronics, including MEMS, microreactors, microanalytical systems and optical devices. Photolithography will continue as the dominant technology in the area of microelectronics for the foreseeable future. Photolithography has, however, a number of limitations for certain types of applications, as discussed in Sect. 3.1.

Soft lithography offers a new strategy for microfabrication. Based on SAMs and molding of organic polymers, this set of techniques represents a non-photolithographic methodology for forming micropatterns, microstructures and microsystems of different materials on a range of substrates. Rapid prototyping enhances the utility of soft lithographic techniques and enables the generation of numerous microstructures and systems with feature sizes $\geq 20\text{ }\mu\text{m}$ at low cost. In a research setting, soft lithographic techniques have generated structures with feature sizes as small as 30 nm . The strengths and weaknesses of these developing techniques are still being defined. Their strengths, however, include low cost (capital and operational), the ability to pattern large areas and the ability to generate structures with feature size $\leq 100\text{ nm}$; limitations include the difficulty in achieving high resolution registration and in controlling distortion of patterns caused by deformation of the elastomers. We are beginning to address these issues in our research, and we believe that new materials, designs and configurations will lead to improvement in these areas.

Acknowledgements. The work in our laboratory was supported in part by ONR, DARPA and NSF (Grant PHY 9312572), and made use of MRSEC shared facilities supported by the NSF under Grant DMR-9400396. The authors thank Dr. J. Michael Ramsey for design of the CE in Fig. 5 A and Professor Michael Grunze for the design of the SAW device in Fig. 5D. JAR gratefully

acknowledges funding from the Harvard University Society of Fellows and RJJ gratefully acknowledges a scholarship from NSERC. The authors thank Andrew J. Black and Scott T. Brittain for proof reading this manuscript.

5 References

1. Heitmann D, Kotthaus JP (1993) *Physics Today* 46(6):56
2. Moreau WM (1988) *Semiconductor lithography: principles and materials*, Plenum, New York
3. Jacobson SC, Hergenroder R, Koutny LB, Ramsey JM (1994) *Anal Chem* 66:1107
4. Manz A (1996) *Chimia* 59:140
5. Bratten CDT, Cobbold PH, Cooper JM (1997) *Anal Chem* 69:253
6. Clark RA, Hietpas PB, Ewing AG (1997) *Anal Chem* 69:259
7. Ananchenko GS, Bagryanskaya EG, Tarasov VF, Sagdeev RZ, Paul H (1996) *Chem Phys Lett* 255:267
8. Song MI, Iwata K, Yamada M, Yokoyama K, Takeuchi T, Tamiya E, Karube I (1994) *Anal Chem* 66:778
9. Briceno G, Change HY, Sun XD, Schultz PG, Xiang XD (1995) *Science* 270:273
10. Kovacs GTA, Petersen K, Albin M (1996) *Anal Chem* 68:407
11. MacDonald NC (1996) *Microelectronic Engineering* 32:49
12. Lee SS, Lin LY, Wu MC (1995) *Appl Phys Lett* 67:2135
13. Wu MC, Lin LY, Lee SS, King CR (1996) *Laser Focus World* 32(2):64
14. Lin LY, Lee SS, Pister KSJ, Wu MC (1994) *IEEE Photonics Technology Letters* 6:1445
15. Van Der Bery A, Gergveld P (1995) *Micro Total Analysis Systems*, Kluwer Academic Publishers, Netherlands
16. Harrison DJ, Fluri K, Seiler K, Fan Z, Effenhauser CS, Manz A (1993) *Science* 261:895
17. Jacobson SC, Moore AW, Ramsay JM (1995) *Anal Chem* 67:2059
18. Tomlinson AJ, Guzman NA, Naylor S (1995) *J Capillary Electrophor* 2(6):247
19. Raymond DE, Manz A, Widmer HM (1994) *Anal Chem* 66:2858
20. Terry SC, Jerman JH, Angell JB (1979) *IEEE Trans Electron Devices* EC-26:1880
21. Ocivirk G, Verpoorte E, Manz A, Grasserbauer M, Widmer HM (1995) *Anal Methods Instrum* 2:74
22. Manz A, Miyahara Y, Miura J, Watanabe Y, Miyagi H, Sato K (1990) *Sens Actuators B* 1:249
23. Jacobson SC, Hergenröder R, Koutny LB, Ramsay JM (1994) *Anal Chem* 66:2369
24. Heeren F, Verpoorte E, Manz A, Thormann W (1996) *Anal Chem* 68:2044
25. Effenhauser CS, Manz A, Widmer HM (1993) *Anal Chem* 65:2637
26. Effenhauser CS, Paulus A, Manz A, Widmer HM (1994) *Anal Chem* 66:2949
27. Tarasevich MR, Bogdanovskaya VA (1996) *Adv Biosens* 3:5
28. Ehrfeld W, Hessel V, Moebins H, Richter T, Russow K (1996) *Dechema Monogr* 132:1
29. Lee SS, Ridean AM, McGown LB (1996) *J Phys Chem* 100:5880
30. Licklider L, Kuhr WG, Lacey MP, Keough T, Purdon MP, Takigiku R (1995) *Anal Chem* 67:4170
31. Davis MT, Lee TD, Ronk M, Hefta SA (1995) *Anal Biochem* 224:235
32. Yi C, Gratzl M (1994) *Anal Chem* 66:1976
33. Yi C, Huang D, Gratzl M (1996) *Anal Chem* 68:1580
34. Craston D (1996) *Chem Britain* October 31:31
35. Goffeau A (1997) *Nature* 385:202
36. Kozal M, Shah N, Shen N, Yang R, Fucini R, Merigan TC, Richman DD, Morris D, Hubbell E, Chen M, Gringeras TR (1996) *Nature Med* 2:753
37. Shoemaker DD, Lashkari DA, Mittmann M, Davis RW (1996) *Nature Genet* 14:450
38. Blanchard AP, Kaiser RJ, Hood LE (1996) *Bios Bioelectronics* 11:687
39. Fodor SPA, Red JL, Pirrung MC, Stryer L, Liu AT, Solas D (1991) *Science* 251:767
40. Fodor SPA, Rava RP, Huang XC, Pease AC, Holmes CP, Adams CL (1993) *Nature* 364:555

41. Fromherz P, Offenhausser A, Vetter T, Weis J (1991) *Science* 252:1290
42. Bryzek J, Petersen K, McCulley W (1994) *IEEE Spectrum* 31(5):20
43. Bryzek J, Petersen K, McCulley W (1994) *IEEE Spectrum* 31(7):6
44. Peterson KE (1982) *Proc IEEE* 70:420
45. Koester DA, Markus KW, Waiters MD (1993) *Computer* 29(1):93
46. Sniegowski JJ (1996) *Solid State Tech* 39(12):83
47. Ohlchers P, Hanneborg A, Nese M (1995) *J Micromech Microeng* 5:47
48. Paula G (1996) *Mech Eng* 118:64
49. Tracey MC, Greenaway RS, Das A, Kaye PH, Barnes AJ (1995) *IEEE Trans on Biomed Eng* 42:751
50. Steinkuhl R, Dumschat C, Sundermeier C, Hinkers H, Rennegerg R, Cammann K, Knoll M (1996) *Biosen Bioelectronics* 11:187
51. Tang WL, Temesvary V, Yao JJ, Tai YC, Miu DK (1996) *J App Phys Part-1* 35:350
52. Wu MC, Lin LY, Lee SS, Pister KSJ (1995) *Sens Actuators A* 50:127
53. Noworolski JM, Klaassen E, Logon J, Petersen K, Maluf NI (1996) *Sens Actuators A* 54:709
54. Xia Y, Whitesides GM (1996) *Adv Mater* 8:765
55. Frazier AB, Ahn GH, Allen MG (1994) *Sensors and Actuators A* 45:47
56. Williams G, D'Silva C (1996) *Sensors and Actuators B* 30:51
57. Emmelius M, Pawlowski G, Vollmann HW (1989) *Angew Chem Int Ed Engl* 28:1445
58. Chou SY, Krauss PR, Renstrom PJ (1996) *Science* 272:85
59. Hutley MC (1982) *Diffraction gratings*, Academic Press, New York
60. Xia Y, Kim E, Zhao X-M, Rogers JA, Prentiss M, Whitesides GM (1996) *Science* 273:347
61. Terris BD, Mamin HJ, Best ME, Logan JA, Rugar D, Rishton SA (1996) *Appl Phys Lett* 69:4262
62. Whitesides GM (1995) *Sci Am* 273:146
63. Beaucage SL, Lyer RP (1992) *Tetrahedron* 48:2223
64. Hanneborg A, Nese M, Ohlckers P (1991) *IEEE MicroElectroMechanical Systems* 1:139
65. Spangler LJ, Wise KD (1990) *Sens Actuators A* 24:117
66. Lasky JB (1986) *Appl Phys Lett* 48:76
67. Hubin N, Noethe L (1993) *Science* 262:1390
68. Thompson LA (1994) *Physics Today* 47(12):24
69. Wilbur JL, Jackman RJ, Whitesides GM, Cheng E, Lee L, Prentiss M (1996) *Chem Mater* 8:1380
70. Rogers JA, Qin D, Schueller OJA, Whitesides GM (1996) *Rev Sci Instrum* 67:3310
71. Xia Y, McClelland JJ, Gupta R, Qin D, Zhao X-M, Sohn LL, Celotta RJ, Whitesides GM (1997) *Adv Mater* 9:147
72. Clarson SJ, Semlyen JA (1993) *Engleword Cliffs, PTR Prentice Hall, Engleword Cliffs, NJ*
73. Rogers JA, Jackman RJ, Schueller OJA, Whitesides GM (1996) *Appl Optics* 35:6641
74. Rogers JA, Whitesides GM (1997) *Appl Optics* 36:5792
75. Qin D, Xia Y, Whitesides GM (1997) *Adv Mater* 9:407
76. Chipman RA, Shamir J, Caulfield HJ, Zhou BQ (1988) *Appl Optics* 27:3202
77. Bonse MH, Mul C, Spronck JM (1995) *Sens Actuators A* 46–47:266
78. Brambley D, Martin B, Prewett PD (1994) *Adv Mater Optics Electronics* 4:55
79. Ulman A (1991) *Introduction to thin organic films: from Langmuir–Blodgett to self-assembly*, Academic Press, Boston
80. Kumar A, Abbott NA, Kim E, Biebuyck HA, Whitesides GM (1995) *Acc Chem Res* 28:219
81. Whitesides GM, Gorman CB (1995) *Self-Assembled Monolayers: Models for Organic Surface Chemistry*. In: Hubbard AT (ed) *Handbook of surface imaging and visualization*, CRC Press, Boca Raton p 713
82. Calvert JM (1995) In: Ulman A (ed) *Thin film*, Academic Press, Boston
83. Huang J, Dahlgren DA, Hemminger JC (1994) *Langmuir* 10:626
84. Chan KC, Kim T, Schoer JK, Crooks RM (1995) *J Am Chem Soc* 117:5875
85. Kim E, Xia Y, Whitesides GM (1995) *Nature* 376:581
86. Zhao X-M, Xia Y, Whitesides GM (1996) *Adv Mater* 8:837
87. Jackman R, Wilbur J, Whitesides GM (1995) *Science* 269:664

88. Xia Y, Whitesides GM (1997) *Langmuir* 13:2059
89. Dubois LH, Nuzzo RG (1992) *Annu Rev Phys Chem* 43:437
90. Xia Y, Zhao X-M, Whitesides GM (1996) *Microelectronic Eng* 32:255
91. Parikh AN, Allara DL, Azouz IB, Rondelez F (1994) *J Phys Chem* 98:7577
92. Folkers JP, Gorman CB, Laibinis PE, Buchholz S, Whitesides GM, Nuzzo RG (1995) *Langmuir* 11:813
93. Cao G, Hong H-G, Mallouk TE (1992) *Acc Chem Res* 25:420
94. Katz HE (1994) *Chem Mater* 6:2227
95. Gardner TJ, Frisbie CD, Wrighton MS (1995) *J Am Chem Soc* 117:6927
96. Xia Y, Tien J, Qin D, Whitesides GM (1996) *Langmuir* 12:4033
97. Jeon NL, Nuzzo RG, Xia Y, Mrksich M, Whitesides GM (1995) *Langmuir* 11:3024
98. Mrksich M, Chen CS, Xia Y, Dike LE, Ingber DE, Whitesides GM (1996) *Proc Natl Acad Sci USA* 93:10775
99. Xia Y, Qin D, Whitesides GM (1996) *Adv Mater* 8:1015
100. Xia Y, Kim E, Whitesides GM (1996) *J Electrochem Soc* 143:1070
101. Xia Y, Kim E, Mrksich M, Whitesides GM (1996) *Chem Mater* 8:601
102. Moffat TP, Yang HJ (1995) *J Electrochem Soc* 142:L220
103. Xia Y, Mrksich M, Kim E, Whitesides GM (1995) *J Am Chem Soc* 117:9576
104. Jeon NL, Glem PG, Payne DA, Nuzzo RG (1996) *Langmuir* 12:5350
105. St. John PM, Craighead HG (1996) *Appl Phys Lett* 68:1022
106. Hidber PC, Helbig W, Kim E, Whitesides GM (1996) *Langmuir* 12:1375
107. Xia Y, Zhao X-M, Kim E, Whitesides GM (1995) *Chem Mater* 7:2332
108. Mrksich M, Whitesides GM (1995) *Trends Biotechnol* 13:228
109. Heinze J (1993) *Angew Chem Int Ed Engl* 32:1268
110. Kumar A, Biebuyck HA, Whitesides GM (1994) *Langmuir* 10:1498
111. Rogers JA, Paul KE, Whitesides GM (1997) *J Vac Sci Tech B* (in press)
112. Jackman RJ, Rogers JA, Whitesides GM (1997) *IEEE Trans Magnetics* 33:2501
113. Rogers JA, Jackman RJ, Whitesides GM (1997) *Appl Phys Lett* 20:2658
114. Rogers JA, Jackman RJ, Whitesides GM (1997) *Adv Mater* 9:475
115. Dijkman JF (1989) *Phillips Tech Rev* 44:212
116. Xia Y, Kim E, Whitesides GM (1996) *Chem Mater* 8:1558
117. Kim E, Xia Y, Whitesides GM (1996) *J Am Chem Soc* 118:5722
118. Kim E, Xia Y, Whitesides GM (1996) *Adv Mater* 8:245
119. Schueller OJA, Brittain ST, Whitesides GM (1997) *Adv Mater* 9:447
120. Zhao X-M, Xia Y, Qin D, Whitesides GM (1997) *Adv Mater* 9:251
121. Zhao X-M, Stoddart A, Smith SP, Kim E, Xia Y, Prentiss M, Whitesides GM (1996) *Adv Mater* 8:420
122. Zhao X-M, Smith SP, Waldman SJ, Whitesides GM, Prentiss M (1997) *Appl Phys Lett* (submitted for publication)
123. Schueller OJA, Brittain ST, Marzolin C, Whitesides GM (1997) *Chem Mater* 9:1399
124. Qin D, Xia Y, Whitesides GM (1996) *Adv Mater* 8:917
125. Economical mask-making using desk-top publishing is described at <http://fas.sfu.ca/ensc/research/groups/micromachining/file2.html> by M. Parameswaran
126. Wilbur JL, Kim E, Xia Y, Whitesides G (1995) *Adv Mater* 7:649
127. Ramos BL, Choquette S (1996) *Anal Chem* 68:1245
128. Chou SY, Krauss PR, Renstrom PJ (1995) *Appl Phys Lett* 67:3114
129. Kim E, Xia Y, Zhao X-M, Whitesides GM (1997) *Adv Mater* 9:651
130. Michaeli W, Bielzer R (1991) *Adv Mater* 3:260
131. Toy C, Palaci Y, Baykara T (1995) *J Mater Pro Tech* 51:211
132. Patel RS, Redmond TF, Tessler C, Tudryn D, Pulaski D (1996) *Laser Focus World* January:71
133. Lizotte T, Ohar O, O'Keefe T (1996) *Solid State Technology* 39(9):120
134. Lehmann O, Stuke M (1992) *Appl Phys Lett* 61:2027
135. Kramer N, Niesten M, Schonenberger C (1995) *Appl Phys Lett* 67:2989
136. Weidman TW, Joshi AM (1993) *Appl Phys Lett* 62:372

137. Miehr A, Fischer R, Lehmann O, Stcke M (1996) *Adv Mater Optics Electron* 6:27
138. Hirsch TJ, Miracky RF, Lin C (1990) *Appl Phys Lett* 57:1357
139. Torres-Filho A, Neckers DC (1995) *Chem Mater* 7:744
140. Wallenberger FT (1995) *Science* 267:1274
141. Lehmann O, Stuke M (1995) *Science* 270:1644
142. Neckers DC (1990) *CHEMTECH* 20(10):615
143. Lochel B, Maciossek A, Quenzer HJ, Wagner B (1996) *J Electrochem Soc* 143:237
144. White V, Ghodssi R, Herdey C, Denton DD, McCaughan L (1995) *Appl Phys Lett* 66:2072
145. Datta M (1995) *J Electrochem Soc* 142:3801
146. Technical Report, Bullen Ultrasonics Inc., Eaton, Ohio, 1995

Micro Total Analysis Systems: Microfluidic Aspects, Integration Concept and Applications

Albert van den Berg and T.S.J. Lammerink

MESA Research Institute, University of Twente, P.O. Box 217, 7500 AE Enschede, The Netherlands. *E-mail: A.vandenBerg@el.utwente.nl*

In this contribution three aspects of miniaturized total analysis systems (μ TAS) are described and discussed in detail. First, an overview of microfabricated components for fluid handling is given. A description of the importance of sampling- and fluid-handling techniques is followed by details of microvalves, micropumps and micro flowchannels. Secondly, the problems associated with system integration are discussed. As a solution for the realization of microfluidic- and micro analysis systems, the concept of a planar mixed circuit board (MCB) as a platform for the integration of different components is described. In addition, the design, modeling and simulation, and realization of several components in the form of standard modules for integration on a MCB is described. As an illustration of the potential of this approach, the realization of a μ TAS demonstrator for the optical detection of the pH change of a pH indicator, is presented. Finally, a number of different applications of μ TAS are described, such as on-line process monitoring, environmental monitoring, biomedical and space applications and DNA-analysis.

Keywords: Microsystem, (bio)chemical analysis, fluid handling, μ TAS, micropump.

1	Introduction	22
1.1	General	22
1.2	(Bio)chemical Analysis Systems vs (Bio)Chemical Sensors	22
1.3	Classifying the μ TAS Field	24
1.4	Elements of a μ TAS	24
2	Sampling and Fluid Handling	25
2.1	Introduction	25
2.2	Sampling Techniques and Components	25
2.3	Fluid Handling Components	26
2.3.1	Microvalves	27
2.3.1.1	Valve Types	27
2.3.1.2	Activating Principles	28
2.3.1.3	Technology	28
2.3.2	Micropumps	29
2.3.3	Micro Flowchannels	33
3	System Integration	35
3.1	Integration Concepts	35
3.2	The Mixed Circuit Board (MCB) Concept	37

3.3	System Modules	37
3.4	Modeling and Design	37
3.4.1	Thermal Flow Sensor	38
3.4.2	Thermopneumatic Micropump	41
3.5	Realization of a Demonstrator System	43
3.5.1	Despcription	43
3.5.2	Results	43
4	Applications	45
5	Conclusions	47
6	References	48

1
Introduction

1.1
General

The subject of miniaturized systems for (bio)chemical analysis is attracting increasing attention from researchers in the biochemistry, analytical chemistry, microsensors and microtechnology field. In Europe as well as North America, and to a lesser extent Japan, many groups are actively studying the subject; micro total analysis systems (μ TAS) have recently been assigned as a strategic research orientation of the MESA Research Institute of the University of Twente [1]. In this contribution, besides a description of several essential components of such μ TAS, concepts for their integration, technologies for fabricating them as well as applications are presented and discussed. The main aim of this work is to inform scientists and engineers active in the analytical and biochemistry fields about the possibilities offered by modern (silicon based) microtechnology, triggering them to think about new and innovative measurement methods.

1.2
(Bio)Chemical Analysis Systems vs (Bio)Chemical Sensors

The analysis of the (bio)chemical state of a system is often described in terms of sensors. These (miniaturized) devices convert the (bio)chemical state (chemical concentration, activity or partial pressure of particles such as atoms, molecules, ions etc. [2] into a (mostly) electrical signal. However, recently miniature components such as mixers, filters, separation columns, reactors etc., have been developed [3, 4] that are capable of pretreating the sample, carrying out a chemical reaction or separating the different components within a sample mixture. The possibility to integrate such components into one miniaturized system leads to a more generalized view on information gathering (see Fig. 1). In general, in order to simultaneously analyze N components using a system

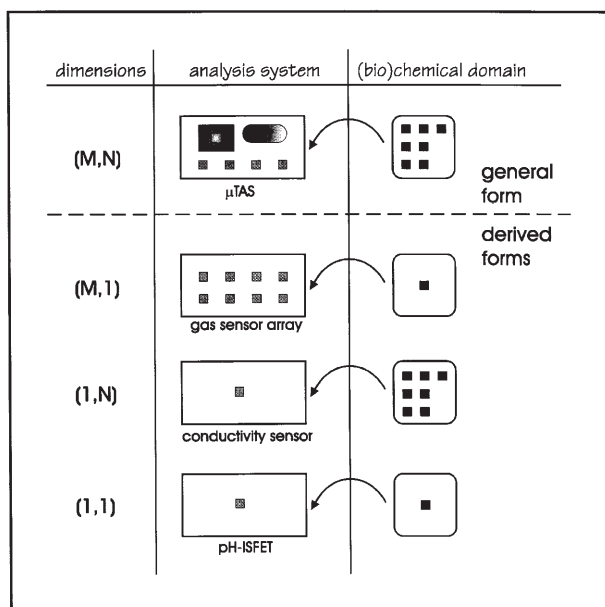


Fig. 1. Transfer of information from the (bio)chemical domain using an analysis system

containing M different sensors, M needs to be larger than N . Special cases are those where M or N equals 1. $N=1$ can be identified with a sensor array where more than one partially selective sensor is used to selectively detect one component in a mixture (e.g. a gas sensor array). $M=1$ is a theoretical case where one analysis system element can be used to detect different (bio)chemical components. As an example, a conductivity sensor can be used to sense the presence of various gases in a gas chromatograph, but not to distinguish them simultaneously. Finally, with $M=N=1$, one sensor may be 'perfectly' selective for one component, such as for instance an ion sensitive field effect transistor (ISFET) for pH. The latter case has been most extensively investigated during the past few decades for a large variety of components [5].

The miniaturized analysis system, however, may also contain components that select one component or a class of components from a mixture (filters, reactors) or components that transform the simultaneous presence of N components in a sequential presence of N different single components (separation devices). The fact that miniaturized analysis systems contain all elements needed to perform the required analysis is reflected in the term μ TAS as first quoted by Manz and colleagues in 1990 [6]. The recent strong interest of many research groups in this subject is stimulated by the fact that finding solutions for chemical measurement problems through development of individual sensors for each of the desired parameters has not been very successful up to now. The main reason for this lies probably in the wide variety of parameters and applications, making one general approach for a sensor very difficult. A solution

for this would be to develop a relatively expensive “overperforming” analysis system instead of a simple sensor. Such a system should be modified for each particular application. Examples of this approach are a micro flow injection analysis system (μ FIA) [7] and micro gas chromatograph (μ GC) [8]. Once such a standard or “generic” solution is widely accepted, the sensor community can focus its efforts to optimize and economize it. In our view this is the only way to obtain optimal synergy from the present quite diversified activities in this field.

1.3

Classifying the μ TAS Field

The research and development field of μ TAS can be differentiated according to several principles. First, the analyte phase (liquid/gas) plays an important role. Clearly, most detection principles can be exclusively used either in the gas or liquid phase. Some detectors, especially those based on thermal principles, can be used in both phases albeit at different ranges of sensitivity. Secondly, the systems can be distinguished according to their mode of operation: flow-type systems or separation-type systems. In the latter type a further differentiation can be made between liquid chromatography and electrophoresis systems. Finally, the application area brings about so many specific requirements that an application-oriented classification seems justified. Examples of application areas are space applications, DNA analysis, and biomedical applications. A classification according to the second criterium appears the most sensible, since the mode of operation influences or even determines the used technology, and is strongly linked to the application as well.

1.4

Elements of a μ TAS

With the first development of piezo micropumps [9], people started to realize that one day such pumps might be integrated together with sensors into a complete microsystem for chemical analysis. In general, four types of sub-systems are thought to comprise a μ TAS: a sampling unit, a microfluidic unit, a detector system and an electronic controller (see Fig. 2). The aspects of electronic control are too specific to be treated in this contribution. The detector system in a μ TAS illustrates many problems related to the small size of the system [10]. An important aspect is the very small size required for the sensing element operating in a microchannel of a few hundreds of microns width. Electrochemical sensors for instance suffer from the lack of a properly functioning micro-reference electrode. In the case of ISFETs a differential setup with two spatially separated ISFETs in combination with a quasi-reference electrode has overcome this difficulty [11]. For optical absorption sensors, widely applied for chemical analysis, the very limited absorption length is the major difficulty. Here, artificially increasing this length by multiple reflection techniques seems the most promising direction. In such a case, using loss-free interference mirrors is preferred over using partly-transparent metal films. Unfortunately, no comprehensive study treating the prob-

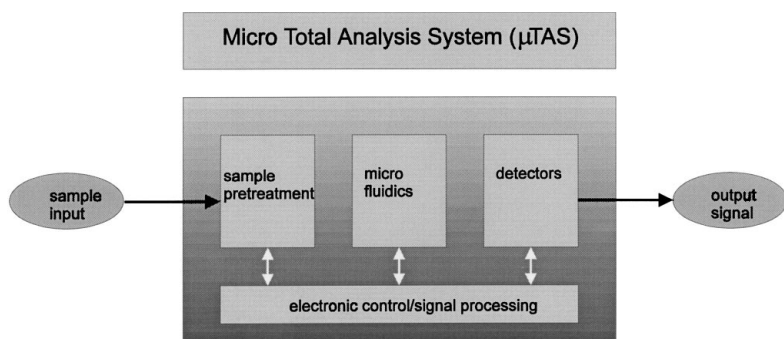


Fig. 2. Elements of a Micro Total Analysis System (μTAS)

lems of miniaturized detector systems has been carried out yet. For this reason we will focus on the sampling and fluidic units and the concept for integration of the different components into one system.

2 Sampling and Fluid Handling

2.1 Introduction

For miniaturized analysis systems, taking samples and manipulating them is of great importance. When miniaturizing macroscopic systems, specific problems include representativeness of the sample and reproducibility of small sample manipulation. Thus, in addition to the whole range of sampling techniques already utilized by analytical chemists in conventional systems, specific techniques and components need to be developed. In particular, attention has to be paid to dead volumes, which give rise to tailing effects in chromatography, and surface properties of the fluid channels, that may cause turn-over effects due to the large surface-to-volume ratio.

2.2 Sampling Techniques and Components

An often underestimated subsystem in miniaturized analyzers is the sampling part. This subsystem incorporates an arrangement that guarantees a representative part of the analyte to be prepared and transported into the analyzer's fluid handling part. The configuration of the analysis system determines the constraints for the sampling. When using silicon micropumps comprising microvalves, for instance the presence of particles (e.g. dust particles, sand grains, living cells) is prohibited because they block the valves. The sampling subsystem should therefore contain a microfilter which may consist of a conventional polymer membrane (e.g. a MilliPore filter) or a microfabricated

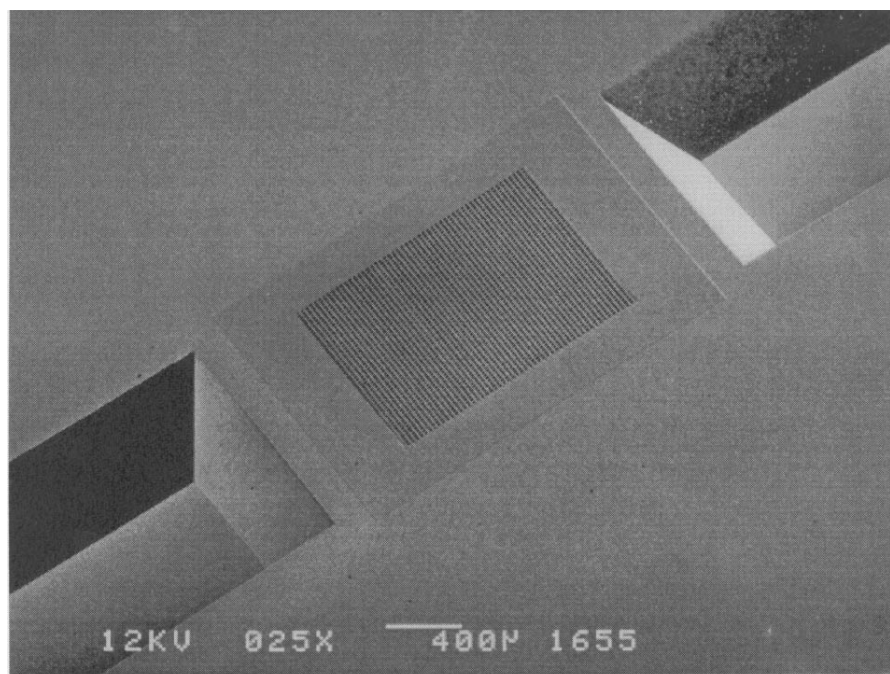


Fig. 3. Micrograph of a silicon microfilter

silicon filter [12] (see Fig. 3). The latter filter has several advantages over conventional (polymer) ones. It has a uniform pore size, low pressure loss, and very small internal volume. Furthermore, it may be used in a setup for rapid (microscale) mixing [13].

In microdialysis sampling, polymeric membranes are used to filter out large biomolecules and cells from the analyte. This technique, introduced some ten years ago, has now become a standard technique in neurochemical laboratories [14] and seems to be well-suited for combination with μ TAS [15, 16]. The great advantage of coupling this sampling technique to a μ TAS is that the internal system volume (comprising connections) remains limited. This means that in spite of flow rates in the order of less than $1 \mu\text{l}/\text{min}$, a high sample throughput can be obtained.

2.3

Fluid Handling Components

Several review articles describing miniaturized devices for fluid handling have been published that give excellent and detailed overviews of the state of the art [3, 4]. Here, some examples of microfabricated valves and pumps will be given to illustrate the possibilities of silicon microtechnology.

2.3.1

Microvalves

2.3.1.1

Valve Types

If we consider a valve as a controlled restriction in a fluid flow channel the following types can be distinguished:

- Type A The first type consists of a plane surface which moves in a direction perpendicular to the flow coming from an orifice (Fig. 4a). We can have a circular orifice surrounded by a valve seat and a plane surface which moves parallel to the valve seat until the flow is shut off.
- Type B The second type consists of the channel being constricted (Fig. 4b).
- Type C The third type is somewhere in between and consists of two mating parts, like the ground glass stopper mated to the neck of bottles used to store chemicals. The mating parts move into each other thereby constricting the flow channel (Fig. 4c).
- Type D A new type of valve is formed by freezing and melting of a part (plug) of a fluid passage. This type is also called the micro electro thermo fluidic (METF) valve [17]. The main advantage of this type of valve is the completely zero dead volume and absence of moving parts.

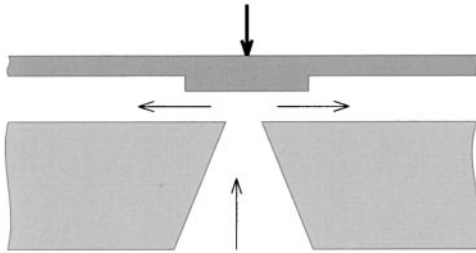


Fig. 4 a. Valve type A; restriction perpendicular to fluid flow

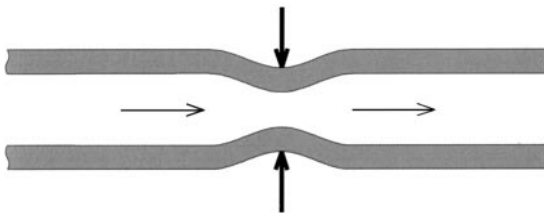


Fig. 4 b. Valve type B; restriction parallel to fluid flow

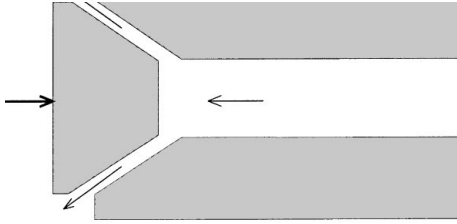


Fig. 4 c. Valve type C; combination of valve type A and B

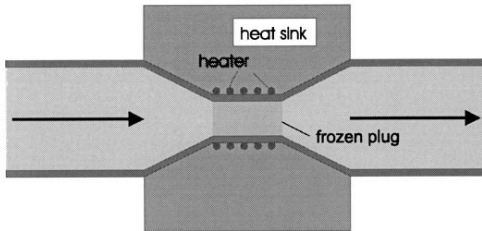


Fig. 4 d. Valve type D; Restriction is formed by frozen part of the liquid

2.3.1.2

Activating Principles

For all types of valves, the parts have to move toward or from each other and therefore an actuator is needed. Although there is no power needed to shut off a flow in the ideal case, this is not true in practice. Controlling a flow (i.e. keeping the constriction in its place in a closed loop configuration) requires a power source, while shutting off a flow requires power to overcome friction or to overcome pressure built up at the orifice during the action. Often a closed valve of type A is secured by a differential pressure. This pressure must be overcome to open the valve. An important requirement in any design is whether the valve should be open or closed when the power goes down (some valves have more than one stable position). From this requirement the valve types ‘normally open’ and ‘normally closed’ can be distinguished.

2.3.1.3

Technology

It cannot be denied that the work on microvalves is in its infancy and it is impossible to classify the valves with respect to the technology used in its production. However, most of the micromachined valves fabricated to date use silicon micromachining. In exceptional cases also other techniques such as LIGA (Lithographie, Galvanoformung, Abformung; a technique involving lithography electro-deposition and molding) may be used [18].

2.3.2

Micropumps

The classification of micropumps is somewhat arbitrary. One might distinguish micropumps according to the type of momentum transfer to the solution (mechanical or electrical), but for practical reasons, we choose here to distinguish them by the presence or absence of mechanical valves, this being a generic element of many pumps. A second classification can be made using the actuation principles (see Fig. 5). Various examples of the different pump-types are listed below.

Valve-type Micropumps.
Piezoelectric Actuation

The very first work on micropumps using piezoelectric actuation was on a peristaltically functioning micropump, which was not published until 1990 [19]. In this micropump, momentum is given to the fluid by a row of valves which give the effect of a restriction moving in the direction of the desired flow. The general structure of a pump with one actuator using two check valves is shown in Fig. 6. A number of check valve type micropumps, all realized using a micro-machined silicon wafer anodically bonded to Pyrex glass, have been developed

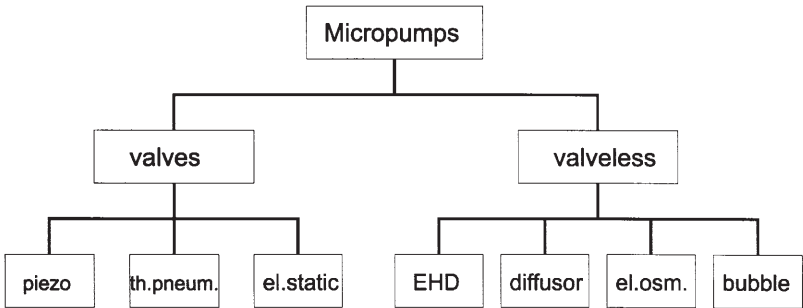


Fig. 5. Classification of micropumps

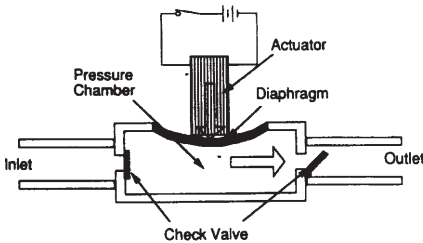


Fig. 6. Principle of check-valve micropump with piezoelectric actuation

at Twente University [9, 20, 21]. The check valves in these pumps are round membranes with orifices and valve seats and they open and close as a consequence of the pressure caused by the driving actuator. In the first model, the driving actuator consists of a bimorph formed by a thin glass membrane and a commercial piezo disc. The seats of the check valves have a surface layer in order to prevent bonding of the check valves when the wafers are bonded. The extra layer is also advantageous in that it give the check valve a small pre-stress.

After the initial work at the University of Twente, other groups optimized [22, 23] or modified [24] piezoelectric actuated micropumps and probably the most advanced micropump to date is the bi-directional one presented by Zengerle et al. [25]. This pump uses an external piezo-actuator and has a complex, actuation frequency dependent mode of operation which creates bi-directional pumping as a function of frequency. The pump has unprecedented specifications: flow rates up to 2 ml/min (8 ml/min for gas), pressure up to 17,000 Pa, bi-directionality and self-priming, which makes this pump actually the best performing one. Unfortunately, contrary to what many researchers have been aiming at during the past few years, there appears to be a growing demand for very precise pumping and dosing in the nanoliter range for applications such as drug delivery and DNA analysis.

Thermopneumatic Actuation

An alternative actuation principle is thermo-pneumatic actuation, as illustrated in Fig. 7. Heating of a confined gas, or gas/liquid mixture, leads to expansion of the gas which deforms a flexible membrane covering the pump chamber. Compared to piezoelectric actuation, the voltages used for heating are much lower, making this pump much more suitable for combination with electrochemical sensors. Even more important is that this design can be fully batch fabricated, be it at the cost of a number of extra silicon and glass wafers forming a six layer stack. Typical yields of this pump are between 10 and 100 $\mu\text{l/min}$ with maximum pressures up to 10,000 Pa. In the operating region of the pump with a counter pressure built up, no measurable backflow occurs, indicating that the closure of the valves is very good. The limiting counter pressure is not deter-

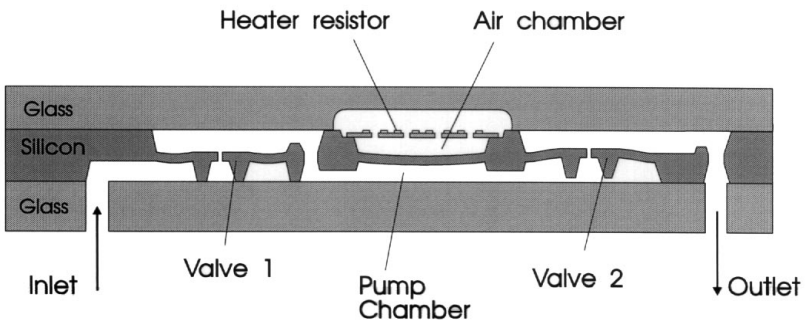


Fig. 7. Principle of a thermopneumatic micropump

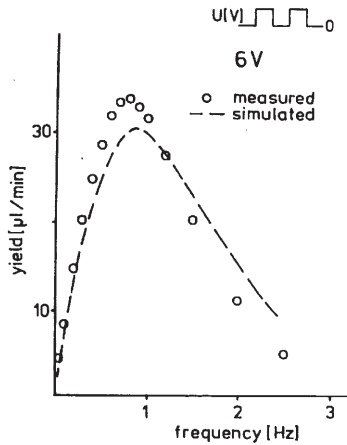


Fig. 8. Pump yield as function of pump frequency for an applied voltage of 6 V at zero back pressure (outlet minus inlet pressure)

mined by backflow but by the pressure balance within the device. In Fig. 8 the measured as well as the simulated [26] pump yield as a function of actuation frequency is shown.

Electrostatic Micropumps

Finally we present a design of Zengerle et al. [27], based on an electrostatic driving principle. A thin pump membrane electrode is electrostatically repelled from a fixed counterelectrode (see Fig. 9). The design contains a stack of four wafers. Here, there is a clear trade off between driving pressure (requiring a small electrode gap, but staying out of the “pull in” regime) and output stroke (requiring a large electrode gap). Quite high voltages are needed to get a reasonable output flow, but the counter pressure that can be overcome with this design is still rather small. However theory predicts a better performance than the experiments show. Again a frequency, much higher than in the thermopneumatic design can be reached giving a smoother outflow.

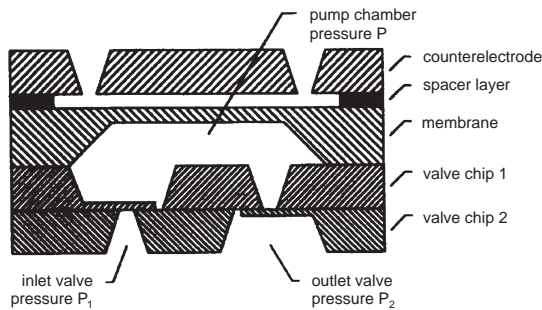


Fig. 9. Principal design of the electrostatically actuated membrane pump [from ref. 27]

Electrohydrodynamic (EHD) Micropumps

The EHD pump of Richter et al. [28, 29] is an example of the “body force” pump. In fact the driving force is created by large electric fields created between two grids, which are positioned orthogonal to the flow direction, or by induction [30, 31]. When using electrodes, a short distance is required to create the necessary high fields, which must be high enough to generate ions at the first grid, which are driven by Coulomb forces and drag the fluid in this driving direction. The process of ionization is complex and depends on electrode material, liquid composition and voltage. With induction pumping, gradients in permittivity or conductivity in the liquid are required. EHD pumps have no moving parts, which is a clear advantage, but it can be imagined that the counter pressure is limited. ‘Backflow’ immediately occurs when the driving force is shut off. Unfortunately, aqueous solutions cannot be pumped as a consequence of the high ionic conductivity.

Electroosmotic Force Pumping

This pumping principle relies on the presence of (immobile) surface charges in glass capillaries. At neutral pH values, the surface of glass (silanol groups) are negatively charged, and positive (mobile) counterions align along the inside of the capillary. When a high voltage is applied the mobile counterions start to move, and take the rest of the fluid column with them.

Electroosmotic flow (EOF)

This type of pumping is frequently employed in separation chemistry for capillary electrophoresis, traditionally in fused silica capillaries, but recently more and more in planar quartz structures [32–34]. It should be noted that this type of pump is of the current-source type. This means that the pressures that can be obtained depend on the internal resistance; in wide glass tubing, with little resistance, very little pressure can be built up, and a very small hydrostatically induced differential in/outlet pressure immediately overrules the electroosmotic pumping. However, in very small capillaries, relatively high pressures can be obtained (up to tens of bars).

Diffuser Pumps

An original pumping principle without moving valves was presented by Stemme et al. [35, 36]. It consists of an actuated pump chamber and diffuser/nozzle elements, that take care of a rectifying action. The principle of operation relies on the fact that the pressure drop Dp over a diffuser/nozzle can be written as:

$$Dp = r u^2 \xi / 2$$

Where r is the fluid density, u is the mean fluid velocity, and ξ is the pressure loss coefficient. The latter coefficient is different for a diffuser and a nozzle, so that the pressure loss depends on the direction of the fluid flow. After a first version

made by conventional machining techniques, a micromachined version was realized which gave yields of 40 ml/min of water and a zero-flow pressure of 50 cm H₂O.

2.3.3

Micro Flow Channels

Recently there has been a great deal of interest in the fabrication of micro-channels in planar substrates. Several etching techniques in silicon (e.g. isotropic and anisotropic wet etching) have been investigated for this purpose. Recently, deep reactive ion etching (DRIE) [37] has been developed as a new technique to make vertical channels with relatively high aspect ratios in silicon (Fig. 10). Vertical channels allow a high density of channels per unit area and therefore provide a long (vertical) absorption path length for optical detection. The high channel density is illustrated by a channel structure for chromatography containing over 300 m of 2.5 μm wide and 25 μm deep channels on one single 3" wafer (see Fig. 11).

The wafers containing the etched trenches are anodically bonded to Pyrex glass to form closed channels. The bond strength thus formed is strong enough to withstand pressures up to 250 bar. At that point a breakdown even takes place in the monocrystalline silicon and not at the bonded interface. Clearly, the indicated structures are useful for HPLC applications.

However, for capillary electrophoresis typically voltages of several kVs are applied, and completely isolating materials such as quartz are used [32]. Unfortunately, wet etching of quartz is not trivial, and little is known about dry

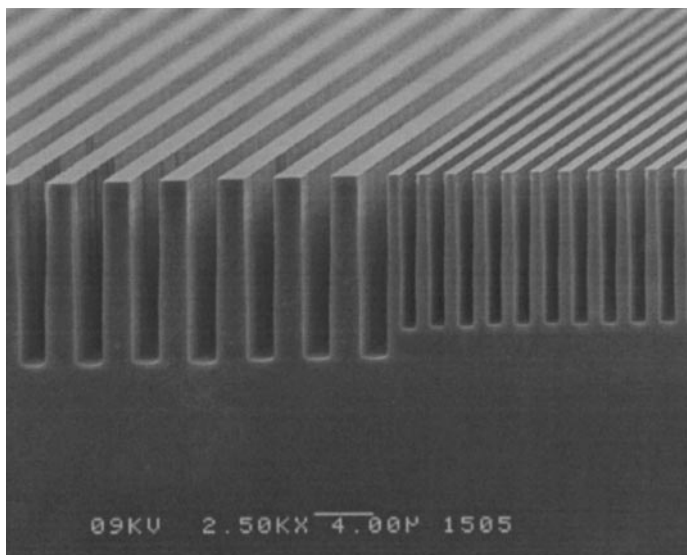


Fig. 10. Vertical channels in silicon made with DRIE

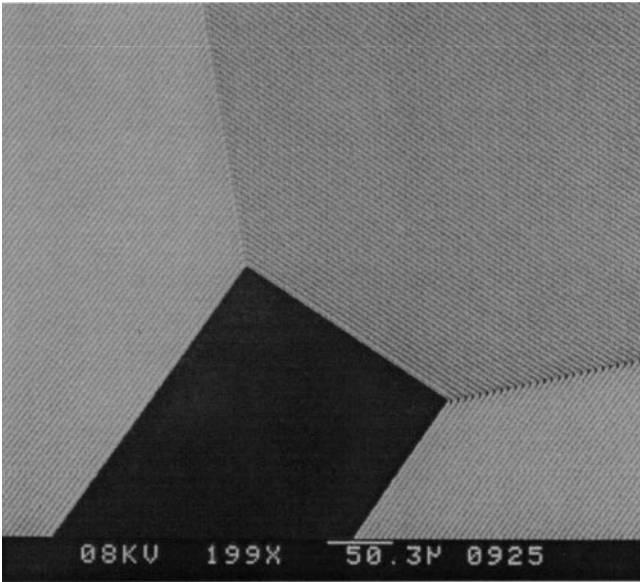


Fig. 11. Anisotropically etched microchannels for chromatography

etching techniques of quartz. It is therefore interesting to transform the etched silicon structures into isolating structures. For this purpose, the etched trenches are filled with silicon oxide and anodically bonded. Subsequently, the reverse side of the silicon is etched back until the oxide is reached, and in such way closed, all-glass microchannels are formed (see Fig. 12).

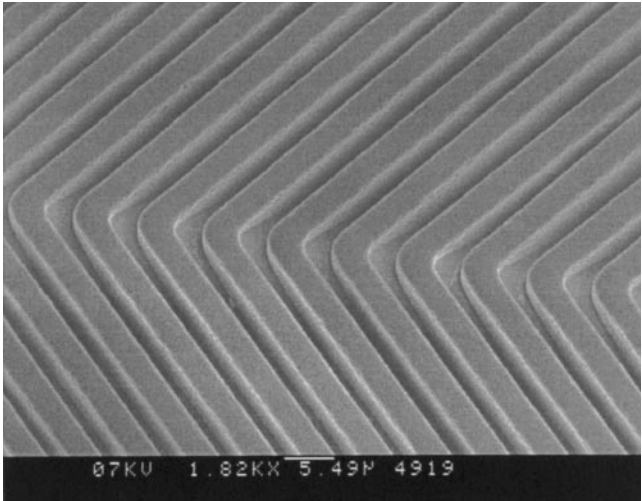


Fig. 12 a. All-glass microchannels formed by DRIE with back-etched silicon

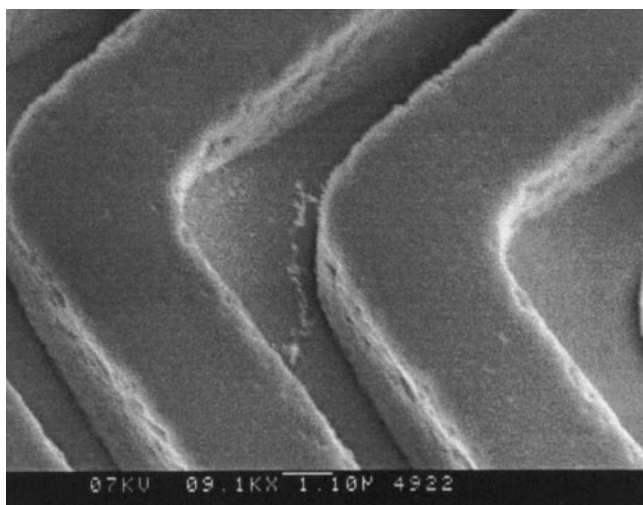


Fig. 12 b. Detailed micrograph of glass-microchannels

3 System Integration

3.1 Integration Concepts

μ TAS configurations often comprise a large variety of components, such as optical, electrochemical, micromechanical and electronic ones. It is clear that covering all the needed expertise for building such a μ TAS is hardly possible for one company or institute. Thus, it should be possible to combine components or subsystems from different developers/suppliers into one microsystem, for which, evidently, some sort of standardization is needed. In addition, although for almost every microsystem a natural tendency exists to look for monolithic integration, as for instance illustrated in the micro liquid dosing system of Lammerink et al. [20], new functions usually start as hybridly integrated components, so that a real life system typically is a mixture of monolithically integrated subsystems and separate components (Fig. 13). Thus, there is a clear need for a flexible concept for microsystem integration.

Two different approaches have been explored for integration of μ TAS. The first approach is to use vertical stacking of components [38, 39]. This builds further on the original disc-stacking concept of Ciba Geigy [40], where planar system components or modules with fixed size are stacked onto each other. The liquid is transported from one module to another through on-module deposited micro sealing rings [5]. An alternative approach is to mount the different system modules on a horizontal baseplate. This method guarantees a better compatibility with standard pick-and-place techniques usually employed for the realization of electronic circuits.

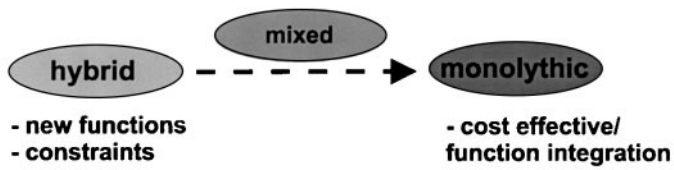


Fig. 13. Possibilities for μ TAS integration

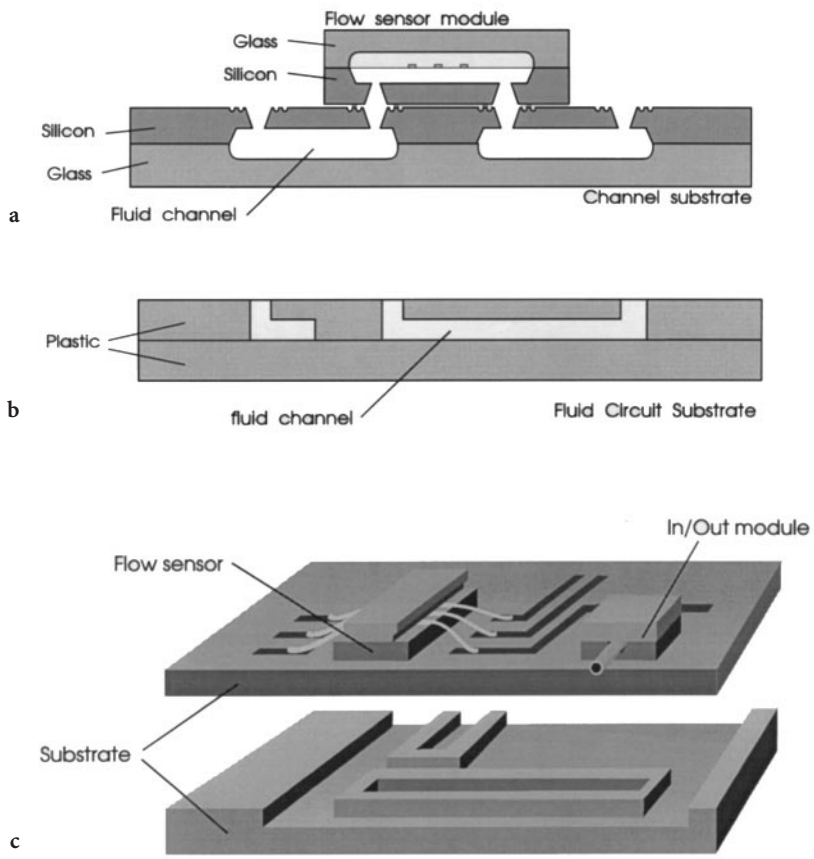


Fig. 14. Planar modular concept for fluid handling micro-systems with functional modules on top of a Mixed Circuit Board

a Flow sensor on top of a silicon- glass MCB,
b MCD made of plastics,
c 3D-view of MCB with flow sensor and input/output

3.2

The Mixed Circuit Board (MCB) Concept

Figure 14 shows schematic diagrams of the so-called mixed circuit board (MCB) which generally consists of two parts to form the fluid channels. The MCB may be built by a glass-silicon sandwich but also by plastics. The modules can be attached with the help of existing bonding techniques such as anodic bonding, glue and soldering. The demonstrated MCB consist of an epoxy printed circuit board attached to a transparent polycarbonate substrate. Versions with machined channels in either one or the other part are used. The top surface of the MCB contains the electric connections and holes for fluid transport from and to the channels. Future developments of the MCB similar to the developments in the printed circuit board technology like flexible versions are feasible.

3.3

System Modules

For the realization of fluid handling microsystems a wide variety of modules is needed. Many of them, like pumps, flow sensors and filters, have already been developed, as described in Sect. 2.3. However, for integration of these components into a system, it was necessary to design them anew. All designs were based on a standard port pitch of 5 mm. Figures 15 to 18, illustrate SEM and/or optical photographs of several system modules.

3.4

Modeling and Design

Because of the enormous diversity in components it is difficult to describe a straightforward design-path for components for the MCB concept. Here we focus on the modeling and the design of the fluid control modules and specific on the thermo-pneumatic actuated micropump used (twice) in the demonstrator. An elaborated model of this micropump is given by van de Pol et al. [21]. The main functions of the fluid control in micro analysis systems are the switching function and the direct flow and/or pressure control. Building blocks are hydraulic inertances, resistors, capacitors and passive and control-valves. Very often an active element like a micropump is needed.

The approach adapted in our group is based on finite element modeling (FEM) in combination with lumped element modeling. FEM is used for specific (mono-, duo-) domain problems. Although the encountered geometries can be rather complex, FEM is not the appropriate tool for modeling the whole system (multi-domain) behavior. The FEM modeling results in specific lumped parameters (e.g., stiffness, capacitance, fluid resistance) which are subsequently used in a lumped element system model. This lumped element system modeling and simulation tool is based on the bond graph description language. Practical implementation of the modeling and simulation is done using the 20SIM program package [26].

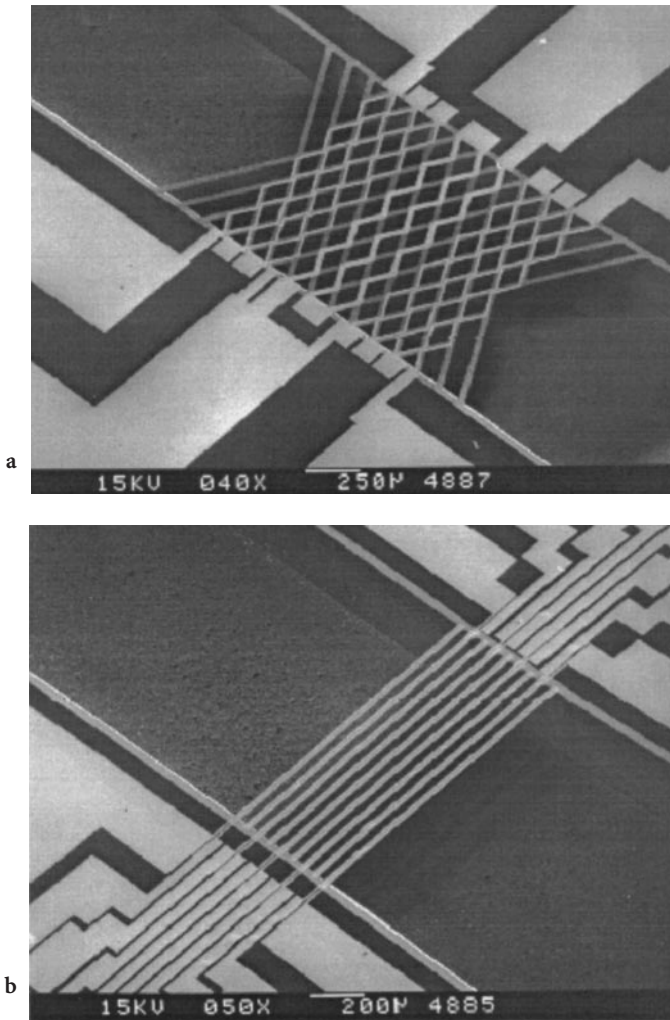


Fig. 15. **a** Grid type flow sensor, **b** beam type flow sensor (the fluid channel width is 1 mm)

The modeling of a thermopneumatic micropump is given as an example of this approach. Simulation results as well as design aspects of a microsystem containing two of these micropumps are discussed.

3.4.1 Thermal Flow Sensor

The demonstrator fluid handling system contains two thermal micro flow sensors illustrated in Fig. 19. Three resistors are located in the middle of the flow channel.

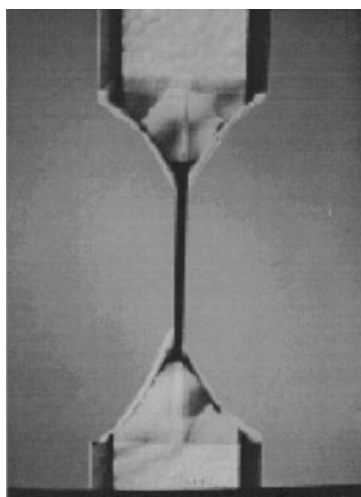


Fig. 16. Hydraulic resistor made of anisotropically etched V-groove

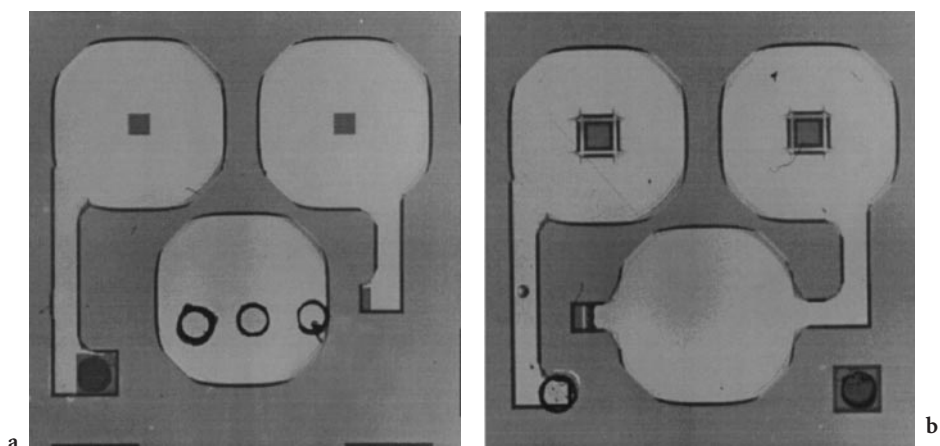


Fig. 17. **a** Micropump (*top*) and **b** micropump (*bottom*)

Heat is dissipated in the middle resistor (H). The resulting temperature distribution is sensed with two temperature sensitive resistors T_u , T_d located symmetrically up- and downstream with respect to the heater. The temperature difference ΔT as function of the flow shows a maximum which limits the usable flow range of the sensor. A typical output signal of the flow sensor is given in Fig. 20.

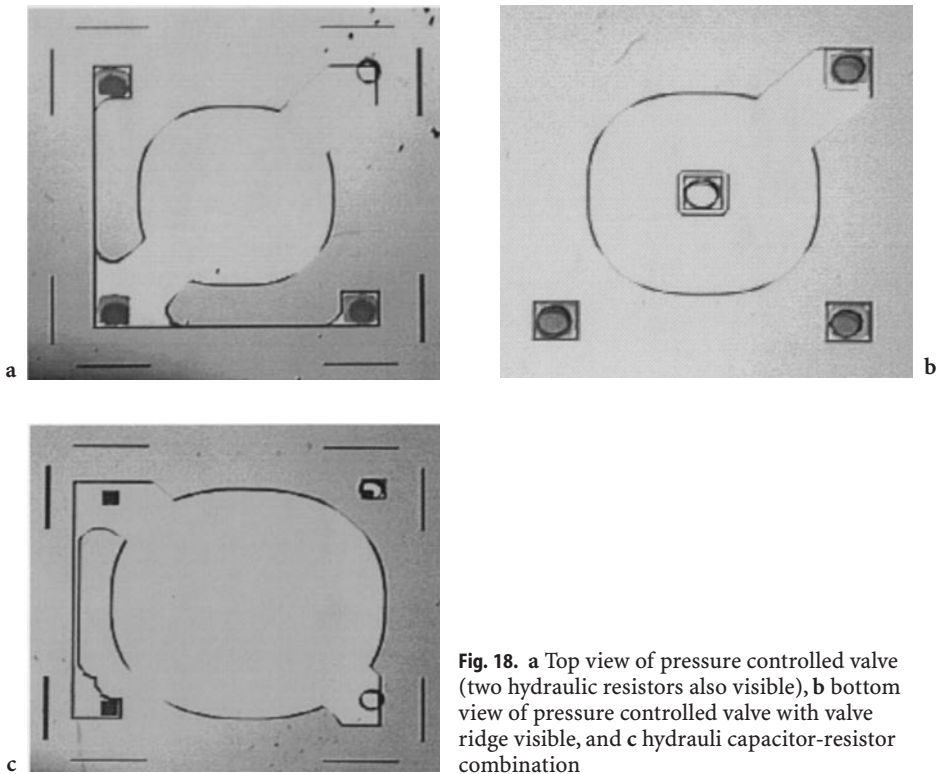


Fig. 18. a Top view of pressure controlled valve (two hydraulic resistors also visible), b bottom view of pressure controlled valve with valve ridge visible, and c hydraulic capacitor-resistor combination

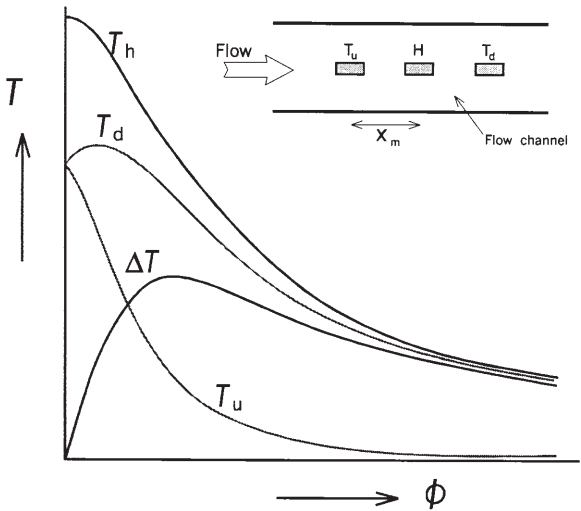


Fig. 19. Resistor temperatures as function of the flow with constant power dissipation in the heater resistor. The insert shows the layout of the thermal flow sensor with three resistive elements in the center of the flow channel

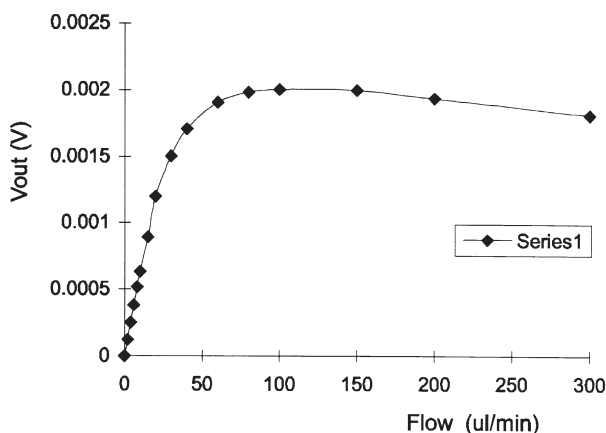


Fig. 20. Typical flow sensor output signal as function of the flow. (For sensor geometry see figure 19; 10 mW dissipation in the heater resistor; 1mW in the sensor resistors; 150 Ω). The sensor can be used up to 100 $\mu\text{l}/\text{min}$ (ethanol)

3.4.2

Thermopneumatic Micropump

The demonstrator analyzing system contains two thermo-pneumatic actuated micropumps (see Fig. 7). The micropumps are of the reciprocating type and consist of three main building blocks: a thermo pneumatic actuator (A), a pump chamber with a flexible pump membrane which acts as a capacitor (C) and two passive circular silicon check valves (V), see Fig. 21.

The pump actuator generates a periodically varying pressure in the air chamber. This pressure acts on a flexible pump membrane between actuator and pump chamber. Due to the deflection of the pump membrane the volume of the pump chamber changes. By means of two check valves, the liquid is periodically sucked in through one valve and forced out through the other valve, thus forcing a flow into one direction. The thermopneumatic actuator consists of a cavity filled with air and a thin film heating resistor supported by thin silicon nitride beams for (periodically) heating the gas inside.

A narrow air channel connects the cavity to the outside and allows a pressure exchange with the surroundings. A typical actuator does have a circular air chamber with a diameter of 8 mm and a height of 400 μm with the resistor mounted in the middle between “floor” and “ceiling”. The “thermal” response (warming up and cooling down of the air) can be described with a “thermal” relaxation time τ_t which is mainly determined by the heat capacity of the heater-resistor and the heat conductivity of the gas [21]. A second relaxation time is determined by the heat capacity of the whole pump body and the heat conductivity of the body to its surroundings. Due to the air channels there is also a (third) ‘pneumatic’ relaxation time τ_p . Since the pneumatic system is non-linear, τ_p can only be approximated.

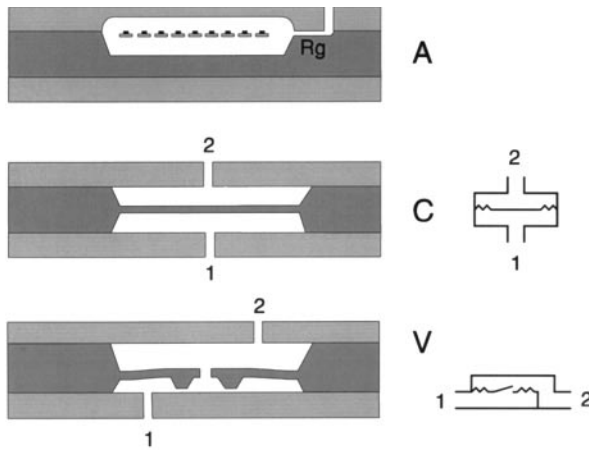


Fig. 21. Cross sections of the glass-silicon-glass structures for the pump actuator, the pump membrane and the valves. Right from the figures, the so-called Ideal Physical Models (IPM's) of the pump membrane and the valve are given

The pump membrane acts as a capacitor (see Fig. 21, C) which stores a volume, related to a pressure drop. In first approximation the volume change under the membrane is linear with the center displacement [42]. The membrane capacitance, however, shows a strong non-linear behavior for center displacements in the range of large deflections.

The normally closed check valves consist of a flexible outer ring and a rigid inner sealing ridge (see Fig. 21, V). When pressure p_1 is higher than p_2 the sealing ridge is lifted, and liquid flows through the valve. When pressure p_2 is higher than pressure p_1 the valve is closed. Due to a thin oxide layer on the valve ridge the valve has a small pre-pressure. Obviously, the valve has a strongly non-linear behavior.

The whole micropump is described in a bond graph model [43]. The pump is driven by a (square-wave) heat source. Simulation results of the pump actuation as well as the pump rate based on this model are given in Figs 22 and 23

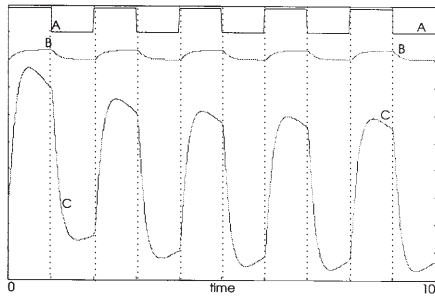


Fig. 22. Simulation of a pump actuator: A = heating power in [W], B = gas temperature in [K] and C = gas pressure in the actuator chamber in [Pa]. The thermal relaxation times are 0.2 and 200 [s] and the pneumatic relaxation time is 2 [s]

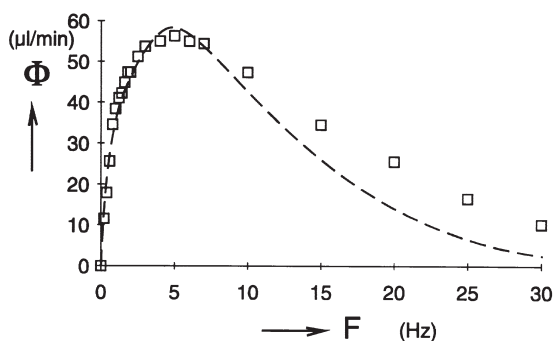


Fig. 23. Simulated and measured pump rate as a function of the excitation frequency. The amplitude of the simulation is fitted with the amplitude of the heating power

respectively. Using the bond graph description language, modeling of more complex systems becomes relatively simple.

3.5

Realization of a Demonstrator System

3.5.1

Description

A schematic diagram of the demonstrator chemical analysis system is given in Fig. 24. The MCB comprises three in/outlets, two micro-pumps, two flow sensors and an optical absorption detector module. The purpose is to measure chemical reaction products by detection of the (spectral) absorption intensity. Sample and reagent liquids are mixed in the appropriate amounts on-board (currently the actual mixing takes place during the propagation in channels) and the optical absorption is measured at the detector side.

The electronic control circuitry is situated in two levels below the MCB layer with the modules. It is based on a microcontroller system for the micro liquid handling and the chemical analysis data. Implemented in the electrical circuitry are driving circuits for the micro pumps, sensing circuits for the flow sensors, optical absorption measurement circuitry, power management and communications using an RS232 interface.

The absorption cell is a glass silicon glass sandwich component ($15 \times 1 \times 0.4$ mm) where optical intensities from different colored LEDs are measured by a 64 pixel CCD detector, see also Fig. 25. A demonstrator system with a total system volume of about 50 ml is illustrated in Fig. 26.

3.5.2

Results

Figure 27 shows test results of the measured pump and flow sensor behavior. The time constant of the pump/flow sensor combination is in the order of 0.2 s. This

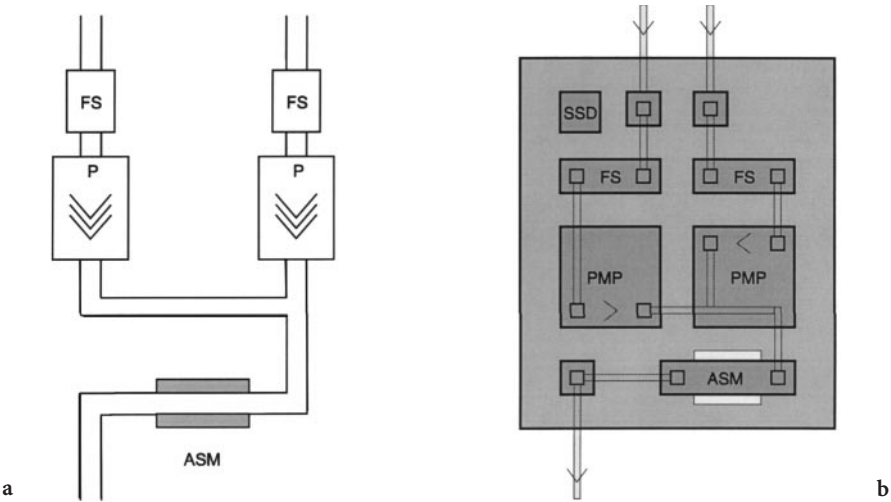


Fig. 24. Micro Analysis System. **a** Structure of NAS with two flow sensors, two pumps and an absorption sensor module. **b** Component lay-out of MAS

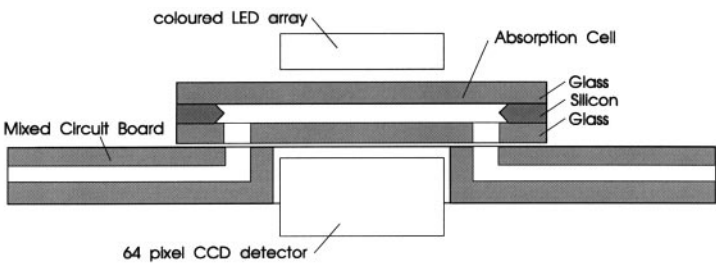


Fig. 25. Cross-section of the optical absorption detector

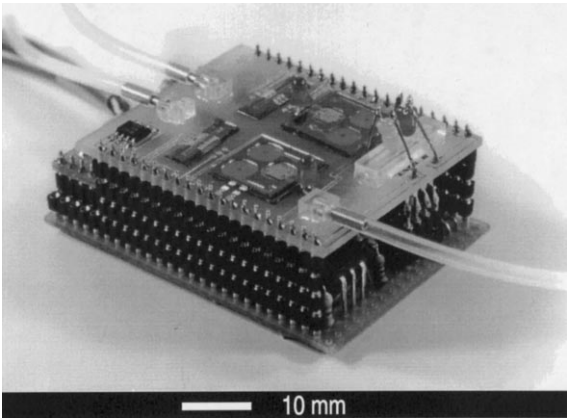


Fig. 26. Demonstrator MAS modules mounted on a MCB

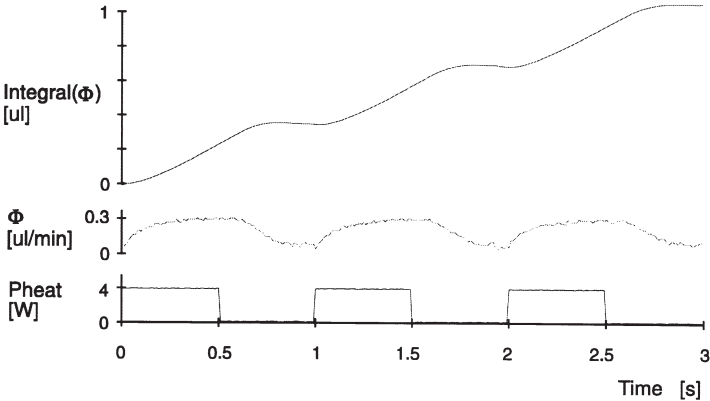


Fig. 27. Measured pump and flow sensor behavior

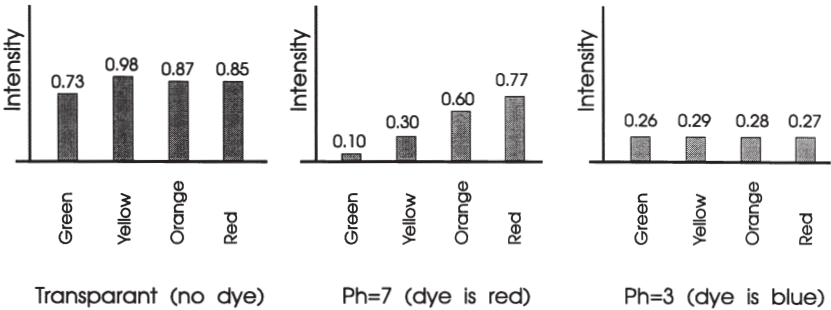


Fig. 28. Measured light intensities with four colored LED's

is in accordance with the simulation results. Integration of the flow sensor signal results in a very smooth dose function.

The operation of the absorption detection is demonstrated by recording absorption intensities. This was done qualitatively at four different wavelengths for three liquids: a transparent fluid, the Congo red indicator at pH=7 (red-colored), and the Congo red indicator at pH=3 (blue-colored). As indicated in Fig. 28, the two differently colored states of Congo red can clearly be distinguished from each other, and from the transparent background solution. Although this demonstration is not optimized, the absorption path length for instance is only 380 μm thick (thickness of a 3" diameter silicon wafer), it clearly illustrates the potential of this approach.

4 Applications

Miniaturized FIA-systems can be used for a variety of applications. First of all, such systems can be used to replace existing conventional FIA-systems, opera-

ted by roller-pumps. The direct advantage is a 10–100-fold reduction in reagent and sample consumption [44, 45]. These systems may find an interesting application for (quasi) on-line process monitoring. The continuous operation in these applications makes the reduction in consumption and waste of chemicals an important advantage.

A second application is as an autonomous instrument for environmental field measurements. The aforementioned advantages are here accompanied by a low power consumption, enabling a long stand-alone time with battery use. Although several research and development projects are actually being carried out in Europe in this direction, up to now no such miniature instrument has been commercialized.

A third application for μ TAS is in the biomedical field. Gumbrecht et al. [46, 47] developed a monolithically integrated, ISFET-based sensor system for (bed-side) monitoring of blood pH, pO_2 and pCO_2 in patients. Here the successful introduction on the market mainly depends on the price of the system, for which reason a CMOS-compatible design of the silicon part is needed. Evidently, such a development is only possible in the case of a high volume market.

In terms of space applications, the low weight accompanied by the small size gives the system a decisive advantage over conventional systems. In addition, the use of silicon processing may also give lower fabrication costs. This is, however, strongly dependent on the type of system and, as mentioned earlier, the production volume. Examples of space applications are the space micro-bioreactor as developed by van der Schoot et al. [48], and the previously mentioned sensor array system [11]. Whereas the first system is meant to be a small-size, low-power experimentation setup for biological experiments, the second one is meant to be incorporated in the life support systems for astronauts. In this case, the light weight, small size and small power consumption are the decisive advantages of the microsystem approach.

Finally, the most promising application area of μ TAS lies in DNA analysis for two reasons. First, microstructures for capillary electrophoresis offer the

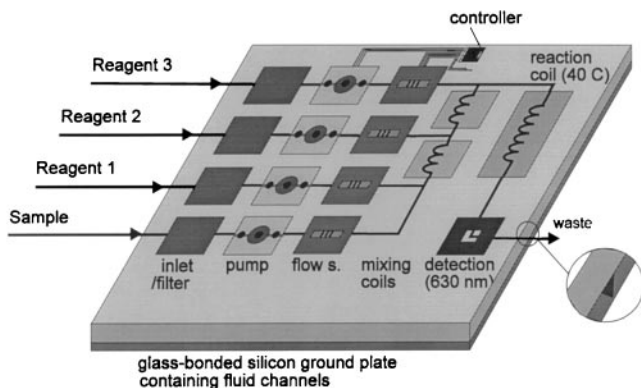


Fig. 29. Ammonia analyzing system according to the proposed MCB-concept

advantage of a high analysis speed [49, 50] which is crucial for DNA-sequencing. Although most of the work on capillary-electrophoresis structures has been carried out with micromachined quartz structures, recently techniques for realization of electrically insulated structures made with silicon microtechnology have been presented, as illustrated in Sect. 2.3.3. The advantage is that micro-detectors such as electrochemical, differential pressure or thermal sensors are much more easily integrated with the microchannels than with quartz structures. The second reason that makes microfabricated structures promising for DNA analysis is that they allow the manipulation of fluids in the nanoliter or even picoliter range. Recently, much work has been done on the realization of micro-titerplates for DNA screening [51–53]. Here a combination of precise fabrication of micro-volume reactors with a clever fluidic system and micro dosing (inkjet) nozzles to charge every microreactor with the appropriate chemicals yields a highly sophisticated microanalysis system with excellent marketing prospects.

5 Conclusions

In this chapter we have described the possibilities of silicon microtechnology for the realization of micro (bio)chemical analysis systems. It can be concluded that, with micro system technology, a variety of components for fluid handling on a micro scale can be realized. Etching techniques can be used for the production of planar microchannels, either in silicon or completely insulating, in silicon oxide. Utilization of micro system technology for a planar fluid-channel plate also facilitates the integration of different components into one system without connecting tubing. Using the same concept, electronic components can also be added. It has been shown that bondgraph modeling provides a valuable tool for the simulation of component and system behavior.

The value of this approach is illustrated by a demonstrator chemical analysis system (μ FIA-system) comprising two micropumps, two flow sensors, an optical absorption cell and control electronics. The capability of detecting a differently colored pH indicator proves that this concept can be used for many miniaturized FIA systems. Given the number of particular properties of μ TAS such as small size, fast response, little consumption of chemicals and electrical power and, potentially, low price, a wide range of potential applications are possible. However, in order to achieve low cost production, large numbers are needed. This is best achieved by focusing efforts onto a few generic systems, that may be finely tuned for particular applications. The selection of these few generic systems appears to be the greatest challenge for the successful implementation of μ TAS. The most promising application seems to be in DNA analysis, where a combination of high analysis speed, extremely small volumes, and precise microsystem fabrication is required and which offers a potentially large market volume.

Acknowledgements. The authors wish to thank Vincent Spiering, Willem Tjerckstra, Meint de Boer and Erwin Berenschot for their valuable contributions. Parts of this work have been car-

ried out with financial support from the Dutch Foundation for Technical Sciences (STW) and with an OSF grant from the University of Twente.

6

References

1. van den Berg A, Bergveld P (1996) Anal Meth Instr Special Issue 1996:9
2. Göpel H (1991) (ed) Sensors, A comprehensive survey, 2, VCH-Verlag, Weinheim, Germany
3. Gravesen P, Branebjerg J, Jensen OS (1993) J Micromech Microeng 3:168
4. Elwenspoek M, Lammerink TSJ, Miyake R, Fluitman JHJ (1994) J Micromech Microeng 4: 227
5. van den Berg A, van der Schoot BH, van den Vlekkert HH (1991) Ion sensitive field effect transistors. In: Sensors – A comprehensive book series in eight volumes, vol 2, chap 10.2, VCH, Weinheim, Germany
6. Manz A, Graber N, Widmer HM (1990) Sens Actuators, B1:244
7. van der Schoot BH, Jeanneret S, van den Berg A, de Rooij NF (1993) Anal Meth Instrumentation 1(1):38
8. Bruns MW (1992) Proc. IEEE Int Conf Industrial Electronics Control Instrumentation 3: 1640
9. van Lintel HTC, van de Pol FCM, Bouwstra S (1988) Sens Actuators 15:153
10. van der Linden WE (1987) Trends Anal Chem 6:37
11. van Steenkiste F, Grünkorn H, Claesen L, Baert K, Hermans L, DeBruyker D, de Cooman M, Spiering V, van den Berg A, van der Schoot BH, Arquint P, Born R, Schumann K(1996) Anal Meth Instr Spec. Issue μ TAS '96:138
12. van Rijn CJM, Elwenspoek MC (1995) Proc MEMS '95, Amsterdam, The Netherlands, 83
13. Miyake R, Lammerink TSJ, Elwenspoek MC, Fluitman JHJ (1993) Proc MEMS '93, Fort Lauderdale, (FA), USA
14. Robinson TE, Justice JB (1991) Microdialysis in neurosciences, Elsevier, Amsterdam, The Netherlands
15. Laurell T, Rosengren L, Drott J (1994) In: van den Berg A, Bergveld P (eds), Micro total analysis systems, Kluwer, Dordrecht, The Netherlands, p 227
16. Künnecke W, Bilitewski U (1994) A novel sampling technique for total analysis systems In: van den Berg A, Bergveld P (eds) Micro total analysis systems, Kluwer, Dordrecht, The Netherlands, p 223
17. Kaartinen N (1996) Proc MEMS '96, San Diego, (CA), USA, 395
18. Schomburg WK, Vollmer J, Büstgens B, Fahrenberg J, Hein H, Menz W (1994) J Micromech Microeng 3:216
19. Smits JG (1990) Sens Actuators, A21 – 23: 203
20. Lammerink TSJ, Elwenspoek M, Fluitman JHJ (1993) Proc MEMS '93, Fort Lauderdale, FA, USA, 254
21. van de Pol FCM, van Lintel HTG, Elwenspoek M, Fluitman JHJ (1990) Sens Actuators A21 – A23:198
22. van der Schoot BH, Jeanneret S, van den Berg A, de Rooij NF (1992) Sens Actuators B6:57
23. Gass V, van der Schoot BH, Jeanneret S, de Rooij NF (1993) Proc MME '93, Neuchâtel, Switzerland, 177
24. Shoji S, Esashi M, van der Schoot BH, de Rooij NJ (1992) Sens Actuators, A32:335
25. Zengerle R, Uhlrich J, Kluge S, Richter M, Richter A (1995) Sens Actuators A50:81
26. 20SIM, Commercially available modeling and simulation package developed at the University of Twente, Control laboratory, Faculty of Electrical Engineering, Enschede, the Netherlands
27. Zengerle R, Richter A, Sandmaier H (1990) Proc MEMS '92:19
28. Richter A, Plettner A, Hoffmann KA, Sandmaier H (1991) Sens Actuators A29:159
29. Richter A, Plettner A, Hofmann KA, Sandmayer H (1991) Proc MEMS '91:271
30. Bart SE, Lee S, Tavrow I (1990) Mehregany M, Lang J (1990) Sens Actuators, A21 – 23:193

31. Fuhr G, Hagedorn R, Müller T, Benecke W, Wagner B (1992) *Proc MEMS '92*:25
32. Harrison DJ, Fluri K, Seiler K, Fan Z, Effenhauser CS, Manz A (1993) *Science* 261:895
33. Jakobson SC, Hergenroder R, Koutny LB, Ramsey JM (1994) *Anal Chem* 66:1114.
34. Manz A, Harrison DJ, Verpoorte EMJ, Lüdi H, Widmer HM (1992) *J Chromatogr* 593:253
35. Stemme E, Stemme G (1993) *Sens Actuators A*39:159
36. Olsson A, Enoksson P, Stemme G, Stemme E (1995) *Proc Transducers '95*, Stockholm, Sweden, 291
37. Jansen HV, de Boer M, Legtenberg R, Elwenspoek M (1995) *J Micromech Microeng* 9:115
38. van der Schoot BH, Verpoorte EMJ, Jeanneret S, Manz A, Verpoorte NF (1994) *Microsystems for analysis in flowing solutions*. In: *Micro total analysis systems*, Kluwer, Dordrecht, The Netherlands, p 181
39. van der Schoot BH, Jeanneret S, van den Berg A, de Rooij NF (1992) *Sens Actuators*, B6:57
40. Fettingner JC, Manz A, Lüdi H, Widmer HM (1993) *Sens Actuators*, B20: 19
41. Arquint Ph, van den Berg A, van der Schoot BH, de Rooij NF, Bühler H, Morf WE (1993) *Sens Actuators*, B13–14:340
42. Lammerink TSJ, Tas NR, Berenschot JW, Elwenspoek MC, Fluitman JHJ (1995) *Proc MEMS '95*, Amsterdam, The Netherlands, 13
43. Lammerink TSJ, Spiering VL, Elwenspoek M, Fluitman JHJ, van den Berg A (1996) *Proc MEMS*, San Diego, USA, 389
44. van der Schoot BH, Verpoorte EMJ, Jeanneret S, Manz A, de Rooij NF (1994) *Micro total analysis systems*, van den Berg A, Bergveld P (eds.), Kluwer Academic Publishers, Dordrecht, The Netherlands, 181
45. van der Schoot BH, Jeanneret S, van den Berg A, de Rooij NF (1993) *Anal Meth Instr* 1(1): 38
46. Gumbrecht W, Abraham-Fuchs K (1996) *Proc Eurosens X*, Leuven, Belgium, 777
47. Gumbrecht W, Peters D, Scheller W, Erhardt W, Henke J, Steil J, Sykora U (1994) *Sens Actuators* B18–19:704
48. Walther I, van der Schoot BH, Jeanneret S, Arquint Ph, de Rooij NF, Gass V, Bechler B, Lorenzi G, Cogoli A (1994) *J Biotechnol* 38:21
49. Effenhauser CS, Manz A, Widmer HM (1995) *Anal Chem* 67:2284
50. Jakobson SC, Hergenröder R, Koutny LB, Ramsey JM (1994) *Anal Chem* 66:1114
51. Effenhauser CS, Bruin GJM, Paulus A, Ehrat M (1996) *Anal Meth Instr Spec Issue μ TAS '96*: 124
52. Northrup MA, Beeman B, Hadley D, Landre P, Lehew S (1996) *Anal Meth Instr Spec Issue μ TAS '96*:153
53. Woudenberg TM, Winn-Deen ES, Albin M (1996) *Anal Meth Instr Spec Issue μ TAS '96*:55

Integrated Chip-Based Microcolumn Separation Systems

Carlo S. Effenhauser

Novartis Pharma AG, Bioanalytical Research, K-127.1.84, CH-4002 Basel, Switzerland

E-mail: Carlo_Stefan.Effenhauser@pharma.novartis.com

The prospects of inexpensive mass production of integrated chemical separation systems with superior analytical performance through modern microfabrication technology has stimulated considerable research activity over the past five years. In addition, these devices hold the promise of being extremely rugged, capable of analysis of very small sample volumes, and suitable for high-throughput analysis through parallel sample processing. The goal of the present article is to review major recent accomplishments in this rapidly advancing field. Since most research efforts up to now have been devoted to electric field driven separation systems, in particular to chip-based capillary electrophoresis, emphasis will be laid on the discussion of the physical-chemical basis of the operation and optimization of these devices.

Keywords: Miniaturization, integration, microcolumn separations, capillary electrophoresis.

1	Introduction	52
2	Miniaturization and Chip-Based Integration	53
3	Capillary Electrophoresis and Related Applications	57
3.1	General Aspects	57
3.1.1	Optimization of Efficiency and Separation Speed	58
3.1.2	Electrokinetic Fluid Handling	60
3.1.3	Sample Injection	63
3.2	Electrophoretic Separations	65
3.2.1	Separations in Free Buffer Solution	65
3.2.2	Separations in Polymer Sieving Media	66
3.2.3	Integrated Precolumn Reactors	69
3.2.4	Integrated Postcolumn Reactors	70
3.2.5	Synchronized Cyclic Capillary Electrophoresis	73
3.3	Electric Field Driven Chromatography	74
3.4	Other Recent Developments	75
4	Free Flow Electrophoresis	76
5	Liquid Chromatography	78
6	Conclusions and Outlook	79
7	References	80

1 Introduction

The exploitation of modern micromechanical fabrication technology for analytical chemical applications has recently created a rapidly advancing interdisciplinary field of research. The separation or fractionation of sample components generally represents an essential step in the sequence of laboratory operations that ultimately generates chemical information (identity and quantity of the constituents of interest), as a look in a modern analytical laboratory readily confirms. Based on a thorough analysis of the physical-chemical basis of the separation mechanisms, the improvement in analytical performance to be gained from miniaturization have been known for quite some time (see [1]). This knowledge has lead to the development of small-diameter packing materials and open-tubular microcolumn separation techniques such as capillary gas chromatography [2], microbore HPLC [3–6] or capillary electrophoresis (CE) [7–9].

In particular, CE has already set new standards in analytical chemistry with regard to separation speed, resolution power and consumption of buffer and sample, even though commercial instruments have not been available before 1988. Column diameters typically range between 25 and 100 μm , a feature size that is conveniently accessible by micromachining technology. It is therefore hardly surprising that the development of micromachined chemical separation systems has been intensively pursued over the past few years, with the earliest roots in capillary gas chromatography dating back to 1975 [10, 11].

However, microfabrication technology has more to offer to the field of analytical science than just a convenient way to manufacture small-bore separation columns. Networks of coupled channels including features such as frits, mixing chambers, flow restrictors, reagent compartments, etc. of virtually any shape can be produced as simple as a single straight channel with negligible additional costs. Therefore, operational functionality, such as integrated sample injectors or on-line modification or synthesis of compounds, can be incorporated in these devices. Most important, this can be done without introducing significant dead volumes into the system, which would be detrimental for the precise handling of pico- to nanoliter sample volumes.

Integration and miniaturization represent of course very general concepts applicable to many aspects of analytical instrumentation (e.g., integrated light sources, detectors, electrodes, electronics for data acquisition and data processing, etc.). The overwhelming success of microfabrication technology in electronics holds the promise that a similar revolutionary approach might be possible for the generation of chemical information. In its ultimate consequence, this route might lead to a so-called “miniaturized total analysis system” (μTAS) or a “lab-on-chip”, where all necessary analysis steps such as sample pretreatment, chemical modification, separation, and detection are carried out in a highly integrated, most desirably monolithic device. This would allow to use these units for on-line and at-site monitoring in a sensor-like manner as presented in detail by Manz et al. [12–16].

The focus of the present chapter is limited to review major accomplishments with “partially” integrated microcolumn separation systems that have been achieved in the last five years. “Partial” integration here refers in most cases to the fluidic part of the system which consists for example of a network of interconnected microchannels. The examples chosen have all been developed at least to the level of functional models and demonstrate principal feasibility. Many aspects of great importance in this context, such as chip fabrication, detection issues, higher levels of functional integration, etc., will be discussed in chap. 1 and 2 of this volume.

2 Miniaturization and Chip-Based Integration

As already mentioned, the concepts of integration and miniaturization are not new in separation science, but the tools at our disposal for the realization of such systems have changed dramatically with the advent of micromechanical fabrication methods. The advantages of this technology are best appreciated by a closer look at earlier attempts to construct integrated small volume analysis systems using “conventional” techniques.

The innovative thermostated separation system published by de Bokx et al. [17] represents an interesting example and comprises a capillary cross intersection for sample injection and a 100 pl fluorescence detector cell based on fiber optics. This apparatus shows basically all features that are required to perform automated fast and efficient electrophoretic separations and has been used to separate a mixture of laser dyes in 35 seconds with moderate efficiency. However, in order to keep all dead volumes at the junctions sufficiently small, the connections had to be done by tedious laser-based drilling of holes through the capillary walls. A similar approach to interconnect capillaries was described for a postcolumn derivatization reactor for CE [18], and many more inventive capillary coupling devices have been designed.

Microfabrication technology offers a much more elegant, precise, and inexpensive (if produced in large numbers) route for the manufacturing of such interconnected systems of microchannels. Figure 1 shows an electron micrograph of an arrangement of channels forming a sample injector for capillary electrophoresis. The microchannels were etched into a glass plate after photolithographic pattern transfer [19]. The intersections are virtually free of void volumes, and the whole arrangement is very rugged due to its monolithic integration into a single chip of glass.

A closer look at the functional models developed so far reveals that the aspect of integration plays a more prominent role than the sheer miniaturization of the characteristic dimensions involved. This is in contrast to the common misconception that micromechanical fabrication techniques result in a dramatic reduction of the physical size of the devices. Although there exist impressive examples of relatively long separation columns folded on a device of a few cm² and below, at the present state of development, the outer dimensions are usually dictated by the constraints of interfacing the chip to the “outside” world (sample, buffer solutions, reagents, etc.).

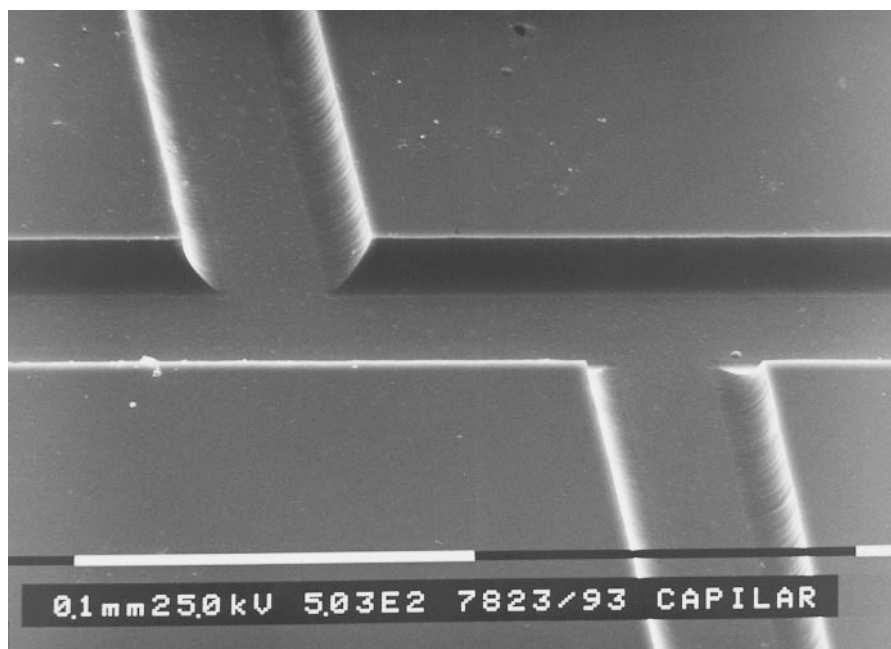


Fig. 1. Electron micrograph of electrophoresis channels formed into a glass substrate by photolithography and wet chemical etching. Channel dimensions: width: 50 μm , depth: 12 μm (reprinted with permission from [19]. Copyright 1993 American Chemical Society)

The main incentives of chip-based integrated chemical separation systems can be summarized as follows:

1. Reduced consumption of sample, reagents, and mobile phase
2. Improved analytical performance in terms of resolution power per time unit
3. Multifunctional, interconnected channel networks with negligible dead volumes
4. Fabrication of arrays of many parallel systems
5. Increased mechanical stability due to monolithic integration
6. Suitability for inexpensive mass fabrication

The first two points represent a general motivation for miniaturization in separation science independent of the actual fabrication technology. The benefit of a reduction of the consumption of sample, reagents, and mobile phase in chemical and biochemical analysis is self-evident and does not need to be discussed further (reduced consumption of precious samples and reagents, reduced amounts of waste, environmental aspects). This advantage is, however, sharply contrasted by its severe implications on the detection side, as discussed elsewhere in this volume in detail. The detection of the separated zones of very small sample volumes critically depends on the availability of highly sensitive detection methods. It is not surprising that extremely sensitive laser-induced-fluorescence (LIF) has been the mostly used detection principle for chip-based separation systems so far.

The effects of miniaturization on the performance of an analytical separation system are often discussed in terms of a reduction of a characteristic length parameter (e.g., column diameter d_c or particle diameter d_p) and the associated consequences for lateral zone dispersion processes and their interplay with longitudinal (axial) zone dispersion. A rigid discussion of the physical-chemical basis is beyond the scope of this chapter. For a general account in terms of scaling laws and proportionality considerations, the reader is referred to the references [12, 14]. A comprehensive and detailed description with emphasis on the underlying physical-chemical processes can be found in the book by Giddings [20].

Poppe has recently summarized the most essential factors in a concise and lucid manner [21]. His reasoning is applicable to a wide range of separation techniques provided that zone dispersion due to lateral non-equilibrium is understood in a very broad sense that includes, for instance, lateral concentration gradients of various origins (e.g., owing to size exclusion effects, partitioning between different phases, external gradients, etc.) and lateral differences in local flow velocities. These lateral non-equilibria can be described by characteristic relaxation time constants τ that measure how long it takes to establish lateral equilibrium. From a molecular point of view, they can also be interpreted as a measure of how long it takes for a molecule to “sample” all the various lateral regions in the system under consideration. The parameter τ is fundamentally related to characteristic size measures d of the system (layer thickness, particle diameter, column diameter, etc.) through a diffusion Eq. of the form:

$$\tau = \gamma \frac{d^2}{D} \quad (1)$$

where D is the diffusion coefficient and γ stands for a numerical factor depending on the geometry of the process considered.

The major reason why a reduction of the particle size or column diameter is expected to lead to an increase of “separation speed” (resolution power per time unit) can be found in its effect to decrease τ . Separation speed is often expressed in the analytical literature in terms of the number of theoretical plates N per time unit t (for a definition of N in terms of experimental parameters see Sect. 3.1.1). For zone dispersion due to lateral non-equilibrium, the ratio N/t will be in general inversely proportional to τ [20]:

$$\frac{N}{t} \sim \tau^{-1} \sim \frac{D}{d^2} \quad (2)$$

Consequently, if a given separation problem requires the generation of a certain number of theoretical plates, the analysis time can be reduced by lowering τ according to Eq. 1. For a given fixed value of d , τ is ultimately limited by the magnitude of the diffusion coefficient. In general, however, τ can be strongly reduced by decreasing the characteristic size measure d . If longitudinal diffusion is also taken into account, a more detailed analysis shows that the

optimum linear flow velocity that leads to an optimum separation efficiency is proportional to the ratio D/d [20]:

$$v \sim \frac{D}{d}. \quad (3)$$

As d is reduced, the linear flow velocity has to be increasingly higher in order to take full advantage of miniaturization according to Eqs. 1 and 2. In liquid chromatography, the mobile phase velocity required by Eq. 3 is limited by the maximum pressure that can be applied to the separation column, thus imposing an instrumental limit to the gain that can be achieved by miniaturization. In CE, the discussion of separation performance indices is strongly facilitated by the absence of a stationary phase. Lateral non-equilibrium in CE is usually dominated by the formation of thermal gradients in the capillary, which can be remedied by decreasing the cross section of the column (see Sect. 3.1.1).

The third point listed above is of utmost importance if the theoretically expected improvement in separation performance should be exploitable with a real instrument. Apart from the inherent contribution of the separation column itself (variance σ_{col}^2), overall band broadening (σ^2) is also caused by the sample injector (σ_{inj}^2), the finite length of the detection volume (σ_{det}^2), and by any contributions of dead volumes (σ_{dv}^2) due to fittings etc. (see for example [22]):

$$\sigma^2 = \sigma_{\text{col}}^2 + \sigma_{\text{inj}}^2 + \sigma_{\text{det}}^2 + \sigma_{\text{dv}}^2 = \sigma_{\text{col}}^2 + \sigma_{\text{excol}}^2 \quad (4)$$

Clearly, any reduction in σ_{col}^2 will only be useful if all other contributions σ_{excol}^2 can also be kept low enough *relation to it*. For example, although sample plugs of only 150 μm length were used in the first demonstration of microchip gel electrophoresis with 3.8 cm separation length, yet about 50% of band broadening was found to be caused by sample injection [23]. Thus, small sample volumes need to be injected, detection has to be carried out in small detection volumes, and all void volumes spoiling the gain from miniaturization must be avoided. Of course, the time response of the detection electronics and data acquisition system has to be fast enough in order to avoid additional dispersion of the detected signal. The necessity of handling very small volumes in the femto- to nanoliter range, although a prerequisite for special applications as for example the analysis of single cells (see for example Ref. [24]), is therefore in many cases simply enforced by the desired analytical performance, which requires small bore separation columns of short length.

The aspect of minimization of all void volumes is particularly important on a micrometer length scale since diffusion then becomes a very fast and dominating mixing process. Any small void volumes will act as efficient “mixing chambers”. For a typical diffusion coefficient of a small ion in solution ($D=10^{-5} \text{ cm}^2/\text{s}$), diffusion over a distance of 10 μm will take place in approximately 100 ms; over a distance of 1 μm only 1 ms is required. Any concentration gradients present on this length scale will be very readily leveled out, i.e. void volumes will be filled. The virtues of microfabrication for the production of virtually dead volume free interconnections can hardly be overestimated. It

should be noted that even a fairly low dead volume (from the separation science point of view) of only 1 femtoliter corresponds to the volume of a cube with 1 μm edge length. Features of this size are considered significant from the standpoint of microfabrication and are easily within the scope of standard photolithographic resolution.

The potential of planar fabrication technology for the batch production of arrays with many integrated units has been convincingly demonstrated by the microelectronics industry. Parallel analysis systems provide a route to high throughput analysis, which is mandatory for many modern developments in the life sciences, as e.g. high throughput screening of combinatorial libraries or high speed sequencing of DNA. The extreme mechanical ruggedness of monolithically integrated columns and the low fabrication costs are self-evident and reflect the origin of this technology for the production of microelectronic components.

3 Capillary Electrophoresis and Related Applications

3.1

General Aspects

Originally pioneered by Harrison and Manz between 1990 and 1991 [25, 26], the development of chip-based integrated CE systems with electrokinetic fluid handling has received ever increasing interest over the past five years. This branch of microfabricated microcolumn separation systems is arguably the most rapidly advancing one and the area where the most spectacular results have been accomplished [27]. The reasons for this can be partly found in the inherent simplicity of the fabrication, operation and control of these devices.

The early phase of development can be characterized by a transfer of concepts from "conventional" CE to the planar format, such as capillary gel electrophoresis, micellar electrokinetic chromatography, sample stacking and pre- and postcolumn sample derivatization. Emphasis was laid on the demonstration of the specific advantages mainly from the separation science point of view. With only very few exceptions, detection has received much less attention yet. LIF detection with confocal imaging has been used in most of the early work owing to its high sensitivity and its relatively easy implementation. If not explicitly mentioned otherwise, all experiments described in the following sections were carried out with LIF detection [28, 29].

As far as substrate materials are concerned, glass and more recently quartz have been predominantly employed. The reasons for this include:

1. micromachining techniques for glass and quartz are well established,
2. the general optical, electrical and chemical properties are favorable and
3. there exists a variety of surface modification methods that can be easily transferred from conventional CE to planar chips.

The devices are usually fabricated by photolithographic pattern transfer followed by a wet chemical etching step (see for example [25, 30, 31] for ex-

perimental details). The channel system is then sealed by thermally bonding of a cover plate to the structured substrate. The cover plate contains reservoir holes which provide access to the channels. In the case of glass, annealing temperatures between 500 and 600 °C usually have to be used for several hours, whereas quartz devices have been bonded at temperatures as high as 1100 °C [32, 33].

Silicon devices covered with insulating layers of thermal oxide and CVD nitride have been shown to suffer from breakdown problems which limit the applicable voltages [34]. For that reason, very few experimental studies on high-speed CE (requiring high field strengths) have appeared in the literature where silicon substrates were used, in contrast to its successful use in other separation techniques as discussed in Sects. 4 and 5.

Only very few studies with alternative materials and fabrication methods have been published. Ekström et al. [35] demonstrated the feasibility of structuring inexpensive polymeric materials by means of a microfabricated master for the production of microchannel systems. The structured polymer film was mechanically clamped between two glass plates to form a closed channel system. Recently, a similar route for the fabrication of microchannel chips that relies on casting of an elastomeric polymer material against a microfabricated master has been presented by Effenhauser et al. [36] (see Sect. 3.4).

3.1.1

Optimization of Efficiency and Separation Speed

Longitudinal diffusion caused by concentration gradients in the capillary (sample plug) will be an omnipresent source of band broadening in CE, even if zone dispersion due to lateral non-equilibrium were completely absent. Furthermore, some extra-column band broadening due to sample injection and detection will always have to be accepted in a real instrument. In this section, the optimization of separation speed and efficiency in CE will be discussed under the assumption that zone dispersion is governed by these three unavoidable sources of band broadening [19]. As already mentioned, lateral non-equilibrium in CE is in many cases dominated by Joule heating of the buffer solution, therefore some relevant aspects of heat dissipation in capillaries will also be discussed here.

The analysis time t in CE is determined by the migration time of the slowest detectable sample constituent i and can be calculated from

$$t = \frac{L}{\mu_i E} = \frac{L^2}{\mu_i V_{\text{sep}}} \quad (5)$$

where L denotes the distance between injection and detection, μ_i the (vector-) sum of the electroosmotic and the electrophoretic mobility of component i , E the absolute value of the electric field strength and V_{sep} the potential drop across L . The most commonly used measures for the efficiency of a sample separation method is either the number of theoretical plates N or the plate height H (more

accurate: height equivalent to a theoretical plate, HETP) respectively, which can be defined as:

$$N = \frac{L^2}{\sigma^2} \quad \text{and} \quad H = \frac{L}{N} = \frac{\sigma^2}{L} \quad (6)$$

Since the variance contributions σ^2 (in length units) of longitudinal diffusion, injection, and detection are not correlated, their variances can be added

$$\sigma^2 = \sigma_{\text{diff}}^2 + \sigma_{\text{inj}}^2 + \sigma_{\text{det}}^2 = 2D_i t + \sigma_{\text{excol}}^2 \quad (7)$$

The molecular diffusion coefficient of the component i is denoted D_i . In this scenario, the corresponding upper limit of N is then given by

$$N_{\text{max}} = \frac{L^2}{\sigma^2} = \left(\frac{2D_i}{\mu_i V} + \frac{\sigma_{\text{excol}}^2}{L^2} \right)^{-1} \quad (8)$$

High plate numbers require the application of high voltages while keeping $\sigma_{\text{excol}}^2/L^2$ as low as possible. It is interesting to note that N depends only on the absolute voltage applied and not on the field strength. Furthermore, since both μ_i and D_i are inversely proportional to the friction coefficient f in the buffer solution [20], N will in general not depend on f .

If, however, efficiency and analysis time are to be optimized at the same time, a different outcome is obtained. As already mentioned above, separation speed is often expressed as the ratio N/t (the rate of “generation of theoretical plates”) and can be calculated by combining Eqs. 5 and 8

$$\left(\frac{N}{t} \right)_{\text{max}} = \frac{\mu_i^2 E^2}{2D_i + \mu_i E \frac{\sigma_{\text{excol}}^2}{L}} = \frac{\mu_i^2 E^2}{2D_i + \mu_i E H_{\text{excol}}} \quad (9)$$

In contrast to N , N/t does not depend on the separation voltage but rather on voltage gradient E . Maximum separation speed can be obtained by application of the highest possible field strength while keeping the plate height due to extra-column band broadening $H_{\text{excol}} = \sigma_{\text{excol}}^2/L$ as low as possible. Note that N/t is inversely proportional to the friction coefficient f in the separation medium [20].

In practical applications, Joule heating imposes an upper limit on the maximum field strength. The heat W generated per time unit and unit volume V in an electrolyte of a electrical conductivity κ is given by:

$$\left(\frac{W}{V} \right) = \kappa(T) E^2 \quad (10)$$

and increases with the square of the electrical field strength. Since the heat is generated uniformly in the electrolyte volume, but can be dissipated only across

the confining boundaries of the electrophoresis compartment, increasing the surface-to-volume ratio provides the major route to improve heat dissipation. Originally, this has been a major motivation for the development of narrow tube electrophoresis and was proposed by Tiselius in 1937 [37]. Apart from a general rise in temperature, Joule heating leads in the case of cylindrical capillaries to the formation a parabolically shaped temperature profile [38–40]. If the applied electric field exceeds a certain limit, this profile becomes a major source of band broadening and causes severe deterioration of the separation efficiency. The general physical-chemical mechanisms leading to band broadening have been discussed in detail by several authors (see for example [41]).

In contrast, microfabricated microchannels in general exhibit more or less rectangular shaped cross sections depending on the fabrication process. The advantage of rectangular channels with respect to heat dissipation are obvious (even better surface-to-volume ratio) [37, 42].

In 1989, Jansson et al. [43] theoretically modeled the performance of electro-driven separation systems in rectangular conduits etched into bulk silicon substrates and proposed their fabrication. As it turned out, however, the additional advantage of a 100-fold higher thermal conductivity of silicon compared to glass or quartz is opposed by dielectric breakdown problems, thus again imposing a limit to E [34]. The thermal properties of thin-walled rectangular capillaries were recently reinvestigated by Cifuentes et al. [44–46]. If cylindrical and rectangular columns of equal cross sections are compared, the latter clearly show improved thermal properties (lower temperature rise, smaller temperature gradients across the column). This improvement gets more pronounced with increasing aspect ratio (width-to-height ratio) of the channel [44], favoring thin and wide separation beds.

A systematic study of microchannel heat dissipation in bulk planar substrates with a thickness in the order of a few mm has not been published yet, but a simple extrapolation of the underlying physics would indicate that the temperature gradients will be low in these channels as well. Using low conductivity buffer solutions, efficient separations at field strengths of up to 2500 V/cm have been demonstrated with these devices [23, 30].

The conductivity of the buffer solution is, however, also of great relevance in this context (Eq. 10) and capillaries of very small diameter with very efficient heat dissipation are commercially available. Using well designed buffer solutions and conventional 50 μm capillaries, fast protein separations at 2000 V/cm have been described by Hjerten et al. [47]. Using a laser photolysis based gating technique, the group of Jorgenson has reported extremely fast CE separations on a subsecond timescale at up to 2500 V/cm in a 6 μm and at 3300 V/cm in a 10 μm inner diameter capillary respectively [48, 49].

3.1.2

Electrokinetic Fluid Handling

In the present context, the term electrokinetic effects is used to cover both electrophoretic and electroosmotic phenomena, which are often inseparably super-

imposed on each other. In contrast to electrophoresis, electroosmosis is a macroscopic phenomenon that relies on the existence of immobilized surface charge at the channel walls when in contact with an electrolyte solution. This charge can be due either to ionizable groups (e.g., silanol groups in the case of glass or quartz capillaries) or can be caused by adsorbed charged species from the buffer. As a result, a thin electric double layer of opposite charged mobile ions (typical thickness κ^{-1} : 10–100 nm) is formed with an associated difference of the electrical potential (“ ζ -potential”) with respect to the bulk buffer solution. Application of an external electric field in axial direction exerts a force on this thin fluid layer where a net charge density exists, and by momentum transfer to adjacent fluid layers (viscous forces), the whole fluid in the capillary will be dragged along. According to numerical simulations by Dose and Guiochon [50], the formation of a steady-state flow profile in general takes place on a 100 μ s time scale. The flow induced by this remarkable phenomenon exhibits a number of very useful features [51, 52]:

1. The average flow velocity is independent of the channel width and geometry over a wide range of dimensions (roughly 10^0 – 10^3 μ m).
2. The velocity profile is virtually flat over the cross section of the capillary, thus causing only little zone dispersion. This is valid as long as the condition $\kappa^{-1} \ll d$ is fulfilled [51].
3. The flow velocity is linearly dependent on the electric field strength applied ($v_{eo} = \mu_{eo} \cdot E$, where μ_{eo} denotes the electroosmotic mobility). In glass or fused silica, linear flow velocities of 100 μ m/s to 1 mm/s can be achieved with field strengths in the order of several 100 V/cm. For a typical channel cross section of 10^{-5} cm² (50 \times 20 μ m) this results in corresponding volume flow rates in the order of 100 pl/s to 1 nl/s.

If external potentials are applied to a system of several interconnected channels, the respective field strength in each channel will be determined by Kirchhoff's laws in analogy to an electrical network of resistors [28]. Ideally, electrokinetically driven mass transport in each of the channels will take place according to magnitude and direction of these fields. This allows for complex fluid manipulation operations in the femtoliter to nanoliter range without the need of any active control elements, such as external pumps or valves. This is of particular relevance due to the demanding limitations with respect to void volumes in the system (see Sect. 2).

The characteristics of electrokinetically controlled fluid flow in microchannel manifolds has been studied in a systematic way by Harrison and coworkers [28, 30]. An illustrative demonstration of the potential of this approach is shown in Fig. 2 for the controlled dilution of a fluorescein solution under voltage control. In parallel with a stepwise decrease of the potential applied to the fluorescein reservoir, a decrease of fluorescence signal downstream after the junction is visible in Fig. 2. As long as the ionic strength and pH in each supply channel is the same (same μ_{eo}), mass balance is automatically fulfilled, and the incoming flows at the intersection will be exactly balanced by the outgoing flow of the mixed components (otherwise, mass balance would be enforced by additional hydrodynamic or secondary internal flows). This way of mixing fluids was also

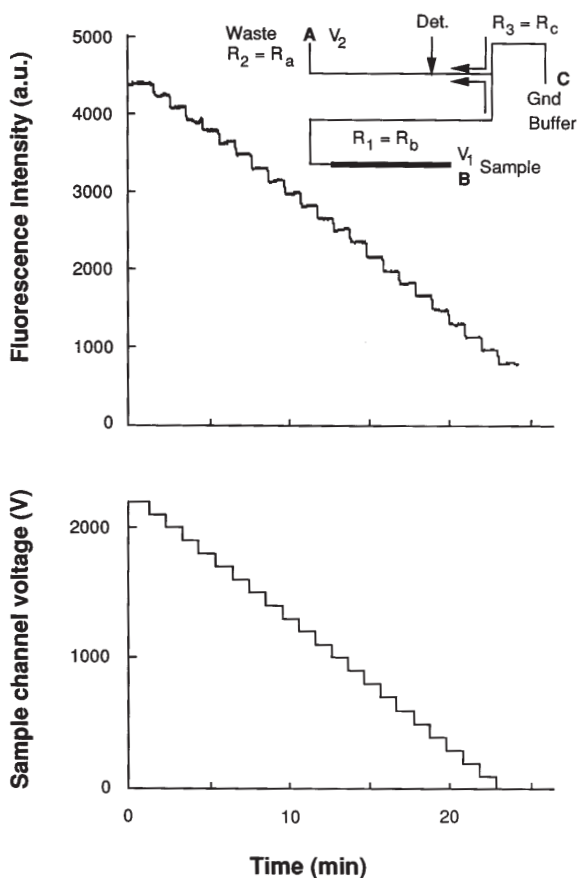


Fig. 2. Fluorescence intensity recorded downstream a T junction after controlled dilution of a fluorescein sample. Dilution is controlled by stepwise reduction of potential V_2 (reprinted with permission from [56]. Copyright 1994 American Chemical Society)

used to perform well controlled chemical reactions on a chip, as for instance with postcolumn sample derivatization for detection purposes [33, 53, 54] (see Sect. 3.2.4).

However, in the same studies, characteristic “leakage” effects at capillary junctions were observed and have been attributed both to hydrodynamic and diffusion effects. For example, a steady flow of buffer in the straight part of a T-junction often induces a small secondary leakage flow from the side channel, although no voltage is applied there (floating potential). Photomicrographs and video imaging were used by several groups for the documentation of these effects [55, 56]. The underlying fluid dynamics is not completely understood yet, and the direction of the secondary flow can be reversed under certain conditions. Numerical simulations of the fluid dynamics at the junction have been carried out very recently and seem to provide better understanding [57]. The

effect disturbs for instance the injection of sample plugs due to a small steady flow of sample into a separation capillary (see Sect. 3.1.3), hence causing a high background signal. However, application of potentials to each of the channels involved can fully suppress this leakage flow, as is described for example in Refs [23, 56, 58, 59].

3.1.3

Sample Injection

A means for sample injection has been the first functionality that was successfully integrated into a planar CE device [19, 25, 27, 30, 56]. The geometrical design used was first proposed by Verheggen et al. and has demonstrated its performance with the injection of microliter sample volumes and sample plug lengths of several cm [60]. A miniaturized and valveless version of this design consists of two closely spaced T-junctions (“double-T injector”) [19] as illustrated in Fig. 3 or, in its most simple version, of a simple channel crossing.

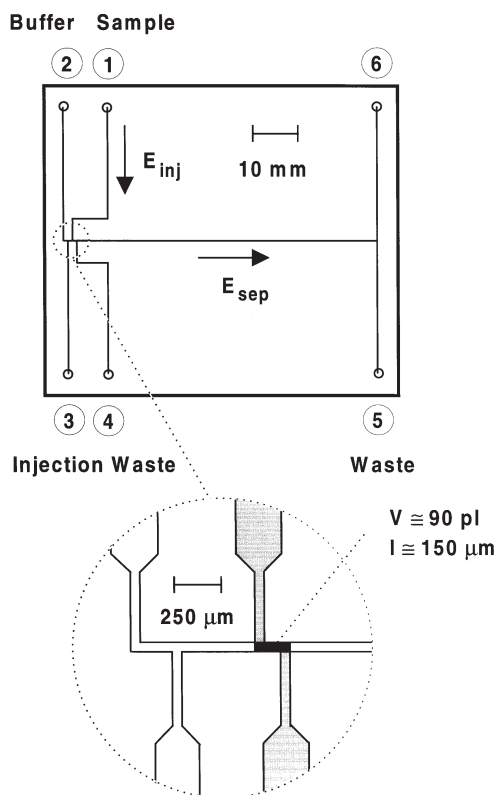


Fig. 3. Layout of a glass chip with integrated sample injection. The *inset* shows details of the channel geometry of the injection region (reprinted with permission from [19]. Copyright 1993 American Chemical Society)

Application of a potential between reservoirs 1 (sample) and 4 (injection waste) electrokinetically pumps sample solution as indicated in Fig. 3. In this way, a geometrically defined 150 μm (90 pl) section of the separation channel can be filled [19]. If the injection potential is applied long enough to ensure that even the slowest sample component has completely filled the injection volume, a representative aliquot of sample can be analyzed (so-called “volume defined” injection). This is in contrast to electrokinetic sample injection in conventional capillaries, which is known to bias the sample according to the respective ionic mobilities [61]. These characteristic differences are shown schematically in Fig. 4. It should be noted that this picoliter sample injector is exclusively controlled by the application of electric fields and does not require any active elements with moving parts such as valves and external pumps. The reproducibility of the peak height of the injected sample plugs has been reported to be within 2 % RSD (relative standard deviation) and less [19, 23].

Leakage from the injection capillaries into the separation channel is often observed after application of the separation voltage. It can be avoided by more sophisticated voltage control protocols during sample injection and separation [23, 56, 58, 59].

A similar volume defined injection protocol where the sample is confined within two controlled side streams of buffer solution has been developed by the group of Ramsey and has been dubbed “pinched injection” scheme [31]. The

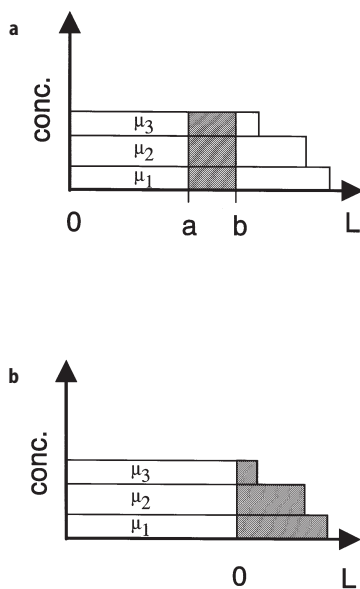


Fig. 4. Schematic representation of electrokinetic sample injection in **a** a volume defined injection scheme (unbiased loading) and **b** conventional CE (biased sample loading). The sample migrates through the injection volume in a way resembling a frontal electropherogram

same group also investigated an injection scheme based on switching of an electrokinetically driven continuous sample flow for a short time (so-called “gated” sample loading) [31]. The performance of both injection techniques was found to be very satisfying, although the latter technique (“gated injection”) again leads to an electrokinetic bias of the sample. The reproducibility of the peak area was found to be around 1–2 % RSD and below.

“Gated” sample injection have also been used in combination with a sample preconcentration technique known as sample stacking. This technique exploits the changes of the ionic migration velocity when crossing a boundary of a discontinuous change of buffer conductivity with an associated step-like change of the electric field strength. Jacobson et al. have shown with fast separations of derivatized amino acids that concentration enhancements up to a factor of 30 can be achieved [62].

3.2

Electrophoretic Separations

3.2.1

Separations in Free Buffer Solution

As has been discussed before, short separation channels in combination with a high electric field strength and minimized extra-column band broadening should result in both fast and efficient electrophoretic separations. Mixtures of fluorescent-labeled (FITC) amino acids were often used as model samples. An example of a high-speed high-resolution separation of a mixture can be found in Fig. 5, which also shows how the separation evolves with increasing migration path [19]. For $L=5$ mm, sample components differing by one unit in effective charge are well separated within 2.5 seconds, and four out of five neutral amino acids with similar effective charges can be resolved. If the separation length is increased to $L=24$ mm, all five neutral amino acids are base-line resolved within 14 seconds [19, 27], and a separation speed index of 8,300 plates/second could be obtained in combination with a corresponding plate height as low as $0.3\text{ }\mu\text{m}$. Other examples of fast separations of amino acids on microchips have been published in Refs. [30, 56].

In the presence of electroosmotic flow, opposite charged dyes can be separated at particularly high separation speed on a time scale of 100 ms generating up to 18,600 theoretical plates/second, as reported by Jacobson et al. [63]. The same group has reported rapid separations of metal ions (Zn^{2+} , Cd^{2+} , Al^{3+}) complexed with a fluorescent quinoline dye on a quartz microchip [32]. Channel walls were coated with polyacrylamide to prevent electroosmotic flow, the separation was achieved in less than 20 s at 870 V/cm and $L=16.5$ mm.

An interesting application of microchip CE is the analysis of serum cortisol immunoassays that have been performed off-chip prior to their injection [64]. Separation and quantitation of the free and bound labeled antigen could be achieved in less than 30 s and allowed the determination of serum cortisol in the clinical range of interest.

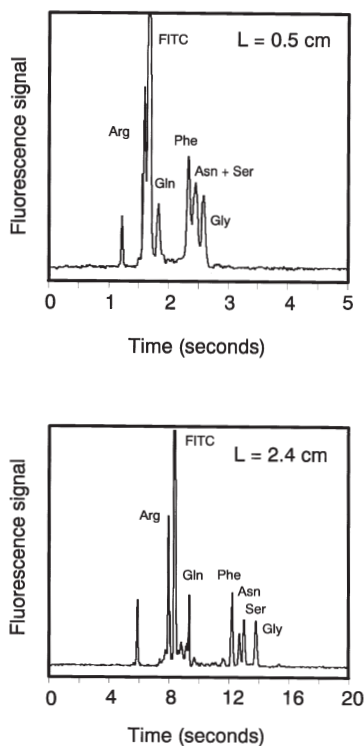


Fig. 5. Electropherograms of a mixture of six FITC labeled amino acids utilizing 5 and 24 mm separation length recorded at 1060 V/cm. Sample was injected and separated on the glass chip depicted in Fig. 3 (reprinted with permission from [19]. Copyright 1993 American Chemical Society)

3.2.2

Separations in Polymer Sieving Media

Today, the majority of electrophoretic separations is performed using polyacrylamide or agarose gels with biopolymer samples. Therefore, in order to widen the range of microchip CE to this central area of bioanalytics, transfer of gel electrophoresis protocols has been investigated very early in the development of microfabricated chemical analysis systems. The first application was described by Effenhauser et al. [23], who used a microchannel system filled with non-cross linked 10% T polyacrylamide for the size separation of phosphorothioate oligonucleotides ranging from 10 to 25 bases in length. A high field strength of 2300 V/cm was employed, resulting in rapid size separation in less than 45 seconds with 0.2 μm plate height as depicted in Fig. 6. Chemical modification of the channel walls was found to be not necessary. As it turned out, resolution was limited in this study by the length of the injected sample plug of 150 μm (separation length: 3.8 cm). In a follow-up study, a longer separation length diminished the relative band broadening contribution of the injected

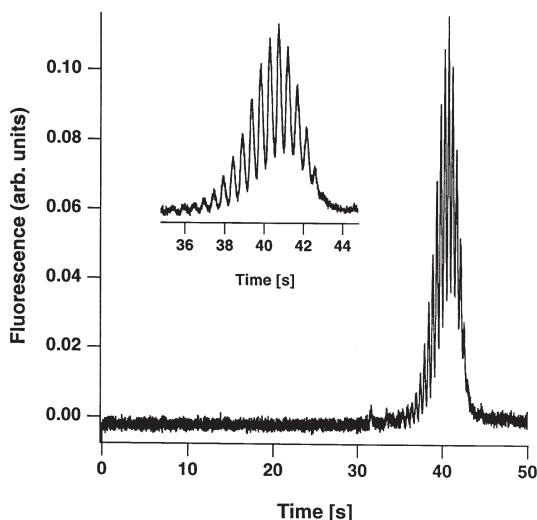


Fig. 6. Electropherogram of fluorescein labeled phosphorothioate oligonucleotides (PS pd (T)_{10–25}) recorded in 10% T, 0% C polyacrylamide matrix at 2000 V/cm, L=38 mm (reprinted with permission from [23]. Copyright 1994 American Chemical Society).

sample plug and lead to baseline resolution of the same sample [65]. The actual aim of this work was the isolation of fractions of single oligonucleotides by electrokinetic manipulation, and was achieved by automated switching of voltages at a T-junction after separation. The voltage switching protocol is shown schematically in Fig. 7. The result of the isolation of a single oligonucleotide (18-mer) is also shown in Fig. 7.

Woolley and Mathies were the first to demonstrate the separation of longer double stranded DNA (ϕ X 174 HAE III restriction fragments) on CE chips [29]. In this study, an entangled hydroxyethylcellulose solution was used as a sieving matrix. The DNA sample was on-column labeled for fluorescence detection by adding an intercalating dye to the buffer solution. Separations of the DNA fragments (with good 271/281 bp fragment resolution) were achieved in 120 seconds with 3.5 cm separation length. The influence of the field strength and the width of the separation and injection channels on the separation efficiency was studied in a systematic manner by fabrication of 15 different width combinations on a single device.

The same authors have exploited the unique combination of speed and resolution for DNA sequencing on a chip, a key application in modern molecular biology. The chip was completely filled with a 9% T, 0% C polyacrylamide sieving medium [66]. Sequencing was performed in a four color labeling and fluorescence detection format. By using a separation distance of 3.5 cm, sequencing resolution of up to ~200 bases could be obtained in less than 10 minutes with 97% accuracy (Fig. 8). Resolution was limited by the length of the injected sample plug, and could be improved to 500 bases by using an optimized chip layout in combination with an optimized sieving matrix.

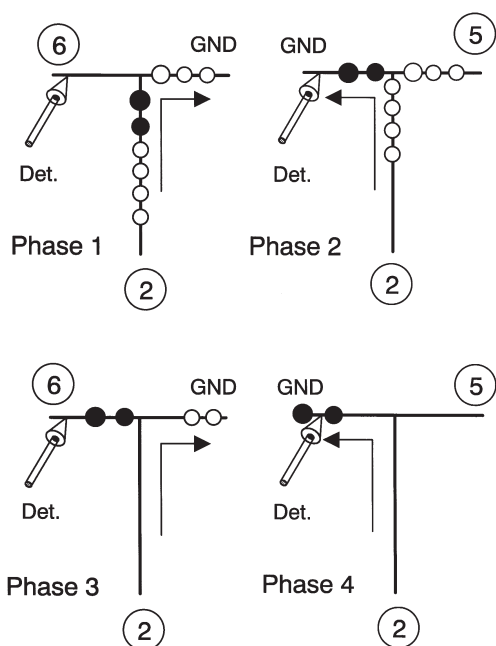


Fig. 7a. Voltage switching protocol for the electric field controlled withdrawal of preselected sample zones at a T-intersection. The same sample used in Fig. 8 was base line separated prior to fraction isolation at 1130 V/cm

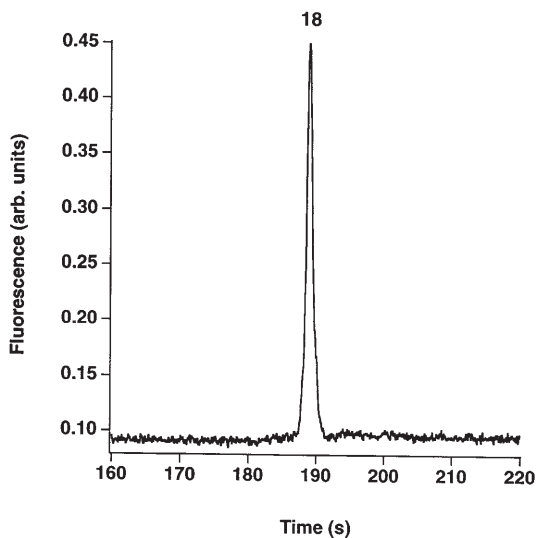


Fig. 7b. Result of the withdrawal of a single oligo (PS pd(T)₁₈) (reprinted with permission from [65]. Copyright 1995 American Chemical Society)

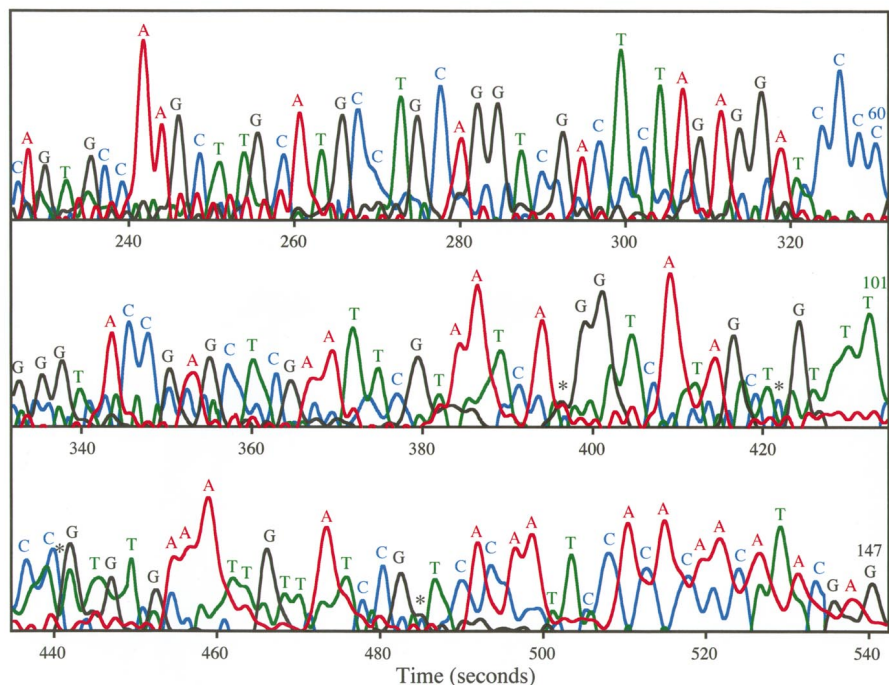


Fig. 8. Analyzed four-color DNA sequencing data (M13mp 18) recorded on a CE chip in a 9% T, 0% C polyacrylamide matrix at 200 V/cm, L=35 mm. Blue: C; green: T; black: G; red: A. (reprinted with permission from [66]. Copyright 1995 American Chemical Society)

3.2.3

Integrated Precolumn Reactors

A variety of pre- and postcolumn sample derivatization schemes has been developed in CE, mainly for the attachment of fluorescent labels for detection purposes. Precolumn sample modification is usually less demanding than postcolumn reactions for reasons discussed in Sect. 3.2.4.

A chip-based integrated precolumn microreactor with 1 nl reaction volume has been explored by Jacobson et al. [67]. The reactor is operated in a continuous manner by electrokinetically mixing of sample (amino acids) and reagent (*o*-phthaldialdehyde) streams. The reaction time is adjusted via the respective flow velocities. By switching of potentials, small plugs of the reaction product were injected into a 15.4 mm separation channel in a “gated” injection scheme (<1.8% RSD in peak area). The separation efficiency achieved was relatively poor, however, electrokinetic control of reaction time (and yield) permitted to monitor the kinetics of the derivatization under pseudo first-order conditions. A similar integrated precolumn reactor operated in a stopped flow mode has been described by Harrison et al. [68].

Another interesting application of an integrated precolumn microreactor with a volume of 0.7 nl is the on-chip digestion of plasmid DNA (pBR322) with

an restriction enzyme (*HinfI*) [69]. The operation procedure is similar to the one described above, apart from the fact that the digestion reaction was carried out either in a continuous flow or a stopped flow mode. Subsequent fast size analysis of the digested DNA fragments was performed with a 1% hydroxyethyl cellulose sieving matrix. The double stranded DNA was labeled on the separation channel by the counterpropagating (positively charged) intercalating dye TOTO-1 and detected by means of LIF. The electropherogram of the fast size separation of the digested DNA fragments is shown in Fig. 9.

Very recently, the coupling of a PCR (polymerase chain reaction) reaction chamber with microchip electrophoresis has been published by Woolley et al. [70]. This instrument can be regarded as a special case of a precolumn sample modification system, although integration is not used here in the sense of monolithic integration as in the examples discussed before. The silicon-based micro PCR reactor (20 μ l) was glued into one of the reservoir holes of the cover plate of a glass CE chip, and served as a “special” sample reservoir. The contents of the PCR reactor was periodically injected into the separation channel and electrophoretically analyzed. In this way, the course of the PCR amplification of a 268 bp β -globin target could be monitored through the determination of the peak area. The product was analyzed in a 0.7% hydroxyethyl cellulose buffer solution. PCR amplification (30 cycles) and the electrophoretic analysis of the sample was done in less than 20 minutes.

3.2.4

Integrated Postcolumn Reactors

Postcolumn derivatization schemes for detection purposes offer a number of advantages over precolumn labeling, such as the avoidance of multiple labeled products with associated differences in migration times (proteins, peptides) and less stringent demands on reaction product stability. On the other hand, apart from the limited number of appropriate reagents with high absorption at the excitation wavelength, high fluorescence quantum yield, low background fluorescence and sufficiently fast reaction kinetics, it is obvious that a compromise has to be found between intimate mixing of the reaction partners on one side (fast kinetics, high product yield) and conservation of the separation efficiency on the other side. In general, this requires a very high degree of control for the mixing of two fluids. A variety of innovative mixing devices has been developed based on conventional plumbing of capillaries, however, all these designs suffer more or less from the complicated fabrication of the capillary junction and from dead volume constraints as discussed in Sect. 2. Chip-based integration of such a mixing device would clearly offer essential advantages in this respect.

The first experimental demonstration of such a device has been published by Jacobson et al. [53]. Amino acids were injected by a “gated” injection scheme, separated in a 7 mm channel and subsequently labeled by controlled mixing with an *o*-phthaldialdehyde reagent solution at a T-intersection. The separation efficiency achieved, however, was relatively poor and the inadequate kinetics of the labeling reaction caused significant band broadening.

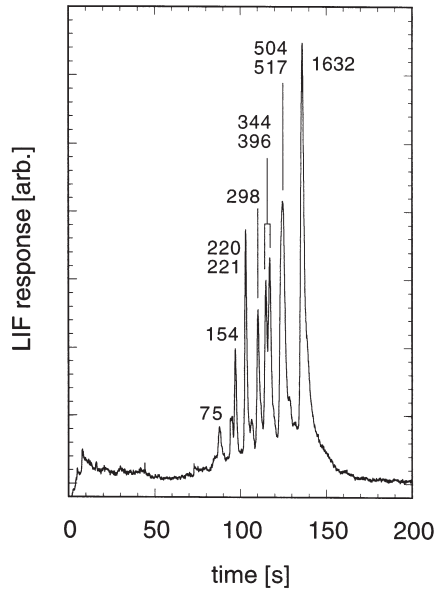
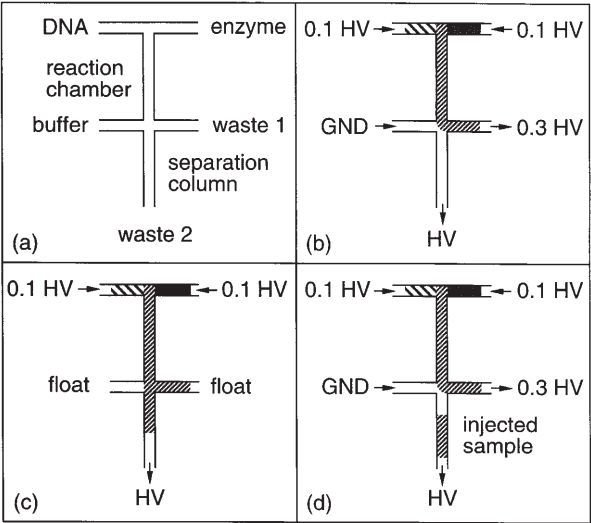


Fig.9. *Upper* – Schematic of the electric field controlled enzymatic digestion of DNA in a manifold of microchannels: **a** principal arrangement, **b** loading of DNA and enzyme, **c** injection of the digested products, **d** separation of the fragments.
Lower – Electropherogram of the digested products (pBR322 digested with the enzyme *Hinfl*) recorded at 380 V/cm, L=67 mm (reprinted with permission from [69]. Copyright 1996 American Chemical Society)

Recently, Fluri et al. [33] have presented optimized chip designs with a very high operation performance due to improved mixing through diffusion. Using the same labeling chemistry as mentioned above, on-chip postcolumn reactions were carried out with only 10% degradation in separation efficiency, permitting fast separations on a time scale of seconds with 0.5 μm plate height (Fig. 10). Postcolumn labeling and detection of bovine serum albumin (BSA) was also demonstrated by these authors.

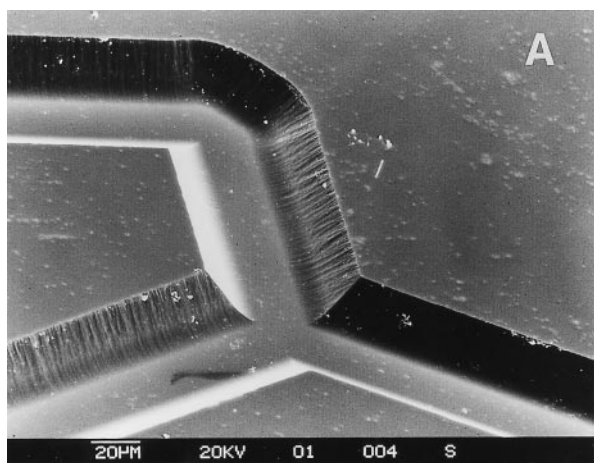


Fig. 10 a. Electron micrograph of an optimized mixing junction for postcolumn reactions microfabricated into a quartz substrate

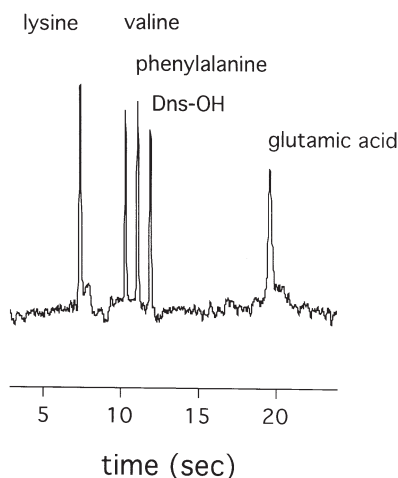


Fig. 10 b. Electropherogram of amino acids and hydrolyzed dansyl chloride with postcolumn derivatization using the reactor shown above (reprinted with permission from [33]. Copyright 1996 American Chemical Society)

3.2.5

Synchronized Cyclic Capillary Electrophoresis

A novel electrophoretic separation concept based on repeated column switching has been achieved by Burggraf et al. [58, 71–73]. Since the column switching procedure is synchronized to one or several analytes of interest, the method has been dubbed “synchronized cyclic capillary electrophoresis” (SCCE). The principle is shown in Fig. 11. Sample injection is performed according to a volume defined injection scheme as described in Sect. 3.1.3. Periodically repeated application of voltages cycles the sample around a system of channels arranged in a square, and permits to employ a separation channel of virtually “infinite” length. The field switching period is synchronized to the migration of a certain analyte of interest (component 2 in Fig. 11.). As indicated schematically in Fig. 11, only components within a small “mobility window” around sample 2 will be kept in the system, whereas both faster and slower components (1 and 3) will be withdrawn. The principle advantage of this concept is that it “mimics” the higher separation effect of a high separation voltage applied a long separation channel resulting in the same field strength. The total potential drop V_{tot} effectively experienced by an ion after the n th cycle is given by its total migration distance s multiplied by the field strength E :

$$V_{\text{tot}} = s \cdot E = 4 \cdot n \cdot d \cdot \frac{V_{\text{app}}}{2d} = 2 \cdot n \cdot V_{\text{app}} \quad (11)$$

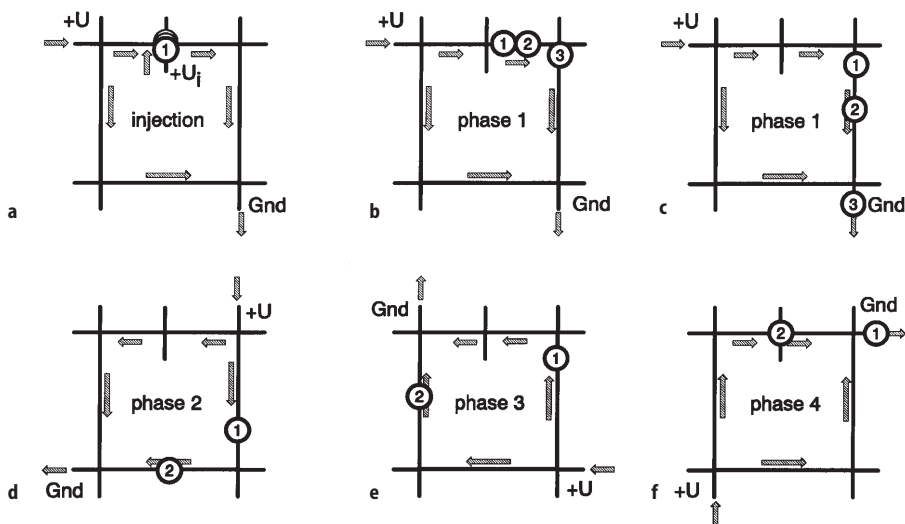


Fig. 11. Principle of synchronized cyclic capillary electrophoresis. Three sample components with different mobility are symbolized. The voltage switching protocol is synchronized to component 2 (reprinted with permission from [73]. Copyright 1994 Hüthig Verlag, Germany)

where d denotes the length of the edge of the square and V_{app} the actually applied potential (the factor 2 reflects the fact that the potential is applied diagonally). Ten complete cycles with 500 V applied mimic the application of 10 kV. The advantage is apparent by recalling Eq. 8, which states that the plate number N is proportional to the voltage drop experienced by the sample ions. High plate numbers should be possible with moderate voltages applied.

Despite the intriguing features of the concept and the demonstrated experimental feasibility [58, 71–73], few applications to real samples have been demonstrated so far. For reasons of the inherent complexity of the many junctions to be controlled and the repetitive character of the experiment, the effects of any non-idealities in the system will rapidly accumulate (e.g. a loss of sample material is frequently observed at each intersection, thus degrading the analytical performance). In order to demonstrate the usefulness of SCCE for real analytical applications, von Heeren et al. have shown that its performance can be improved when fluid flow is suppressed by filling the device with an entangled polymer solution [74]. The same authors have also used SCCE microstructures for MECC separations of biological samples [59] (see Sect. 3.3).

3.3

Electric Field Driven Chromatography

Electrophoresis chips can be readily adapted to perform electrochromatographic separations in open channels, as has been demonstrated by Jacobson et al. [75]. In this work, the channel walls were coated with a thin film of stationary phase by pumping chlorodimethyloctadecylsilane (ODS) through the whole channel system for 18 h at 125 °C. Loading of sample was performed in the same way as described for the CE experiments with a “pinched” injection scheme, and the mobile phase was electroosmotically pumped through the serpentine shaped separation channel (length: 165 mm). Application of a field between 27–163 V/cm resulted in a linear flow velocity of the mobile phase between 0.13 and 0.78 mm/s. The feasibility was demonstrated with separations of three coumarin dyes on a time scale of a few minutes with plate heights in the range between 4 and 5 μm .

Another format of chromatography which has been performed on electrophoresis chips is micellar electrokinetic capillary chromatography (MECC). This technique represents a very powerful extension of CE for the separation of both neutral species and ionic compounds, and has been originally developed by Terabe et al. [76]. Transfer of MECC to CE microchips has been first demonstrated by Moore et al. [77]. The experimental procedure used is identical to high speed CE, apart from the fact that a MECC buffer with 50 mM SDS and 10% methanol was used. Again three coumarin dyes were used as a model sample. Separation was achieved within a few minutes. At low applied field strengths (< 400 V/cm), the reproducibility was found to be excellent (below 1 %).

Very recently, von Heeren et al. [59] have performed MECC separations with SCCE. In particular, these authors demonstrated the application of microchip MECC to biologically relevant samples such as labeled urine. A competitive immunoassay for monitoring patient serum levels of theophylline was carried

out by off-line MECC quantitation of the labeled theophylline tracer. In the same publication, a series of video micrographs is depicted that illustrate the precision of sample injection and the speed of separation achieved.

3.4

Other Recent Developments

By far most of the work discussed in this review has been based on LIF detection, usually with an 488 nm Ar-ion laser as the excitation source. Only very few other examples exist in the literature where other detection principles were investigated. One of these exceptions is an integrated detection cell for chip CE that has been described by Liang et al. [78]. In combination with the U-shaped separation channel, two additional well aligned channels to take up the excitation and collection fibers where micromachined in a glass plate. The U-cell provides a longitudinal path of 120–140 μm in length parallel to the flow direction and can be used both for absorption and fluorescence measurements. The absorption detection limit was 0.003 AU ($\approx 6 \mu\text{M}$ of a fluorescein dye); in the fluorescence mode a detection limit of 3 nM fluorescein (20 000 molecules) was achieved.

A micromachined CE device featuring a truly monolithically integrated detector has been recently reported by Webster et al. [79]. A semiconductor radiation detector was fabricated together with a separation channel on a silicon substrate in a 10-mask process. The preliminary results achieved with the detection of beta decay events of ^{32}P -labeled DNA at 27 V/cm demonstrate the feasibility of the concept.

Very recently, new materials and fabrication procedures have been explored in order to overcome a number of disadvantages associated with glass and quartz substrates. One of these new approaches is based on casting of the micro-

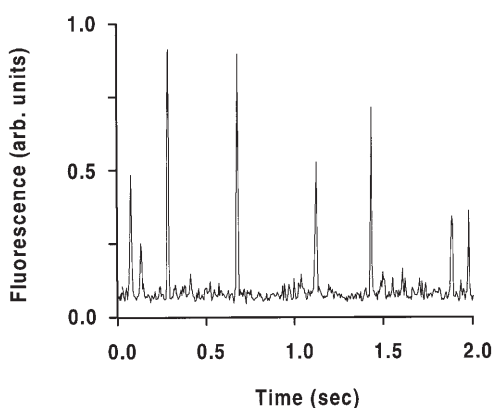


Fig. 12. Fluorescence burst transients originating from individual YOYO-1 stained λ -DNA passing through a focused laser beam molecules in a molded PDMS electrophoresis chip. DNA concentration: 82 fM, $E=200 \text{ V/cm}$

channel systems from a micromachined silicon master with polydimethylsiloxane (PDMS), an elastomeric polymer material that is curable at room temperature [36]. The PDMS replicas show sufficiently good adhesion on smooth and clean surfaces, thus avoiding any bonding process to generate a closed channel system. The performance of these inexpensive devices was demonstrated with the separation of labeled DNA digests. Single λ -DNA molecules (multiply labeled with an intercalating dye) could also be detected with high efficiency in a PDMS channel under electrophoretically controlled flow conditions (see Fig. 12) [36].

4 Free Flow Electrophoresis

A very useful and versatile technique for sample pretreatment and fraction collection on a preparative scale is free flow electrophoresis (FFE). In FFE, a narrow stream of sample solution is continuously injected into a carrier buffer that flows through a shallow separation bed. Perpendicular to the carrier stream, an electric field is applied. The trajectory of a charged sample constituent through the separation bed is then given by the superposition of the longitudinal hydrodynamic flow velocity and its individual electrophoretic migration component in perpendicular direction, as shown schematically in Fig. 13. This technique has been successfully applied to the isolation of a wide range of biologically and medically relevant objects, such as nucleic acids, proteins, viruses, bacteria, cell organelles, and cells. A recent review including the discussion of currently available commercial instruments is given in [80].

A miniaturized and integrated version (“ μ -FFE”) fabricated onto a silicon wafer has been published by Raymond et al. [81, 82]. The device includes a 25 μ l

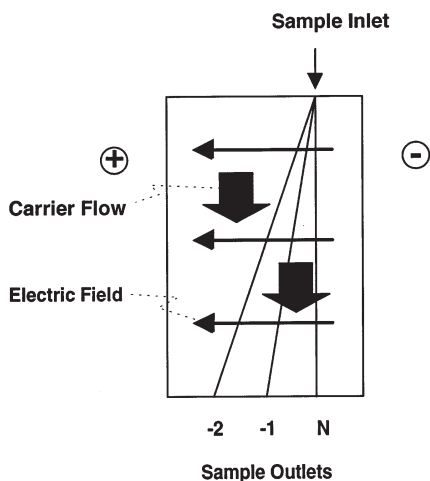


Fig. 13. Concept of FFE. N, -1, and -2 denote the positions where a neutral compound, a mono-anion, and a dianion, respectively, are expected to exit the system (reprinted with permission from [81]. Copyright 1994 American Chemical Society)

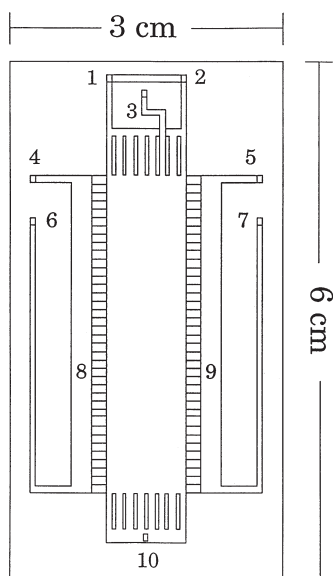


Fig. 14 a. Layout of a silicon FFE device. (1) and (2): buffer inlets, (3) sample inlet, (4) and (5): side bed inlets, (6) and (7) side bed outlets, (8) and (9) side beds containing Pt electrodes, (10) outlet

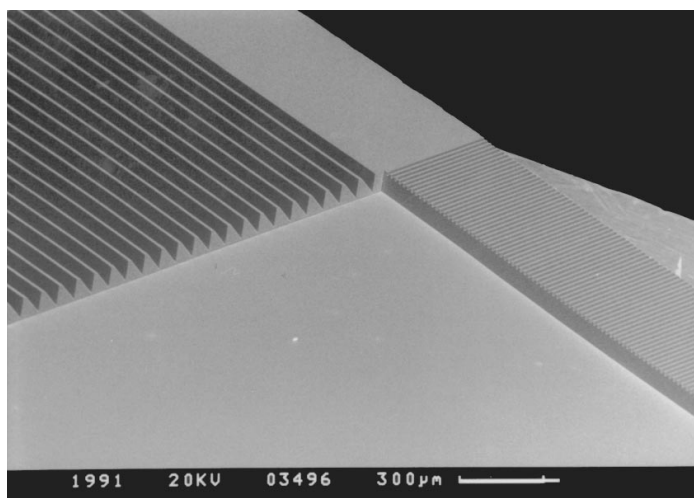


Fig. 14 b. Electron micrograph showing the inlet and side bed channel arrays (reprinted with permission from [81]. Copyright 1994 American Chemical Society)

separation bed of 50 μm depth, two electrode side beds, two arrays of 2500 channels for isolation of the side beds from the separation bed (mimicking the membranes in conventional instruments), and two arrays of 125 inlet and outlet channels, respectively. The layout of the device and an electron micrograph of the inlet and side bed channel arrays is shown in Fig. 14. For electrical insula-

tion, the silicon device was coated with a 100 nm thermal oxide layer and a 600 nm layer of silicon nitride (breakdown voltage: 200–300 V). The device was sealed through anodic bonding of a glass cover plate. Platinum wire electrodes were manually inserted into the side beds. Buffer was delivered into the separation and side beds using syringe pumps under computer control; detection was done by means of LIF very similar to the set-up used for microchip CE.

The feasibility of the approach has been demonstrated with base-line resolved separations of tagged amino acids at a electric field strength of 50 V/cm applied across the “separation length” (bed width) of 1 cm [81]. However, it is clear that high resolution separations will not be the domain of this technique, for the absolute magnitude of the separation voltage across the separation bed is limited to ~100–200 V (see Eq. 8). The flow through the outlet channels was combined into one hole in the cover plate, therefore fraction collection experiments were not possible in this study.

In a follow-up study, the same authors examined the applicability of the same device for relevant protein samples and investigated the main contributions to band broadening [82]. As a consequence of the small depth of the beds, zone spreading caused by Joule heating was shown to be negligible (see Sect. 3.1.1). Cross fields of up to 100 V/cm were applied for the separation of human serum albumin, ribonuclease A and bradykinin. The feasibility of fraction collection was demonstrated with four collected fractions of a whole rat plasma sample. Off-line analysis of these four isolated fractions by CE indicated the separation of serum albumins and globulins.

5 Liquid Chromatography

The very first realizations of integrated chip-based chemical separation techniques can be found in the field of chromatography. The complete gas chromatograph fabricated on a silicon wafer by Terry et al. [10, 11], first reported in 1975, represents an outstanding achievement and laid the basis for the current developments in this field (although an “incubation time” of more than 15 years was required). This work has been reviewed several times (see for example [14]) and will not be further discussed here.

More recently, the description of a small-bore liquid chromatography by Manz et al. [83] on a 5×5 mm silicon chip revived the interest of the analytical chemical community. The chip incorporated an open tubular column of 6×2 μm cross section (column volume: 1.8 nl) and a conductometric detector with a detection volume of only 1.2 pl. Although this work was an important benchmark study, the actual functioning of the chromatograph was never demonstrated with separations.

The first experimental investigation and performance demonstration of an integrated liquid chromatography chip was carried out by Ocuvirk et al. [84]. The device is shown schematically in Fig. 15 and comprises a split injector, a small-bore separation column, a frit, and a detector cell, all integrated in a monolithic manner. An electron micrograph of the silicon chip is also depicted in Fig. 15. The whole device was composed of two 350 μm Si chips and a 50 μm interme-

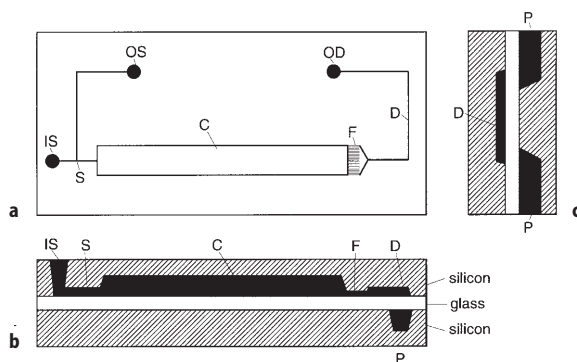


Fig. 15. Schematic layout of the HPLC chip: **a** layout of the channel system, **b** cross section along the channel axis, **c** cross section along the detector cell axis. *IS*: sample and mobile phase inlet, *S*: split injector, *OS*: outlet for rejected sample and mobile phase, *C*: separation channel, *F*: frit, *D*: optical detector cell, *OD*: outlet to waste, *P*: positioning grooves for optical fibers (reprinted with permission from [84]. Copyright 1995 John Wiley)

diate glass layer, all sealed and mutually bonded by an anodic bonding process. Note that the total dead volume in this rather complex 500 nl separation system amounts to only 0.5%. The column was packed with 5 μm particles through application of a pressure of up to 130 bar. Much attention had to be paid to the interfacing of the chip and the sealing of all external fluidic connections. Unfortunately, the injected sample volume could not be kept at a low enough level, and the analytical performance did not reach the theoretically expected plate numbers (80 plates could be obtained for a separation of two dyes in an analysis time of one minute). Nevertheless, this work demonstrates the feasibility of integrated small volume liquid chromatography.

6 Conclusions and Outlook

The past 5 years have witnessed an impressive rate of progress in the field of integrated chip-based separation systems. A variety of functional models has been developed that very clearly demonstrate the feasibility of the general approach. In particular, chip-based electrophoretic separations show unique features with respect to separation speed, sample injection, and the consumption of sample and buffer solution. The analysis time is often reduced by a factor between 10 and 100 compared to conventional CE systems, without a significant decrease of separation efficiency.

The achievements discussed in this chapter also underline that such systems are more than just separation systems. They should rather be regarded as generally applicable fluid handling systems for small volume samples. In particular in the case of electric field controlled systems, the fluid handling requires only control of electric potentials and can be easily automated. Electrophoresis experiments on the level of single DNA molecules have already been demonstrated

in chip-based devices [36]. The combination of electrokinetic control of picoliter sample volumes and single molecule detection would result in a novel and valuable tool for the identification, selection, and manipulation of single molecular objects in solution (enzymes, receptors, genes, viruses etc.). Fast drug screening and molecular diagnostics could profit from such an approach [85, 86].

In order to develop the concept from novelty to utility, many practical issues with respect to economical device fabrication and general handling (e.g. fluidic interfacing of the chip) still have to be solved and currently prohibit routine applications. However, the commercial opportunities have been very well recognized and the critical issues are being directly addressed, e.g. by a growing number of instrumental biotech companies [87]. The shift in research activities towards commercially interesting applications is also reflected by the most recent presentations of active researchers in this field (e.g. parallel CE arrays [88], coupling of microchip CE to mass spectrometry [89, 90], new polymer substrate materials [36, 91], on-chip immunoassays [92, 93]. Judged from the current pace of development and the tremendous commercial opportunities, microfabrication technology is very likely to substantially impact the fields of analytical chemistry and medical diagnostics in the next decade.

Acknowledgement. The author is grateful to Drs. Gerard J.M. Bruin, Alfredo E. Bruno, and Aran Paulus (Novartis Pharma AG, Basel, Switzerland) for their critical reading of the manuscript and helpful comments.

7

References

1. Novotny MV, Ishii D (1985) *J Chromatogr Lib*, 30, Elsevier, Amsterdam
2. Golay MJE (1958) In: Coates VJ (ed) *Gas Chromatography*. Academic Press, New York
3. Knox JH (1980) *J Chromatogr Sci* 18:453
4. Novotny M (1981) *Anal Chem* 53:1294A
5. Novotny MV, Ishii D (1985) *J Chromatogr Lib*, 30
6. Tsuda T, Novotny M (1978) *Anal Chem* 50:632
7. Virtanen R (1974) *Acta Polytech Scand* 123:1
8. Mikkers FEP, Everaerts FM, Verheggen TPEM (1979) *J Chromatogr* 169:11
9. Jorgenson JW, Lukacs KD (1981) *Anal Chem* 53:1298
10. Terry SC (1975) *A Gas Chromatography System Fabricated on a Silicon Wafer Using Integrated Circuit Technology*, Ph. D. Thesis, Stanford University
11. Terry SC, Jerman JH, Angell JB (1979) *IEEE Trans Electron Devices* ED-26:1880
12. Manz A, Graber N, Widmer HM (1990) *Sens Actuators B* 1:244
13. Manz A, Harrison DJ, Verpoorte EMJ, Fettingner JC, Lüdi H, Widmer HM (1991) *Chimia* 45: 103
14. Manz A, Harrison DJ, Verpoorte E, Widmer HM (1993) In: Brown PR, Grushka E (eds) *Advances in Chromatography*, vol 33. Marcel Dekker, New York, p 1
15. Manz A, Verpoorte E, Effenhauser CS, Burggraf N, Raymond DE, Harrison DJ, Widmer HM (1993) *J High Resolut Chromatogr* 16:433
16. Manz A, Verpoorte E, Raymond DE, Effenhauser CS, Burggraf N, Widmer HM (1995) In: van den Berg A, Bergveld P (eds) *Micro Total Analysis Systems*. Kluwer, Dordrecht, p 1
17. de Bokx PK, Gillissen EEA, van de Weijer P, Bekkers MHJ, van Bommel CHM, Janssen HG (1992) *J Chromatogr* 598:115
18. Pentoney SL, Huang X, Burgi DS, Zare RN (1988) *Anal Chem* 60:2625

19. Effenhauser CS, Manz A, Widmer HM (1993) *Anal Chem* 65:2637
20. Giddings JC (1991) *Unified Separation Science*. John Wiley, New York
21. Poppe H (1994) *Analisis* 22:M22
22. Gluckman JC, Novotny M (1985) In: Novotny MV, Ishii D (eds) *Microcolumn Separations* (J Chromatogr Lib), 30. Elsevier, Amsterdam
23. Effenhauser CS, Paulus A, Manz A, Widmer HM (1994) *Anal Chem* 66:2949
24. Ewing AG, Strein TG, Lau YY (1992) *Acc Chem Res* 25:440
25. Harrison DJ, Manz A, Fan Z, Lüdi H, Widmer HM (1992) *Anal Chem* 64:1926
26. Manz A, Harrison DJ, Verpoorte E, Fettinger JC, Paulus A, Lüdi H, Widmer HM (1992) *J Chromatogr* 593:253
27. Harrison DJ, Fluri K, Seiler K, Effenhauser CS, Manz A (1993) *Science* 261:895
28. Seiler K, Harrison DJ, Manz A (1993) *Anal Chem* 65:1481
29. Woolley AT, Mathies RA (1994) *Proc Natl Acad Sci USA* 91:11348
30. Fan ZH, Harrison DJ (1994) *Anal Chem* 66: 177
31. Jacobson SC, Hergenröder R, Koutny LB, Warmack RJ, Ramsey JM (1994) *Anal Chem* 66: 1107
32. Jacobson SC, Moore AW, Ramsey JM (1995) *Anal Chem* 67:2059
33. Fluri K, Fitzpatrick G, Chiem N, Harrison DJ (1996) *Anal Chem* 68:4285
34. Harrison DJ, Glavina PG, Manz A (1993) *Sens Actuators B* 10:107
35. Ekström B, Jacobson G, Öhman O, Sjödin H (1990) *WO* 91/16966
36. Effenhauser CS, Bruin GJM, Paulus A, Ehrat M (1997) *Anal Chem* 69:3451
37. Tiselius A (1937) *Trans Faraday Soc* 33:524
38. Hinckley JON (1975) *J Chromatogr* 109:209
39. Brown JF, Hinckley JON (1975) *J Chromatogr* 109:218
40. Coxon M, Binder MJ (1975) *J Chromatogr* 107:43
41. Gobie WA, Ivory CF (1990) *J Chromatogr* 516:191
42. Brown JF, Hinckley JON (1975) *J Chromatogr* 109:225
43. Jansson M, Emmer A, Roeraade J (1989) *J High Resolut Chromatogr* 12:797
44. Cifuentes A, Poppe H (1994) *Chromatographia* 39:391
45. Cifuentes A, Xu X, Kok WT, Poppe H (1995) *J Chromatogr A* 716:141
46. Cifuentes A, Rodriguez MA, Garcia-Montelongo FJ (1996) *J Chromatogr A* 737:243
47. Hjerten S, Valtcheva L, Elenbring K, Liao JL (1995) *Electrophoresis* 16:584
48. Moore AW, Jorgenson JW (1993) *Anal Chem* 65:3550
49. Monnig CA, Jorgenson JW (1991) *Anal Chem* 63:802
50. Dose EV, Guiochon G (1993) *J Chromatogr A* 652:263
51. Rice CL, Whitehead R (1965) *J Phys Chem* 69: 4017
52. Li H, Gale RJ (1993) *Langmuir* 9:1150
53. Jacobson SC, Koutny LB, Hergenröder R, Moore AW, Ramsey JM (1994) *Anal Chem* 66: 3472
54. Harrison DJ, Fluri K, Fan Z, Seiler K (1995) In: van den Berg A, Bergveld P (eds) *Micro Total Analysis Systems* (MESA Monographs). Kluwer, Dordrecht, p 105
55. Burggraf N (1993) Unpublished results
56. Seiler K, Fan ZH, Fluri K, Harrison DJ (1994) *Anal Chem* 66:3485
57. Harrison DJ (1996) In: Widmer HM, Verpoorte E, Barnard S (eds) *2nd International Symposium on Miniaturized Total Analysis Systems (μTAS 96)*, Basel, Switzerland
58. Burggraf N (1995) *Synchronized Cyclic Capillary Electrophoresis*, Ph. D. Thesis, University of Neuchâtel, Switzerland
59. von Heeren F, Verpoorte E, Manz A, Thormann W (1996) *Anal Chem* 68:2044
60. Verheggen TP, Beckers JL, Everaerts FM (1988) *J Chromatogr* 452:615
61. Huang X, Gordon MJ, Zare RN (1988) *Anal Chem* 60:375
62. Jacobson SC, Ramsey JM (1995) *Electrophoresis* 16:81
63. Jacobson SC, Hergenröder R, Koutny LB, Ramsey JM (1994) *Anal Chem* 66:1114
64. Koutny LB, Schmalzing D, Taylor TA, Fuchs M (1996) *Anal Chem* 68:18
65. Effenhauser CS, Manz A, Widmer HM (1995) *Anal Chem* 67:2284
66. Woolley AT, Mathies RA (1995) *Anal Chem* 67:3676

67. Jacobson SC, Hergenröder R, Moore AW, Ramsey JM (1994) *Anal Chem* 66:4127
68. Harrison DJ, Fluri K, Chiem N, Tang T, Fan Z (1995) *Transducers '95 – Euroensors IX*, Stockholm, Sweden p 752'
69. Jacobson SC, Ramsey JM (1996) *Anal Chem* 68:720
70. Woolley AT, Hadley D, Landre P, deMello A, Mathies RA, Northrup MA (1996) *Anal Chem* 68:4081
71. Burggraf N, Manz A, Effenhauser CS, Verpoorte E, de Rooij NF, Widmer HM (1993) *J High Resolut Chromatogr* 16:594
72. Burggraf N, Manz A, de Rooij NF, Widmer HM (1993) *Anal Methods Instrum* 1:55
73. Burggraf N, Manz A, Verpoorte E, Effenhauser CS, Widmer HM, de Rooij NF (1994) *Sens Actuators B* 20:103
74. von Heeren F, Verpoorte E, Manz A, Thormann W (1996) *J Microcolumn Sept* 8:373
75. Jacobson SC, Hergenröder R, Koutny LB, Ramsey JM (1994) *Anal Chem* 66:2369
76. Terabe S, Otsuka K, Ichikawa K, Tsuchiya A, Ando T (1984) *Anal Chem* 56:111
77. Moore AW, Jacobson SC, Ramsey JM (1995) *Anal Chem* 67:4184
78. Liang Z, Chiem N, Ocvirk G, Tang T, Fluri K, Harrison DJ (1996) *Anal Chem* 68:1040
79. Webster JR, Jones DK, Mastrangelo CH (1996) *MEMS '96* p 491
80. Roman MC, Brown PR (1994) *Anal Chem* 66:86A
81. Raymond DE, Manz A, Widmer HM (1994) *Anal Chem* 66:2858
82. Raymond DE, Manz A (1996) *Anal Chem* 68:2515
83. Manz A, Miyahara Y, Miura J, Watanabe Y, Miyagi H, Sato K (1990) *Sens Actuators B* 1:249
84. Ocvirk G, Verpoorte E, Manz A, Grasserbauer M, Widmer HM (1995) *Anal Methods Instrum* 2:74
85. Eigen M, Rigler R (1994) *Proc Natl Acad Sci U.S.A.* 91:5740
86. Keller RA, Ambrose WP, Goodwin PM, Jett JH, Martin JC, Wu M (1996) *Appl Spectrosc* 50:12A
87. Dutton G (1996) *Gen Eng News* September 15:18
88. Mathies RA (1996) *Microfabrication Technology for Biomedical Applications*. Cambridge Healthtech Institute, San Jose, California
89. Foret F, Xue Q, Dunayevskiy Y, Karger BL (1996) In: Widmer HM, Verpoorte E, Barnard S (eds) *2nd International Symposium on Miniaturized Total Analysis Systems (μ TAS 96). Analytical Methods & Instrumentation*, Basel, Switzerland p 81
90. Ramsey JM (1996) *Microfabrication Technology for Biomedical Applications*. Cambridge Healthtech Institute, San Jose, California
91. Soane D (1996) *Microfabrication Technology for Biomedical Applications*. Cambridge Healthtech Institute, San Jose, California
92. Harrison DJ, Chiem N (1996) In: Widmer HM, Verpoorte E, Barnard S (eds) *2nd International Symposium on Miniaturized Total Analysis Systems (μ TAS 96). Analytical Methods & Instrumentation*, Basel, Switzerland p 31
93. Regnier F (1996) *Microfabrication Technology for Biomedical Applications*. Cambridge Healthtech Institute, San Jose, California

Biological Application of Microstructures

G. Fuhr · S.G. Shirley

Humboldt-Universität zu Berlin, Institut für Biologie, Lehrstuhl für Membranphysiologie,
Invalidenstraße 43, 10115 Berlin, Germany.

The investigation of living cells, isolated organelles, viruses and macromolecules in microstructures fabricated by semiconductor technology is a new field of research and has found its first biotechnological and medical uses. This chapter contains selected examples of three-dimensional structures to characterise, manipulate and separate suspended and adherently growing cells. It addresses the problem of cell cultivation in strong electric fields. In addition, some theoretical and experimental results dealing with dielectrophoresis, trapping of sub-micron particles and cryoconservation of cells in microstructures are given. The behaviour of adherently growing animal cells on artificial surfaces is described. Combinations of electrical and optical methodologies are discussed and the perspectives for such semiconductor- or glass-based devices are outlined.

Keywords: Three dimensional microstructures, electric field, field cage, cell adhesion, cell migration.

1	Introduction	84
2	Miniaturisation	84
2.1	The Available Forces	86
2.2	Dielectrophoresis	87
2.3	Cooling	89
2.4	Gradients	91
3	Manipulation of Cells in Suspension	92
3.1	Positioning, Moving and Sorting of Cells and Submicron Particles	92
3.2	Single Cell Characterisation	97
3.3	Resonances	97
4	Adherent Cells	100
4.1	Fibroblasts as Model Cellular Systems	100
4.2	Cell Migration	102
4.3	Artificial Control of Cell Migration	103
4.4	Long Term Exposure of Cells to Electric Fields	105
4.5	Micropores	106
5	Cryo-Conservation	109
5.1	Cryo-Conservation of Cells in Micro-Structures	110
5.2	Cell Adhesion Patterns	111

6	Perspectives	114
7	References	114

1

Introduction

Great strides have been made over the past few years in biotechnology. Genetic engineering now allows us to transform cells and, to an extent, construct organisms with properties to our advantage. There are, however, other branches of biotechnology and this article deals with one of them – the interactions of living cells and their components with inanimate matter and how those interactions can be put to use.

For the last ten years or so, a handful of groups world-wide have been working to develop microtools for cell handling. The aim is to develop a series of basic elements which can be juxtaposed and connected to build useful devices. This work draws heavily on techniques pioneered for semiconductor manufacture. The results are promising and the number of groups is increasing as the result of industrial interest.

The first generation of instruments is likely to include devices for sorting and selecting cells, devices for accurately positioning one or more cells in a mixture and cell based biosensors with long shelf lives. New measurement techniques at the single cell level and new ways of probing cell-cell interactions will open up possibilities in basic research.

The aim of this article is to give an introduction to this new field of research with enough background to make it easily accessible to both biologists and physical scientists. We explain the basic principles by the use of selected examples and try to cast some light on the complex process of interfacing artificial and biological systems. Although some of the devices described are constructed of silicon, we are not here concerned with its semi-conductor properties [1, 2] concentrating rather on cell-manipulation devices. While we give some literature sources, we do not attempt to give a complete overview of the literature of the several branches of science on which this work is based. Neither do we give a detailed mathematical explanation of the effects as this may be found elsewhere [3–10].

2

Miniaturisation

Miniaturisation is not simply a “down-scaling” of well known devices. The relative importance of different forces and processes changes with scale. While this prohibits the use of some familiar techniques, it opens up possibilities for novel ones. Accurate positioning and manipulation of cells requires that devices be structured on or near the same scale as the cells themselves and, in this sense, miniaturisation is essential (Fig. 1). It also brings other benefits such as the short response times associated with small devices, ease of sterilisation and, most

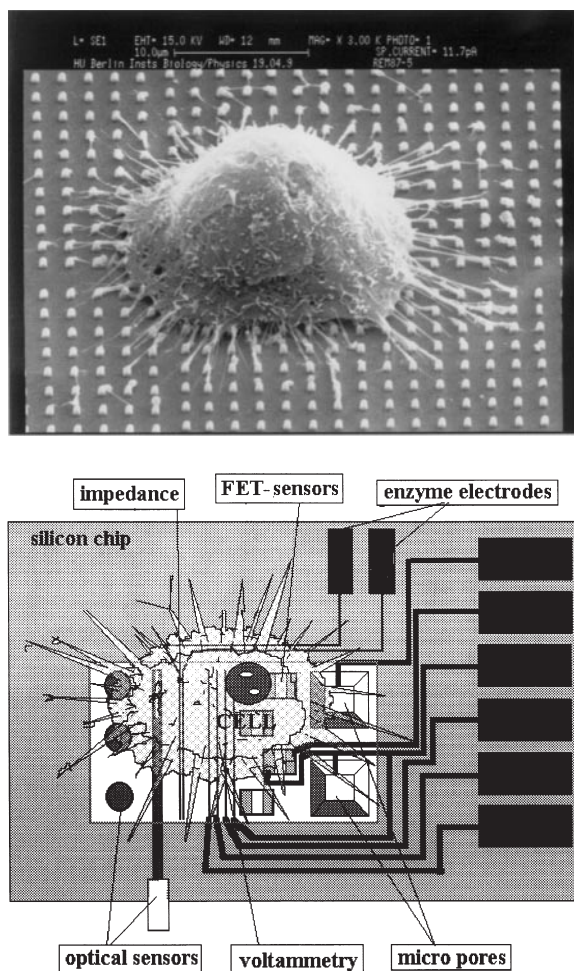


Fig. 1. The accuracy of e-beam lithography is illustrated in the scanning electron micrograph (*top*). The size of the features formed in the silicon oxide is $0.5\ \mu\text{m}$ and the typical animal cell (a fibroblast) has a diameter of $20\ \mu\text{m}$. This kind of cell adheres actively to surfaces, forming thin filopodia which here have all attached to the micro-hillocks. Semiconductor technology is capable of manufacturing micro-electrodes, sensors, pores and electronic networks with sizes smaller than that of the cell. The lower illustration summarises the main detection and measuring methods currently in use

importantly, it allows the construction of complex systems. Also many cells and tissues are sensitive to pH and other ionic gradients. Only in microsystems can such gradients be generated, stabilised and controlled on a micron scale.

Another advantage of miniaturisation is that small devices can work with small quantities of biological material, a single cell or a few viruses or macromolecules. This is a highly desirable feature in pharmaceutical screening devices and diagnostic systems.

2.1

The Available Forces

It is worth reviewing the forces that act and can be used for the manipulation of cells in microstructures. Random thermal (Brownian) motion becomes important for objects of cellular size and very important for smaller ones. The energy associated with this (about 2×10^{-21} J/particle, regardless of size at room temperature) provides a yardstick to which the strengths of the other forces can be compared. For instance, a perfectly controlled force of 10^{-15} N would be capable of holding a particle within about $2 \mu\text{m}$ of a target position.

Most important are the chemical forces. The energy of a single C–C bond is about 10^{-18} J and the energies of reactions involving covalent bonds are typically a few $\times 10^{-19}$ J/molecule with many molecules being involved in cellular interactions. Neither must the secondary chemical forces be overlooked. For example, the energy associated with the exclusion of water from between two hydrophobic surfaces of $1 \mu\text{m}^2$ (hydrophobic bonding) is about 10^{-13} J. The chemical forces are short range, requiring contact. But, once a cell has contacted a surface and chemical interactions have occurred, they will dominate its behaviour. These interactions may be incidental or those controlled by the cell itself as part of the cascade of physiological responses following contact. They may also be used deliberately and the structuring of the “chemistry” of the surface is one method of controlling cell behaviour (see Sect. 4.3).

The physical forces are long range, more suited to manipulating cells in suspension. There are four main considerations:

How strong can the force be made?

How does the strength vary with particle size?

How does the force vary with particle nature?

How easily can the force field be structured and controlled?

Gravity does noticeably affect objects of cellular size in suspension. The combined gravitational/buoyancy force on a cell of $10 \mu\text{m}$ diameter and density 1.01 is about 5×10^{-14} N. This is sufficient to cause slow sedimentation but too weak to be used as a primary manipulative tool. The gravitational force can be enhanced by the use of a centrifuge or by changing the density of the suspending medium but there is no practical way of structuring such changes.

Much stronger forces are available by utilising hydrodynamic flow. The force on a $10 \mu\text{m}$ cell in water streaming at 1 mm/s is about 10^{-10} N. It is worth noting that liquid flows in microstructures occur with low Reynold's numbers and that they are very stable and predictable. It is also possible to achieve a degree of structure in a flow regime, e.g. by the use of local convective streaming. Unlike most of the other forces mentioned here, the viscous drag on a particle depends on its radius not its volume and this fact can also be used to advantage. It is likely that many future devices will use flow to impose one of their controlling forces on particles.

Electrophoresis is a well known macroscopic technique which can also be applied in microstructures [11]. Forces can be quite high. A cell with a net imbalance of a thousand electronic charges in a field of 50 kV/m experiences a force of about 10^{-11} N. The heat that such fields and the resulting currents pro-

duce can be removed in microstructures (see Sect. 2.3) but there are difficulties in structuring dc fields. Some coarse structure can, in principle, be achieved by the use of channels to connect with external electrodes, but fine structuring requires the use of electrodes within the device itself and this is prohibited by electrolysis with dc.

Dielectrophoresis (DEP) is less widely known and, for that reason, it is explained in more detail in the next section, see [3]. There are only a small number of practical macroscopic devices based on the principle. Fundamentally, it utilises the force experienced by a (charged or uncharged) particle in an electric field gradient. As devices are scaled down, gradients can be made steeper and fields can be made stronger. DEP becomes very important in small devices. The force on a 10 μm cell in a field varying from 50 kV/m to zero in the space of 50 μm is of the order of 10^{-10} N. Very importantly, DEP occurs in dc or ac fields and the use of high frequency ac eliminates electrolysis problems. Also, the dielectrophoretic force is frequency dependent in a way that reflects cellular properties and good use can be made of this fact. Negative DEP (see next section) has the advantage of moving cells to regions of low field strength where they experience the least possible stress.

Laser tweezers can and have been used to manipulate cells [12–17]. A particle in a laser beam experiences two forces. The first is radiation pressure which drives the particle in the direction of the beam. The second is a force akin to DEP which drives the particle toward regions of highest intensity (the beam's focus). This force is only found with optically transparent material but, with suitable beam geometry, it can be made larger than the first. The optical forces are of the same order of magnitude as DEP (10^{-10} to 10^{-14} N for a typical cell). Laser tweezers suffer from the disadvantage that they drive cells towards a region where the light intensity can be damagingly high but, properly controlled and used short-term, they have characteristics complimentary to DEP. A laser beam manipulates a single chosen particle. In principle, multiple-particle manipulation is possible but it requires multiple controlled laser beams. DEP on the other hand affects all particles in the chosen region with possible discrimination between particle types. Hybrid devices are quite plausible. For instance a system might screen a cell mixture by means of DEP and flow, use a short laser exposure to select a particular cell and then hold it in position using the gentler dielectrophoretic force again (Fig. 2).

It is worth remembering that the breaking of chemical bonds requires displacements of only a small fraction of a nanometer. The energies associated with even the strongest of these physical forces acting on an object of cellular size with displacements of this order are only comparable to the energy stored in a very small number of chemical bonds.

2.2

Dielectrophoresis

The full theory of DEP and related phenomena can be found elsewhere [3, 6, 18–21]. We give just a short, non-mathematical introduction outlining the main features.

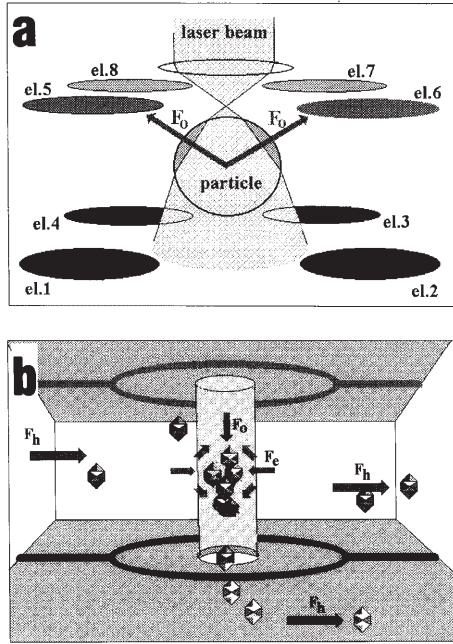


Fig. 2. Schematic diagram showing how electrical, optical and hydrodynamic forces could be combined for handling particles. **a** In negative DEP, a particle experiences a force driving it toward a region of lower field strength; in this case the field minimum formed at the centre of an eight electrode cage. A steeply divergent laser beam exerts two forces on a particle. One (not shown) is the radiation pressure which acts in the direction of the beam. The second is a force akin to DEP which moves the particle towards the focus of the beam. Under the right conditions, the second force can be made stronger than the first. **b** Diagrammatic view of a channel with two ring electrodes, each surrounding a central opening which leads to a parallel channel. Such electrodes create a field which has a minimum at the centre of each ring (at the openings). Viruses or other particles brought into the device by streaming (F_h the hydrodynamic force), would normally be concentrated and forced by the field (F_e the electrical force) through one or other of the holes into the parallel channels. Particles can be sorted to the correct hole by switching the direction of a parallel sided laser-beam (F_o the optical force, radiation pressure)

A particle in an electric field polarises and the resulting dipole is aligned either parallel or anti-parallel to the external field depending of whether the permittivity of the particle is greater or less than that of the surrounding medium. A non-uniform electric field exerts a force on the induced dipole and this force drives a particle toward regions of high field strength (positive DEP) if the particle has higher permittivity than that of the medium or towards low field strength (negative DEP) if it has lower permittivity. The dielectric force becomes large only when the field strength varies significantly from one side of the particle to the other, steep gradients are required.

When an alternating, non-uniform field is used, the situation is similar. The induced dipole is still aligned (spatially) with the field but it oscillates and, in

general, there is a phase difference between it and the field. Positive or negative DEP occurs according to whether the phase angle is less or greater than 90° . The phase angle depends on both the permittivity and conductivity of particle and medium and on the frequency. DEP is a frequency-dependent force (even for homogenous particles with frequency-independent dielectric properties).

A living cell is a highly structured particle with several dielectric interfaces (at minimum, external medium/membrane and membrane/cytoplasm) [5, 22]. A force is developed at each interface. These forces have different frequency dependencies and can sum to give a complicated “force spectrum”. The usual pattern for cells in solutions of low conductivity is for positive DEP at low frequencies crossing over to negative DEP at high ones. With high external conductivity, the DEP stays negative at all frequencies. Although the force-frequency relationship is complex, it is very reproducible and can be used to determine cell dielectric properties.

2.3

Cooling

Another advantage of miniaturisation is the ease with which heat can be removed from systems. The application of strong electric fields to conducting solutions such as cell culture media produces considerable heating. Heat production *per se* not damaging to cells and other biological material, it is high temperatures that must be avoided. Small devices allow easy removal of heat and prevent excessive temperature increases. To illustrate the point, consider a rectangular film of liquid of thickness t , cooled at the top and bottom faces and exposed to an electric field of strength E . The power is deposited in the liquid at a density of $p = gE^2$ where g is the electrical conductivity. Considering conductive cooling only, the temperature rise at the centre of the film is $\Delta\theta = pt^2/8k$, where k is the thermal conductivity of the liquid.

For an aqueous solution with an electrical conductivity of 1 S/m (typical of cell culture media) and a field of 100 kV/m, the power density is 10^{10} W/m³. Without cooling this would be sufficient to take the liquid from room temperature to boiling point in 30 ms. Despite the low thermal conductivity of water ($k = 0.59$ W/m °C at 15 °C), the steady state temperature rise at the centre of a 50 μ m thick cooled film is only 5.3 °C.

This illustrates two points. First the temperature rise is proportional to the square of the film thickness and as devices are scaled down cooling improves dramatically. Secondly (and counter-intuitively), conduction becomes the dominant cooling process in such devices. To obtain the same degree of cooling by forced convection alone would necessitate totally replacing the liquid in the film some 500 times per second. Convection does of course occur in devices and is sometimes used to advantage but conduction is usually responsible for transporting most of the heat. This is another example of the relative importance of processes changing with scale.

The distribution of heat production which occurs in and around a living cell in an electric field is also important. This is illustrated in Fig. 3.

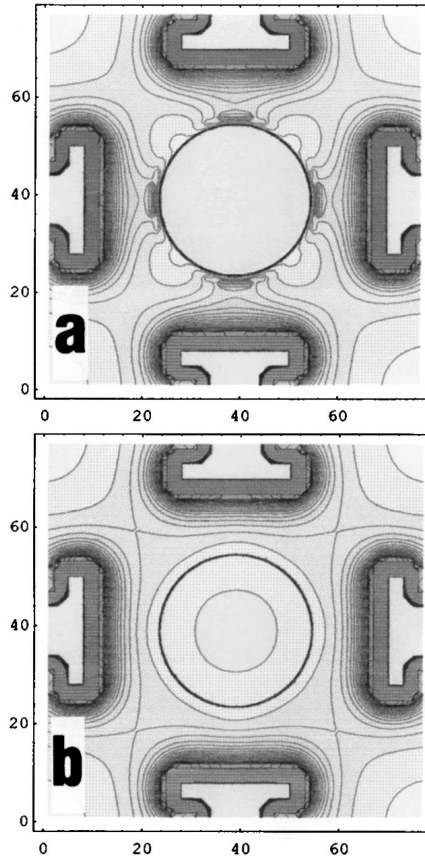


Fig. 3. Heat production is an important consideration for devices using electric fields in the liquid near cells. This figure shows the theoretical distribution of heat production in and around a spherical cell at the centre of a quadrupole electrode chamber in a solution of low electrical conductivity (*top*) and high conductivity (*bottom*). The heat production is given by gE^2 where g is the conductivity of the solution or cell component and E is the (local) electric field strength. The contour interval is 7% of the maximum in each case. The cell is modelled as an electrically conductive sphere enveloped by an insulating but capacitive membrane.

In both cases, the region of highest heat production is at and near the electrode edges. However, this component of the heat is easily removed into the substrate. It is the heat production in and near the cell which is important. At high external conductivity the heat production is fairly uniform with some heat being produced within the cell. Some heat production can be tolerated and while this sets a limit on the driving voltages which can be applied, useful fields and forces can still be developed. It may seem attractive to use solutions of lower conductivity as less heat is then produced and it is produced external to the cell. But the appearance of local “hot-spots” means that it may not be possible to increase voltages and fields as much as might be expected. The figure shows the situation at high frequencies (1 MHz) and for solution conductivities of 0.1 mS/m and 1.4 S/m. At low frequencies, heat production becomes fully external to the cell and its distribution becomes less dependent on solution conductivity

Heat must also flow through the walls of a device. DEP utilises electric field inhomogeneities which means that the fields (and heat production) within the liquid tend to be quite localised. The external heat flows can occur over much wider areas so it is sometimes possible to use even poorly conducting materials such as ordinary glasses and quartz. In critical cases, silicon, which has a high thermal conductivity ($150 \text{ W/m s } ^\circ\text{C}$), is used.

2.4

Gradients

Thermal gradients in microdevices can be made very steep, stable and controllable. Although the actual temperature variations are quite small, the gradients can be of the order of $10^5 \text{ } ^\circ\text{C/m}$. Most cells have temperature sensitive behaviour and an example of the use of controlled local heating to exploit this can be found in Sect. 4.4. But thermal gradients of this magnitude may have wider applications than guiding cell growth. Techniques such as thermophoresis [23], up until now a theoretical curiosity, may become practical with gradients of this order.

Ionic gradients can be generated as well as thermal ones. In particular, a measure of pH control can be achieved. By correctly pulsing dc electrodes, it is possible to generate useful, local pH changes while the electrolytically generated hydrogen and oxygen dissolve rather than appear in gaseous form. Such acidic and alkaline clouds (Fig. 4) can be moved over and near a micro-electrode array by suitable switching [24]. In principle, it should be possible to move them away from the array with a suitable flow regime to produce pH pulses in a field-free region. Controllable pH clouds might be used for signal transmission to living cells as well as for titration applications in micro-chemical devices.

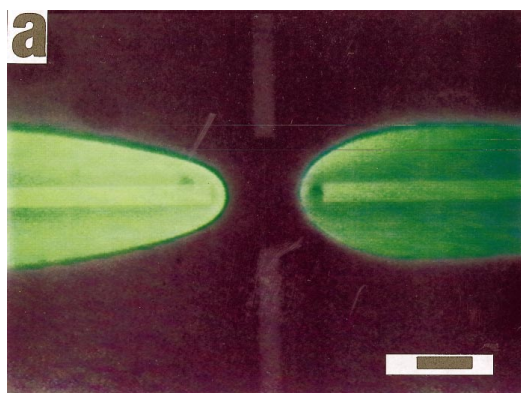


Fig. 4. The pH shifts around electrodes can be visualised with fluorescein isothiocyanate which fluoresces in alkaline solution. (The tip-tip distance between opposite electrodes is $200 \text{ }\mu\text{m}$. **a** The horizontal electrodes are negative and the vertical ones positive. The alkaline clouds formed around the cathodes are clearly visible

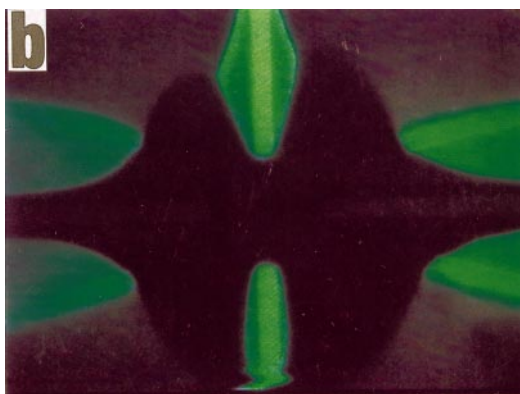


Fig. 4b. 3 seconds after reversing the polarity, new alkaline zones have formed around the vertical electrodes and dark, acidic regions have been created near the horizontal ones

3 Manipulation of Cells in Suspension

DEP and related phenomena are very useful for handling cells in microdevices. Macroscopically, dielectrophoretic particle manipulators have a long history [3, 25–32] but, except for dust filters, they have found few commercial applications. The basic reason is that precise particle positioning requires strong gradients and fields which are structured on a scale comparable with the size of the particles themselves. In macroscopic devices this is very difficult to achieve. But semiconductor fabrication technology is now capable of making electrode systems on the micrometer and sub-micrometer scale and precise cell handling systems are becoming a reality.

3.1 Positioning, Moving and Sorting of Cells and Submicron Particles

Positive DEP drives particles towards field maxima and negative DEP moves them to field minima. It is only possible to create field maxima at the surfaces of the electrodes, no maximum can exist elsewhere in an isotropic solution. Trapping or positioning of particles by positive DEP therefore requires the dielectrophoretic force to be balanced by some other force (e.g. sedimentation, buoyancy or flow) and to be subjected to feedback control. This was first done with a two electrode system by Jones and Kaler [33–37].

They also developed a system using negative DEP [37]. Field minima (unlike maxima) can be created remote from electrode surfaces and negative dielectrophoretic traps do not need balancing forces and active control circuitry.

Steep gradients could not be achieved in these macroscopic devices and high excitation voltages were needed to compensate for this. The situation changed with the advent of 3-dimensional micro-electrodes fabricated on glass and

silicon substrates. It is now possible to build cages working at MHz frequencies and low voltages which will hold a cell at a given position within a physiological (highly conductive) solution [38] (Fig. 5). The motion of the particle is strongly damped by the surrounding liquid and trapping is stable, without oscillation or complex trajectories.

The simplest negative dielectrophoretic trap does not require control circuitry but control circuitry can, of course, be used. By modulating the amplitude and/or phase of the driving voltages, the caged cell can be moved to a desired position in three dimensions with micron accuracy and it can also be rotated about any axis [38, 39]. Currently, there is a system for positioning a cell by means of a joystick and direct computer control is an obvious next step (unpublished data).

Such cages compare favourable with laser tweezers. The precision of control is about the same but rotation is much easier to achieve with cages. The electrode assemblies themselves can be fairly robust, cleanable and sterilisable and can be manufactured to fit and work in a conventional microscope. The cost of the assemblies in medium scale production would be sufficiently low that they could almost be regarded as "disposable elements" and interchangeable electrode systems for different applications are perfectly feasible. The cost of a complete system including h.f. generators and control circuitry is much less than the cost of the corresponding laser equipment and there are advantages too in terms of overall size and the virtually "maintenance free" reliability associated with modern electronics. Field cages hold cells much more gently than do laser tweezers, cells can be held for days if necessary and can be seen to grow and divide during this time [38, 40]. An additional advantage is that multiple cages can be fabricated on the same chip and individual control of many cells simultaneously is feasible.

The field cage principle is not only applicable to cells, smaller particles can be held. The dielectrophoretic force varies with particle volume and this, ultimately, puts a lower limit on the size of particle which can be handled. But fields in microstructures can be made very strong and very non homogeneous and this allows the manipulation of particles much smaller than was previously thought possible. Viruses can be concentrated from suspensions and trapped [41–43]. The concentration occurs because convective streaming induced by the thermal gradients created by the device itself carries particles into the cage. The fields are strong enough to induce particle-particle interactions and virus aggregation occurs within the cage. The smallest cages fabricated to date have electrode gaps of 500 nm.

Field cages can also be used to create layered particle aggregates of defined shape which can then be made permanent by e.g. photopolymerisation (Fig. 6) [44]. Possible applications of this technique range from the encapsulation of drugs in micron scale structures with controlled release pores to the creation of ordered aggregates of living cells.

As particle sizes fall, Brownian motion becomes more important. For small particles, trapping becomes a statistical process. A given particle will have a "lifetime" within the cage. For particles of 10 nm, numerical simulations show that this lifetime is a few minutes, in comparison to microseconds without field,

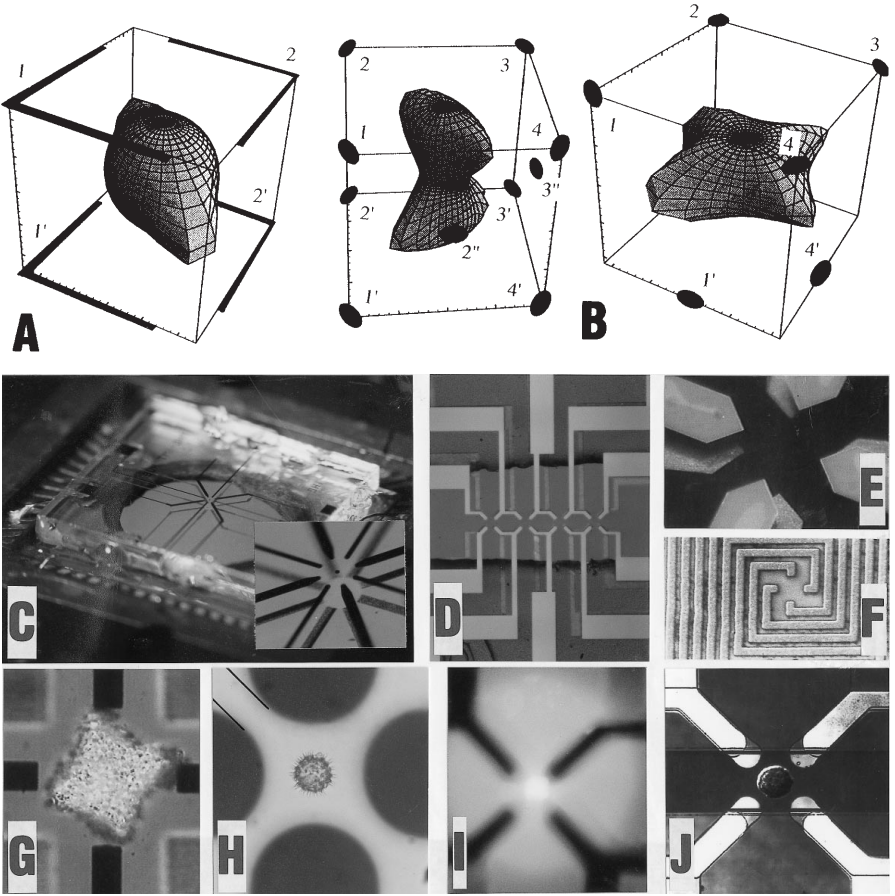


Fig. 5. The upper part of the figure (A, B) gives two examples of the different force distributions which can be generated within field cages. The surface of constant, centrally directed force is shown in each case. An aggregate of small particles within the cage would take on the shape of this surface. The shape is determined by the number of electrodes and their positions and by the amplitude and phase of the driving voltage applied to each. Great variety is possible even with a fixed electrode geometry. By suitable choice of the driving regime, the surface can be moved or distorted, even to the point of creating an opening to allow the release of a trapped particle in a specified direction. The lower part of the figure shows some examples of cages made by semiconductor manufacturing techniques. C Shows a field cage composed of two glass plates (spaced 100 μm apart) each of which carries eight electrodes. D Is a top view of 4 octopole cages arranged along a channel of 20 μm width. The terminals are arranged symmetrically. E Shows a cage where the upper electrodes are twisted slightly, rather than lying exactly above the lower set. This electrode arrangement gives force distributions as seen in B. F Shows the smallest quadrupole electrode system fabricated. The meander (square-spiral) electrodes are 200 nm wide and surround a central gap of 500 nm. G Confirms that the aggregate created by a twisted electrode cage is of the “pin cushion” shape predicted in B. The aggregate is about 100 μm in diameter and is formed of latex particles. H Shows a grain of *Helianthus annuus* pollen (50 μm) trapped in a large cage. I is a fluorescence image of submicron particles trapped in a 20 μm (tip-tip) cage. J Shows a fibroblast (10 μm diameter) trapped in one of the cages pictured in D

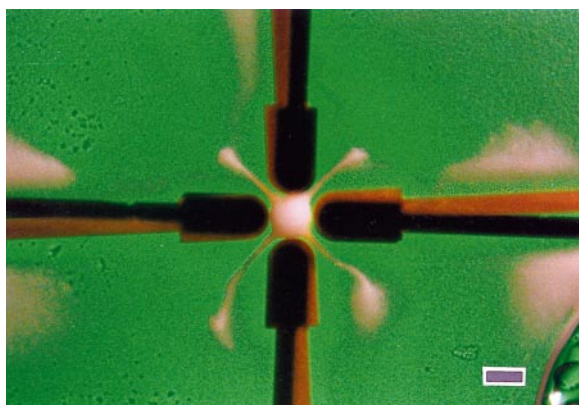


Fig. 6. This particle aggregate was formed in an octopole field cage. It has six tails of which four are visible here. The cage was 200 μm in diameter and energised by 25 V at 1 MHz. The aggregate is formed of 3.9 μm diameter latex beads levitated and held by the forces in the cage. By alterations of driving regime, different shapes are possible and suitably prepared particles can be crosslinked to form a permanent structure by photo-polymerisation or by chemical means. The bar is 200 μm

so even particles of this size can be handled. This opens up possibilities for handling cell organelles and even the largest macromolecules.

Cages can hold a cell and make fine adjustments to its position. A cell handling system may also need to move cells from one place to another and this calls for different arrangements. One solution to the problem utilises travelling waves. These can be generated over an array of parallel electrodes and were first used by Melcher [45, 46] to induce liquid pumping (electro-hydrodynamic pumping). In principle, the fluid flow induced by such pumps could be used to move cells but most effort has centred on the use of travelling waves to move cells directly. A synchronous “linear motor” for moving cells in microsystems was first demonstrated by Masuda et al. [47].

We have developed an asynchronous system (particle velocity \ll wave propagation velocity) using high frequency travelling waves [48, 49] (Fig. 7). A feature of this system is that particle movement is the result of two forces. First, there is DEP, this is simply the result of the electric fields being more intense near the track. This force either attracts particles to the track (positive DEP) or repels them and levitates them above it (negative DEP). The frequency and dielectric properties of the particle determine whether positive or negative DEP occurs. The second force occurs because the electrodes are energised with a travelling wave and this force is directed along the track. Mathematically, this force is analogous to the torque experienced by a particle in a rotating field and, very importantly, its frequency spectrum is quite different to that of DEP [48–50]. It is possible to choose conditions so that cells of one type are levitated and then propelled through the solution while different cells are attracted to the track where they are immobilised by friction or roll slowly. So not only is it possible to transport cells by travelling waves, it is also possible to sort them.

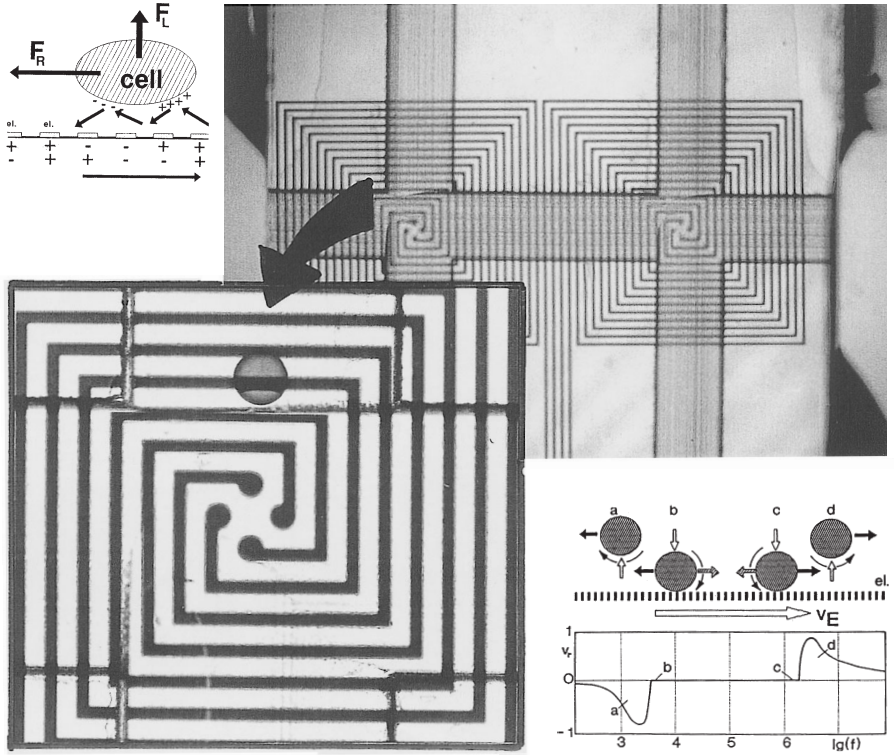


Fig. 7. A cell near a travelling wave array experiences two forces. The first is dielectrophoretic as the electric fields are most intense near the array. Depending on the frequency, this force may be positive (*b* and *c* in the inset) or negative (*a* and *d*). The positive force attracts particles to the track where they are either immobilised or roll slowly due to friction. Particle velocity is, therefore, near zero over the central part of the frequency range where positive DEP occurs. At low and high frequencies, there is negative DEP. The force (F_L) levitates the particle above the track. Since the particle is then free to move, the effects of the second force can be seen. The travelling wave force (F_R) is related to the torque generated by a rotating field and derives from the phase gradient inherent in a travelling wave. (There is a close analogy to the electro-rotation spectrum.) The combination of DEP and travelling wave force produces a velocity spectrum as shown in the inset. The structures shown are fabricated by photolithography and consist of gold electrodes on a glass substrate. The width of each electrode is 30 μm and the gaps are 55 μm . The crossed channels are formed in thin (100 μm) glass which covers the non-working areas of the electrodes

This is not the only kind of cell sorter which is possible. Basically there are three different types. Firstly, there are those which utilise electrical forces only. The travelling wave device is an example of this. Since the electrical forces scale with particle volume, this kind will sort according to the passive electrical properties of the cells [51–53]. Secondly, there are those which use an electrical and another force in combination. Flow is the most promising candidate. As the

hydrodynamic force scales with particle radius, very sensitive size-based separations should be possible even for cells with very similar electrical properties in a dielectrophoretic/flow sorter [54]. The third kind is the active sorter, where cells are guided by electrical fields which are switched in response to some trigger signal derived from a sensor. This could be as simple as a yes/no optical signal giving an inexpensive device which would perform the task of a fluorescence activated cell sorter (Fig. 8). Or, given the favourable geometry and microscope-compatibility of the microdevices, it could involve complex pattern recognition.

3.2

Single Cell Characterisation

A cell (like any other polarisable body) will spin when suspended in a rotating electric field [55]. It becomes, in effect, the rotor of a dielectric motor. The torque and hence rotation speed induced in a complex-structured body like a cell is frequency dependent. In the kHz frequency range, it reflects mainly the properties of the cell membrane. At MHz frequencies, rotation depends primarily on the electrical properties of the cytoplasm. Also, feature such as large organelles, membrane mobile charges and surface structure may leave signatures in the rotation spectrum. The technique of measuring rotation speed as a function of field frequency is known as single cell dielectric spectroscopy. A detailed theory and many examples of its use can be found elsewhere [4, 10, 18, 56].

Until now, measurements were made in macroscopic devices. This limited the technique to using solutions of very low conductivity. Microdevices allow the use of a range of conductivities up to and even beyond physiological [40]. In some cases the use of physiological solutions is essential. For cells which will tolerate variations in ionic strength, much more information is available when measurements are made at a range of external conductivities. For instance, by adjusting the permittivity and conductivity of the external solution it is possible to suppress the main cytoplasm peak of the spectrum and see the signatures of other polarisation processes which were masked by it (Fig. 9). This allows the study of membrane components such as mobile charges [10, 57].

An additional advantage of microdevices is that the cell under study can be centred in the electrode chamber by DEP. This removes the main reason for manual intervention in the measurements and opens the possibility for automating the spectroscopy. It is likely that instruments of this type will become commonplace in the next decade.

3.3

Resonances

With increasing miniaturisation, the area of electrodes in contact with the solution becomes smaller and its behaviour becomes more capacitive. Microelectrode structures typically have a resonant frequency [58]. Usually, this occurs at hundreds of MHz. While this is above the frequency of most generators it can accentuate harmonics when square wave drive is used. Also, by the addition of

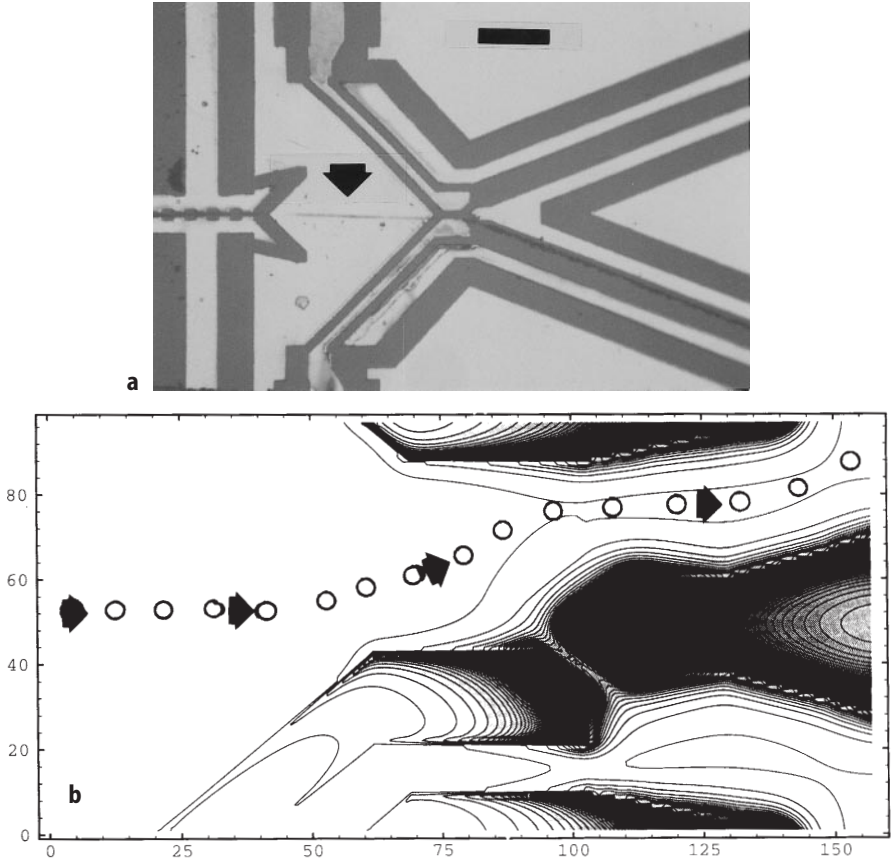


Fig. 8. One design for an active particle sorter. **a** The device consists of two parallel glass plates 50 μm apart. The lower one, which is visible here, has platinum/titanium electrodes shaped by laser ablation. The electrodes of the upper plate are formed in indium-tin oxide (ITO), a transparent conductor, to allow the working of the device to be viewed. (The bar is 50 μm). There is a flow of electrolyte from left to right through the device. The particles have been concentrated from the 1000 μm wide input stream and “collimated” by another dielectrophoretic device, part of its last element is visible at the left of the figure. Due to the laminar nature of the flow such single-file particle “beams” (arrowed) will travel considerable distances without degradation. The sorter itself consists of two steering electrodes (club ended) and two output “channels” formed by the “V” electrode at the right and the two “tick-shaped” electrodes (all five electrodes have their counterparts on the upper plate). The output channels are permanently energised and confinement of particles here is purely electrical, there are no mechanical barriers. The four large, roughly triangular areas are non-working. When the upper pair of steering electrodes are energised, particles are deflected into the lower channel and vice versa. (Lower and upper here refer to the figure, corresponding electrodes of the upper and lower plates are energised simultaneously.) The few particles visible in the upper channel have been removed from the main stream by transient switching of the steering electrodes. In a practical application, this switching would be controlled by signals from an optical or other sensor examining the incoming particles. **b** The passage of particles through the device is determined by the left to right fluid flow and by the field-strength valley created by the steering and channel electrodes. Plotted here are the force contours when the lower steering electrode pair is energised. The numbers on the axes are a scale of μm

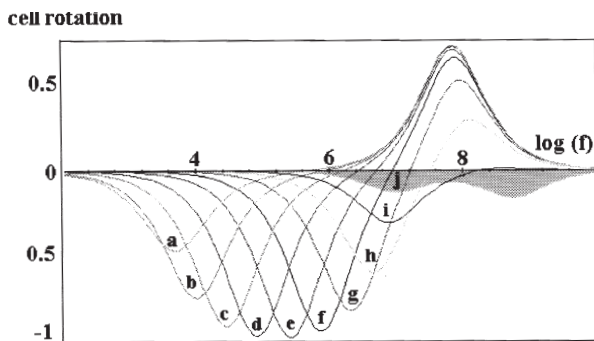


Fig. 9. A rotation spectrum is produced by observing the motion of a cell in a rotating electric field of constant amplitude and plotting the rotation speed of the cell against frequency of the field. In solutions of low conductivity, the cell rotates in the opposite direction to the field (anti-field rotation) at low frequencies. This rotation reaches a peak when the field frequency corresponds to the charge relaxation time of the membrane. The position of this peak therefore contains information about membrane permittivity and conductivity. As the frequency increases further, the rate of cell spinning falls, becoming zero at about 1 MHz. Above this frequency, the cell starts to spin with the field (co-field rotation) and a second peak is reached. The frequency at which this peak occurs depends in practice mainly on the conductivity of the interior of the cell. It may be used for non-destructive determination of cytosolic electrolyte concentration.

The curves (a) to (j) show rotation spectra with increasing external conductivity (a – 10^{-4} S/m; b – 3×10^{-4} S/m; c – 10^{-3} S/m; d – 3×10^{-3} S/m; e – 10^{-2} S/m; f – 3×10^{-2} S/m; g – 0.1 S/m; h – 0.3 S/m; i – 1 S/m; j – 3 S/m). In solutions whose conductivity reaches that of the cytosol (curve i) the second peak is suppressed. When the conductivity greatly exceeds that of the cytosol (curve j), two anti-field peaks are observed. To obtain most information, rotation spectra should be measured at a range of concentrations.

In addition to the general behaviour outlined above, rotation spectra can contain signatures from such features as cell walls, large organelles, surface structure and membrane mobile charges. This allows the spectra to be used in a variety of investigations

capacitance and inductance the resonant frequency can be lowered and the effect put to use. Most of the devices described here need to be energised with only a few volts and such drives are easy and cheap to generate. A few, however, need higher voltages, up to about 100 V. Such voltages can be produced in the device itself from a low voltage source by the correct control of resonance, circumventing the need for expensive high-voltage generators.

A typical example of a resonance assisted device might be a cell separator designed to discriminate between cells which have only a small difference in dielectric properties. The cross over frequencies from positive to negative DEP will be similar but not identical for the two cells. By working at a frequency between the two crossovers it is possible to separate the cells but the forces produced will be small unless very high fields are used (Fig. 10). Controlled resonance can be used to boost the fields at the working frequency.

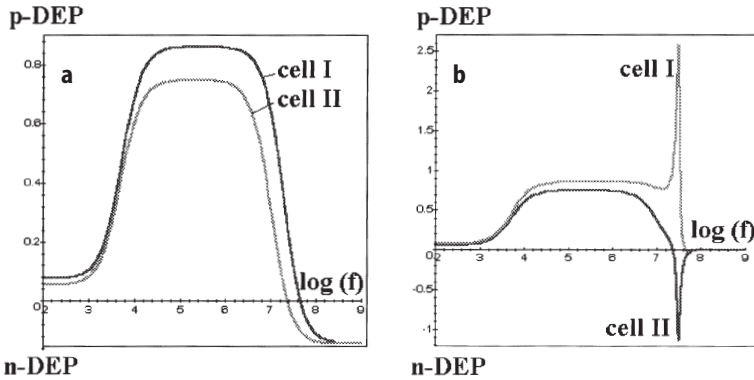


Fig. 10. Modifying the resonances in an electrode system can be useful when two cell types have only small differences in passive electrical properties and in dielectrophoretic force spectra. The best frequency to achieve a separation lies near the crossover frequencies when one cell is showing positive DEP and the other negative. But at such a frequency the forces are small. By suitable adjustment of capacitive and inductive elements at each electrode, it is possible to make a system resonate at the desired frequency, thereby increasing the drive voltage (and force) many fold without the need for expensive high voltage signal generators. The real dielectrophoretic force spectra (a) can be transformed into effective spectra (b)

4 Adherent Cells

4.1 Fibroblasts as Model Cellular Systems

Many cells of medical and pharmaceutical importance grow adherently. Typical examples are macrophages and fibroblasts. These human and animal cells have quite different properties to the cells of plants and bacteria (Fig. 11). First, they do not have a cell wall and, as a consequence, they do not have a well defined and constant shape. Rather, a cell's shape is determined by its cytoskeleton, a network of protein fibres which is dynamically controlled by the cell itself. It is this feature which allows directed movement and allows the cell to change shape in response to its environment. A second feature is that a high degree of surface structure is found in these cells, microvillae are common. Cells adhere to (some) surfaces or to each other within seconds of contact (Fig. 11 a–d). Cells also migrate over surfaces at speeds of several $\mu\text{m}/\text{h}$. Both processes are actively controlled. Cell division is a rupture utilising the forces acting on the substrate surface and, indeed, cells will only divide when suitably anchored (Fig. 12).

It was shown over two decades ago that animal cells could grow and develop on artificial substrates. “In vitro cell culture” is now a routine process in medical, pharmaceutical and biological laboratories world-wide. However, the glass and plastic substrates are not structured and cell growth and migration are random. Photo- and e-beam-lithography are capable of structuring surfaces on the sub-micrometer scale and this opens up possibilities for directed cell growth and movement.

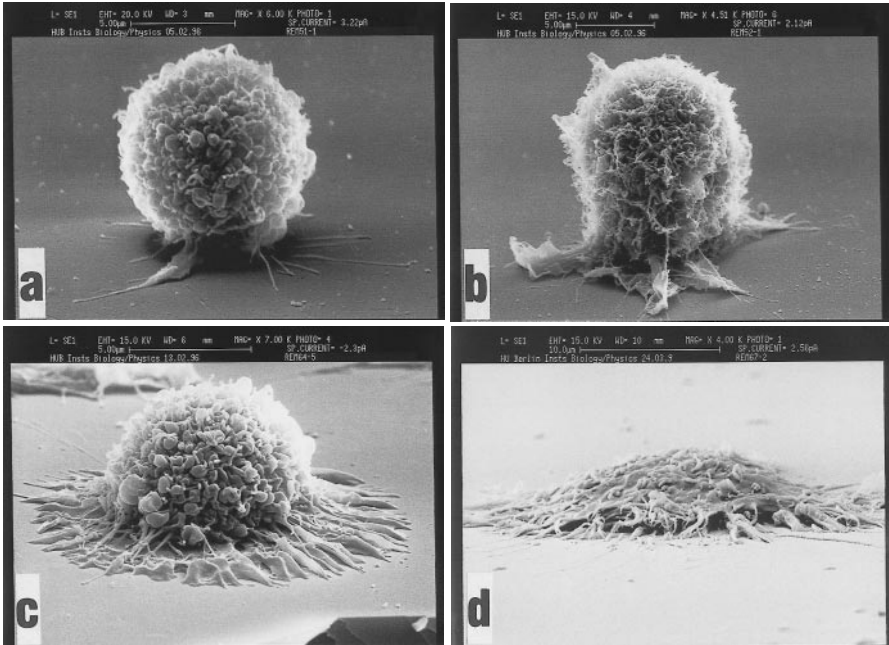


Fig. 11. Scanning electron micrographs (a–d) shown sequential stages in the early part of the adhesion process for mouse fibroblasts from initial contact with a surface to the assumption of a more or less final morphology. The cytoskeleton has the ability to change cell shape quickly and an individual cell may pass from the initial spherical form to the final flattened one in a few minutes. The initial adhesion process at the points of contact between cell and surface is also very rapid but there are subsequent changes at the adhesion sites affecting the nature and strength of the bonds which may continue for many hours. These can be studied by TIRF microscopy

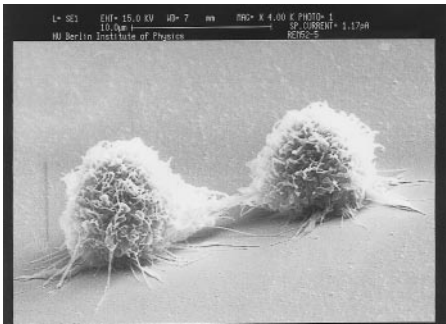


Fig. 12. In this scanning electron micrograph of the final stage of cell division both daughter cells are more or less spherical and adhering to the surface by filopodia. After disrupting the connecting filaments they will flatten and start migration over the surface with velocities of several micrometers per hour

4.2 Cell Migration

The process of cell migration is essential for organisms. Macrophages migrate continually through body tissues and capillary walls to attack cells and particles marked by the immune system and fibroblasts move to fill gaps in tissue during wound healing.

The molecular mechanisms of cell migration are complex but are becoming understood (Fig. 13). Contact is mediated by cadherins and integrins, two families of membrane proteins with special binding epitopes. On the cytoplasm side of the membrane, vinculin and other macromolecules serve to link the integral membrane proteins to the cytoskeleton. Aggregation and deaggregation of micro-tubuli generate cell motion and determine its direction while material is actively recycled from the back of the cell to the front. The process is controlled to produce a strong binding at the front edge of the cell and weaken that at the back.

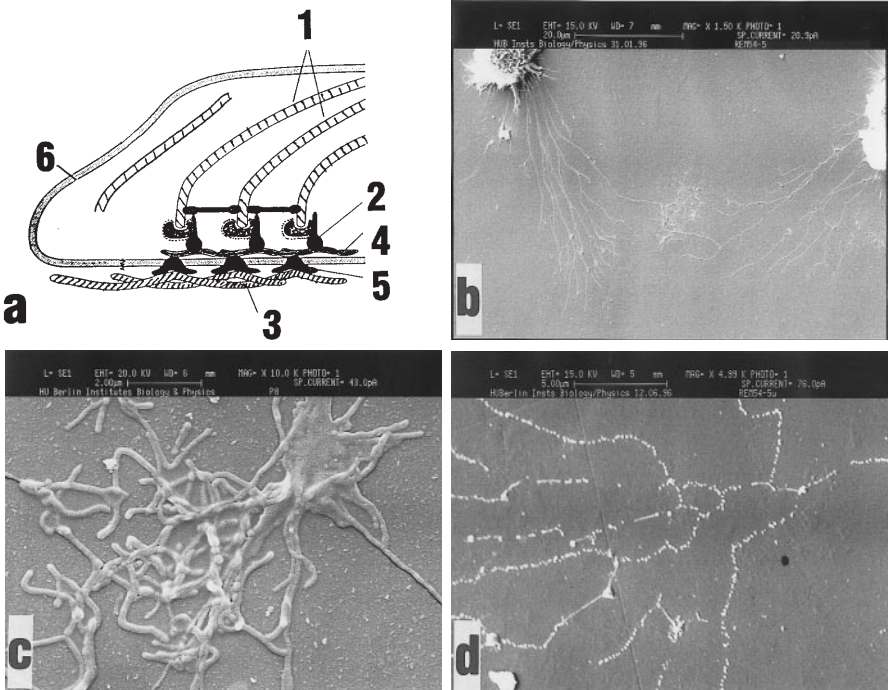


Fig. 13. **a** Schematic description of the molecules involved in the processes of cell adhesion and migration. Inside the leading edge of the cell, actin filaments (1) are connected via vinculin (2) and talin (4) to integrins, a family of proteins (5) which span the membrane (6). Outside, the integrins have epitopes which normally bind to fibronectin (3) but they can also adhere to artificial surfaces. At the other end of the cell the molecular contacts are broken and the material is recycled. **b** On artificial surfaces recycling is hindered and cell trails can be observed. **c** and **d** Under higher resolution cell trails are seen to be filament like structures or patches

Cells also migrate on artificial surfaces like silicon or glass but there is a difference. When a cell migrates over another cell, adhered material is scavenged and reincorporated into one or other partner. A cell migrating on an artificial surface loses material and leaves a trail. These trails can be investigated by total internal reflection fluorescence (TIRF, see legend to Fig. 19) microscopy and atomic force microscopy as well as by scanning electron microscopy. Typically, strips or tubes of material of about 200 nm dimension and membrane patches are left on the surface. Different kinds of cell leave different trails and the properties and structuring of the surface also have an effect.

The trails left by cells are unavoidable and they can influence the long-term stability of micro-systems, especially sensors. But they can also be used to advantage. Since a trail is characteristic of the cell which made it, trails can be used to identify cells, if necessary on an "occasional monitoring" basis. Also the rate at which trails appear in a unit area can give information about cell vitality or the effect of pharmaceuticals.

4.3

Artificial Control of Cell Migration

Cell-based micro-systems would be greatly advanced if ways could be found to control the direction, speed and timing of cell migration. Cells interact by direct surface contacts and by releasing transmitters which affect neighbouring cells. Achieving some measure of control over these processes on a cell by cell basis would, ultimately, lead to such things as artificial tissues and working neural nets [1, 2]. More immediately, even a very crude level of control of cell adhesion, growth and movement could be used to direct cells to the correct place in a device and to avoid cells clustering and blocking channels.

Three kinds of method are currently under investigation in different laboratories:

1. Surfaces can be treated to provide chemical cues to the cells (by e.g. coating with thin films containing charged molecules).
2. Surfaces can be microstructured to provide topographic cues to the cells [59,60].

Both these methods are essentially static in that once a device has been manufactured its characteristics cannot be changed.

3. A third possibility is the use of high frequency electric fields to shield areas of the device.

Examples of these techniques are shown in Fig. 14.

Electrical forces are not strong enough to dislodge a cell once it has attached to a surface. But they can be made strong enough to prevent the initial contact since fields near a surface can be very large and very non homogeneous. A simple array of parallel conductors with a spacing of a few hundred nanometers is particularly useful. With this geometry, fields can rise from virtually zero at 1m above the electrode plane to several MV/m in the plane itself. When such an array is energised at MHz frequencies, cells are strongly repelled [38]. Alterna-

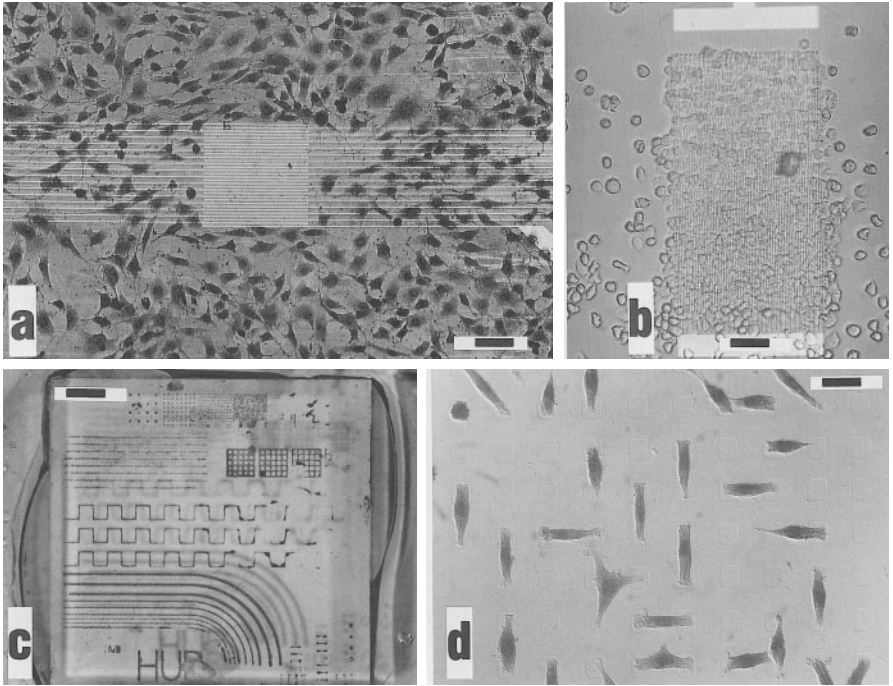


Fig. 14. Two of the possible methods for controlling adherent cells are illustrated here. **a** The electric field in the area of electrode interdigitation is of a frequency which produces strong negative DEP. Cells cannot settle onto this area and so grow elsewhere. (They may eventually migrate across the surface into the central region as the electrical force is not strong enough to prevent active cell movement.) The bar is 50 μm . **b** This is a similar electrode system to that shown in **a**) except that the frequency has been chosen to produce positive DEP. Cells are attracted to the interdigitated area where they grow in several layers. This photograph was taken two days after the abdominal implantation of the device in a pig. Most of the cells are macrophages. The bar is 50 μm . **c** This 9 \times 9 mm chip is made from glass (to which cells can adhere) coated with a thin plastic layer (to which they cannot). The plastic layer has been structured by laser ablation to expose the glass in places. Cells cultivated on this structure grow only in the cleared areas and show up as *dark lines* and *points*, following the underlying pattern. **d** Magnified detail from the upper part of **c**. The small, laser-cleared squares which are visible are of 10 μm side. Suitable choice of the size and spacing allows cells to be aligned and ordered

tively, at lower frequencies, cells can be attracted to the electrodes by positive DEP.

For the reasons given in Sect. 2, heating is not a problem with devices of this kind. (In fact, the situation is favourable since the heat is generated very close to the cooling surface). Even with animal cells in highly conductive (several S/m) culture media, fields of 50 kV/m or more can be used.

4.4

Long Term Exposure of Cells to Electric Fields

If cells are to be used long-term in electrical devices, especially for medical applications, then the effect of electric fields on cells must be considered. Possible effects of fields on cells are summarised in Fig. 15. It is important to distinguish between processes occurring within the cell itself, those occurring in the membrane and those which are external. It is also necessary to discriminate

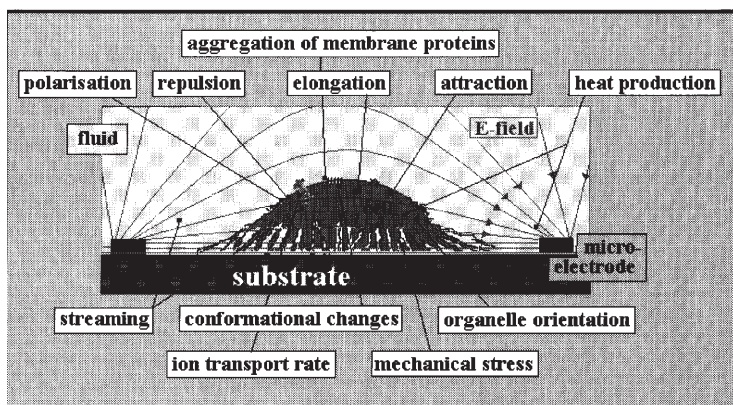


Fig. 15. The possible mechanisms by which a strong electric field can affect cells in suspension or adherently growing. Most of the heat is produced near the electrodes and, therefore, tends not to be a direct problem as it can be easily dissipated into the substrate. This heating can, however, induce convection currents which, in turn, may impose mechanical stress on an adherent cell. There is also some heating between the electrodes. At low frequencies, this occurs only in the medium although it may be concentrated in regions surrounding the cell. At high frequencies, this heating becomes more uniform but, because high frequency currents can flow inside the cell, there is some internal heat production. The total amount of heat evolved depends on the conductivity of the medium and on the square of the applied voltage.

At low frequencies, the external field induces an alternating voltage which is superposed on the resting (dc) transmembrane potential. As frequencies rise and the membrane capacitance dominates its electrical behaviour, this induced voltage drops to a very low level.

The dielectrophoretic (or electro-rotation) force imposed on an adherent cell is not strong enough to dislodge it from the substrate. The force will, however, create mechanical stress in the immobilised cell. At higher frequencies (when there is a field inside the cell) a force may also be imposed on organelles. The dielectrophoretic force tends to be small as the internal field is fairly uniform but with rotating fields it is sometimes possible to observe distortion or rotation of large organelles.

The frequencies used are well below those needed to induce electronic or vibrational transitions in molecules. But it is possible that an alternating field might produce a quivering motion of, say, a protein as the molecular dipoles attempt to align with the field. In the vast majority of cases, the energy involved would be less than the random thermal energy of the molecule but the strongest possible fields might just have a noticeable effect on the most polarised species. Effects on proteins are much more likely to be indirect, mediated by the induced membrane potential or by mechanical stress. Possibilities include the aggregation/deaggregation of membrane proteins, conformational changes and "knock-on" effects such as changes in ionic transport rates

between thermal effects and true electrical ones. Microstructures allow the investigation of these matters under well defined conditions of field distribution and heat production. Indeed, the experiments are only possible in microstructures as high fields applied to physiological solutions in macroscopic devices will produce boiling (see Sect. 2.3) and the use of low-salt solutions brings its own artefacts to the problem.

Electrical breakdown of the membrane sets an upper limit on the fields that can be applied. Controlled electrical breakdown of the membrane is a fairly well understood process which is used in the techniques of electrofusion and electroporation but it is clearly undesirable in the devices under discussion. Surprisingly, fibroblasts can be cultivated for days with no apparent adverse effects in fields inducing *trans*-membrane potentials of 80 % of the breakdown voltage (unpublished data).

The induced *trans*-membrane potential varies with frequency, being highest at low frequencies (Fig. 16a). At high frequencies, very high fields can be applied and this allowed investigation of thermal effects as it is possible to produce local heating of the solution by 1 or 2 °C. Fibroblasts will only grow in the temperature range 30–40 °C. When a device is at a temperature just below the lower limit of this range, cells will only survive in the warm area between the electrodes (Fig. 16b). With the device just below the upper limit, the electrode area remains clear (Fig. 16c). At first sight, either figure alone might be taken to indicate an electrical effect on the cells but the two together show that the process is thermal. The heating produced by the electrical currents in a microdevice can be quite localised and it is very controllable. In principle, it offers one possibility for cell growth guidance.

The experimental results indicate that sustained, high frequency electric fields in the kV/m range do not have gross deleterious effects on fibroblasts. The cells will grow, divide and migrate, apparently normally [40]. There are many potential mechanisms by which an electric field might have subtle effects on a cell. For instance, at high frequencies, external fields produce currents within the cell itself and these currents will cause heating. Also, the dielectrophoretic force acting on an anchored cell will cause mechanical stress and it is possible, in principle, for an electric field to affect ion carriers and transport proteins within the membrane. Microstructures are a necessary tool for investigating these possibilities and for exploiting any phenomena which might be found [61].

4.5

Micropores

Square pores can be made in a monocrystalline silicon membrane by the process of anisotropic etching. The accuracy of the technique lies in the submicron range. Fibroblasts moving on the membrane surface show interesting behaviour when they encounter a pore, Fig. 17. It is possible for a cell to bridge across a pore (staying on the same side of the membrane). It is also possible for a cell to travel through the pore to the other side of the membrane. To do so it must negotiate edges with angles of more than 270 degrees. In some cases, there must be con-

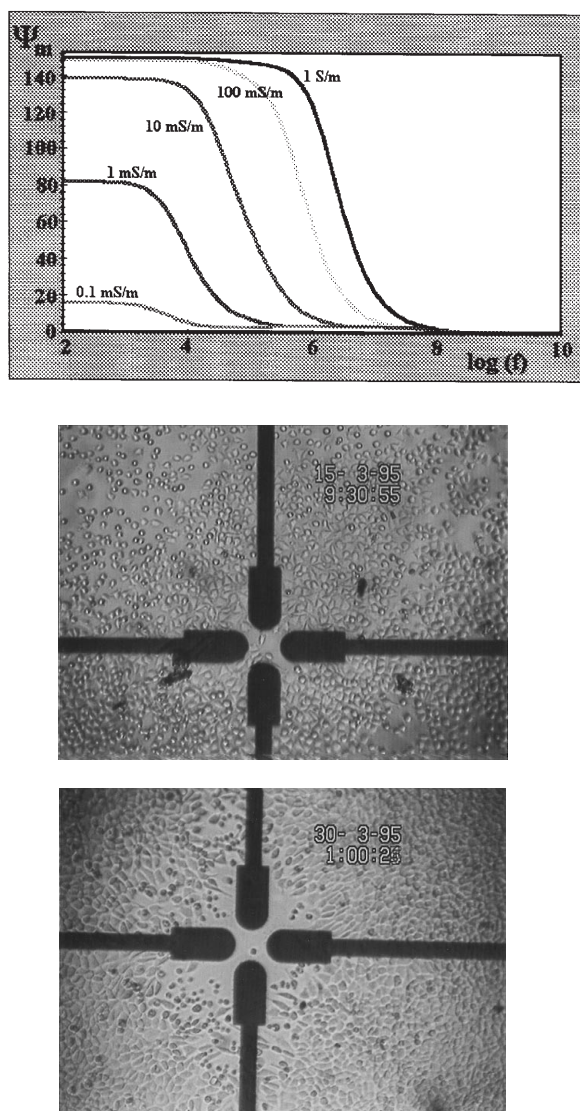


Fig. 16. *Top* The illustration shows the variation of the induced transmembrane potential of a cell with frequency and with the conductivity of the external medium. The induced potential increases with external conductivity. However, it also decreases with frequency and above about 5 or 10 MHz the induced potential has fallen below 10 mV in most practical cases. Cells can be cultivated for days in fields of high MHz frequencies.

Centre Fields may have thermal as well as direct electrical effects on cells. This chip is cultivated at 30 °C, too cold for fibroblast growth. An electric field (50 kV/m) in the area of electrodes interdigitation warms this zone, taking it to a tolerable temperature. Cells near the electrodes are both more numerous than elsewhere and have the characteristic flattened shape. Cells further away have a more spherical, inactive form.

Bottom This chip is cultivated at 40 °C, just below the upper temperature limit for fibroblasts. The electric field again raises the temperature locally, creating a zone where cells cannot grow

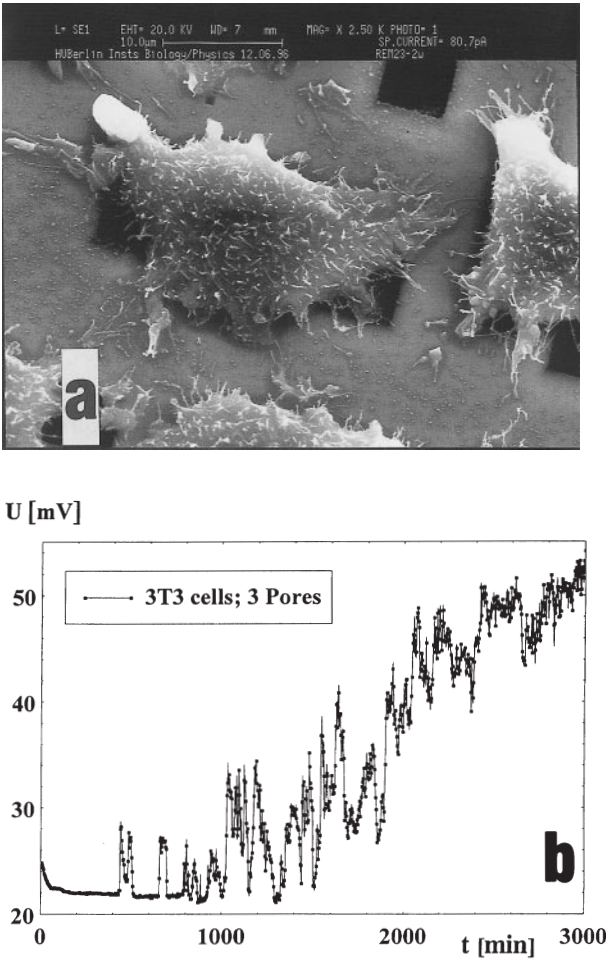


Fig. 17. **a** A scanning electron micrograph of square pores etched in a 3 micrometer thick silicon membrane. The pores were produced by anisotropic etching and their width on this side of the membrane is 6 μm . Cells (fibroblasts 3T3) attach to the surface and migrate over the pores. **b** Electrodes are placed on either side of the membrane and a constant current passed through it (mainly through the pores). The presence of cells is easily detected and movements of cell filopodia of less than 100 nm and the passive electric properties of the cell body can be determined by analysis of the signal fluctuations and impedance

siderable additional deformation because a fibroblast can traverse a pore smaller than the typical cell body dimension. A third possibility is that the cell lodges within the pore and extends filopodia to the other side.

The case of a cell in or near a pore presents an excellent geometry for the measurement of impedance since any electrical currents must flow through the pore provided the silicon is suitably insulated. Any movement of the cell will result in a change of the impedance measured between one side of the mem-

brane and the other. The ideal situation occurs when the pore size has been chosen so that a cell lodges within. In this case, movements of filopodia of less than 100 nm can be detected [62].

Since cell and filopod movement depends on the chemical environment of the cell, a pore-impedance device could function as a chemosensor for substances of medical and pharmacological importance, especially if the cells themselves have been genetically engineered for the purpose. Another use of such a device would be the study of cell-cell interactions as different kinds of cell could be separated by the membrane and allowed to interact through the pore.

The pore-based device has two main advantages over systems which try to acquire the same information from unaided microelectrodes. In a pore-impedance device, the size and position of the electrodes is relatively non-critical, the electrodes can be made large enough to avoid polarisation problems. Secondly, the pore itself is robust and formed in an inert material, it is not destroyed by attack from the cells and is fairly resistant to accidental damage. It may become blocked by a cell but it is easily cleaned after use.

Electrodes and pores can be arranged in several ways. A single pore can be interrogated by its own electrode pair. This gives unambiguous information about a single cell. A few (between 2 and 4) pores can be addressed by a single pair of electrodes. Usually, this will give information about a single cell but with an enhanced chance of getting a suitably positioned cell in the device. A large number (hundreds or thousands) of pores can have a common pair of electrodes which give an averaged signal from a large cell population. It is also possible to imagine a device one side of which is a series of channels, each with its own electrode and a pore through to a common space on the other side of the "membrane". This would allow many (possibly different) measurements to be made simultaneously.

5 Cryo-Conservation

Cryo-conservation of cells is a standard laboratory technique. A properly frozen cell suspension can be stored for years if necessary at liquid nitrogen temperatures. However, in a suspension, the position of an individual cell is unknown, as are the temperature gradients to which a particular cell has been subjected. For some purposes it would be advantageous to freeze cells in known positions. An example would be a diagnostic device, pre-cultivated with the correct cells in position on the sensor elements. In fact, devices incorporating living cells will probably only find wide application if they can be stored stable for long periods and easily transported. The use of liquid nitrogen for this purpose seems attractive.

5.1

Cryo-Conservation of Cells in Micro-Structures

There are three problems to be avoided:

1. Damage to the micro-structure during freezing and thawing.
2. Damage to the cells during freezing and thawing.
3. Loss of cell adhesion.

Damage to the microstructure is fairly easy to avoid. Liquid containing structures cannot be sealed during freezing and materials must be carefully chosen. Both silicon and quartz are stable under the conditions met during the fast freezing and thawing of cells. Despite the fact that both these materials have thermal expansion coefficients smaller than those of metals, many metalizations also seem to be stable. Silicon is especially suitable for this kind of work due to its high thermal conductivity.

Cells in suspension must be frozen rapidly in order to encourage the formation of small ice crystals rather than the large ones which would rupture membranes. The same principle holds for cells attached to surfaces but there is a complication. When cells are frozen in suspension, it is usual to choose conditions which promote some degree of cell shrinkage to prevent rupture of the cell membrane (Fig. 18). However, shrinkage of a cell adhered to a surface creates

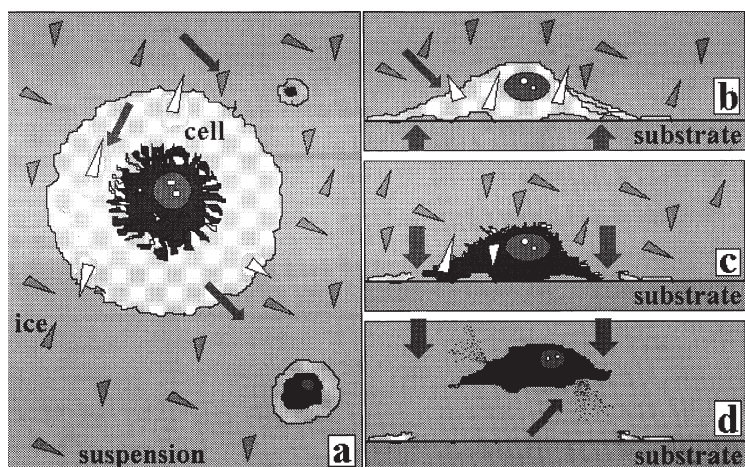


Fig. 18. Diagrams illustrating the differences and difficulties during freezing of cells in suspension (a) and on surfaces (b, c and d). In both cases, large ice crystal formation must be avoided, this means that freezing must be rapid and often involves the use of cryo-protectants. In suspension, the use of hypertonic solutions to shrink cells by osmosis helps to avoid membrane rupture. But with cells fixed to surfaces, shrinkage can lead to rupture of the filopodia or to parts of cytoskeleton or cell membrane (c). Additionally, animal cells under stress (including this kind of osmotic stress) tend to build up into a spherical shape. This means they would lose many of their surface contacts before freezing and disappear into solution after re-thawing. Cryo-conservation of adhered cells in defined positions requires very precise control of the conditions

mechanical stress and can rupture the filaments of the cytoskeleton. It is therefore necessary to control osmotic and ionic conditions very carefully to achieve a constant cell size during freezing. When this is done, survival rates of fibroblasts frozen on glass or silicon surfaces can be higher than 80%.

The maintenance of cell adhesion is also vital and therefore it is of fundamental interest to visualise the adhesion points and understand the dynamics of the process.

5.2

Cell Adhesion Patterns

For biotechnological purposes, it is necessary not only that cells remain viable but also that adhesion is maintained so that a cell can be found in the expected position. The adhesion pattern that a cell has adopted before freezing is crucial to successful cryo-preservation. Adhesion patterns can be visualised by (TIRF microscopy, [63]) mentioned above and also by confocal laser scanning fluorescence (CLSM, [64]) microscopy. We have investigated the adhesion patterns of fibroblasts as a function of adhesion time and various surface treatments [65]. Some examples are shown in Fig. 19.

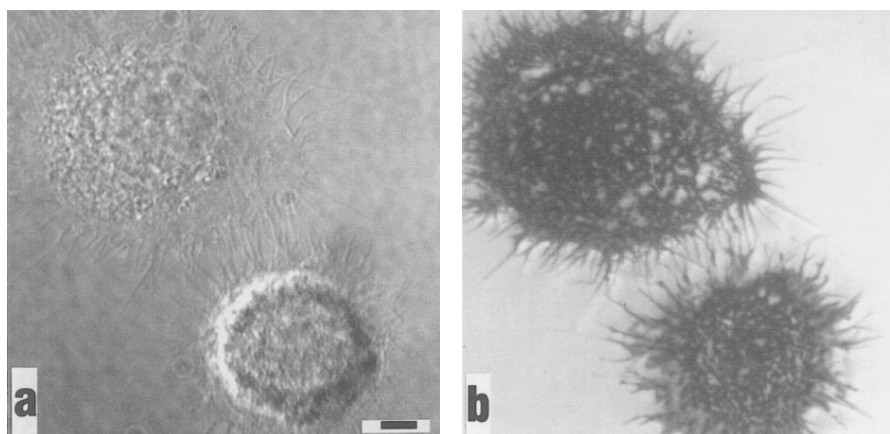


Fig. 19 a, b. This set of photographs illustrates the complexity of cell adhesion. **a** Two fibroblasts growing on a polylysine coated glass plate as seen in transmission microscopy. (Polylysine promotes cell adhesion by creating a surface rich in negative charge.) The bar is 4 μm . **b** The same cells seen by total internal reflection fluorescence (TIRF) microscopy. The TIRF technique utilises the evanescent wave produced in the solution when light strikes the glass/solution interface at a shallow angle and undergoes “total” internal reflection. The evanescent wave exists only near the surface and is used to excite fluorescence in the fluorescein-containing culture medium. Areas where a cell has contacted the surface and excluded the solution therefore appear dark against a light background. These polylysine fixed cells contact the surface (with gaps of less than 10 nm) over most of their area and therefore have little freedom of movement

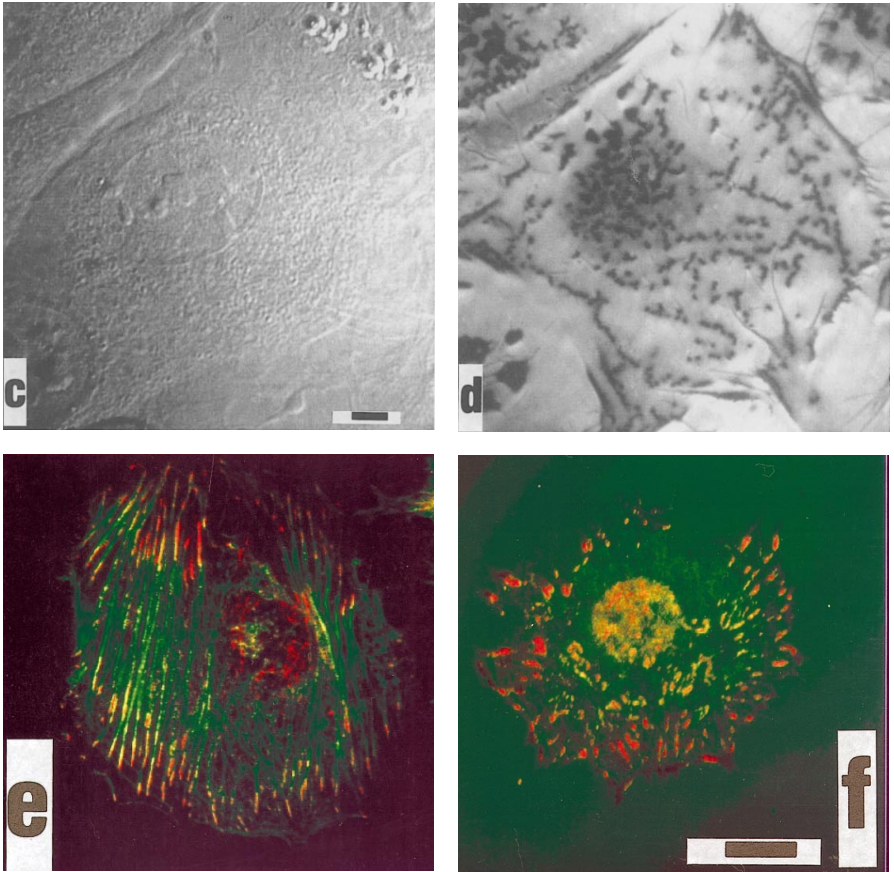


Fig. 19 c–f. **c** Transmission micrograph of a cell growing on glass with no polylysine coating. The bar is 4 μm. **d** The same cell as in **c** visualised by TIRF microscopy. The strongly localised adhesion plaques are clearly visible. **e** This confocal laser scanning image shows the actin filaments of the cytoskeleton labelled immunofluorescently. **f** Vinculin, which connects the cytoskeleton to the adhesion molecules, is here shown fluorescently labelled under the confocal laser scanning microscope. The bar is 5 μm

As well as visualisation, quantitative measurements are necessary in order to understand the adhesion process. One possible method involves streaming the cells over a surface and measuring the maximum speed of flow at which adhesion can occur [see 64]. Another technique uses the atomic force microscope for measurements at a single molecule [66].

We have developed a new micro-system using rotating electric fields for measuring adhesion (unpublished data). A schematic representation of this is given in Fig. 20. A cell is allowed to sediment onto a surface which carries four electrodes. The electrodes are driven to produce a field which rotates at MHz frequencies, but the direction of rotation is periodically reversed. This leads to a

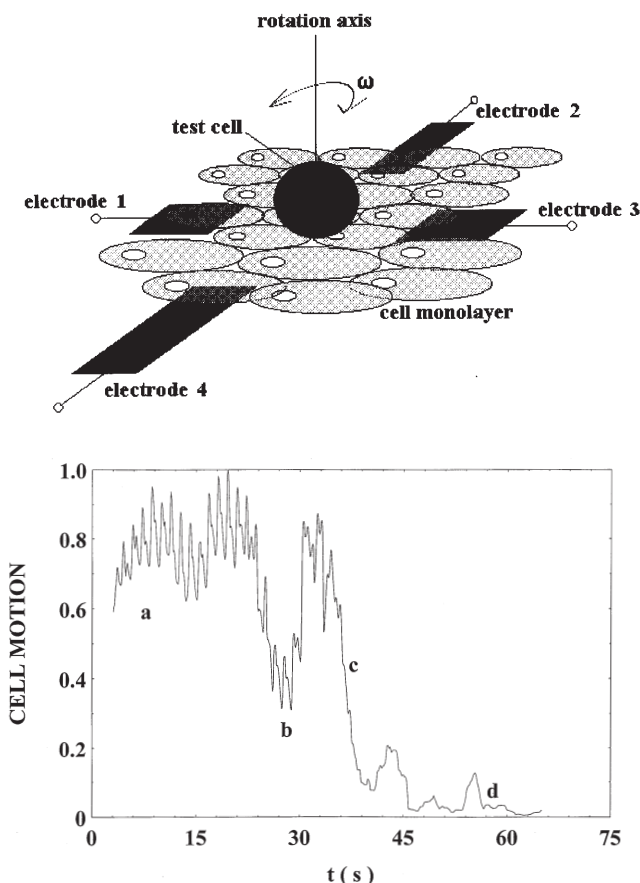


Fig. 20. A diagram of the measurement of cell-cell adhesion and a measured curve. **a** The substrate with four planar electrodes is first prepared as desired, e.g. a cell monolayer could be grown. A high frequency electric field (say 10 MHz) used to spin a test cell about an axis perpendicular the surface. As this cell sediments, its rotation velocity is measured. This allows the calculation of the induced torque from the frictional torque ($N = 8\pi R^3 \eta \omega$, where η is the viscosity of the solution, R is the cell radius and ω the angular velocity of the cell). After reaching the surface, the test cell is driven alternately clockwise and counter-clockwise (initially through 45° to avoid large shearing forces). As the test cell forms more molecular contacts with the cells of the monolayer, the amplitude of the oscillation becomes smaller and smaller until the cell is immobilised. The cell motion can be detected automatically by noise analysis. **b** The example shown is the adhesion process of a fibroblast sedimenting on a cleaned glass surface. The graph is of normalised amplitude of cell oscillation vs time. The curve can be divided into four main parts:

- a** The first molecular contacts occur but there is no fixation.
- b** There is transient fixing.
- c** The cell undergoes rapid adhesion.
- d** With an increasing number of contacts and flattening of the cell body, the specimen becomes immobilised.

The advantages of this method are that the cell is in a known position and that the torque applied has been accurately calibrated.

slow clockwise/anticlockwise oscillation of the cell. The torque applied to the cell can be deduced from measurements of the amplitude of oscillation as the cell sediments toward the surface. When the cell reaches the surface and molecular contacts develop, the amplitude of oscillation is reduced until, finally, the motion is abolished by adhesion.

6 Perspectives

Microstructure based biotechnology is a fascinating field of research which is beginning to produce its first applications. It is not a simple down-scaling of existing techniques but an attempt to find new cell handling methods and to create new interfaces between living material and inanimate objects.

The first practical applications are likely to include field cages for cell positioning, inexpensive cell sorters and single cell cultivation depots. But once the basic elements for cell handling have been developed, very many kinds of device will become easy to produce. We can expect to see new systems for use in medical diagnosis and pharmaceutical testing within the next decade and a range of cell based biosensors.

Microtechnology continues to develop and new techniques such as three dimensional structuring by laser ablation and deposition will doubtless be used in bio-systems opening up a new range of possibilities.

Looking further ahead, the understanding of and the ability to control cell-surface and cell-cell interactions is the key to developing much more sophisticated devices such as those incorporating biological contractile elements and even working neural nets. Ultimately this road might even lead to artificially grown tissues and organs. Microstructures have a bright future in the biological world.

Acknowledgements. We would like to thank the following people for the use of the photographs and diagrams shown here.

Dr. S. Fiedler (Fig. 4; 5c–e, g, i; 6; 8a)

H. Glasser (Fig. 16b, c; 20b)

Dr. R. Hagedorn (Fig. 17b)

J. Hornung (Fig. 19a–d)

Dr. T. Müller (Fig. 14a, b)

Dr. E. Richter (Fig. 1a; 11; 12; 13b–d; 14c, d)

Dr. Th. Schnelle (Fig. 3; 8b)

Our thanks also go to Dr. B. Wagner and I. Lisec of the Fraunhofer Institute für Siliziumtechnologie for the fabrication of multi-layer structures by photo- and e-beam-lithography and for the anisotropic etching of silicon membranes.

7 References

1. Fromherz P, Offenhäusser A, Vetter T, Wels JA (1991) *Science* 252:1290
2. Weis R, Müller B, Fromherz P (1996) *Phys Rev Lett* 76:327
3. Pohl HA (1978) *Dielectrophoresis*. Cambridge University Press, Cambridge, 1978
4. Sauer FA, Schlögl RW (1985) Torques exerted on cylinders and spheres by external electromagnetic fields: A contribution to the theory of field induced cell rotation. In:

- Chiabrera A, Nicolini C, Schwan HP (eds) Interactions between electromagnetic fields and cells. Plenum, New York, p 203
5. Pauly H, Schwan HP (1959) *Z Naturforsch Teil B*, 14:125
 6. Washizu M, Jones TB (1994) *J Electrostat* 33:187
 7. Sauer FA (1983) Forces on suspended particles in the electromagnetic field. In: Fröhlich H, Kremer F (eds) *Coherent Excitations in Biological Systems*. Springer, Berlin Heidelberg New York, p 134
 8. Sauer FA (1985) Interaction-forces between microscopic particles in an external electromagnetic field. In: Chiabrera A, Nicolini C, Schwan HP (eds) *Interactions between electromagnetic fields and cells*. Plenum, New York, p 181
 9. Pastushenko VPh, Kuzmin PI, Chizmadshv YuA (1985) *Stud Biophys* 110:51
 10. Fuhr G, Zimmermann U, Shirley SG (1996) Cell motion in time-varying fields: principles and potential. In: Zimmermann U, Neil GA (eds) *Electromanipulation of cells*. CRC Press, Boca Raton, p 259
 11. Harrison DJ, Fluri K, Seiler K, Fan Z, Effenhauser CS, Manz A (1993) *Science* 261:895
 12. Ashkin A (1970) *Phys Rev Lett* 24:156
 13. Ashkin A, Dziedzic JM (1987) *Science* 235:1517
 14. Ashkin A, Dziedzic JM, Yamane T (1987) *Nature* 330:769
 15. Buican TN, Smyth MJ, Crissman HA, Salzman GC, Stewart CC, Martin JC (1987) *Applied Optics* 26:5311
 16. Block SM, Goldstein LSB, Schnapp BJ (1990) *Nature* 348:348
 17. Tadir Y, Wright WH, Vafa O, Ord T, Asch RH, Berns MW (1990) *Fertil Steril* 53:944
 18. Pethig R (1991) *Institute of Physics Conference Series* 118:13
 19. Washizu M (1992) *J Electrostat* 29:177
 20. Molinari G, Viviani A (1978) *J Electrostat* 5:343
 21. Jones TB (1995) *Electromechanics of Particles*. Cambridge University Press, Cambridge
 22. Irimajiri A, Hanai T, Inouye A (1979) *J Theor Biol* 78:251
 23. Derjaguin BV, Churaev NV, Muller VM (1985) *Poverkhnostnye Sily, Moskva, Nauka* 322
 24. Fiedler S, Hagedorn R, Schnelle Th., Richter E, Wagner B, Fuhr G (1995) *Anal Chem* 67:820
 25. Pohl HA, Hawk I (1966) *Science* 152:647
 26. Glaser R, Pescheck C, Krause G, Schmidt KP, Teuscher L (1979) *Z. f. Allgemeine Mikrobiologie* 19:601
 27. Robinson R (1969) The early history of the electrodeposition and separation of particles. In: Pohl HA, Pickard WF (eds) *Dielectrophoretic and electrophoretic deposition*. The Electrochemical Society, NY, p1
 28. Zebel G (1965) *J Colloid Sci* 20:522
 29. Hall HJ, Brown RF (1966) *Lubrication Engineering* 488
 30. Verschure RH, Ijlst L (1966) *Nature* 211:619
 31. Benguigui L, Lin IJ (1982) *Sep Sci Technol* 17:1003
 32. Lin IJ, Benguigui L (1982) *J Electrostat* 13:257
 33. Jones TB, Kallio GA (1979) *J Electrostat* 6:207
 34. Kaler KVIS, Jones TB (1990) *Biophys J* 57:173
 35. Jones TB, Kraybill JP (1986) *J Appl Phys* 60:1247
 36. Kaler KVIS, Xie J-P, Jones TB, Paul R (1992) *Biophys J* 63:58
 37. Jones TB, Bliss GW (1977) *J Appl Phys* 48:1412
 38. Fuhr G, Müller T, Schnelle Th, Hagedorn R, Voigt A, Fiedler S, Arnold WM, Zimmermann U, Wagner B, Heuberger A (1994) *Naturwissenschaften* 81:528
 39. Schnelle Th., Hagedorn R, Fuhr G, Fiedler S, Müller T (1993) *Biochim Biophys Acta* 1157:127
 40. Fuhr G, Glasser H, Müller T, Schnelle Th (1994) *Biochim Biophys Acta* 1201:353
 41. Fuhr G (1995) *Proc. St. Andrews Meeting, Animal and Cell Abstracts C2.18*, p.77, St. Andrews
 42. Green N, Morgan H, Wilkinson CD (1995) *St. Andrews Meeting, Animal and Cell Abstracts C2.20*, St. Andrews, p.77
 43. Schnelle Th., Müller T, Fiedler S, Shirley SG, Ludwig K, Herrmann A, Wagner B, Zimmermann U (1996) *Naturwissenschaften* 83:172

44. Fiedler S, Schnelle Th, Wagner B, Fuhr G (1995) *Microsyst Technol* 2:1
45. Melcher JR (1966) *Physics Fluids* 9:1548
46. Melcher JR (1983) Electrodynamic surface waves. In: *Waves on fluid interfaces*, Academic Press, New York, p 167
47. Masuda S, Washizu M, Kawabata T (1988) *IEEE Trans Ind Appl* 24:217
48. Fuhr G, Hagedorn R, Müller T, Benecke W, Wagner B, Gimsa J (1991) *Studia Biophys* 140:79
49. Hagedorn R, Fuhr G, Müller T, Gimsa J (1992) *Electrophoresis* 13:49
50. Wang X-B, Huang Y, Becker FF, Gascoyne PRC (1994) *J Phys D Appl Phys* 27:1571
51. Gascoyne PRC, Pethig R, Burt JPH, Becker FF (1993) *Biochim Biophys Acta* 1149:119
52. Pethig R, Huang Y, Wang X-B, Burt JPH (1992) *J Phys D Appl Phys* 24:881
53. Gascoyne PRC, Huang Y, Pethig R, Vykoukal J, Becker FF (1992) *Meas Sci Technol*, 3:439
54. Pohl HA, Kaler K, Pollock K (1981) *J Biol Phys* 9:67
55. Arnold WM, Zimmermann U (1982) *Z Naturforsch* 37c:908
56. Arnold WM, Zimmermann U (1988) *J Electrostat* 21:151
57. Sukhorukov VL, Zimmermann U (1996) *J membrane Biol* 153:161
58. Gimsa J, Müller T, Schnelle Th, Fuhr G (1996) *Biophys J* 71:495
59. O'Neill C, Jordan P, Riddle P, Ireland G (1990) *J Cell Sci* 95:577
60. Curtis ASG, Clark P (1990) *CRC Revs Biocompatibility* 5:342
61. Giaever I, Keese CR (1991) *Proc Natl Acad Sci USA* 88:7896
62. Hagedorn R, Fuhr G, Lichtwardt-Zinke K, Richter E, Hornung J, Voigt A (1995) *Biochim Biophys Acta* 1269:221
63. Gingell D, Heavens OS, Mellor JS (1985) *J Cell Biol* 100:1334
64. Bongrand P, Claesson PM, Curtis ASG (1994) (eds) *Studying cell adhesion*, Springer Verlag, Berlin, Heidelberg
65. Hornung J, Müller T, Fuhr G (1996) *Cryobiol.* 33:260
66. Ducker WA, Senden TJ, Pashley RM (1991) *Nature* 353:239

Polynucleotide Arrays for Genetic Sequence Analysis

Rolfe C. Anderson · Glenn McGall · Robert J. Lipshutz

Affymetrix Inc, 3380 Central Expressway, Santa Clara, CA 95051.

E-mail: rolfe_anderson@affymetrix.com

We describe a new paradigm for genetic analysis based upon high density arrays of polynucleotide probes. Methods for light-directed polynucleotide array synthesis, as well as array packaging, sample preparation, array hybridization, epifluorescence confocal scanning, and data analysis are described. Applications to discovery, genotyping, expression, and resquencing are presented.

Keywords: Polynucleotide arrays, hybridization, sequencing, DNA chip.

1	Introduction	117
2	Array Fabrication	118
3	Applications	124
3.1	Design of Polynucleotide Arrays	125
3.2	HIV Resequencing Application	126
3.3	mRNA expression monitoring	127
3.4	Other Applications	128
4	Conclusion	128
5	References	128

1 Introduction

The Human Genome Program and related public and private research programs are rapidly determining the full sequence of the human genome and the genomes of other medically and economically relevant organisms. The motivation for these programs is the identification of new targets for therapeutic intervention, new diagnostic markers for human disease, and the development of improved agricultural and industrial products. The resulting databases provide the primary structural information for the genome; as such, they are the foundation of future research. The next phase is to associate functions with newly discovered genes.

Building on these databases, researchers are asking which genes are associated with human disease (discovery), where these genes are located within the genome (mapping), the extent to which the genes are being translated into protein (expression), and how the genes of individuals differ (genetic variation).

The existing tools to address these questions are slow and cumbersome. We describe a new paradigm for genetic analysis based upon high density arrays of polynucleotide probes. Methods for light directed polynucleotide array synthesis, as well as array packaging, sample preparation, array hybridization, epifluorescence confocal scanning, and data analysis are described. Applications to discovery, genotyping, expression, and resquencing are presented.

2 Array Fabrication

In the development of polynucleotide arrays for sequencing applications, one of the principal challenges has been to fabricate arrays of sufficient size and complexity with the highest possible density of encoded sequence information. To fabricate the high-density arrays needed for large-scale sequence-analysis applications, we have made use of light-directed synthesis [1–4]. In this technique, 5'-terminal protecting groups are selectively removed from growing polynucleotide chains in pre-defined regions of a glass support by controlled exposure to light through photolithographic masks. This approach can be applied to the synthesis of other biopolymers as well. The advent of this technology has made it possible to fabricate DNA probe arrays with densities as high as 10^6 unique probe sequences per cm^2 .

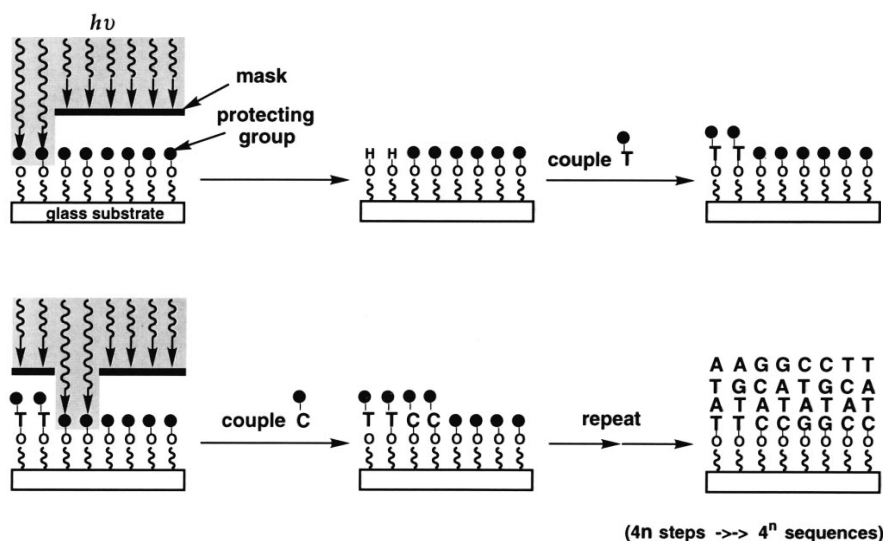


Fig. 1. Light-directed synthesis of polynucleotide probe arrays. Exposure to light through a photolithographic mask is used to remove protecting groups from surface sites in pre-defined regions of a functionalized glass substrate. A solution of an activated polynucleotide building block is then applied, which reacts specifically in the exposed regions of the substrate. Repeated cycles of illumination-deprotection and monomer coupling are used to construct a two-dimensional array of probe sequences

Figure 1 illustrates the overall process of photolithographic polynucleotide array synthesis. The process begins with a planar glass or silica substrate, which has been covalently modified with linker molecules bearing terminal hydroxyl groups to provide reactive sites for polynucleotide synthesis. Hydroxyl groups on the linker molecules are protected with a photolabile protecting moiety (see below). Specific regions of the surface, defined by a mask, are exposed to light, causing the selective removal of protecting groups from linkers exclusively in the illuminated regions. The entire substrate is then treated with one of four similarly protected nucleoside phosphoramidite building blocks (dA, dG, dC or T), activated using standard DNA synthesis protocols. The monomer reacts specifically with unmasked hydroxyl groups on the exposed regions of the substrate. Cycles of photo-deprotection and nucleotide addition are repeated to build the desired array of sequences. The process is very efficient: a simple combinatorial masking scheme [1, 2] (Fig. 2) will generate an array containing 4^n

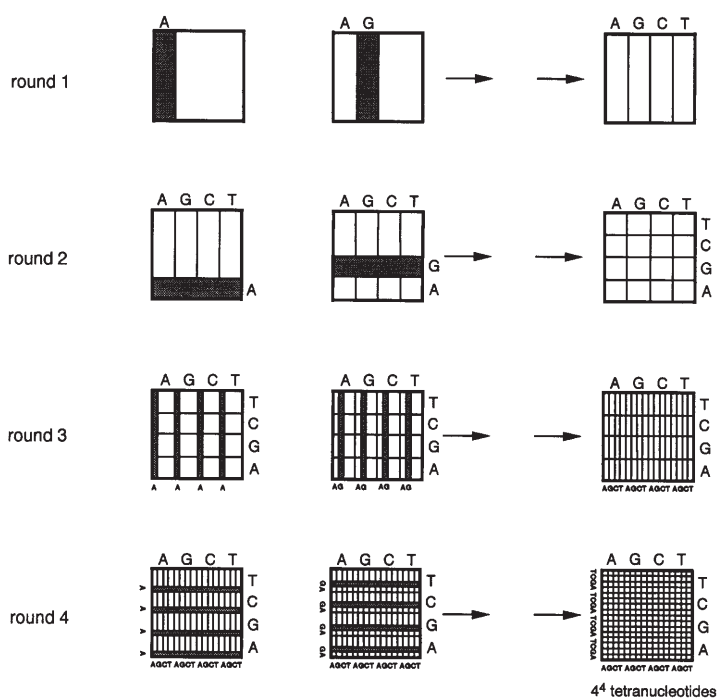


Fig. 2. Masking strategy for the combinatorial synthesis of all possible polynucleotide tetranucleotides. In *round 1*, a mask is used to add all four nucleotides, to four separate regions of the substrate, as the first base in the array. An orthogonal mask is used in *round 2* to subdivide each mononucleotide "cell" into quarters for the addition of the four nucleotides as the second base. This generates a 4×4 array of all possible dinucleotides. The mask used in *round 3* further subdivides the dinucleotide cells into quarters for the addition of the third base. After 4 rounds, an array of all 256 dinucleotides is obtained. This process can be continued, using masks which subdivide cells into increasingly smaller regions, to obtain complete arrays of longer polynucleotide sequences

unique sequences in only $4n$ chemical steps. For example, the complete array of all possible 10mer probes ($>10^6$ sequences) requires only 40 steps. Table 1 illustrates the relationship between the number of synthesis cycles and the total number of unique sequences of a given length that can be prepared. Although complete sets of polynucleotide probes of certain lengths are being studied for potential use in generic sequencing applications, current applications (see Applications Section) employ specific *subsets* of probes for detecting and/or resequencing known sequence fragments. However, any set of probes of length L or less (probe length can be varied within an array) can be synthesized using at most $4L$ chemical synthesis steps. A unique set of photolithographic masks can readily be generated for each specific probe array.

Currently, this process employs nucleoside phosphoramidite monomers in which the 5'-hydroxyl is blocked with a photo-removable MeNPOC [5] protecting group. The latter is based on a well-known class of photolabile 2-nitrobenzyl derivatives, and is well suited to the synthesis of DNA probes, since the photocleavage reaction occurs from an $n-\pi^*$ excited state resulting from irradiation with light in the near-UV region ($\lambda_{\max} \sim 350$ nm, $\epsilon = 5500$ M $^{-1}$ cm $^{-1}$). This has several advantages, including the ability to use filtered 365 nm I-line emission from readily available high-intensity collimated Hg light sources. The use of longer wavelengths also avoids potential photochemical modification of the DNA probes or quenching of the photolysis reaction due to electronic interactions between the nucleic acid bases and the MeNPOC excited state. Photolysis involves an intramolecular redox reaction which requires no special solvents, catalysts or coreactants (Fig. 3), and complete deprotection requires about one minute using standard photolithography exposure systems.

The stepwise efficiency of polynucleotide synthesis using this method is in the 92–96% range [2, 4]. These values reflect the chemical yield of the photochemical deprotection reaction after complete (exhaustive) photolysis. The other chemical reactions involved in the base addition cycles are essentially quantitative. For instance, a large excess of activated monomer and additional capping steps are used to make sure that no unreacted sites remain which can be extended in subsequent synthesis cycles. This ensures that significant levels of insertion or deletion sequences do not accompany the desired full-length probe sequences. Despite the presence of incomplete or "truncated" probes, the performance characteristics of the arrays when they are used for hybridization-based sequencing is very good. Array hybridizations are typically carried out

Table 1. Combinatorial synthesis of polynucleotide probe arrays

Probe Length	Chemical Steps	Number of Possible Probes
4	16	256
8	32	65 536
12	48	16 777 216
16	64	$\sim 4.3 \times 10^9$
20	80	$\sim 1.1 \times 10^{12}$

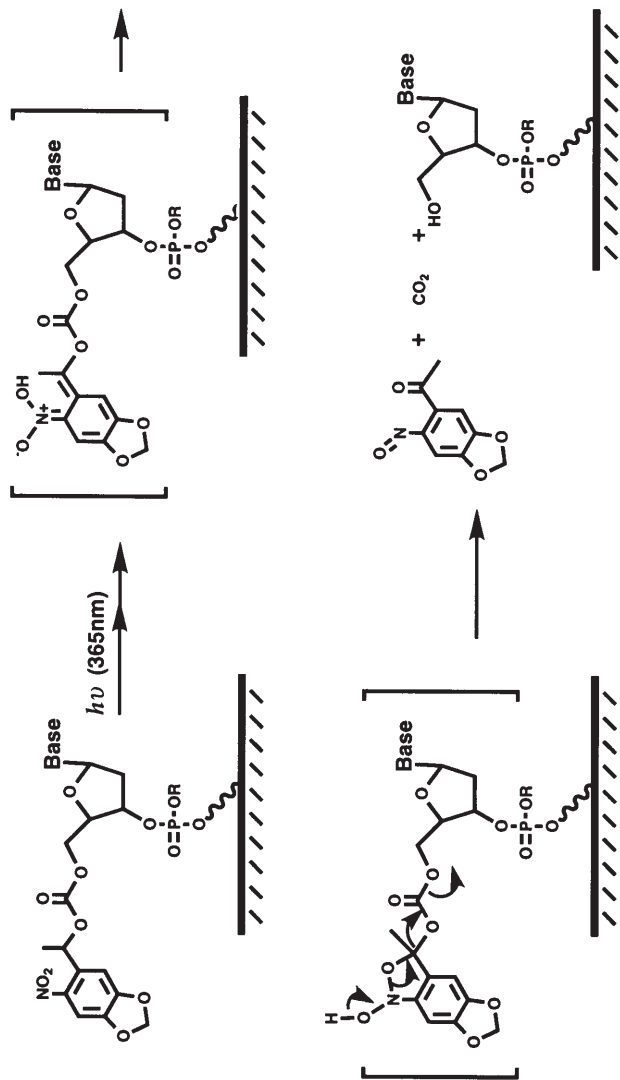


Fig. 3. Photolysis of 5'-MeNPOC protecting group

under stringent conditions so that hybridization to significantly shorter ($< n - 4$) oligomers is negligible, and statistically, the full-length probe is the major species able to hybridize under such conditions. Thus, sequence information can routinely be “read” from array hybridization data with single-base resolution.

DNA probe arrays are currently manufactured on a large-scale by automating the entire process using techniques and equipment similar to those used in the microelectronics industry. For example, two wafers, each containing replicate arrays of 65,000 unique 20-mer probes, can be completed in less than 15 hours. After synthesis, wafers are briefly treated to remove base protecting groups from the immobilized polynucleotides, and then diced to yield individual arrays for packaging in injection-molded cartridges. Additional increases in capacity and throughput will accompany further improvement and scale-up of these production techniques.

The resolution of the photolithographic process determines the maximum achievable density of the array (i.e. the amount of sequence information encoded on the chip). Table 2 shows the relationship between the resolution, in terms of smallest feature size, and the maximum density at which an array can be “printed”. Application of the photolithographic process using photolabile protecting groups currently provides a spatial resolution that allows arrays to be fabricated with densities on the order of 10^6 sequences/cm², which corresponds to an individual feature size of $\sim 10 \times 10$ m. This feature size is near the limit of resolution that can be achieved by this method using standard photolithography equipment.

By comparison, imaging materials and processes currently used in the semiconductor industry are capable of sub-micron resolution [6]. For this reason, we have been exploring new processes for synthesizing DNA probe arrays which combine standard solid-phase DNA synthesis chemistry with polymeric photoresist films serving as the photoimageable component [7–9]. In addition to the potential for higher resolution, this approach has the advantages of using standard dimethoxytrityl (DMT)-based DNA synthesis reagents and conventional semiconductor microlithography tools exclusively. Furthermore, photoresists typically require much shorter exposure times, compared to the photolabile protecting groups described above.

One way to use a photoresist film for array synthesis is to employ the image-patterned film as a physical barrier to mask selected regions of the substrate from exposure to reagents used in DNA synthesis. Figure 4A (*Left*) outlines a

Table 2. Photolithographic resolution and maximum array density

Resolution (mm)	Array Density (sequences/cm ²)
500	400
200	2 500
100	10 000
50	40 000
10	1 000 000
1	100 000 000

simple process in which the resist is used as a barrier to the acid solution used for the selective removal of DMT protecting groups from the surface polynucleotide chains, thereby activating the exposed regions of the chip for building block addition. Initial efforts to implement this strategy were somewhat hampered by the generally poor compatibility between the surface chemistry and the conditions necessary to develop the resists. This problem is resolved, however, by the introduction of an inert underlayer to protect the surface from the resist processing. This bilayer technique is illustrated in Fig. 4B (*Right*). Arrays have been prepared using the resist bilayer process which show identical performance to those made using photo-protecting group chemistry [7–9]. The production of 8 m features was demonstrated using this method, and higher resolution is likely with further process optimization.

An alternative and potentially much simpler photoresist-based process is one in which a polymer film containing a photo-acid generator is applied to the substrate (Fig. 5) [8, 9]. Here the film does not function as a physical mask. Instead, exposure to light through a mask creates localized acid development in regions of the film which are adjacent to the substrate, resulting in direct removal of DMT protecting groups from the growing DNA oligomers in those regions. No development or image-transfer steps are required. Substrate-resist compatibility must be optimized resolved in order to implement this approach. In particular, the acid strength and concentration must be carefully controlled to achieve

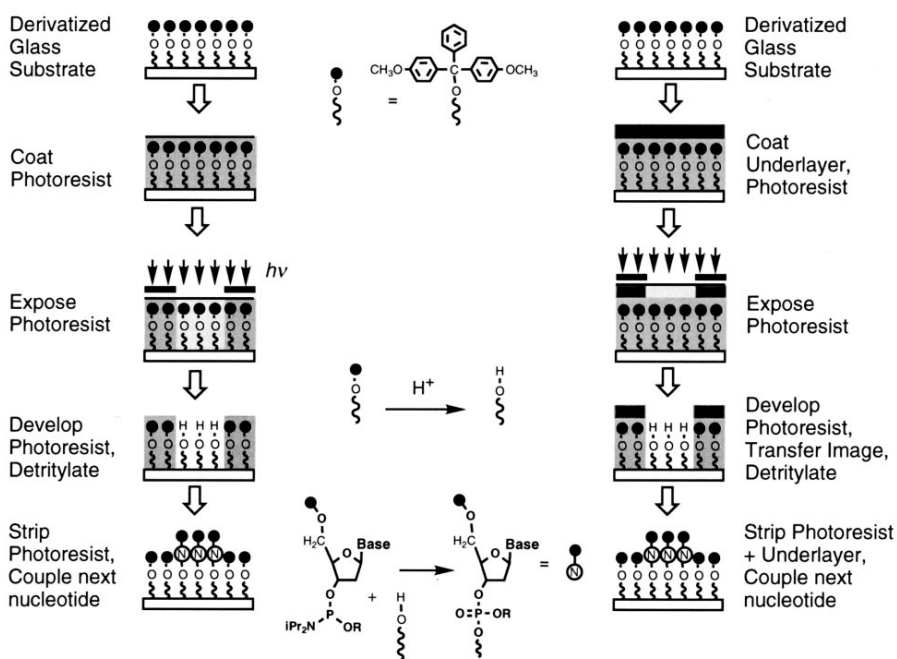


Fig. 4. Polynucleotide array fabrication processes using polymeric photoresists. *Left:* A single layer resist process. *Right:* A “bilayer” process using a protective underlayer

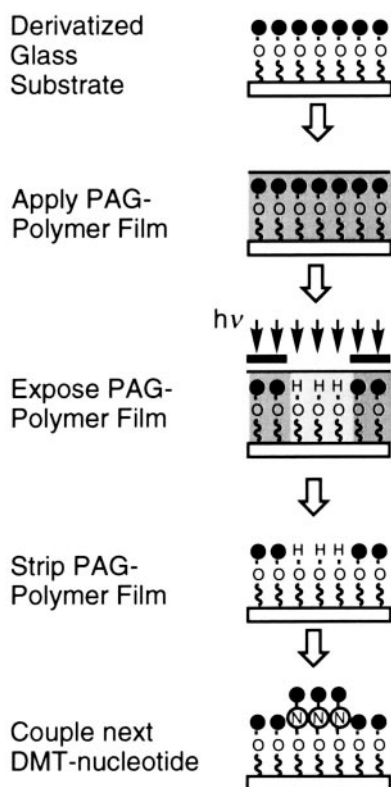


Fig. 5. Polynucleotide array fabrication process using photo-acid generator. In this process, acid is generated photochemically in a polymer film to effect light-directed surface activation

efficient deprotection without causing degradation of the surface chemistry. With further optimization and refinement, high resolution photoresist-based processes should soon enable high-throughput production of polynucleotide arrays with features on the order of one micron or smaller.

3 Applications

In hybridization-based sequence analysis, an analyte nucleic acid, or “target” is incubated with the GeneChip™ array, and the extent of hybridization with each DNA probe on the array is assessed in order to identify those which are perfect complements to the target. This requires the preparation of a fragmented and labeled target mixture from a genetic sample. Confocal epifluorescence scanning is used in conjunction with fluorescent labeling to monitor hybridization. The protocols for sample preparation are application specific and described below. Analysis of the scanned digitized images is carried out using specially developed software to determine the sequence of the sample.

3.1
Design of Polynucleotide Arrays

Careful design of the polynucleotide array can enhance the accuracy and reliability of information gathered from hybridization-based assays. These designs are facilitated by the high density of features available on GeneChip™ arrays. For example, whereas the absolute intensity of hybridization is a strong function of sequence [10], selective binding is more easily detected by monitoring the intensity relative to a reference probe. Redundant probes provide the opportunity for local intensity reference standards and therefore a higher quality of information.

One standard array design takes advantage of the empirical fact that the sensitivity to probe-target mismatches is highest at the center of the oligomer probe [11]. As shown in Fig. 6, a frame is selected around a section of the target sequence, representing the perfect match allele complimentary to the wild type probe. For example, with a 20-mer probe a frame size of 20 would be used. A set of four probe features are generated that are complimentary to this frame with an A, C, T, and G substituted at the center position. A second set of four probe features are generated by translating the frame by one base and carrying out the substitutions at the new location. This approach exploits the strength of detection using relative intensities. Within each set of four features at a given frame position, the brightest feature is the correct base assignment at that substitution position. This approach to probe design has been used for monitoring mutations in HIV [12].

A somewhat more complex approach is necessary to sense clusters of mutations. In this tiling, eight additional sets of four features are added that interrogate for mutations directly adjacent to, and one base away from, the center of the frame. These additional sets assume either wild type or one specific mutation at the frame center. This strategy has been applied to the detection of cystic fibrosis gene mutations [13].

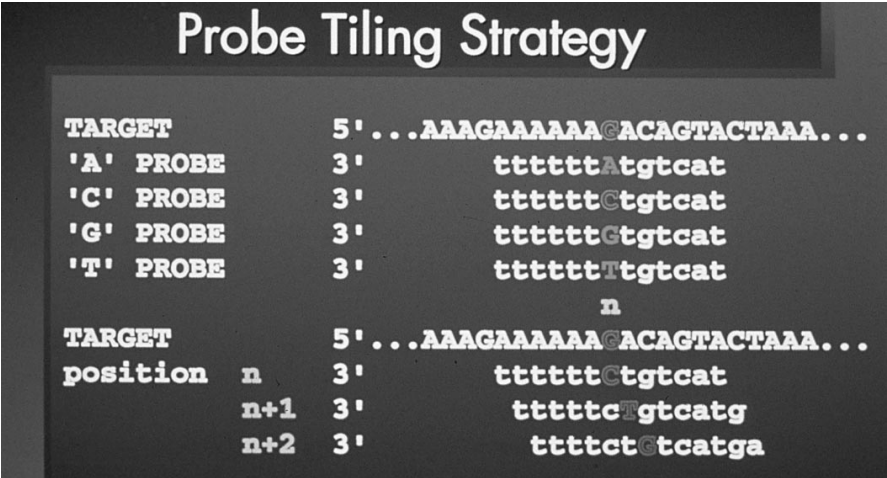


Fig. 6. Design of polynucleotide array using first tiling method

3.2
HIV Resequencing Application

Genotype diversity in HIV viruses increases with the progression of the disease, and in one hypothesis HIV overcomes the immune system through the accumulation of these mutations [14]. Studies on HIV therapy have resulted in the putative assignment of certain mutations in the RT and protease regions of the HIV genome as conferring drug resistance. Research on HIV therapy demands methods for rapidly screening these regions of the viral genome. As shown in Fig. 7, a GeneChip™ array with over 10,000 features has been developed for this purpose.

Genetic samples are prepared by extracting the viral RNA from serum or plasma and reverse transcribing it to DNA. A portion of the HIV genome is amplified using PCR [15]. As shown in Fig. 8, transcription promoter regions are included in the PCR primers. Labeling is carried out by in vitro transcription [16] in the presence of fluorescenated UTP's, and fragmentation by heating in the presence of magnesium salt. This GeneChip™ assay is currently in use at several research laboratories and is commercially available.

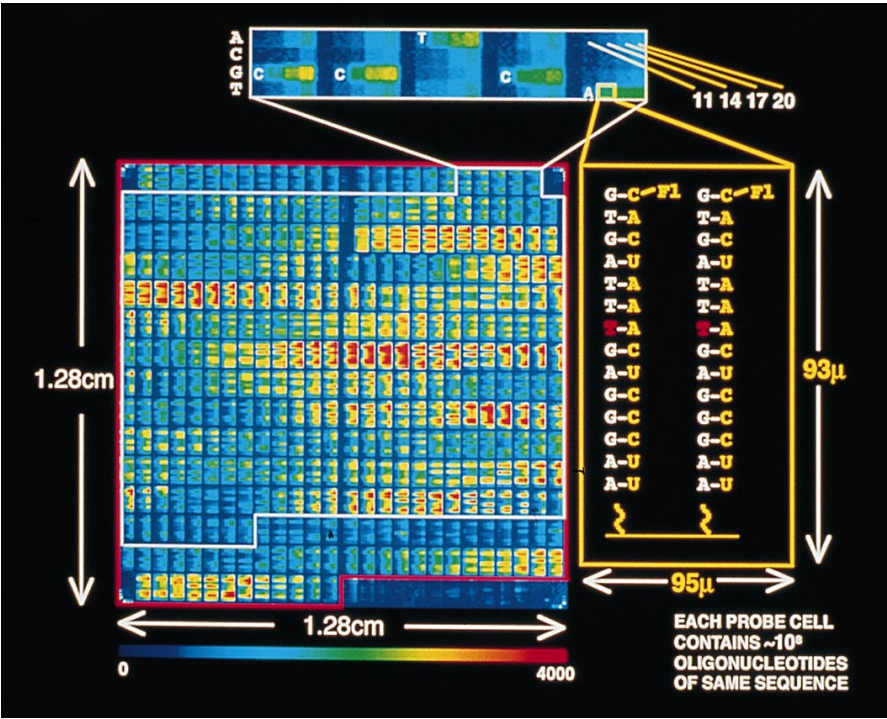


Fig. 7. False color image of fluorescent intensities on a GeneChip™ array that analysis sequences within the HIV-1 genome

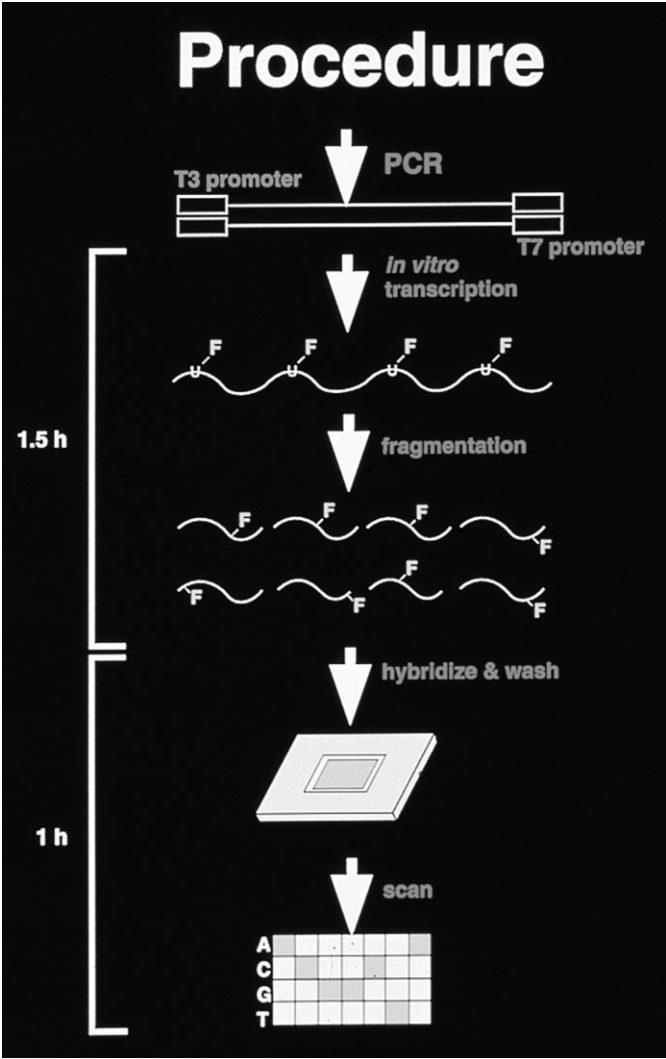


Fig. 8. Series of reactions used to prepare labeled and fragmented RNA target

3.3
mRNA Expression Monitoring

Gene expression is one of the fundamental mechanisms used by organisms to control their function. Proteins are translated from regions of genomic DNA through an mRNA intermediate that is relatively shortlived, referred to as a “message”. By monitoring levels of different mRNA molecules over time, insight into the state and activity of an organism can be gained. A set of such ex-

periments can be used to decipher the function of various genes resulting in a better understanding of how an organism works. This improved understanding can lead to improved therapeutics (i.e. drugs) and diagnostics.

In contrast to the resequencing arrays, the goal in this application is to detect the presence and quantity of certain known sequences. This is accomplished by designing two polynucleotide array features for each 20-mer mRNA segment to be detected: a perfectly complimentary probe and a reference probe that differs only by a single base substitution in the central position [17]. A GeneChip™ array with 65,000 features has been developed that quantitatively detects the presence of 118 murine genes. The level of mRNA was detected over three orders of magnitude while maintaining specificity in the presence of complex cellular mRNA backgrounds. These results were used to develop a four chip set covering 6,500 of the 100,000 human genes.

3.4

Other Applications

Some mutations in genomic DNA have been correlated with the predisposition towards, onset and progression of certain cancers. For example, mutations in the familial early onset breast cancer gene, BRCA1 have been monitored using these polynucleotide arrays [18]. The rapid development of new applications for genetic analysis continues. For example, GeneChip™ arrays have been developed that analyze the entire human mitochondrial genome in a single experiment [19].

4

Conclusion

Methods for the synthesis, hybridization, scanning, and analysis of high density arrays of polynucleotides have been developed. These methods have been applied to polymorphism discovery, genotyping and expression. These new tools are significantly changing the way scientists are exploiting the information in rapidly growing genetic databases, assisting in the transition from structure to function.

Many benefits will be realized by incorporating these polynucleotide arrays into an integrated analysis system. Decreased assay cost and contamination, along with improved throughput and reproducibility can be achieved by integrating sample preparation processes with the polynucleotide arrays; these systems under development at Affymetrix [20–21].

5

References

1. Fodor SPA, Read JL, Pirrung MC, Stryer LT, Lu A, Solas D (1991) *Science* 251:767
2. Pease AC, Solas D, Sullivan EJ, Cronin MT, Holmes CP, Fodor SPA (1994) *Proc Natl Acad Sci USA* 91:5022
3. Lipshutz RJ, Morris D, Chee M, Hubbell E, Kozal MJ, Shah N, Shen N, Yang R, Fodor SPA (1995) *Biotechniques* 19:442

4. McGall GH, Barone AD, Diggelmann M, Fodor SPA, Gentalen E, Ngo N (1997) *J Amer Chem Soc* 119:5081
5. MeNPOC=1-(3,4-methylenedioxy-6-nitrophenyl)ethoxycarbonyl
6. Willson CG (1994) In: Thompson LF, Willson CG, Bowden MJ (eds) *Introduction to Micro-lithography*, 2nd edn. American Chemical Society, Washington, DC, p 139
7. McGall G, Labadie J, Brock P, Wallraff G, Nguyen, T, Hinsberg W (1996) *Proc Natl Acad Sci USA* 93:13555
8. Wallraff G, Labadie J, Brock P, Nguyen T, Huynh T, Hinsberg W, McGall G (1997) *Chemtech*, February, p 22
9. Beecher JE, McGall GH, Goldberg MJ (1997) *Preprints Amer Chem Soc Div Polym Mater Sci Eng vol. 76: Natl Meeting, San Fransisco, CA, April*, p 597
10. Cantor C, Schimmel P (1980) *Biophysical chemistry part 3, The behavior of biological macromolecules*. W.H. Freeman, New York, p 1109
11. Wallace RB, Shaffer J, Murphy RE, Bonner J, Hirose T, Itakura K (1979) *Nucleic Acids Research* 6:3542–3557; Fodor SPA, Lipshutz RJ, Huang X (1993) *DNA sequencing by hybridization, Proceedings of the Robert A. Welch Foundation 37th Conference on Chemical Research – 40 Years of the DNA Double Helix*. Robert A. Welch Foundation, Houston, p 3–9
12. Kozal MJ, Shah N, Shen N, Yang R, Fucini R, Merigan T, Richman D, Morris, D, Hubbell E, Chee MS, Gingeras TG (1996) *Nature Medicine* 2:7:753
13. Cronin MT, Ficini RV, Kim SM, Masino RS, Wespi RM, Miyada CG (1966) *Human Mutation* 7:244
14. Wolinsdy SM, Korber BTM, Neumann AU, Daniels M, et al. (1996) *Science*, Apr 26, V272 N5261:537; Mellors JW, Rinaldo CR, Gupta P, White RM, et al. (1996) *Science*, May 24, V272 N5265:167
15. Saiki RK et al. (1985) *Science* 230:1350
16. Sambrook J, Fritsch EF, Maniatis T (1989) *Molecular Cloning, A Laboratory Manual*. 2nd edn. Cold Spring Harbor, p 5.58
17. Lockhart DJ, Dong H, Byrne MC, Follettie MT, Gallo MV, Chee MS, Mittmann M, Wang C, Kobayashi M, Horton H, Brown EL (1996) *Nature Biotechnology*, December 14:13:1675
18. Hacia JG, Brody LC, Chee MS, Fodor SPA, Collins FS (1996) *Nature Genetics*, December 14 14:441
19. Chee M, Yang R, Hubbel E, Berno A, Huang XC, Stern D, Winkler J, Lockhart DJ, Morris MS, Fodor SPA (1996) *Science*, October 25, 274:610–614
20. Anderson RC, Bogdan GJ, Lipshutz RJ (1996) *Miniaturized genetic analysis system. Technical Digest of 1996 Solid-State Sensor and Actuator Workshop, Hilton Head Island, South Carolina*, p 258
21. Anderson RC, Bogdan GJ, Barniv ZB, Dawes TD, Winkler J, Roy K (1997) *Microfluidic Biochemical Analysis System. Technical Digest of Transducers 97, 1997 International Conference on Solid-State Sensors and Actuators, Chicago, June 16–19*, p 477–480

Microtechnical Interfaces to Neurons

Thomas Stieglitz · J.-Uwe Meyer

Fraunhofer Institute for Biomedical Engineering, Sensor Systems/Microsystems Department,
Ensheimer Strasse 48, 66386 St. Ingbert, Germany. *E-mail: meyeru@ibmt.fhg.de*

In this chapter, different concepts of microtechnical interfaces to neurons are introduced. A description of hand-crafted neural devices is given which demonstrates the principle applications, limitations and needs of advanced interfaces. The postulation for advanced neural interfaces leading to the discussion on utilizing microelectromechanical systems for neural prostheses. Two on-going research projects are presented highlighting the technical possibilities for the design of neural interfaces. The first example describes a neural prosthesis for an amputee model to control an artificial limb. Secondly, concepts and realization steps are given for a sensory prosthesis which will aid people suffering from a special kind of blindness. A discussion on future concepts follows that outlines possible directions of research and development with the aim of clinical use, implantability of the whole system, wireless signal and energy transmission and closed-loop control of and with biological systems. Possible applications not only include restorative and rehabilitation purposes but also therapeutic applications for pain relief or bio-artificial drug delivery.

Keywords: Neural prostheses, microsystem technology, biotechnical interface, electrical stimulation, nerve signal recording.

1	Introduction	132
2	Some Fundamentals of Neurons and Electrostimulation	133
3	Conventional Approaches to Interface with Neurons	134
3.1	Surface and Needle Electrodes	134
3.2	Nerve Surrounding Electrodes	134
3.2.1	Helix-Electrodes	135
3.2.2	Cuff Electrodes	135
3.3	Book Electrodes	137
3.4	Epineural Electrodes	138
3.5	Interfascicular Electrodes	138
3.6	Electrodes for Contacting the Central Nervous System in Clinical Practice	139
3.7	Potentials of Microtechnologies	140
4	Micromachined Neural Prostheses	140
4.1	Cultivation of Neurons on Microsystems	141
4.2	Shaft Electrodes	142

4.3 Three-Dimensional Electrode Arrays 143

4.4 Electrodes to Contact Regenerating Nerves 143

4.5 Requirements for Electrodes and Insulation Material 144

5 Flexible, Micromachined Neural Prostheses with Integrated Cables 146

5.1 Process Technology 146

5.2 Artificial Limb Control with a Microsystem 149

5.2.1 In vitro Device Characterization 151

5.2.2 Chronic Implantation of Microimplants 153

5.2.3 Evaluation of Design 154

5.3 A Concept for a Retina Implant for the Blind 154

5.3.1 Epiretinal Microdevices 155

5.3.2 Design and Development of a Biocompatible Retina Stimulator . . 156

6 Future Trends 158

7 References 159

1

Introduction

The most welcome technical achievements in life science are the ones that enhance well-being or restore impaired or lost biological functions. Rehabilitation engineering is a research field that has devoted its full spectrum of efforts to compensate for malfunctions and disorders in human biological systems. This includes the development of devices for the rehabilitation of neural disorders which are termed neural prostheses. Neural prostheses directly interface with the central and peripheral nervous system. The most commonly known neural prosthesis is the cardiac pacemaker, which has existed for more than 30 years. A variety of other lesser known devices have been developed to partially restore neural functions in disabled people.

The age of microtechnology provides ample opportunities to design a new breed of neural interfaces that exhibit small dimensions, less weight, and improved performance. Miniaturization of electrodes yields a higher number of contact sides per unit area for stimulation and nerve signal recording. Integrated electronics and wireless communication by radio frequency links allows large data throughputs. Despite all technical achievements, implantable neural devices have to interact with the highly delicate, protective and complex biological system that also exerts chemical and mechanical forces. The devices need to be non toxic for the organism, light and soft to prevent mechanically induced traumatization, and biostable in the body over decades. Evolution has generated a nervous system characterized by massive data flows, huge redundancies, and the most sophisticated data processor, our brain. Neural micro-devices are facing the formidable task of interacting with such a complex system. Even though the most sophisticated technology appears to be crude when compared to nature, chances are high that beneficial effects will be achieved. In the follow-

ing, conventional approaches for interfacing the nervous system are summarized. The features on conventional electrode types are then compared to the ones of micromachined electrode arrays. Examples of current research projects are given which highlight the potentials of neural micro devices but also the difficulties to be overcome in the future.

2 Some Fundamentals of Neurons and Electrostimulation

Since the first experiments of Galvani and Volta [1] it has been known that muscles and nerves can be electrically stimulated to bring about muscle contraction. Physicians investigated the possibility of using electricity to cure diseases and to observe the secrets of electrical nerve signals. Surprisingly, the scientific work on Functional Electrical Stimulation (FES) only started about 45 years ago [1]. The mechanism of nerve excitation and the generation of action potentials was first described analytically by Hodgkin and Huxley in 1952. Their basic differential equations were investigated for over 30 years and provide the fundamentals to model even advanced mechanisms [2]. The anatomy and physiology of the nervous system is highly complex. Therefore, here we will address just some basic principles which are necessary to understand the different concepts described below. In a highly simplified scheme, the nervous system can be divided into the central nervous system (CNS) which consists of the brain and the spinal cord and the peripheral nervous system (PNS) which consist of the “remaining” nerves. Most of the scientific approaches that are presented below, deal with traumatizations of the CNS, e.g. paraplegia, the recording of nerve signals, or the stimulation of peripheral nerves. If central paralysis has occurred, the nerves below the trauma are intact, it is just the information from the brain which is affected. Different mechanisms occur when peripheral nerves are damaged. A retrograde degeneration will evolve which may alter excitation of the nerve. One nerve consists of many single nerve fibers that are organized in nerve bundles, so-called fascicles. They are surrounded by a layer of connective tissue, the perineurium. The whole nerve is also embedded in loose connective tissue, the epineurium. Small capillaries provide the nerve with oxygen. They pass in parallel to nerve and have orthogonal connections between the interior vessels. Nerve fibers exhibit different diameters relating to their tasks in the body. Thick fibers conduct nervous signals very fast and have a low excitation threshold. Thin fibers are slower with a higher threshold. The nerve signals are generated asynchronously by the brain and thin fibers are often activated first. If electrical stimulation is used, the thick fibers are activated first due to their lower threshold and this is called inverse recruitment. Unfortunately, these thick fibers often innervate fast fatiguing muscle fibers. Additionally, an activation of muscles with FES is always a more or less synchronous activation. Therefore, sophisticated training and stimulus protocols have to be used to allow a long term activation with diminished muscle fatigue. Different standard concepts are established to investigate basic mechanisms at nerves and at the nerve cell membrane. The most famous perhaps is the patch clamp electrode which allows the investigation of single ion channels on nerve

cell membranes. In this article, we would like to focus on technology used in rehabilitation and clinical settings to improve the daily life of people with neural disorders.

3 Conventional Approaches to Interface with Neurons

Different types of contacts between technical systems and the nervous system are common in experimental medicine and clinical application. In the following an overview is given on the main concepts for recording nerve signals and their advantages and disadvantages are discussed.

3.1 Surface and Needle Electrodes

Clinical electrodiagnosis of diseased nerves and muscles with surface and needle electrodes is well established [3]. The surface electrodes consist of stainless steel rings or plates that are positioned on the skin during examination. The needle electrodes are manufactured from stainless steel cannulae or platinum wires. They are pierced into the muscle or down to nerves for performing acute stimulation or recording of muscle and nerve signals, respectively. The surface electrodes are non-invasive and easy to apply for a trained person. Infections during long-term use can be prevented. If a part of a system fails, it can be replaced in a very simple and inexpensive way because all components are extracorporeal. This is a reason for the widespread use of surface electrodes not only for diagnostics but also for therapy [4], e.g. to reduce spasticity [5–7], and for FES of upper [8, 9] and lower limbs [10, 11] in paralyzed people. Unfortunately, there are many disadvantages inherent in this approach. The large electrodes stimulate with very low selectivity. Due to the extracorporeal position of the electrodes, the energy consumption is very high. Burning of the skin can occur, if stimulation parameters were chosen too high and electrodes were used without gel or saline solution to decrease the electrode-skin resistance. Reproducible electrode positioning is time consuming and needs well trained and highly motivated physicians and patients. In daily use, normally the physiological benefits will outweigh the technical disadvantages; the training of the paralyzed muscles by FES will improve blood supply and helps to prevent decubitus.

3.2 Nerve Surrounding Electrodes

Since the 1970s, nerve surrounding electrodes have become the most successful types of implantable biomedical electrodes in clinical use. For example, they have been used for stimulation of the lower limb [12], the urinary bladder [13], and for recording neural signals [14, 15]. Some electrodes have been safely in use for over 15 years [16]. They have been investigated intensively and many efforts have been made in respect to spatial selectivity and nerve fiber recruitment.

3.2.1

Helix-Electrodes

Helix-electrodes contact peripheral nerves on a small area due to their open structure. They consist of a silicone rubber substrate with one or two embedded platinum wire electrodes (Fig. 1). They were developed at the Huntington Medical Research Institute (HMRI) in a monopolar and a bipolar version [17]. The latest versions have been applied in paralyzed people at the sacral spinal roots for micturition control and incontinence. Their advantage can be seen in the self-sizing properties due to the spiral structures when the nerve is affected by edematous swelling after the implantation trauma.

A disadvantage can be seen in their open structure with insufficient homogeneity of the electrical field for multipolar electrode settings compared to closed devices .

3.2.2

Cuff Electrodes

Extraneural Cull-electrodes are available in two variations. The early “split cylinder” models consist of SILASTIC designs which have a stiff closing mechanism and only a few electrode channels. They have to be carefully adjusted to the nerve diameter.

For an effective stimulation they have to fit snugly to the nerve. If the nerve has post-implantation swelling due to mechanical or chemical irritation, an increase of 0.3% for a nerve diameter of 1.0 mm is sufficient to build up a pressure of 20 mm Hg. This may influence the intraneural blood flow in a way that damage may occur to the nerve due to a lack of oxygen [16]. If a larger cuff diameter is chosen, fibrotic tissue may grow between the cuff and the nerve with a high electric resistance. This results in much higher energy being necessary for stimulation. The mechanical disadvantages can be improved with a different design, the spiral cuff electrode (Fig. 2). It is built of two silastic sheets and platinum foil electrodes with Teflon insulated wires. The platinum electrodes are fixed on one foil. The second foil is stretched, electrode windows cut inside and then is glued on the basic foil and electrodes. Due to the stretching of the inner



Fig. 1. Monopolar helix electrode of the HMRI [17]

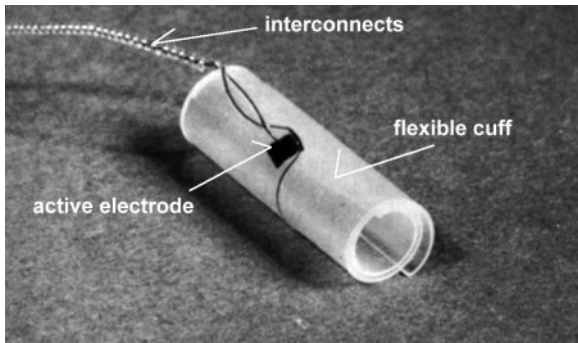


Fig.2. Monopolar Spiral Cuff-Electrode with cable before implantation [17]

foil, the electrode curls to a cuff in respect to the amount of stretching before the gluing procedure. With this concept, a nerve swelling up to 21% for a 1.0 mm nerve may develop before irreversible damage occurs [16]. Typical dimensions of the electrodes are 20 mm in length, an inner diameter of 4 mm, and a thickness of 0.3 mm for a silastic foil. With proper selection of material and electrode arrangement, the electrical field for the stimulation is limited to the internal cuff [18]. For a good spatial selectivity, many electrodes are placed radially on the circumference of the nerve. They could be used independently in any electrode configuration [19]. The most popular electrode configurations [18] are:

- a) monopolar electrode configuration: one electrode inside the cuff is used against a large counter electrode outside the cuff, placed on body parts distant to the cuff. The electrical field exceeds the location of the nerve.
- b) bipolar electrode configuration: two electrodes are stimulated against each other. This arrangement is rarely used in cuffs [19] but quite common in surface and intraneural electrodes.
- c) tripolar electrode configuration: one cathode in longitudinal direction of the cuff and nerve is placed in-between of two anodes. In this way, the electrical field is focused on to a small area inside the cuff.
- d) steering electrodes: they are used additionally to mono- or tripolar electrodes. They are arranged opposite to the cathode. Superficial nerve areas are turned in a refractory state to reach deep nerve areas for selective stimulation [20]. The refractory state is achieved with transversally applied subthreshold steering currents.

In experiments with a twelve channel cuff electrodes, different muscles were selectively activated by stimulating the adequate nerve with a different tripolar electrode configuration and transversal steering currents [12, 21].

Although cuff electrodes were originally only designed for nerve stimulation, it was shown that recording of nerve signals is also possible [22, 23]. The signals of mechanoreceptors of the paw of a cat were recorded during skin contact [23–25] and slip detection [26]. The method was developed to clinical relevance.

First systems for footdrop correction after stroke [27] use recorded nerve signals from the calcanean nerve of the foot for the control of an electrostimulation system.

3.3

Book Electrodes

A common form of electrodes in clinical use are the book electrodes for urinary bladder stimulation. The prototype was introduced in 1972 by G.S. Brindley [28] (Fig. 3) to contact the anterior sacral spinal roots. The devices consist of a silicone rubber block with four slots. In each slot, three platinum foil electrodes were embedded, each of which can be addressed independently.

The spinal roots were placed in the slots comparable to a bookmark laid in-between the pages of a book. The slots were covered with a medical epoxy resin to prevent the roots slipping out. After more than 10 years of development, the Brindley group were able to report the first 50 cases of an radio frequency controlled implant called a sacral anterior root simulator (SARS) in humans [29]. Meanwhile, there are over 500 patients with an urinary bladder stimulator [30]. Besides the intradural surgical implantation, an epidural implantation procedure was developed [31] to enhance the group of patients that may benefit from this kind of neural prosthesis. The implantation was mostly combined with a deafferentation of the posterior sacral roots to interrupt reflex circles and to restore continence. The disadvantages of this surgical procedure include the loss of reflectoric defecation and of reflectoric erection and ejaculation in male patients. It could be shown that the SARS could be also used to restore male sexual and reproductive functions [32, 33]. Even after a long clinical experience with excellent results, the electrodes seem to be very bulky from a technical point of view. There is a high demand of miniaturization above all with regard to minimal invasive surgery, because operations on the open vertebral column are still very risky.

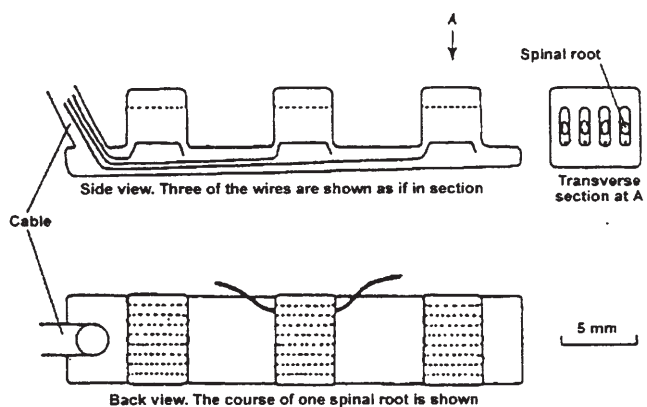


Fig. 3. Prototype of a book electrode [28]

3.4
Epineural Electrodes

Phrenic nerve stimulation for respiration is backed up by more than 10 years of experience [34]. It is used for patients where a high lesion of the spinal cord causes chronic respiratory insufficiency. The Vienna phrenic pacemaker stimulates the two branches of the phrenic nerves with four electrodes each. The cyclic combination of the electrodes, called roundabout stimulation, changes over time to prevent fatigue of the diaphragm during the 24 hours of stimulation per day.

The electrodes are manufactured from single or multistrand stainless steel wires (Fig. 4). The interconnection cables are coated with silicone. Besides a simple manufacturing technology, the electrodes demonstrate good electrical and mechanical properties [35]. In long term implantations the nerve damage due to continuous electrical stimulation was below 4.8%. Explantation of the electrodes is easy to perform [36].

3.5
Interfascicular Electrodes

Another electrode type takes into consideration that the nerve fibers are organized in bundles. In the case of SPINE (“slowly penetrating interfascicular nerve electrode”), small silicone pads with platinum foil electrodes inserts incorporated vertically [37] (Fig. 5) or radially into the nerves between the nerve fascicles.

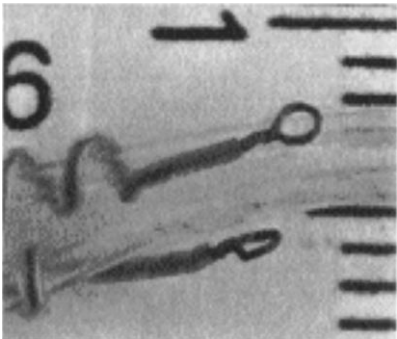


Fig. 4. Epineural electrodes with connection cable (Medi-
mplant, Inc.)

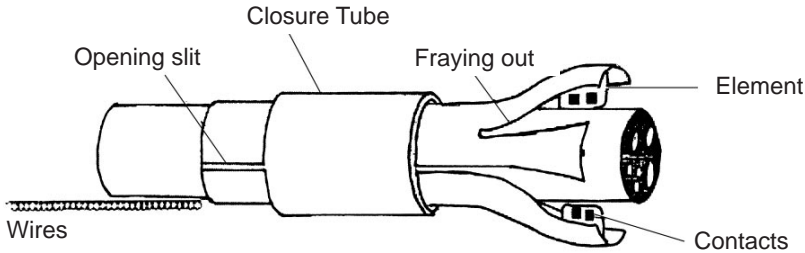


Fig. 5. Interfascicular electrode made of silicone rubber [37]

They separate the nerve into electrically insulated compartments and allow a selective stimulation of the nerve. The SPINE combines the advantages of a relatively small traumatization of the nerve with the high selectivity of intraneural implanted electrodes. The disadvantage of this design is again the relatively bulky size, especially at the site where cables are interconnected.

3.6

Electrodes for Contacting the Central Nervous System in Clinical Practice

The acute recording of evoked potentials and the stimulation at the spinal cord has been a well-established method for more than 20 years. The procedures require electrodes that are similar to pacemaker electrodes. Applications can be found in the field of scoliosis correction [38, 39] and the repair of aorta aneurysms [40]. An intraoperative stimulation of fibers of the sacral spinal cord was performed during dissection of unilateral testicle tumors to preserve ejaculation [41]. The main application of implants for chronic stimulation of the spinal cord is the handling of chronic pain [42]. There are two types of electrodes: the percutaneous electrodes resemble the pacemaker electrodes. They consist of a mandrel with up to four ring electrodes of a platinum iridium alloy (Fig. 6). They have a length of 3 mm with an interelectrode distance of 6 mm or a length of 6 mm with an interelectrode distance of 12 mm.

The electrodes are manufactured and distributed by MEDTRONIC (Minneapolis, USA). The epidural implantation is performed under local anesthesia. The second electrode type consists of four platinum disks that are embedded in a silicone rubber carrier. They have a diameter up to 6 mm (Fig. 7). They are implanted close to the spinal cord under complete anesthesia. Surgical procedures have been developed from the early 1970s up to the present [43]. Current designs offer the possibility of externally correcting small dislocation of electrodes [44]. Meanwhile more than 300 patients have benefitted from this therapy.

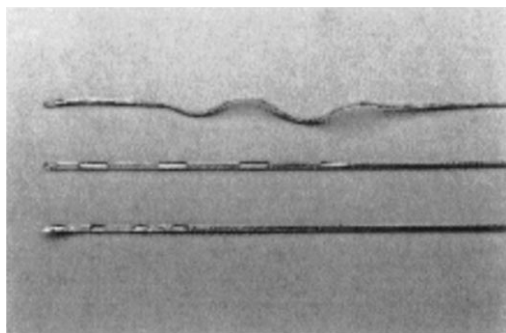


Fig. 6. Percutaneous four pole electrodes (Medtronic, Inc.)

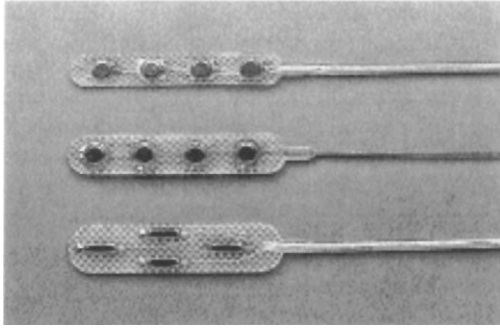


Fig. 7. Surgical four pole electrodes (Medtronic, Inc.)

3.7

Potentials of Microtechnologies

The conventionally systems presented above are relatively simple. Many of them are highly reliable, some of them implanted and in daily use for over 15 years [16]. Their advantage lies in the relative simple implantation procedures and only a few possible reasons for failure, e.g. broken wires, electrode corrosion or insulation failure. Normally, electrode areas and insulation thickness are “oversized” to guaranty a long lifetime. Nevertheless, there are limitations to the current designs in regard to size and functionality. Advanced microtechnologies offer the advantage to overcome the limitations. “Microtechnologies” offer the following advantages:

The dimensions of devices can be dramatically decreased while increasing the number of electrode channels. In this way, a higher spatial resolution is achieved, resulting in a higher selectivity. Downsizing device sizes reduces weight and therefore the mechanical load when attached to the nerve. In addition, small dimensions offer the possibility of minimal invasive surgery for implantation thus reducing surgical trauma. From the cost point of view, batch processing of the devices yields higher productivity and lower the costs of products. The dimensions and properties of the devices can be created with higher reproducibility when compared to hand-crafted designs.

4

Micromachined Neural Prostheses

For more than 10 years, researchers have investigated different concepts of utilizing microsystems to contact single neurons or whole structures in the central and peripheral nervous system.

The main approaches will be presented in the following, starting with single neurons and leading to more complex structures and systems intended for use in daily life. The demands on microsystems for their use in a physiological environment will be pointed out in examples while describing the devices in

detail. Finally, a specification of an optimal micromachined neural prosthesis will be given and compared to existing and possible future developments.

4.1

Cultivation of Neurons on Microsystems

Cultivation of neurons on technical microsystems is one approach for interfacing the nervous system. Planar and three-dimensional microprobes and microelectrode arrays are needed to investigate neural activities, growth, and adhesion of the cells. Experiments with cultivated embryonic nerve cells from chickens have elucidated that the structure's topology, e.g. the width of grooves, have an important impact on the growth of the cultivated cells [45–47]. Fromherz et al. were able to demonstrate the guided growth of nerve cells from leeches on a laminine coated substrate [48, 49]. In further experiments, they obtained a current-free measurement of the membrane potential of a single neuron of a leech, a so-called retzius cell. The cell adhered directly to the gate of a field effect transistor (FET) [50]. Using an array of FET's, a multielectrode array for a network of cultivated neurons will be possible. Usually, metallic electrodes are used for a bidirectional information exchange with nerve cell cultures for recording and stimulation. The activity of embryonic spinal cord cells of mice have been recorded simultaneously over a period of several month on a planar glass substrate with 64 indium tin oxide (ITO) electrodes [51]. Autonomous signals, generated from the cultivated neural network were examined [52]. An axonal outgrowth of embryonic nerve cells from rats was observed and electrical activity was recorded in a microstructure with 16 electrodes, which were connected with grooves, [53, 54]. Other groups applied silicon micro-machining to create wells with gold electrodes on the bottom and a grillwork at the top (Fig. 8) [55, 56].

The cells were seeded into the wells. The grillwork prevented the neurons from migrating. The Jerry Pine group managed to plant single hippocampus cells of the rat into a three-dimensional silicon structure which was termed a

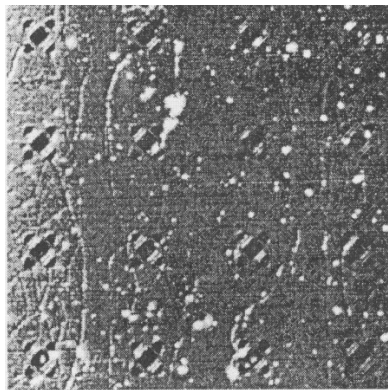


Fig. 8. Cultured neurons in microwells [55]

“cultured neuron probe” [57]. They were able to demonstrate that the transplanted cells inside the microcompartments retain their capacity for axonal outgrowth. Nerve action potentials were directly recorded extracellularly from the soma of the cells.

4.2

Shaft Electrodes

Planar shaft electrodes are the most common microstructures to contact the nervous system. The “Center for Integrated Sensors and Circuits” at the University of Michigan (USA) is most experienced in the microfabrication of this kind of penetrating electrodes [58–63]. The center has established a distribution service providing microprobes to researchers all over the world. A basic illustration of the electrode design is seen in Fig. 9.

The multichannel device consists of a micromachined silicon substrate with up to 36 thin-film metal electrodes. The width of the electrodes and interconnections on the shaft is only 140 m. The structures are insulated with a CVD dielectric at the bottom and the top. Only the active electrode areas are opened. Monolithically integrated analog CMOS circuitry is located on the same device for signal amplification and data encoding. The circuitry occupies an area of 2.5 mm² on the device. Other researchers have adopted the Michigan design of shaft electrodes [64, 65]. They have micromachined their own versions. The electrodes were used in animal experiments. Recordings have been achieved in the peripheral nervous system [66] as well as from the central nervous system of the honey bee [65]. Intracortical recording and stimulation at guinea pigs and rats has been performed [67, 68]. High spatial resolution is obtained when electrodes are placed inside the nerve or cortex. Multishank electrodes allow stimulation and recording of nervous signals in a (two-dimensional) plane. Different designs are available. The shanks of the silicon shafts are stiff and brittle. This carries the risk of nerve traumatization during implantation which may adversely influence the long term stability of the devices in the peripheral nervous system.

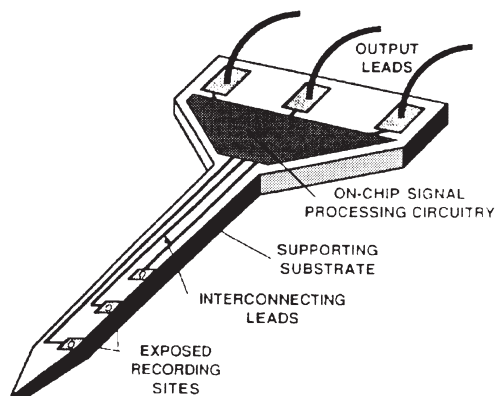


Fig. 9. Schematic of a “Michigan” shaft electrode

4.3
Three-Dimensional Electrode Arrays

A three-dimensional device was obtained by an hybrid assembly of comb-like multishank electrodes. The final structure resembled a bed of nails [69,70]. The array contains 256 electrodes with a lateral and horizontal spacing of 120 μm and 150 μm , respectively (Fig. 10). The assembly was sealed with glass and was implanted into the subarachnoidal space without any significant tissue damage.

4.4
Electrodes to Contact Regenerating Nerves

Micromachining allows the fabrication of micro sieves and microstructures through which regenerating peripheral axons may grow. Electrodes on the sieve will give rise to extracellular recordings in close proximity to single neurons. Different designs have been investigated. The long term vision describes a neural prosthesis that controls the artificial limb of an amputee by autogenous nerve signals. Micromachining is an integral part of all designs. A typical design is shown in Fig. 11 and comprises a silicon die, guidance channels, and connection cables in a hybrid assembly.

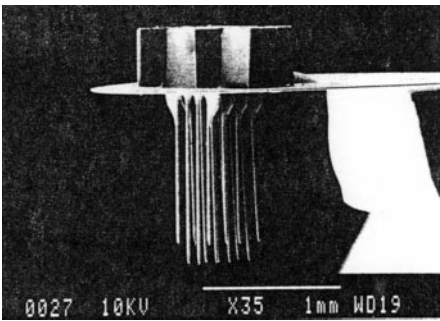


Fig.10. Threedimensional electrode area [69]

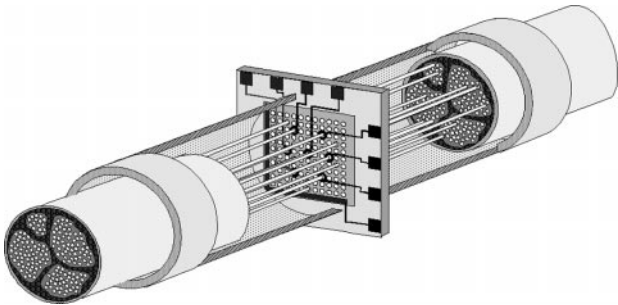


Fig.11. Schematic of a silicon sieve electrode for a regenerating nerve

The openings in the silicon structures are shaped as slots [71] or via holes [72]. Monolithic integration of circuits for signal processing and encoding into the device has been reported [73]. A particular challenge are the connections of the microsystem to the “outer world”. On some silicon structures, contact pads are offered as sites for electrical contact [71, 74]. The fabrication of integrated cables and round shaped via requires a complex process technology [75]. The via holes are etched in silicon membranes, which vary in thickness from 50–100 μm [76] to 4 μm in thickness [77]. The fabrication of round via holes has been demonstrated in thinner membranes [77]. The glossopharyngeal nerve of a cat regenerated and reinnervated after an implantation time of only 100 days [78].

Silicon sieve electrodes were also achieved by European groups (Fig. 12) [79]. Regeneration of the sciatic nerve of a rat has been demonstrated [80–82].

4.5

Requirements for Electrodes and Insulation Material

The design of microelectrodes is a critical part in neural prostheses. Electrode design requirements need to include aspects of biocompatible and biostable operation. One requirement may exclude the other. An optimum stability, life-time, and safe performance has to be combined with a minimum of toxicity. The optimal requirements are as follows [83, 84]:

- a) minimal energy consumption for stimulation concomitant with effective charge delivery at a small (geometric) electrode surfaces,
- b) low tendency to create irreversible electrochemical reaction products that may cause inflammatory reactions when a high reversible charge delivery capacity is reached,
- c) low polarization of the phase boundary, as well as low afterpotentials,
- d) low and stable impedance of the phase boundary,
- e) low cut off frequency of the impedance,
- f) low tendency for artifacts, e.g. electrochemically induced noise.

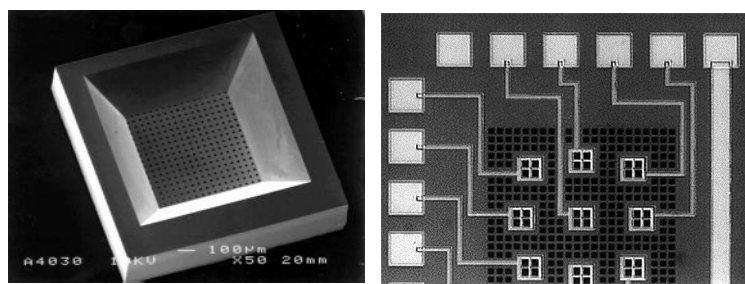


Fig. 12. Sieve electrode in silicon technology. **a** SEM, dimensions 1.4 mm × 1.4 mm; **b** light micrograph, sieve with platinum thin-film electrodes

Microelectrodes are fabricated utilizing thin film technologies. Electrode materials are used for which thin film processes are established. The “classical” materials are gold and platinum [85, 86] but their charge delivery capacity is quite low (Au: 20 $\mu\text{C}/\text{cm}^2$, Pt: 75 $\mu\text{C}/\text{cm}^2$). At fast charge delivery rates, the maximum charge injection capacity is often one magnitude lower [87, 88] and the electrodes may corrode [89]. As electrode areas become smaller to obtain a higher spatial resolution, their impedance increases progressively and the charge delivery decreases. There are two alternative solutions to this problem: one is the enlargement of the electrochemical active surface. Rough or even fractal surfaces help to increase the charge delivery capacity substantially. Fractal titanium nitride (TiN) is known as a material with a low cut-off frequency and excellent charge injection limits are achieved with a large electrochemical surface area [90]. A second excellent material is iridium oxide which belongs to the group of electroactive materials. Iridium can be deposited with evaporation or sputter technology. The oxide is generated electrochemically using cyclic voltammetry. The electroactive mechanism of the AIROF (activated iridium oxide films) is based on valence changes in its oxidation state at different potentials at the phase boundary [91, 92]. The charge delivery capacity is in the range of 3000 $\mu\text{C}/\text{cm}^2$. Different densities of iridium and AIROF may induce stress in the films, which needs to be reduced to obtain films that are stable over a long stimulation period.

A further challenge is the formation of biocompatible and long-term stable insulation layers with means of semiconductor technology. As shown in Sect. 3, most of the hand-crafted neural prostheses are insulated with a silicone rubber coating. These coatings are quite thick when compared to dimensions of the micromachined devices presented in this section. Therefore, many research groups are working on the development of biostable coatings of semiconductor insulation materials. Mostly, the technology of chemical vapor deposition (CVD) is used. In a physiologic environment, materials like silicon nitride and silicon oxide are not stable as monolayers [47, 93, 94]. An excellent stability is achieved when combining the layers to multilayers (Fig. 13) [95, 96]. Insulation

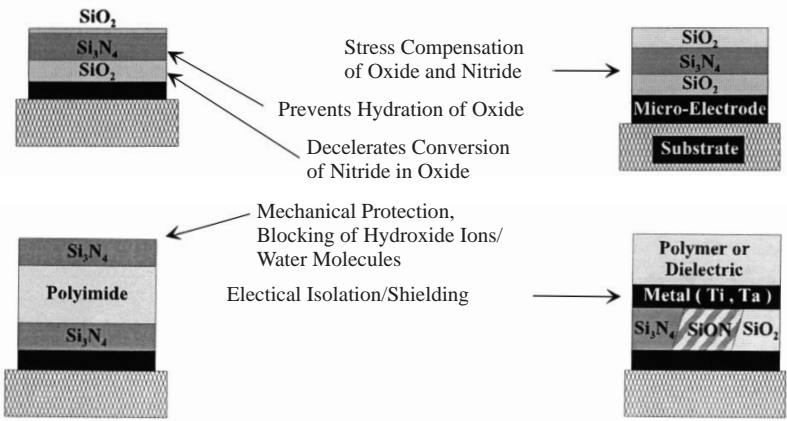


Fig. 13. Different combinations for biostable insulation layers in microsystem technology

decays when exposed to physiologic environment. Problems include the trapping of hydrogen atoms in oxide layers [97], the degradation of silicon nitride [98, 99], the change of silicon oxide to water soluble silicate [100], and the diffusion of ions (Na, Cl) in the insulation layers [97]. Furthermore, insulation deficiencies often arise from pin holes in the materials, e.g. from small particles. The use of combination layers also alleviates this problem. The possibility of minimizing the intrinsic stress of the complete multilayer by compensating compressive stress in the nitride with tensile stress in the oxide enhances the mechanical durability and life-time of the devices.

5

Flexible, Micromachined Neural Prostheses with Integrated Cables

Our research group has investigated materials other than silicon for interfacing nervous structures. The ideal material combines biocompatibility with proper mechanical characteristics while still applying microtechnologies. We have developed microtechnologies for the fabrication of ultra light-weight and flexible devices. In the search for a non-toxic material, we have chosen polyimide [101–103], which is well known in microelectronics [104–107], e.g. as a stress buffer in multi-chip-module (MCM) assemblies [108]. Hybrid assemblies of micromechanical systems are possible on a base of polyimide substrates and interconnections. Hybrid designs allow adaptation of the system to many applications, in a relatively low development time and with less costs than the complete redesign of silicon-based integrated system. Further more, flexible polyimide based assemblies may be transformed from planar structures into three-dimensional shapes.

In the following, a detailed description of the process technology is given. Different designs of neural prostheses will be presented and two applications will be discussed in detail.

5.1

Process Technology

The fabrication of polyimide based microstructures with a single metallization layer is described. The silicon wafer is merely used as a supporting structure to perform the photolithographic steps and thin film procedures in the cleanroom. The wafer is removed at the end of the process.

As the first step, a silicon wafer is spin coated with resin-like precursors of polyimide. From the broad selection of polyimides, we have chosen the Pyralin PI 2611 (DuPont) (Fig. 14a). It belongs to the new generation of polyimides with low water absorption and a thermal coefficient of expansion (TCE) that is adapted to the TCE of silicon nitride. The polyimide is dried on a hotplate and fully imidized in a curing process at 350 °C under a nitrogen atmosphere. The bottom layer can vary between 2 μm and 7 μm with a typical thickness of 5 μm . The thickness is a compromise between flexibility and mechanical stability. In a second step, we use thin film technology to deposit platinum electrodes, multi-strand ribbon cables, and connection pads in a single process step utilizing the

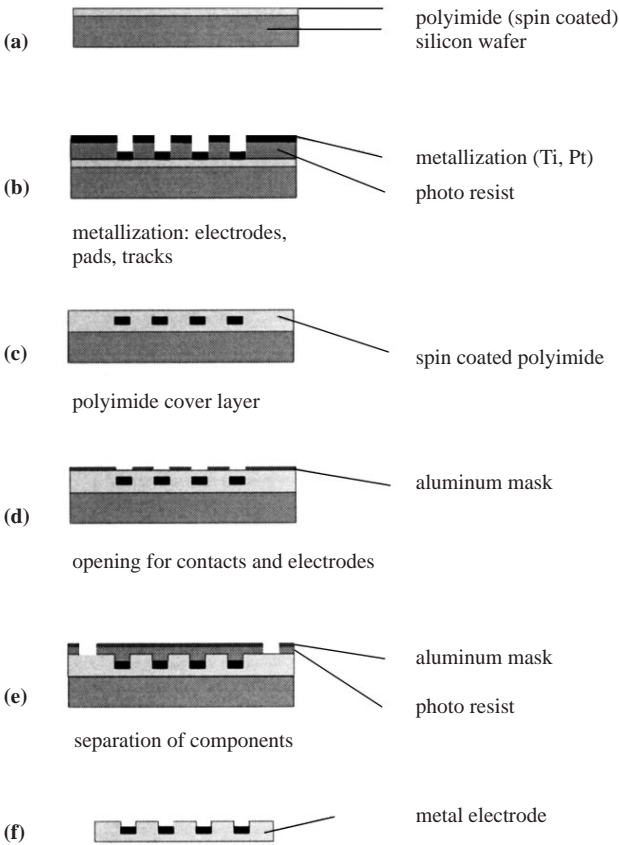


Fig. 14. Fabrication process of flexible neural prostheses

so-called lift-off. After roughening the polyimide surface in an oxygen plasma to enhance the adhesion properties, a photoresist layer is deposited onto the wafer. The pattern of the metallization is removed by photolithography and the metallization of platinum (300 nm) on a titanium adhesion layer (30 nm) is sputtered on the complete wafer (Fig. 14b). The mechanical stress inside the metallization depends on many process parameters. We optimized the process to achieve good adhesion combined with low mechanical tensile stress. Lift-off technology is applied which yields remaining patterns for electrodes, cables, and connection pads. A polyimide top layer of 5 μm thickness provides additional mechanical support and insulates the metallization (Fig. 14c). Reactive Ion Etching (RIE) is utilized to open the electrode areas and connection pads while leaving the interconnections insulated. A patterned aluminum layer (300 nm) served as an etching mask (Fig. 14d). An oxygen plasma was generated in the RIE reactor to obtain structures with sharp edges and a low surface roughness.

In the next step, the outer shape and holes are produced. After removing the aluminum, a resist layer is spun on, which protects the electrode and pad areas.

An aluminum etching mask is deposited (Fig. 14e) and patterned corresponding to the shapes of the devices. RIE is used to etch the polyimide down to the support wafer and to separate all devices in one etching step. After removing the aluminum and the resist, the single devices are separated from the support wafer. The resulting components have a total thickness of 10 μm (Fig. 14f).

Finally, it is possible to generate the three-dimensional shapes of the micro-devices. For this, the devices are bent to their desired position and tempered at 300 °C for 2 hours. The devices maintain their three-dimensional shapes. Typical shapes of neural interfaces comprise gutters (Fig. 15), cuffs (Fig. 16), or helically rolled interconnections to attain a better longitudinal elasticity (Fig. 17).

The number of tracks for interconnections is limited by the width of the interconnecting cable. A higher number of electrodes and interconnections is achieved when multi-layer strands are fabricated. We have developed double layer strands with sandwiched insulation layers of about 5 μm in thickness. Multiple metallization layers are used when concentric bipolar electrodes are fabricated. Bipolar concentric electrodes minimize the electrical stray field when applying current pulses. In this way, energy consumption for stimulation is reduced.

A main problem in all biomedical signal recording is the capacitive coupling of undesired signals into electrodes or interconnections. These so-called

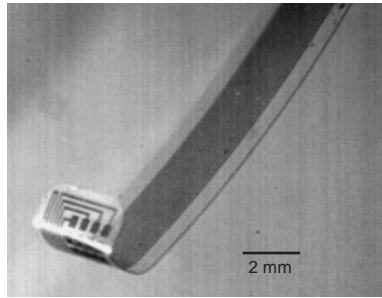


Fig. 15. Gutter-shaped electrode array

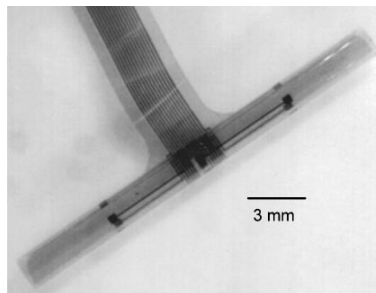


Fig. 16. Multichannel cuff electrode with four tripoles

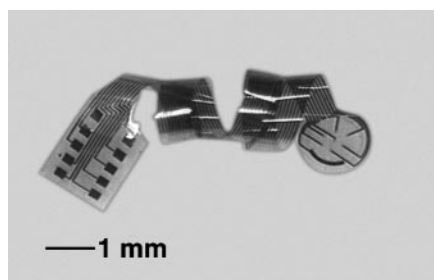


Fig. 17. Electrode with rolled interconnections to receive a higher longitudinal elasticity

artifacts could be, for instance, the signals of nearby muscles of some mV when trying to record nerve signals in the order of μV . Additionally, crosstalk occurs between conducting tracks when package density is increased. This led us to develop coaxial, electrically shielded interconnections in thin film technology.

5.2

Artificial Limb Control with a Microsystem

It is still a vision to be able to control an artificial limb by autologous neural signals. Many research groups have pursued this idea. The first approaches started in 1945, when a lower limb was lost and acute recordings of nerve signals were taken to control a wooden artificial limb [109, 110]. Decades later, with the emerging of micromachining technology, miniaturized devices have been developed. Some silicon-based microsystems had been introduced above. The idea of all sieve shaped electrodes is to entrap regenerating nerve in a microsystem after amputation. The working hypothesis is to record nerve signals that come “down” from the brain when intending to move of the limb. As a feedback, a stimulus would deceive a “movement” or “grip” in the sensoric areas of the brain to which the limb was innervated. The neural microdevice and a miniaturized telemetric implant will exchange data with an artificial limb. By this, an “intelligent” artificial prosthesis is created that is controlled by the brain. Current upper limb prostheses are controlled differently. Many types of artificial arms are cable-activated with a harness control. The most sophisticated prostheses feature myoelectric, two-channel controls. They are equipped with a microcontroller that allows the choice of several programs for hand opening, turning and closing.

If a microsystem should interface a regenerating nerve, some basic demands have to be taken into consideration: the system must be absolutely non toxic, it must be stable in the physiologic environment for a long time, and the mechanical load on the severed nerve should be as minimal as possible during muscle contraction and limb movement. The neural prostheses should be equipped with multiple electrodes for recording nerve signals and for stimulation of different portions of the nerve.

We have developed basic structures of a light-weighted microsystem in the framework of the European INTER-project (Intelligent Neural Interface,

ESPRIT, #8897). The regeneration of a dissected nerve through a sieve was investigated in an animal model at the sciatic nerve of rats. The basic components of the implant are illustrated in Fig. 18: a multichannel sieve electrode with long integrated interconnections, two guidance channels, and the nerve stumps that were inserted very carefully into the channels. The sieve electrode was fabricated with the single-metallization layer process described above.

The implant has a total length of 30 mm with ribbon-cable 1 mm wide (Fig. 19). The sieve is circular shaped with a diameter of 2 mm. The sieve is perforated with 281 round holes having a diameter of 40 μm and a center-center distance of 70 μm (Fig. 20). They have an electrode area of 1,473 μm^2 and 10,300 μm^2 for the counter electrode, respectively. The via holes feature steep edges and a smooth surface (Fig. 21). By using combinations of O_2 and CF_4 for RIE or a higher HF power, we obtained higher etching rates, but the surface roughness increased and resembled the structure of a sponge.

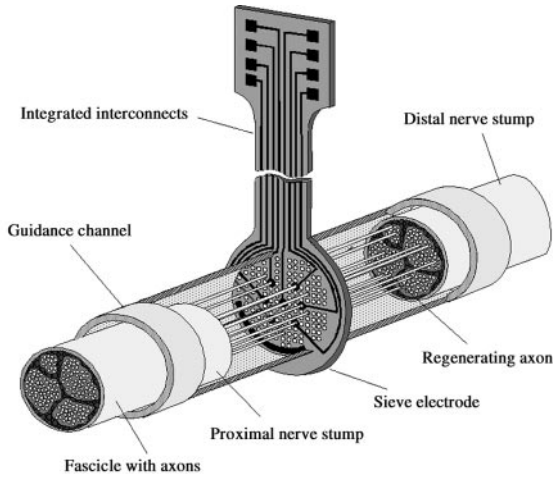


Fig. 18. Schematic of a flexible multichannel sieve electrode with integrated interconnections



Fig. 19. Sieve with integrated cables (length 21 mm) and connection pads (light micrograph)

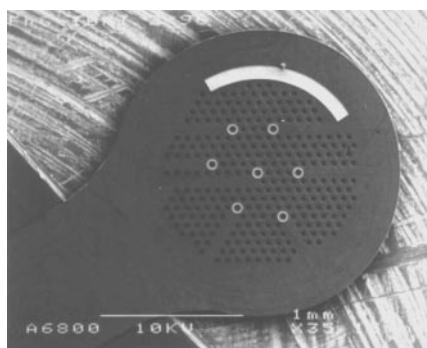


Fig.20. Sieve with 281 holes, 7 electrodes and a large counter electrode (SEM)

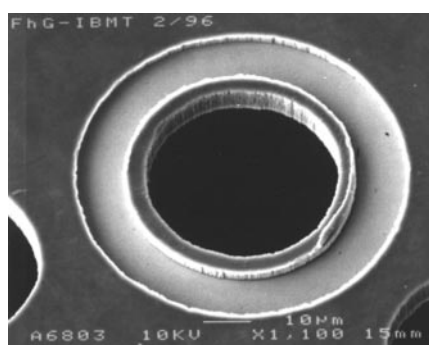


Fig.21. Detailed view of an circular electrode around a via hole (SEM)

5.2.1

In Vitro Device Characterization

Before implantation several in vitro tests were performed. For evaluation of a possible toxic reaction, we investigated the material and the whole devices in vitro with cell culture methods. Direct contact and extraction tests with a mouse fibroblasts cell line (L 929) and a neuroblastoma cell line (neuro-2-a) were performed according to the international standard ISO 10993 (“Biological Evaluation of Medical Devices”). The materials and devices showed no toxicity, i.e. no significant differences in membrane integrity of the cell membranes, mitochondrial activity and DNA synthesis rate. The neuro-2-a cell line is so sensitive that even small changes in process technology are detectable. The flexible polyimide structures proved to be non toxic.

Neural implants need also to be biostable in a “wet” environment. Therefore, mechanical bending tests were performed in physiologic saline solution at room temperature to simulate loading stresses of movements. In dynamic tests the electrodes were fixed at the ends and bent for 130,000 times at an angle of 120° with a repetition frequency of $1/3$ Hz. The devices remained stable. No cracks or

delamination were observed with means of light and electron microscopy. Soaking the devices in saline solution provides a rough estimation of the degradation behavior of the material. After more than 26 months of soaking, no alterations of the devices are detectable.

Designing neural implants requires thorough investigations on the electrical and electrochemical properties of the microelectrodes before implantation. Injectible stimulation charges are estimated and electrode recording impedances are determined. Proper impedance match between the recording electrodes and the amplifier-filter electronics yields high signal-noise ratio and allows the detection of small nervous signals. Well established electrochemical methods were used for electrode characterization. Using a three-electrode setup (device under test – platinum counter electrode – Ag/AgCl reference electrode) and a potentiostat we performed electrode impedance spectroscopy with an amplitude of 100 mV in the range between 1 Hz and 100 kHz. Based on the results (Fig. 22), we can model the equivalent circuit of the electrode that helps

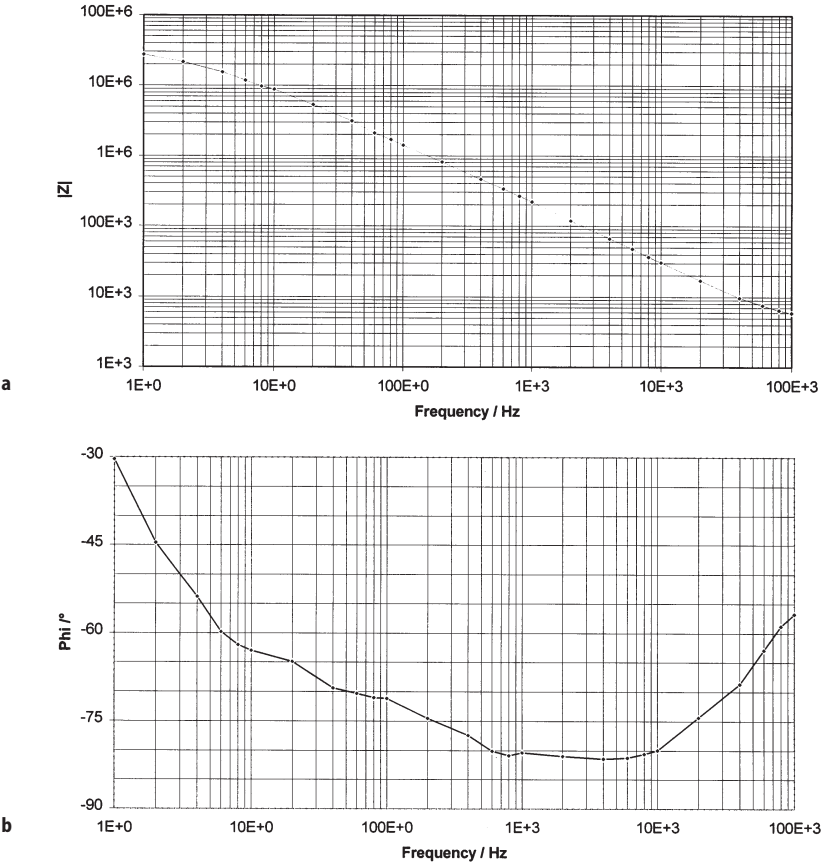


Fig. 22 a, b. Electrode impedance spectrograph obtained from a platinum electrode (a Value; b phase)

to understand the mechanisms at the phase boundary and derive the coefficients for amplification and signal filtering.

A further standard method for electrochemical analysis is cyclic voltammetry. A voltage ramp is increased and decreased between two potential limits and the current is monitored. In the resulting curve, electrochemical reactions in the equilibrium state can be detected. At platinum electrodes, the formation of Pt-H complexes and the oxidation and reduction at the metal surface can clearly be observed (Fig. 23).

The enclosed area of the curve is a measure of the reversible charge delivery capacity of the electrode. For fast current pulses, a different measurement method is used to determine the charge injection limits without gassing. Current pulses are applied and the voltage over two electrodes is monitored just below the gassing limits (Fig. 24). Once having passed the extensive *in vitro* testing, the electrodes were tested in chronic animal experiments.

5.2.2

Chronic Implantation of Microimplants

The group of X. Navarro (Barcelona, Spain) implanted our microsystems in rats under pentobarbital anesthesia. The sciatic nerve was sharply transected at the midhigh. The nerve stumps were introduced into the ends of the silicone tubes and fixed with one 10-0 suture at each end, leaving a short gap between. The wound was closed by muscle and skin sutures. Regeneration of the nerve was proved with histological and electrophysiological methods over two to six month postimplantation. One rat was reanesthetized and the sciatic nerve was reexposed. There was a thick regenerated nerve cable inside the guidance channels. The nerves were organized in fascicles corresponding to the grid pattern of the via holes. Electrical stimulation of the sciatic nerve over the electrode elicited muscle

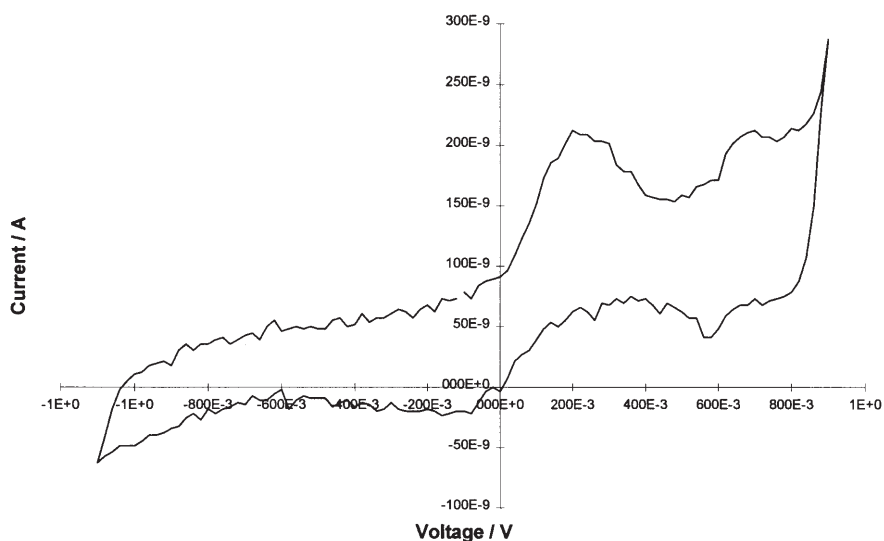


Fig. 23. Cyclic voltammogram of a platinum electrode (1.5 V/s scan rate)

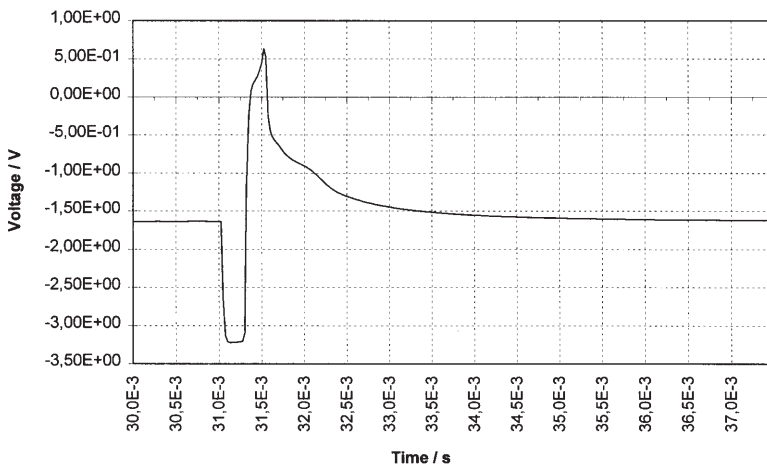


Fig. 24. Potential over an electrode after a current pulse (200 μ A, 250 μ s)

action potentials similar to those evoked by nerve stimulation over conventional metal hook electrodes. Direct recordings from the interface connection pads allowed to record nerve action potentials in response to electrical stimulation of distal regenerated nerve, and in response to functional sensory stimulation, e.g. toe stretching, heat, pinching [111]. The quality of the regenerates was better than of those grown through silicon dice [82].

5.2.3

Evaluation of Design

The design of a ultra-light weighted neural prostheses showed excellent results in our hands. The flexible material properties only caused slight mechanical induced tissue reactions. The devices were biostable for an implantation time of over 6 months. The regeneration rate was better than in all silicon based systems tested before. Though these results are very promising, they mark only the beginning of efforts to obtain a neural prosthesis for humans. Long-term stability testing has to be performed under normal and accelerated aging conditions. A stability over some decades is required for an implantation in humans. A telemetric unit is currently developed to transceive signals to a controller system outside the body and vice versa. Until now, there are only few notions about the signal processing of the nerve data and their use for an artificial limb control. A major challenge will be the examination of nerve regeneration when the distal end of the nerve is really missing. Even enthusiastic estimation predict ten or more years of development until the first clinical systems will be available.

5.3

A Concept for a Retina Implant for the Blind

In Germany, 30,000 patients are suffering from vision impairment or blindness. Different research groups are focusing their work on the development of a

neural prostheses to aid people suffering from blindness. Three main approaches are investigated relating to different traumatization mechanisms. In one approach, the visual cortex is directly contacted with a three-dimensional microsystem [112]. In the second effort, the electrode array is directly interfacing the optic nerve. Alternative to the approaches above, the retina is contacted directly with micromachined devices subretinally [113, 114] or epiretinally [115, 116]. The authors work with a consortium which develops an epiretinal visual prosthesis [117, 118]. An epiretinal prosthesis is indicated when patients suffer from retinitis pigmentosa (RP). In RP patients the light sensitive receptor cells -rods and cones- are damaged. Light is not transduced into electrical impulses and therefore no visual information is received in the visual cortex of the brain. Proper electrical stimulation of the ganglion cells of a patient with a needle electrode evokes a sensation is evoked that is described as a lightning, “pea-shaped” spot, termed phosphene [119].

5.3.1
Epiretinal Microdevices

A consortium of 13 technical and medical partners works on different tasks to develop a complete system for a visual prosthesis (Fig. 25). The neural prostheses comprises a unit to record and process ambient light, an encoder that transforms visual information into a sequence of stimulation pulses, a micro-electromechanical system that is implanted into the eye for interfacing the retina and for generating the appropriate stimuli.

A similar project on contacting the retina is pursued at MIT for more than five years.

The main difference of our project is the development of a retina encoder which simulates the signal processing of the different layers of the retina. The encoder transforms visual information into stimuli for the ganglion cells. The stimulation patterns should resemble the ones obtained from a non damaged retina. In detail, a high speed, pixel addressable camera with a light sensitivity of

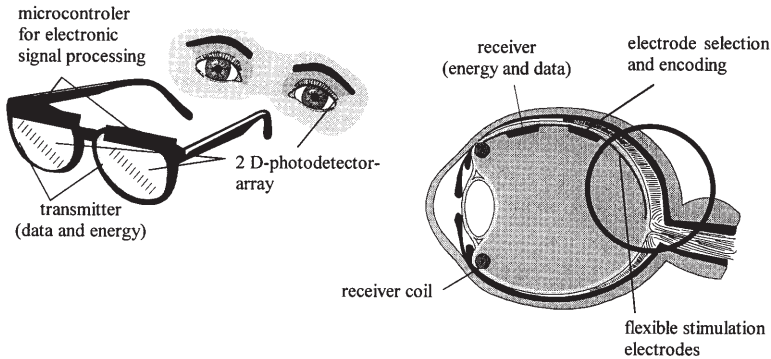


Fig 25. Concept of the retina implant of the German EPI-RET consortium

7 decades has been developed. Optical and electromagnetic telemetry systems for the energy and data transmission are under current investigation. Pictures were preprocessed with spatio-temporal filters in a so called “retina encoder” to simulate the properties of the retina. Artificial neural nets help to derive the filter parameters which are particular in each future patient. Monolithic integration of CMOS circuitry is being developed for signal transmission, generation, and control. Supporting electronics is connected to the flexible, micromachined stimulator structures. Ophthalmologists investigate different strategies for an epiretinal fixation and develop new operation and implantation techniques. Function tests of implants are under way. It is objective of the project to deliver a first demonstrator of the complete prosthesis for evaluation in an animal model after four years. Even very optimistic estimations deal with a time frame of 10 to 15 years until a first generation of retina implants will reach be clinical significance for patients.

5.3.2

Design and Development of a Biocompatible Retina Stimulator

Since the begin of the project in August 1995, the authors work on the design, development, and characterization of biocompatible retina stimulator structures. We have screened various substrate and insulation materials for biocompatibility applying our standardized cytotoxicity tests. Several test geometries for stimulator structures were designed and evaluated. First demonstrators were fabricated and implanted in rabbits for acute studies. For an early evaluation of the microelectrode properties, we designed test structures to stimulate the retina. While stimulating the retina with our microelectrodes, correlated electrical evoked potentials (EEP) were recorded with clinical standard electrodes on the top of the visual cortex at thresholds similar to other groups [120]. These initial investigations led to the design of a round stimulator structure with long interconnections and connection pads at the terminal end. Our microfabrication process was utilized to design the highly flexible, light-weighted stimulation structures that adhere to the retina because of their three-dimensional deformability.

The actual retina contact structure incorporates 12 or 24 independent electrodes, respectively. The electrodes were arranged concentrically to minimize the electrical stray field during stimulation. We established the microfabrication process for double metallization layers needed to obtain concentric microelectrodes. In a temper step, the electrodes were formed into a convex shape according to the curvature of the eye. The generation of convex shapes was possible since the stimulator was designed in concentric rings interconnected by s-shaped bridges (Fig. 26).

In acute and first chronic implantations in rabbits, the stimulator structures showed an excellent performance. Only minor foreign body reaction occurred. The fixation support structures are located apart from the stimulation site. By this, more choices are available to fix the structure to the retina. Possible ophthalmologic fixation methods include laser scar formation and retinal tacks without affecting the ganglionic structures directly under the stimulation elec-

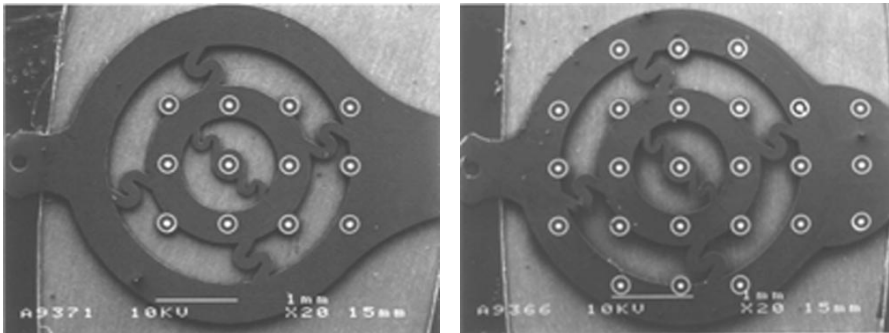


Fig 26. Flexible multichannel retina stimulator (SEM) with 12 (*left side*) and 24 (*right side*) independently addressable bipolar electrodes, respectively

trodes. The pads at the end of the interconnections will be connected to micro-electronic circuitry. The interconnect length is designed in a way that bulky electronic can be modularly assembled in the periphery and will not affect the area where the stimulation occurs.

Future work will focus on real three-dimensional electrodes that may slowly penetrate the superficial layer of the retina. We hope to improve the spatial selectivity of a stimulator structure and to lower the energy consumption during stimulation, when the microelectrode is in close proximity to the somata of the ganglion cells. A possible design of this structure is shown in Fig. 27. It demonstrates the design potentials that microfabrication of polymer based micro-structure offer.

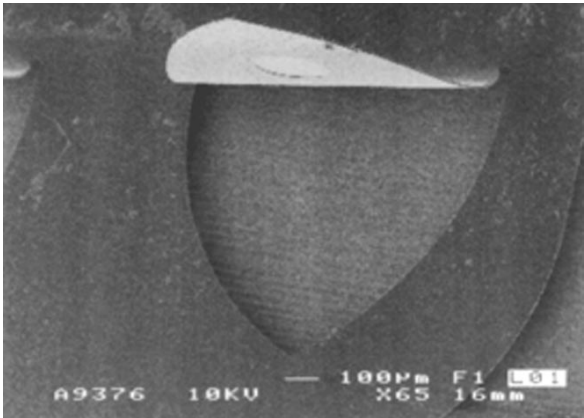


Fig.27. Approach of three-dimensional, penetrating electrodes (SEM)

6

Future Trends

At the end of this chapter, some readers may wonder why we did not present one of the three most famous and beneficial neural prostheses that are in clinical use since several years: the cardiac pacemaker, the cochlea implant and the urinary bladder stimulator of Brindley. In our view, the devices may not be considered microsystems. Only the electronic parts are built of monolithic integrated circuitry in silicon technology. The electrodes are still manufactured in a conventional way not reaching miniaturization levels that were presented here. We foresee a tremendous progress in the development of neural prostheses in the next 20 years. Developments will focus on microimplants that could help neurally impaired people to restore activities of daily life.

Many of the microsystems based neural prostheses described above bear already the aspect of future and vision. Even being most enthusiastic about the possibilities of neural microsystems we hesitate to postulate that technical systems will provide all the functionality that a biological system is able to offer. To our understanding it is less desirable and probably not feasible to interface each of the billion neural pathways with microsystems. Future effects should rather be directed to built contact to functional units or to utilize the control strategies of the body. This may be illustrated by the example of an upper limb prosthesis. Grasping is normally a perfect interplay between sensory feedback and applied muscle forces. It is a future challenge of a neural prosthesis to record sensory inputs for adapting the parameters that result in grasping. This system would mimic the closed loop control strategies of our body preventing slipping.

Neural microsystems of the future will employ the myriad of functionalities biology provides. We envision the coupling of cells with microsystems to control the syntheses of bioagents or to create highly complex and sensitive biosensors. Examples are dopamine cells on a microsystems that are implanted into the basal ganglia of the brain. The microsystem controls the dopamine production of the cells according to the needs of a patient with Parkinson's disease. In bio-sensing, microsystems will utilize the neural signals of cell complexes and organs that pursues high sensitivities to agents. In the example of lobster tentacles one may detect traces of amino acids simply by recording the nervous activity of the tentacles. There, the biohybrid system is transducing the chemical signal into multiple action potentials that are recorded simultaneously by a microsystem.

The examples above has demonstrated that future microtechnical interfaces to neurons will converge from microelectromechanical systems in biohybride microsystems.

7 References

1. McNeal DR (1977) 2000 Years of Electrical Stimulation. In: Hambrecht FT, Reswick JB. (eds) *Functional Electrical Stimulation. Applications in Neural Prostheses*. Marcel Dekker, Inc. New York, p 3
2. Rattay F, Aberham M (1993) *IEEE Trans Biomed Eng* 40:1201
3. Kimura J (1989) *Electrodiagnosis in Diseases of Nerve and Muscle: Principles and Practice*. F.A. Davis Company, Philadelphia
4. Benton LA, Baker LL, Bowman BR, Waters RL (1983) *Funktionelle Elektrostimulation*. Steinkopff, Darmstadt
5. Vossius G, Holländer H-J, Frech R (1990) *Biomedizinische Technik* 35:118
6. Dewald JPA, Given JD, Rymer WZ (1996) *IEEE Trans Rehab Eng* 4:231
7. Daly JJ, Marsolais EB, Mendell LM, Rymer WZ, Stefanovska A, Wolpaw JR, Kantor C (1996) *IEEE Trans Rehab Eng* 4:218
8. Nathan RH (1990) *Medical & Biological Eng Computing* 28:249
9. Nathan RH (1989) *Medical & Biological Eng Computing* 27:549
10. Franken HM, Veltink PH, Boom HK (1994) *IEEE EMBS Magazine* 564
11. Bajd T, Kralj A, Karcnik T, Savrin R, Benko H, Obreza P (1997) *Proc of the 5th Vienna International Workshop on FES*. Vienna, Austria, p 27
12. Grill WM, Mortimer JT (1993) *Proceedings of the Annual International Conference of the IEEE EMBS* 15:1328
13. Rijkhoff NJM, Koldewijn EL, Kerrebroeck PEV, Debruyne FMJ, Wijkstra H (1993) *Proceedings of the Annual International Conference of the IEEE EMBS* 15:1257
14. Loeb GE, Peck RA (1996) *J Neurosci Meth* 64:95
15. Popovic DB, Stein RB, Jovanovic KL, Dai R, Kostov A, Armstrong WW (1993) *IEEE Trans Biomed Eng* 40:1024
16. Naples GG, Mortimer JT, Scheiner A, Sweeney JD (1988) *IEEE Trans Biomed Eng* 35, No. 11:905
17. Naples GG, Mortimer JT, Yuen TGC (1990) In: Agnew WF, McCreery DB (eds) *Neural Prostheses*. Prentice Hall, Englewood Cliffs, p 107
18. Sweeney JD, Ksienski DA, Mortimer JT (1990) *IEEE Trans Biomed Eng* 37, No 7:706
19. Rozman J (1991) *Proceedings of the Annual International Conference of the IEEE EMBS* 13, No. 2:914
20. Veraart C, Grill WM, Mortimer JT (1993) *IEEE Trans Biomed Eng* 40, No. 7:640
21. Grill WM, Veraart C, Mortimer JT (1991) *Proceedings of the Annual International Conference of the IEEE EMBS* 13:904
22. Sinkjær T, Haugland M, Haase J, Hoffer JA (1991) *Proceedings of the Annual International Conference of the IEEE EMBS* 13:900
23. Sinkjær T, Hinge B, Jørgensen A, Jensen ML, Haugland M (1992) *Proceedings of the Annual International Conference of the IEEE EMBS* 14:1330
24. Hoffer JA, Haugland MK (1992) *Signals from Tactile Sensors in Glabrous Skin Suitable for Restoring Motor Function in Paralyzed Humans*. In: Stein RB, Peckham PH, and Popovic DB. (eds) *Neural Prostheses. Replacing Motor Function after Disease or Disability*. Oxford University Press, New York, Oxford, p 100
25. Haugland MK, Hoffer JA, Sinkjær T (1994) *IEEE Trans Rehab Eng* 2:18
26. Haugland MK, Hoffer JA (1994) *IEEE Trans Rehab Eng* 2, No.1:29
27. Haugland MK, Sinkjær T (1995) *IEEE Trans Rehab Eng* 3:307
28. Brindley GS, Br J Physiol (1972) 222, p 135p
29. Brindley GS, Polkey CC, Rushton DN, Cardozo L (1986) *J Neurol Neurosurg Psychiatry* 49:1104
30. Brindley GS (1995) *The Sacral Anterior Root Stimulator as a Means of Managing the Bladder in Patients with Spinal Cord Lesions*. In: Brindley GS and Rushton DN. (eds) *Neuroprostheses*. Ballière Tindall, London Philadelphia Sydney Tokio Toronto, p 1

31. Sauerwein D, Ingunza W, Fischer J, Madersbacher H, Polkey CE, Brindley GS, Colombel P, Teddy P (1990) *Journal of Neurology, Neurosurgery and Psychiatry* 53:681
32. Stief CG, Sauerwein D, Thon WF, Allhoff EP, Jonas U (1992) *J Urol* 148:107
33. Brindley GS (1995) Neuroprostheses to Restore Male Sexual or Reproductive Function. In: Brindley GS and Rushton DN. (eds) *Neuroprostheses*. Baillière Tindall, London Philadelphia Sydney Tokio Toronto, p 15
34. Mayr W, Bijak M, Girsch W, Holle J, Lanmüller H, Thoma H, Zrunek M (1993) *ASAIO Journal* 39:729
35. Thoma H, Girsch W, Holle J, Mayr W (1989) *ASAIO Transactions* 35:490
36. Koller R, Girsch W, Liegl C, Gruber H, Holle J, Losert U, Mayr W, Thoma H (1992) *PACE* 15:108
37. Tyler DJ, Durand DM (1994) *IEEE EMBS Magazine* 575
38. Burke D, Hicks RG, Stephen JPH (1990) *J of Physiol* 425:283
39. Adams DC, Emerson RG, Heyer EJ, McCormick PC, Carmel PW, Stein BM, Farcy JP, Gallo EJ (1993) *Anest Analg* 77:913
40. Okamoto Y, Murakami M, Nakagawa T, Murata A, Moriya H (1992) *Electroencephalography and Clinical Neurophysiology* 84:315
41. Huland H, Diekmann K-P, Sauerwein D (1992) *Der Urologe* 31:1
42. Koeze TH (1995) Neuromodulation for pain and epilepsy. In: Brindley GS and Rushton DN. (eds) *Neuroprostheses*. Baillière Tindall, London Philadelphia Sydney Tokyo Toronto, p 167
43. Krainick JU (1991) *Der Schmerz* 5:247
44. Winkelmüller W (1991) *Der Schmerz* 5:243
45. Wilkinson DW, Dow JAT, Curtis ASG, Connolly P, Clark P (1987) *Development* 99:439
46. Clark P, Connolly P, Curtis ASG, Dow JAT, Wilkinson CDW (1990) *Development* 108:635
47. Connolly P, Moores GR, Monaghan W, Shen J, Britland S, Clark P (1992) *Sens and Act B*, 6:113
48. Fromherz P, Schaden H, Vetter T (1991) *Neuroscience Letters* 129:77
49. Fromherz P, Klingler J (1991) *Biochimica et Biophysica Acta* 1062:103
50. Fromherz P, Offenhäuser A, Vetter T, Weis J (1991) *Science-Reprint Series* 252:1290
51. Droge MH, Gross GW, Hightower MH, Czisny LE (1986) *J Neurosci* 6:1583
52. Gross GW, Kowalski J (1991) Experimental and theoretical analysis of random nerve cell network dynamics. In: Antognetti P and Milutinovic V. (eds) *Neural Networks: Concepts, Applications, and Implementations*. Englewood City, New Jersey, Prentice-Hall, p 47
53. Jimbo Y, Robinson HPC, Kawana A (1993) *IEEE Trans Biomed Eng* 40, No. 8:804
54. Jimbo Y, Kawana A (1992) *Bioelectrochemistry and Bioenergetics* 29:193
55. Tatic-Lucic S, Tai Y-C, Wright JA, Pine J, Denison T (1993) *Transducers Yokohama, Japan*
56. Tatic-Lucic S, Wright JA, Tai Y-C, Pine J (1996) *Proceedings of Eurosensors X*, p 159
57. Pine J, Tai Y-C, Buzsaki G, Bragin A, Carpi D (1994) *Quarterly Progress Report, NIH-NINDS, Neural Prosthesis Program No. 4, NO1-NS-3-2393*
58. Ji J, Wise KD (1990) *IEEE Trans SC* 107
59. Ji J, Najafi K, Wise KD (1990) *Sens and Act A21 – A23:589*
60. Ji J, Najafi K, Wise KD (1990) *IEEE Trans Biomed Eng* 37, No. 1:1
61. Najafi K, Wise KD, Mochizuki T (1985) *IEEE Trans ED* 32:1206
62. Najafi K, Hetke JF (1990) *IEEE Trans Biomed Eng* 37:474
63. Najafi K, Jin J, Wise KD (1990) *IEEE Trans Biomed Eng* 37:1
64. Blum NA, Carkhuff BG, Charles JHK, Edwards RL, Meyer RA (1991) *IEEE Trans Biomed Eng* 38:68
65. Pickard RS, Wall P, Ubeid M (1990) *Sens and Act B1:460*
66. Meier JH, Rutten WLC, Zoutman AE, Boom HKB, Bergveld P (1992) *IEEE Trans Biomed Eng* 39:122
67. Anderson DJ, Najafi K, Tanghe SJ, Evans DA, Levy KL, Hettke JF, Xialon X, Zappia JJ, Wise KD (1989) *IEEE Trans Biomed Eng* 36:693
68. Drake KL, Wise KD, Farraeye J, Anderson DJ, BeMent SL (1988) *IEEE Trans Biomed Eng* 35:719

69. Hoogerwerf AC, Wise KD (1991) IEEE Int Conference on Solid-State Sensors and Actuators, p 120
70. Hoogerwerf AC, Wise KD (1994) IEEE Trans Biomed Eng 1136
71. Edell DJ (1986) IEEE Trans Biomed Eng 33:203
72. Kovacs GTA, Storment CW, Halks-Miller M, Belczynski CR, Della Santina CC, Lewis ER, Maluf NI (1994) IEEE Trans Biomed Eng 41:567
73. Najafi K, Wise KD (1986) IEEE Trans SC 21:1035
74. Kovacs GTA (1991) IEEE Trans Biomed Eng 38:116
75. Akin T, Najafi K, Smoke RH, Bradley RM (1994) IEEE Trans Biomed Eng 41:305
76. Kovacs GTA, Storment CW, Rosen JM (1992) IEEE Trans Biomed Eng 39:893
77. Akin T, Najafi K (1991) Int. Conference on Solid State Sensors and Actuators (Transducers), San Francisco, CA, USA, p 128
78. Bradley RM, Smoke RH, Akin T, Najafi K (1992) Brain Res, p 1
79. Dario P, Cocco M, Soldani G, Valderrama E, Cabruja E, Meyer J-U, Giesler T, Beutel H, Scheithauer H, Alavi M, Burkner V (1994) Technology and Fabrication of Hybrid Neural Interfaces for the Peripheral Nervous System. In: Reichl H and Heuberger A. (eds) Microsystem Technology, p 417
80. Meyer J-U, Beutel H, Valderrama E, Cabruja E, Soldani G, Dario P (1995) Proc of the 8th Int Workshop on Micro Mechanical Systems, p 358
81. Laurell T, Drott J, Zhao Q, Wallman L, Montelius L, Bjursten LM, Lundborg G, Danielsen N (1994) Proceedings of the Annual International Conference of the IEEE EMBS
82. Navarro X, Calvet S, Butí M, Gómez N, Cabruja E, Garrido P, Villa R, Valderrama E (1996) Restorative Neurology and Neuroscience 9:151
83. Schaldach M (1992) Electrotherapy of the Heart. Springer-Verlag, Berlin, Heidelberg, New York
84. Bolz A (1995) Die Bedeutung der Phasengrenze zwischen alloplastischen Festkörpern und biologischen Geweben für die Elektrostimulation. Fachverlag Schiele und Schön, Berlin
85. Anderson DJ, Hetke JF, Najafi K, Tanghe SJ, Wise KD, Altschuler RA, Kim C-H, Pielemeier W, Wakefield GH, Xue X (1992) University of Michigan
86. Rose TL, Robblee LS (1990) IEEE Trans Biomed Eng 37:1118
87. Tanghe SJ, Wise KD (1992) Iridium Oxide High-Performance Stimulating Sites for Multielectrode Probe Arrays, Center for Integrated Sensors and Circuits, Course of the University of Michigan
88. Robblee LS, Rose TL (1990) Electrochemical Guidelines for Selection of Protocols and Electrode Materials for Neural Stimulation. In: Agnew WF and McCreery DB. (eds) Neural Prostheses. Prentice Hall, Englewood Cliffs, New Jersey, p 25
89. Twardoch UM (1994) J Appl Electrochem 24:835
90. Hubmann M, Hardt R, Bolz A, Schaldach M (1992) Proceedings of the Annual International Conference of the IEEE EMBS 14:2378
91. Beebe X, Rose TL (1988) IEEE Trans Biomed Eng 35:494
92. Anderson DJ, Najafi K, Tanghe SJ, Evans DA, Levy KL, Hetke JF, Xialon X, Zappia JJ, Wise KD (1989) IEEE Trans Biomed Eng 36 No. 7:693
93. Riedmüller J, Bolz A, Brehm B, Schaldach M (1991) Biomedizinische Technik 36, Ergänzungsband:104
94. Edell DJ, Devaney LP, Rescoe G, Heetderks WJ (1993) IEEE Trans Biomed Eng, submitted
95. Edell DJ (1986) IEEE Trans Biomed Eng 33:203
96. Cogan SF, Liu Y-P, Mc Caffrey M, Twardoch UM (1993) Quarterly Progress Report, NIH-NINDS, Neural Prosthesis Program No.5, N44-NS-2-2311:
97. Pliskin WA, Gdula RA (1980) Passivation and Insulation. In: Keller SP. (eds) Materials, Properties and Preparation. North-Holland Publishing Company, Amsterdam
98. Yoshida S, Okuyama K, Kanai F, Kawate Y, Motoyoshi M, Katto H (1988) IEEE-IEDM 22
99. Shimaya M (1995) IEEE 292
100. Vogt M, Hauptmann R (1995) Surface Coatings and Technology 74-75:676
101. Richardson RR, Miller JA, Reichert WM (1993) Biomaterials 14:627

102. Loeb GE, Walker AE, Uematsu S, Konigsmark BW (1977) *Journal of Biomed Mat Res* 11:195
103. Haggerty HS, Lusted HS (1989) *Acta Otolaryngol* 107:13
104. Frazier BA, Ahn CH, Allen MG (1995) *Sens and Act A* 45:47
105. Beebe DJ, Denton DD (1994) *Sens and Act A* 44:57
106. Chang L, Goodner R (1991) SPIE, Metallization:Performance and Reliabilty Issues for VLSI and ULSI 1596:34
107. Kim YW, Allen MG (1991) *IEEE TransED* 651
108. Rossi RD, Machiesky PD (1990) *Solid State Technology* 21
109. Keidel WD (1989) *Biokybernetik des Menschen*. Wissenschaftliche Buchgesellschaft, Darmstadt
110. Keidel WD. Personal communication
111. Stieglitz T, Navarro X, Calvet S, Blau C, Meyer J-U (1996) *Proceedings of the Annual International Conference of the IEEE EMBS*, no. 417
112. Hambrecht FT (1995) Visual prostheses based on direct interfaces with the visual system. In: Brindley GS and Rushton DN. (eds) *Neuroprostheses*. Baillière Tindall, London Philadelphia Sydney Tokyo Toronto, p 147
113. Perlman JL, Chow AY, Peachey NS (1996) *Invest Ophthal & Vis Sci* 37 (Suppl.):96
114. Chow AY, Chow VY, Peachey NS (1996) *Invest Ophthal & Vis Sci* 37 (Suppl.):349
115. Rizzo JF, Miller S, Denison T, Herndon T, Wyatt JL (1996) *Invest Ophthal & Vis Sci* 37 (Suppl.):707
116. Mann J, Edell DJ, Rizzo JF, Raffel J, Wyatt JL (1994) *Invest Ophthal & Vis Sci* 35 (Suppl.):1380
117. Schwarz M, Hosticka BJ, Scholles M, Eckmiller R (1995) *Proc of the 5th Vienna International Workshop on FES* 413
118. Eckmiller R (1996) *Proceedings of the RESNA Research Symposium* 21
119. Humayun MS, de Juan E, Dagnelie G, Greenberg RJ, Philips DH (1996) *Arch Ophthalmol* 114:40
120. Narayanan MV, Rizzo JF, Edell DJ, Wyatt JL (1994) *Invest Ophthal & Vis Sci* 35 (Suppl.):1380

Fluids for Sensor Systems

Shuichi Shoji

Department of Electronics, Information and Communication Engineering, Waseda University,
3-4-1, Ohkubo, Shinjuku-ku, Tokyo, 169 Japan. *E-mail: shojis@mn.waseda.ac.jp*

Several techniques for miniaturization of simple chemical and medical analysis systems are described. Miniaturization of total analysis systems realizes a small sample volume, a fast response and reduction of reagents. These features are useful in chemical and medical analysis. During the last decade many micro flow control devices, as well as the micro chemical sensors fabricated by three dimensional microfabrication technologies based on photofabrication, termed micromachining, have been developed. Miniaturized total analysis systems (μ TAS) have been studied and some prototypes developed. In microfabricated systems, “microfluidics”, which represent the behavior of fluids in small sized channels, are considered and are very important in the design of micro elements used in μ TAS. In this chapter microfluidics applied flow devices, micro flow control devices of active and passive microvalves, mechanical and non-mechanical micropumps and micro flow sensors fabricated by micromachining are reviewed.

Keywords: Microfluidics, micro total analysis system (μ TAS), microvalve, micropump, micro flow sensor.

1	Introduction	164
2	Examples of Micro Total Analysis Systems	165
2.1	Chemical Analysis	165
2.2	Medical Analysis	165
3	Microfluidics Applied Devices	167
3.1	Mixer	167
3.2	Flow Switch	168
3.3	Fluid Filter	168
4	Micro Flow Control Devices	169
4.1	Actuators	169
4.1.1	Miniaturized Conventional Actuators	170
4.1.2	Micromachinable Actuators	172
4.2	Microvalves	174
4.2.1	Active Microvalve	174
4.2.2	Passive Microvalves (Check Valve)	176
4.3	Micropumps	178
4.3.1	Mechanical Micropumps	178

4.3.2 Non-Mechanical Micropumps 181

4.4 Micro Flow Sensors 183

5 Conclusions 186

6 References 187

1

Introduction

Miniaturization of chemical sensors and biosensors is proceeded by three dimensional micro fabrication technologies based on photofabrication commonly used in the integrated circuits, termed micromachining. Very small devices controlling or sensing flow in the order of ml/min are named micro flow control devices. Many micro flow devices of microvalves, micropumps and micro flow sensors made by micromachining have been developed during the last 10 years [1]. Microvalves and micropumps fabricated by micromachining have a very small dead volume that enables precise control of $\mu\text{l/min}$ or ml/min flow with a very fast response time. By integrating these devices with micro flow sensors to obtain feedback control, very precise liquid dosing or controlling systems are realized [2, 3]. In this case, discrete, standard connecting ports used in the conventional systems are not necessary. This is useful for the reduction of dead volume.

Micro flow control devices open new possibilities for the miniaturization of conventional chemical and biochemical analysis systems. The micro total analysis system (μTAS) including microfabricated detectors (e.g. silicon based chemical sensors, optical sensors), micro flow control devices and control/detection circuits is a practical micro electro mechanical system (MEMS). μTAS realize very small necessary sample volume, fast response and the reduction of reagents which is very useful in chemical and medical analysis. Two approaches of monolithic and hybrid integration of these devices have been studied. Monolithic and hybrid types of flow injection analysis (FIA) systems were already demonstrated [4, 5]. The combination of the partly integrated components and discrete components is useful in many cases [6]. To fabricate such systems, bonding and assembling methods play very important roles [7].

Behavior of the fluids in the microfabricated channels are different from those in the millimeter scale channels. Miniaturization of micro flow devices opens a new research field, “microfluidics” which represents the behavior of the fluid in the micro channel [8]. Since the Reynolds number in the micro channel is usually below 200, the flow is laminar and special design concepts are necessary for the fluidic elements of mixers, reaction coils etc. in the μTAS . Some components of flow switches and fluid filters were developed using laminar flow behavior.

Microvalves are classified into two categories: active microvalves (with an actuator) and passive microvalves (without an actuator). Micropumps are also

classified into two groups: mechanical and non-mechanical pumps. In active microvalves and mechanical micropumps the miniaturized conventional actuators and the micromachinable actuators have been studied most widely and used. The characteristics of these devices depend strongly on the features of the microactuator used. Pumping without mechanical actuators is obtained by electrohydrodynamics, electroosmosis and ultrasonic behavior. Electrically driven liquid handling using electroosmosis are applied for flow injection analysis (FIA) systems, liquid chromatography (LC) systems, etc., because of their simple planar structures [9, 10]. Good matching with electrophoresis separation is useful in FIA applications. An immunological μ TAS is also realized by this method [11]. In practical use, mechanical components for introducing samples and for providing reagents are required. To miniaturize conventional total analysis systems, mechanical micro flow control devices are still indispensable.

In this chapter, first the simple μ TAS concepts for chemical and medical analysis using mechanical micro components are presented. Micro components of μ TAS considering the microfluidics are described next. The micro flow control devices of microvalves, micropumps and micro flow sensors are then reviewed.

2

Examples of Micro Total Analysis Systems

2.1

Chemical Analysis

In order to realize automatic chemical analysis, integration of the elements to obtain sample handling, treatment and detection is necessary. A basic flow system can be built up using standard components of micro chemical sensors, a reaction coil, a 3-way microvalve, suction and injection micropumps as shown in Fig. 1. The sample flow is controlled by suction pump and introduced up to the reaction coil part. The reagents are introduced through the 3-way microvalve and mixed to the sample in the reaction coil. After the reaction between sample and reagent, the product is measured in the detector cell. Finally the calibration solution is introduced through the reaction coil by the injection pump to calibrate the microsensors. At the same time, the reaction coil and the detector cell are cleaned. The advantage of this system is that the samples do not enter the micropumps where the unfiltered solution might cause degradation of pumping. Similar systems the detection of ion concentrations have been realized using the ISFET as the detector by stacking the wafers on which the components are fabricated [5].

2.2

Medical Analysis

For medical and biomedical applications, a μ TAS has to be designed considering property of the sample fluid especially in whole blood analysis. Prototypes of

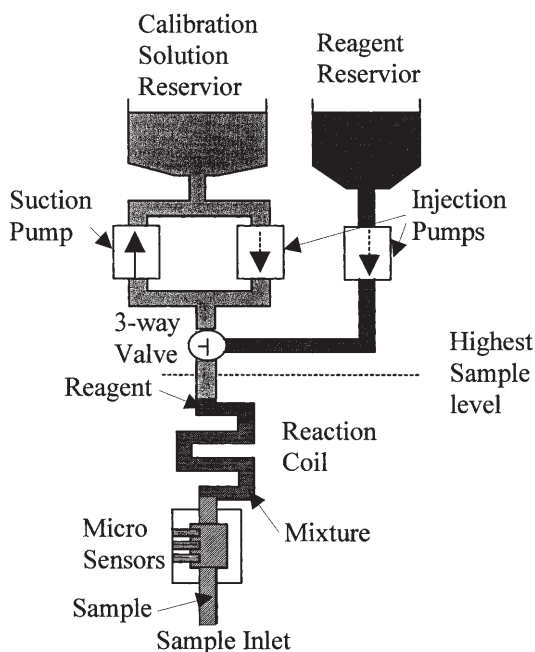


Fig. 1. Setup of a simple micro total analysis system for chemical analysis

whole blood gas analysis systems using pH ISFET and micro valves driven by shape memory alloy (SMA) actuators and piezobimorph actuators were developed [12, 13]. Problems of blood coagulation and protein adhesion have to be solved in such systems. Another problem is that body fluids like whole blood have high viscosity so as to make the microchannel resistance high. Pumping pressure of the sample flow control micropump should be higher than those used in the chemical μ TAS.

Disposable μ TAS will be ideal for medical use [14]. However, the high fabrication cost of sophisticated μ TAS including micropumps and microvalves is a real problem. One of the basic components of medical μ TAS taking this into account is illustrated in Fig. 2. A detector cell consists of micro sensors and a 3-way microvalve is placed at the sample inlet. Flow is controlled by a suction pump and an injection pump connected to the detector cell. The calibration solution flow is also controlled by an individual pump and a 3-way valve. In this system, only sample flow reaches the detector cell. The upper parts of the system are free from contamination and corrosion so that they can be reused many times, while the detector cell has to be disposed of. To realize this system, a 3-way microvalve which can handle whole blood is indispensable. A separable channel type microvalve whose channel part is disposable while actuator part is reusable is useful for the 3-way microvalve of the detector cell [15]. Mechanically fixed stack structures including disposable parts are useful in many medical μ TAS.

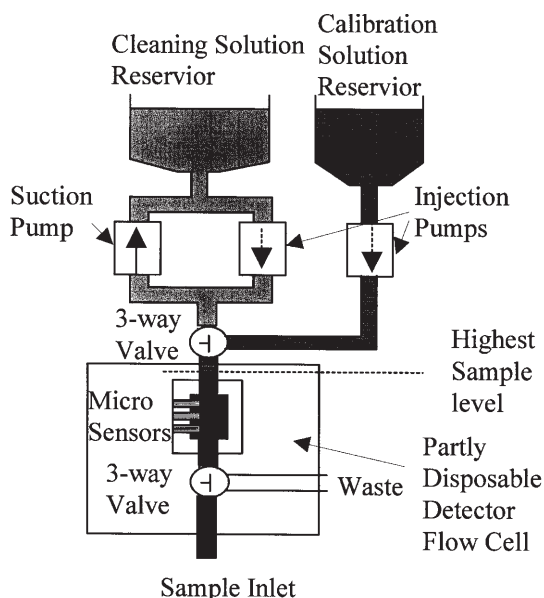


Fig. 2. Setup of a simple micro total analysis system for medical analysis [15]

3 Microfluidics Applied Flow Devices

3.1 Mixer

Effective mixing of the sample solution and reagent is important in μ TAS. Fast mixing is necessary to reduce the analyzing time in μ TAS like FIA and flow cytometry analysis systems. Mixing is generally a two-step process [16]. First, segmentation where a heterogeneous mixture of two fluids is formed by convection; and secondly the inter-diffusion of molecules between domains.

In microfluidics, segmentation by stirring or creation of turbulent flow can not be expected because Reynolds numbers do not exceed 2000 (the limit for turbulent flow). Some methods for mixing in microfluidics have been developed.

1. Mixing by inertial forces has been demonstrated using a 80 zigzag micro-channel ($300\ \mu\text{m} \times 600\ \mu\text{m} \times 1\ \text{mm}$). The mixing time achieved in this case is 1 second at the Reynolds number of 33 [17].
2. Segmentation has also been achieved by injecting one liquid into another through micro nozzles [18].

Segmentation in fluids with Reynolds numbers below 1 is only possible by the way in which two fluids are merged. Since the width of the microfabricated channels on the planer wafers is usually larger than the depth, a method for reducing mixing time is to stack the two flow streams as thin layers in one

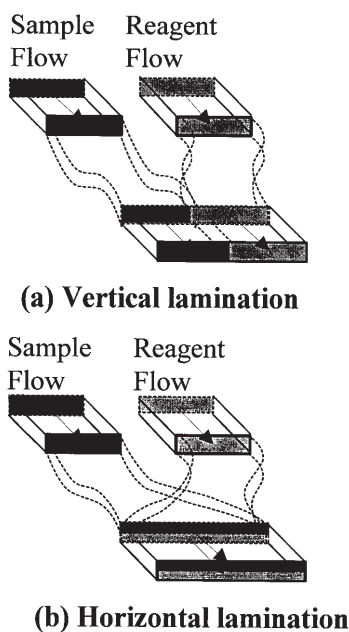


Fig.3. Schematic of the micro fluidics mixer [16]

channel, thus increasing the contact area as well as reducing the diffusion length as shown in Fig. 3. A multi-stage multi-layer lamination of two liquids is very effective to realize fast mixing. To realize this lamination of two liquids, many structures have been tested [19, 20].

3.2

Flow Switch

Flow switches using fluidics in small Reynolds number are fabricated. The principle of the flow switch is shown in Fig. 4 [21]. Mixing of the sample stream and carrier liquid is negligible when the contact area is small and the contact time within subsecond range. The width of the sample stream is controlled by two carrier flows. This structure can be applied for a valveless sample injection in FIA and for sorting of particles and living cells in flow cytometry. A flow switch having 5 outlets has also been obtained by this method.

3.3

Fluid Filter

Fluid filters were realized in the low Reynolds number regime [22, 23]. It separates the particles and molecules based on the diffusion coefficient while diluting their concentration. The concept of the diffusion-based filtration is shown in Fig. 5. As the two flow streams of sample and dilutant are introduced

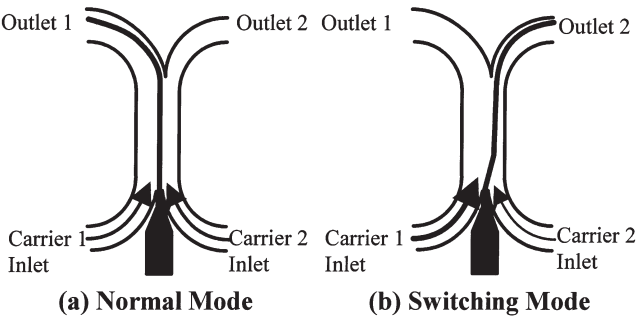


Fig. 4. Schematic of the micro fluidics switch [22]

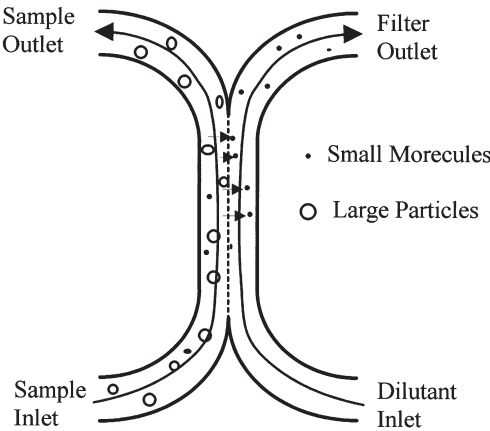


Fig. 5. Schematic of the micro fluidics filter [23]

to the central channel, no mixing occurs at low Reynolds number although some molecules diffuse across the fluid. At the end of the central channel, the flow is split into two streams of a filter outlet and waste. Since the smaller molecules have a larger diffusion coefficient compared to those of the larger ones, the stream to the filter output is preferentially enriched with smaller molecules.

4 Micro Flow Control Devices

4.1 Actuators

The performances of mechanical micro flow control devices depend strongly on the features of the actuator [1]. In fact, the sizes of these devices are determined

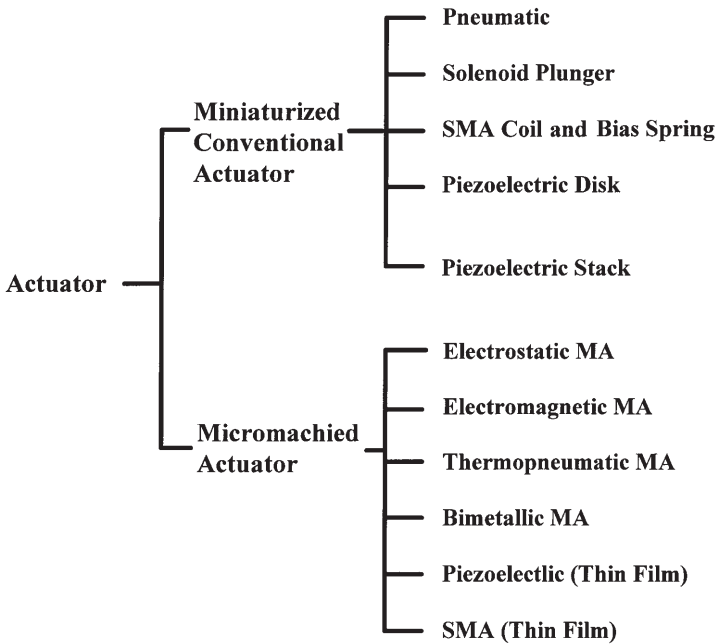


Fig.6. Actuators for micro flow control devices

by that of the actuator used. The actuators developed so far have been classified into two categories, miniaturized conventional actuators and micromachinable actuators. Many actuators listed in Fig. 6 have been studied and some have been used in micro flow control devices. A schematic of the typical miniaturized conventional actuators and micromachinable actuators is given in Figs. 7 and Fig. 8.

4.1.1

Miniaturized Conventional Actuators

Miniaturized conventional actuators have to be glued or mechanically assembled on the microfabricated valve or pump structure.

- a) **Electromagnetic.** Electromagnetic actuation was realized with a solenoid plunger as shown in Fig. 7a. This is the first microvalve which has been used in the gas chromatography system fabricated on a silicon wafer [24]. The force generated by this actuator depends on the applied current to the solenoid coil and on the number of the turns. A large stroke is one of the advantages of this actuator.
- b) **Piezoelectric.** Actuators using the piezoelectric effect have been widely used from a very early stage. Some types of miniaturized piezoelectric actuators, disk (Fig. 7b), cantilever (Fig. 7c) and stack (Fig. 7d) are commercialized.

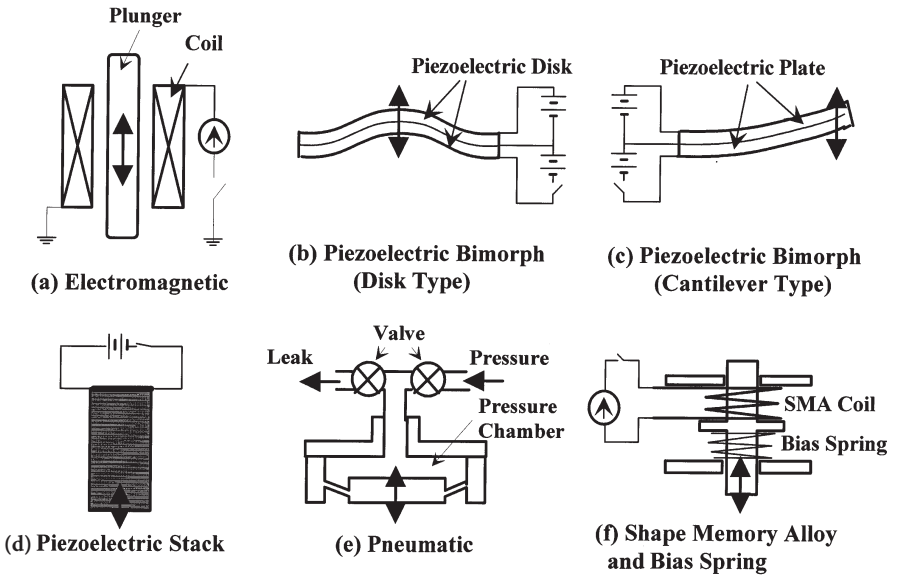


Fig. 7. Schematics of the miniaturized conventional actuators [1]

These actuators consist of the piezoelectric plates and metal electrodes. Since disk type actuators can be easily glued with resin to the structure, these are used in the micropumps. The disk and cantilever type show a large deformation and fast response although the generated pressure is not large.

To generate large pressure, a stack structure of many piezoelectric plates and metal electrodes is used. Pressures greater than 350 kgf/cm^2 are obtained. The maximum stroke is, however, small. The stroke to length of the actuator is smaller than 10^{-3} . A high applied voltage of over 100 V and a small current are features of this actuator.

- c) Pneumatic. Typical pneumatic driving system has electromagnetic valves and an air compressor or nitrogen supply (Fig. 7 e). The displacement and generated force can be widely controlled. However, fast response and small size cannot be expected.
- d) Shape memory alloy and bias spring. Small actuators are obtained using a shape memory alloy (SMA) coil memorizing the expanded state and a bias spring (Fig. 7 f). The SMA coil regains its original shape when it is heated above the critical temperature. The critical temperature of Ti-Ni SMA is 40–50, achieved by the Joule effect. To obtain a reasonable response time, a large current of about 1 A is required. It is difficult to control the displacement.

4.1.2

Micromachinable Actuators

- a) Electrostatic. The principle of the electrostatic actuator is very simple as shown in Fig. 8a. The electrostatically generated pressure P_{el} is calculated by:

$$P_{el} = 1/2 \epsilon_0 \cdot \{V / (d_o + \epsilon_{ox} d_{ox})\}^2$$

where d_o , d_i and V are the gap between the electrodes, the isolating layer thickness and the applied voltage respectively. The generated force is inversely proportional to the second power of the distance d_o . Hence the available stroke is limited when reasonable pressure is required.

- b) Electromagnetic. A miniaturized electromagnetic actuator is shown in Fig. 8b. It consists of a soft magnetic mass suspended by a spring beam and external coil. The generated pressure P_{em} is calculated by:

$$P_{em} = M_m / A \int \delta / \delta x H_x dx$$

where A , M_m and H_x are the area, the magnetization of the mass and the vertical component of the magnetic field produced by the external coil respectively.

Another type of electromagnetic actuator is shown in Fig. 8c. It consists of a deflectable membrane having a metal conductor and a external permanent magnet. A current applied to the conductor perpendicular to the magnetic field generates the Lorentz force.

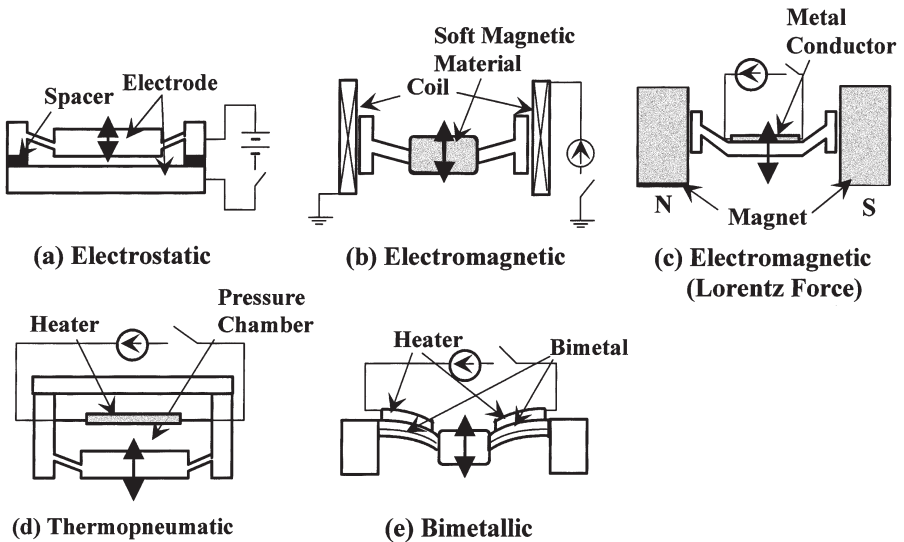


Fig. 8. Schematics of the micromachinable actuators [1]

c) Thermopneumatic. A typical thermopneumatic actuator has a sealed pressure chamber and movable diaphragm as shown in Fig. 8d. The pressure chamber is filled with either gas or liquid. The inner pressure is increased by electrical dissipation in a heater resistor incorporated in the chamber. Generated pressure P_{tp} in the chamber is given by:

$$P_{tp} = P_o \exp (-L_o/RT)$$

where P_o , L_o , R and T are the initial pressure, the latent heat of vaporization, gas constant and temperature respectively. The rising time of the actuator depends on the heat capacitance and the available power of the heater, while the relaxation time is determined by the heat transfer to the outside.

d) Bimetallic. The structure of a bimetallic actuator is shown in Fig. 8e. It consists of two materials having different thermal expansion coefficients and micro heater. The generated pressure P_{bm} is proportional to the difference between the thermal expansion coefficient of the two materials ($\gamma_b - \gamma_a$) and the heating temperature ΔT :

$$P_{bm} \propto (\gamma_b - \gamma_a) \Delta T$$

The general features of the miniaturized conventional actuators and the micromachinable actuators are listed in Table 1.

Table 1. Features of the miniaturised conventional actuators and the micromachinable actuators [1]

Actuators	Pressure	Stroke (Displacement)	Response Time	Reliability
<i>External</i>				
Soleniod Plunger	small	large	midium	good
Disk Type	small	midium	fast	good
Piezoelectric				
Stack Type	very large	very small	fast	good
Pneumatic	large	large	slow	good
Shape Memory Alloy and Bias Spring	large	large	slow	not enough
<i>Micromachinable</i>				
Electrostatic	small	very small	very fast	very good
Thermopneumatic	large	midium	midium	good
Electromagnetic	small	large	fast	good
Bimetallic	large	small	midium	enough

4.2 Microvalves

4.2.1 Active Microvalves

Almost all kinds of actuators described above have been applied to fabricate gas flow control microvalves [1, 25]. However, for liquid flow control only a few microvalves have been developed.

- a) Piezoelectric actuator. Fig. 9 shows a 3-way microvalve using a piezoelectric stack [26]. It has a 2-ring movable diaphragm to obtain one inlet and two switching outlets. To reduce the leakage of the normally closed gap, a suspended Ni valve seat is used. A sample injector was fabricated using a pair of this valve. A very small dead volume 3-way microvalve was developed using a piezoelectric stack as shown in Fig. 10. It consists of the separable channel part and actuator part [14]. Since the channel part is disposed of after use while the actuator part can be used frequently, cost is reduced and can be applied in medical systems. The cantilever type piezoelectric bimorph is also used as an actuator for the microvalve in medical systems [13].
- b) SMA coil and bias spring. Normally open and normally closed microvalves have been developed for blood flow control [12]. Structures are shown in

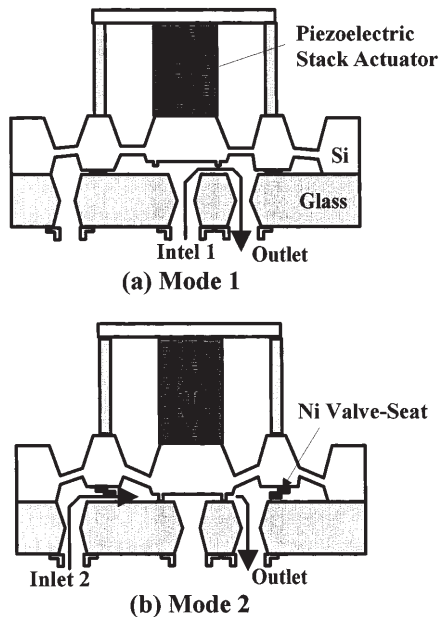


Fig. 9. Structure of the 3-way microvalve using the piezoelectric stack actuator [26]

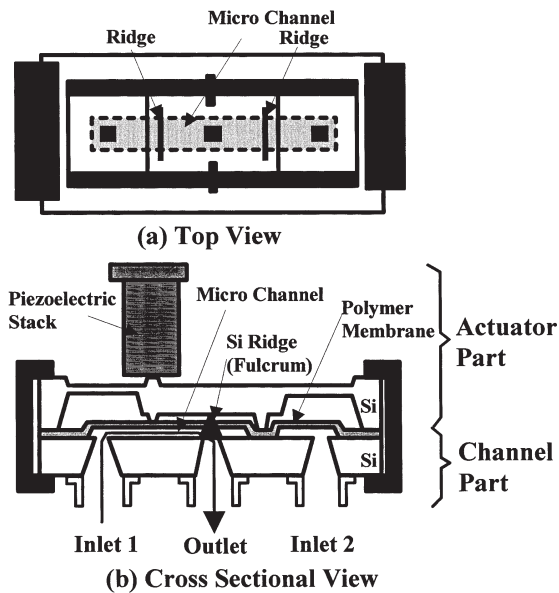


Fig. 10. Structure of the separable type 3-way microvalve using the piezoelectric stack actuator [14]

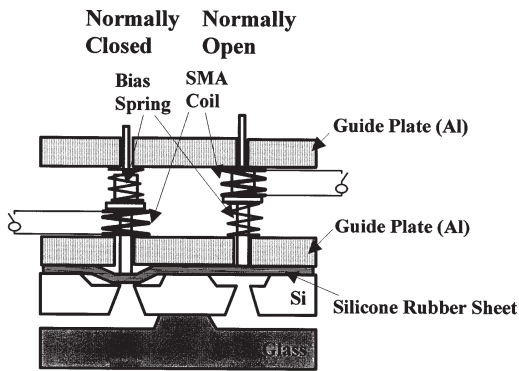


Fig. 11. Structure of the microvalve using SMA coil and bias spring actuator [12]

Fig. 11. A silicone rubber membrane is used as a soft sheet which covers the hole in the flow channel. A larger stroke enables larger flow conductance suitable for the control of blood flow. This valve, however, can be used only as an on-off valve.

c) Thermopneumatic. Thermopneumatically driven microvalves have also been fabricated [27]. An example of the normally open microvalve is shown in

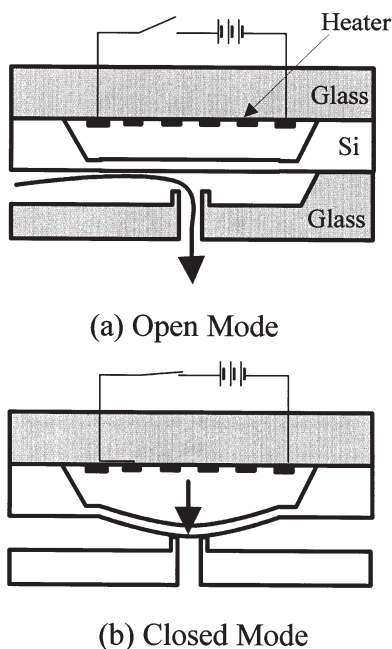


Fig. 12. Structure of the thermopneumatic microvalve [27]

Fig. 12. A resistive metal thin film heater is formed on the upper glass. Using the liquid-gas phase system of methyl chloride, the generated pressure is increased and the response time reduced. The dynamic range of this type of valve can be broad by adjusting cavity shape, quantity of gas and liquid molecules.

4.2.2

Passive Microvalves (Check Valve)

Microvalves without actuators are mainly used for check valves of micropumps. Very small leakage under reverse applied pressure and large reverse-to-forward flow resistance ratio are required in the micropump. The response time that is the transition time during the open-to-close or close-to-open is also an important parameter in the check valve. Structures and operation schemes of the check valves developed so far are shown in Fig. 13. Figure 13a shows a ring mesa structure having a hole through the center and a surrounding ring diaphragm [28]. Fig. 13b shows a simple cantilever structure [29, 30] while Fig. 13c depicts a round disk suspended by four thin beams made of polysilicon which is fabricated by surface micromachining [31]. Figure 13d illustrates a thin V-groove with a small slit [32]. The valve consists of a perforated thin polyimide membrane stretched over an opening in the titanium membrane as shown in Fig. 13e

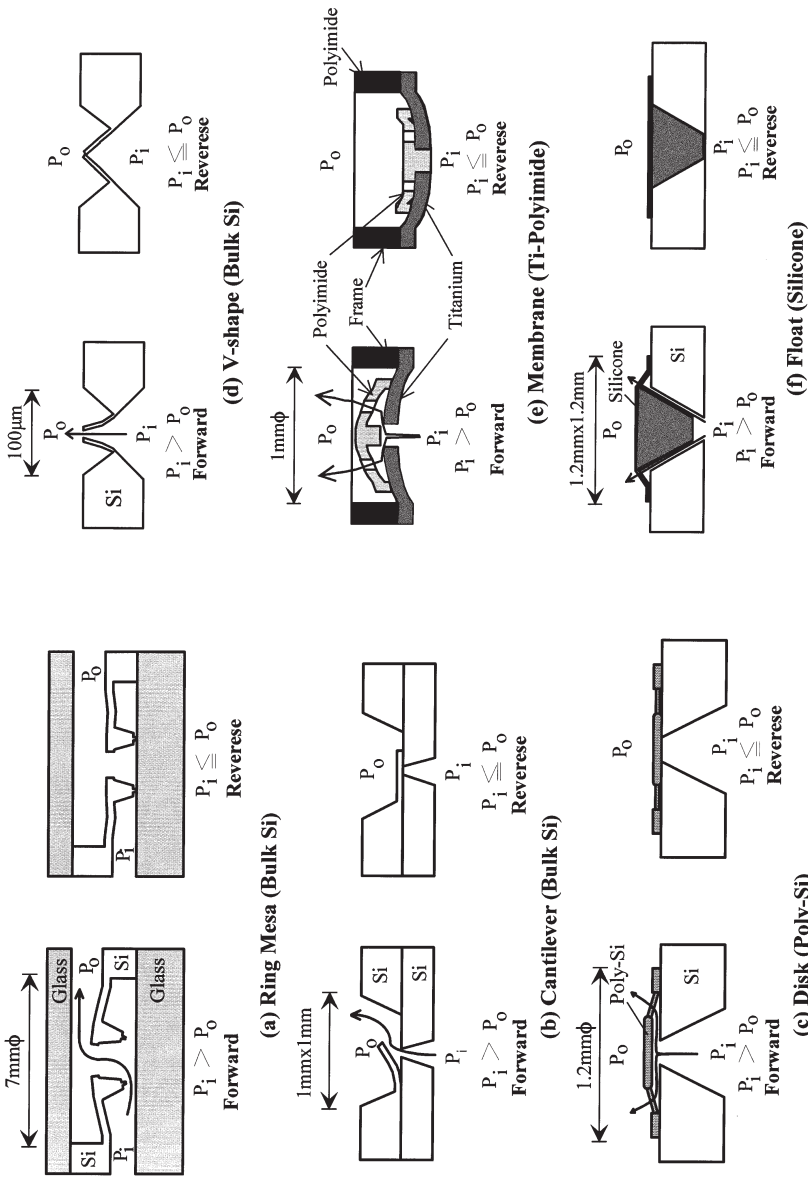


Fig. 13. Structure and operation of the micro check valves [1]

Table 2. Features of the micro check valves [1]

Type	Structure	Size	Reverse Leakage	Forward/Reverse Flow Rate
Ring Mesa (Bulk Si)	Fig. 13 a	7 mm ϕ		
Cantilever (Bulk Si)	Fig. 13 b	1 mm \times 1 mm	1 μ l/min (0.6 mH ₂ O)	5 \times 10 ³ (1.0 mH ₂ O)
Disk (Poly-Si)	Fig. 13 c	1.2 mm ϕ (1.0 mH ₂ O)	5 μ l/min	200 (1.0 mH ₂ O)
V-shape (Bulk Si)	Fig. 13 d	80 μ m \times 100 μ m		6 \times 10 ² (6.0 mH ₂ O)
Membrane (Ti-Polyimide)	Fig. 13 e	1.0 mm ϕ	360 μ l/min (0.1 kgf/cm ² :He)	2.6 \times 10 ³ (0.1 kgf/cm ² :He)
Float (Silicone)	Fig. 13 f	1.2 mm \times 1.2 mm	0.26 μ l/min (10 mH ₂ O)	2.1 \times 10 ⁴ (10 mH ₂ O)

[33]. Fig. 13 f shows a silicone rubber float and through hole, made by molding so as to fit precisely into the hole [34]. This structure is suitable for the high pressure micropump. The size and characteristics are summarized in Table 2.

4.3

Micropumps

4.3.1

Mechanical Micropumps

Two kinds of micropumps have been developed: reciprocating (diaphragm) and peristaltic. The majority of the micropumps developed so far are the reciprocating type (Fig. 14). These consist of a pressure chamber driven by an actuator and inlet and outlet check valves. Many types of micropumps have been constructed with the combinations of the actuators and the check valve described above.

- a) Piezoelectric. Figure 15 shows the micropump developed in the early stage and used in some micro flow systems [28]. It consists of a piezoelectric disk and ring mesa type bulk silicon check valves. The driving frequency of this micropump is limited by the feature of the check valve. A microfabricated nozzle/diffuser elements instead of the check valves can be used for the micropump [35]. Fig. 16 shows the pumping system connecting two micropumps in parallel [36]. One of the disadvantages of micropumps using check valves is the restriction of the driving frequency. This type of the micropump can be driven at frequency of a few kHz. The other types of micropump using piezoelectric stack and poly-silicon check valves are shown in Fig. 17.

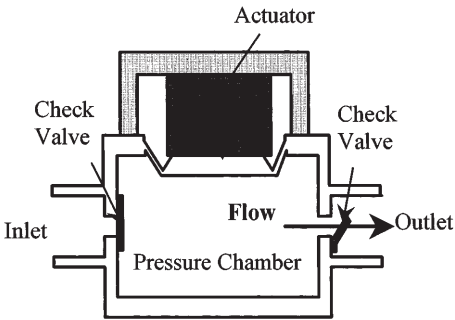


Fig. 14. Schematic of the reciprocating (diaphragm) micropump

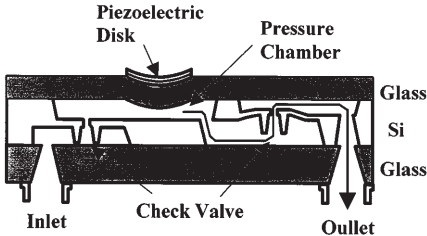


Fig. 15. Structure of the micropump using piezoelectric disk actuator [28]

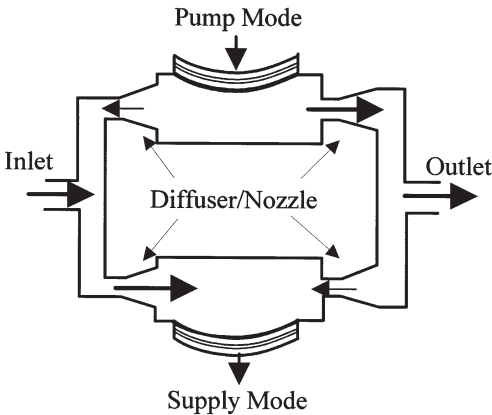


Fig. 16. Schematic of the nozzle/diffuser parallel connected micropumps [36]

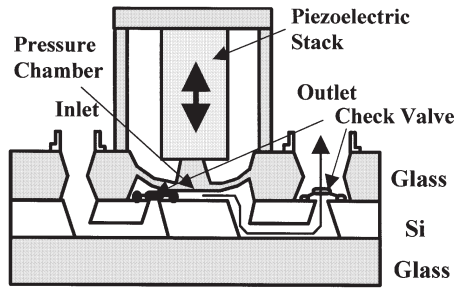


Fig. 17. Structure of the micropump using piezoelectric stack actuator [6]

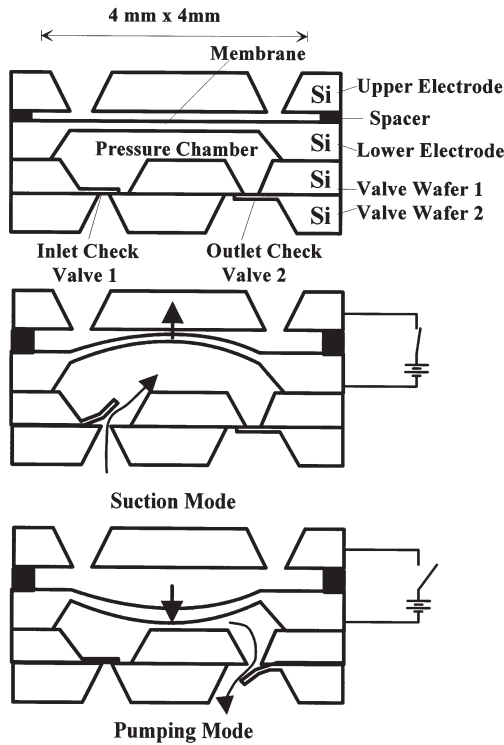


Fig. 18. Structure of the micropump using electrostatic actuator [37]

- b) Electrostatic. The structure and operation of the electrostatically driven micropump is shown in Fig. 18 [37]. The cantilever type check valves are used. High driving frequencies of a hundred Hz can be realized by this combination. This can be fabricated by the simple batch process.
- c) Thermopneumatic. Two types of thermopneumatic micropumps are developed as shown in Figs. 19 and 20. The micropump of Fig. 19 has stacked glass-

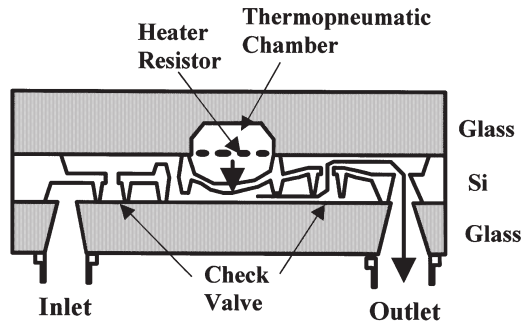


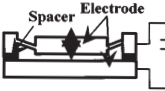
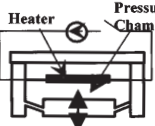


Fig. 19. Structure of the micropump using thermopneumatic actuator fabricated on a silicon wafer [2]

Table 3. Features of the actuators used in the typical micropumps

Actuator	Pressure	Stroke (Displacement)	Response Time
<div> (a) Piezoelectric Disk</div>	Midium < 1 kgf/cm ²	Midium < 50 μm	Fast >0.1 msec
<div> (b) Piezoelectric Stack</div>	Very Large < 350 kgf/cm ²	Small < 10 μm	Fast >0.1 msec
<div> (c) Electrostatic</div>	Small < 0.5 kgf/cm ²	Very Small < 5 μm	Very Fast <0.1 msec
<div> (d) Thermopneumatic</div>	Large <10 kgf/cm ²	Large < 100 μm	Slow > 5 msec

ses and a silicon structure fabricated by anodic bonding [10]. The micropump of Fig. 20 uses a plastic as the body material fabricated by molding [38, 39].

The characteristics of the actuators, check valves and micropumps which have been used in flow systems are listed in Table 3, Table 4, and Table 5 respectively. The characteristics depend on the dimensions designed so that these are only typical values.

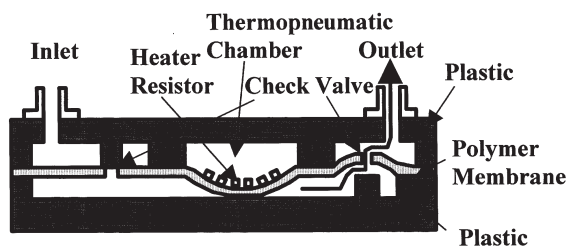


Fig. 20. Structure of the micropump using thermopneumatic actuator fabricated by plastic molding [38]

Table 4. Features of the micro check valves used in the typical micropumps


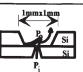
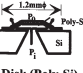
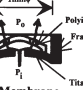

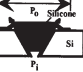

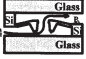


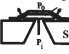
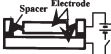



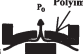
Check Valve	Rverse Leakage (Pressure)	Forward/ Reverse Flow Rate	Dynamic Response
 Diffuser/Nozzle	—	—	<div>Fast</div> <div>↑</div> <div>↓</div> <div>Slow</div>
 Cantilever (Bulk Si)	$< 0.5 \mu\text{l/min}$ ($0.4\text{mH}_2\text{O}$)	$> 2.8 \times 10^4$ ($0.4\text{mH}_2\text{O}$)	
 Disk (Poly-Si)	$< 5 \mu\text{l/min}$ ($1.0\text{mH}_2\text{O}$)	> 200 ($1.0\text{mH}_2\text{O}$)	
 Membrane	$24 \mu\text{l/min}$ ($2.3\text{mH}_2\text{O}$)	< 75 ($2.3\text{mH}_2\text{O}$)	
 Ring Mesa (Bulk Si)	—	—	
 Float (Silicone)	$< 0.2 \mu\text{l/min}$ ($10 \text{ mH}_2\text{O}$)	$> 2.1 \times 10^3$ ($10 \text{ mH}_2\text{O}$)	

Table 5. Characteristics of the typical micropumps

Actuator	Check Valve	Flow Range	Maximum Output Pressure
 (a) Piezoelectric Bimorph (Disk Type)	 (a) Ring Mesa (Bulk Si)	8 μ l/min (100V, 1Hz)	1.0mH ₂ O
	 (b) Diffuser/Nozzle	2.3ml/min:H ₂ O (1kHz)	7.6mH ₂ O
 (b) Piezoelectric Stack	 (c) Disk (Poly-Si)	40 μ l/min (100V, 40Hz)	1.5mH ₂ O
 (c) Electrostatic	 (e) Cantilever (Bulk Si)	350 μ l/min (200V, 400Hz)	3.1mH ₂ O
 (d) Thermopneumatic	 (a) Ring Mesa (Bulk Si)	58 μ l/min (2.5W, 5Hz)	0.3mH ₂ O
	 (f) Membrane (Polyimide)	Air: 218 μ l/min (150mW, 30Hz)	Air: 98 hPa

4.3.2
Non-mechanical Micropumps

Electrohydrodynamic pumps, electroosmotic pumps, ultrasonic pumps and thermocapillary pumps have been reported as non-mechanical micropumps.

a) Electrohydrodynamic. Two types of electrohydrodynamic micropumps are presented: a powerful DC-charge injection micropump and a traveling wave voltage driven micropump. The motive force of the DC-charge injection pump is the Coulomb force exerted on the charges between two electrodes as shown in Fig. 21 [40, 41]. Under conditions of high field injection of charge from the electrodes occurs. This phenomenon can be controlled by the electrochemical reaction at the electrode-liquid interface that is dependent on the composition and geometry of the electrodes. The mesh-like parallel electrodes and multi pole electrode array placed along the channel are used. Since the injected ions are moved by the attractive electrostatic force, the gap between the electrodes should be as small as possible. Pumping fluids are limited to liquids of low conductivity and to dielectric liquids.

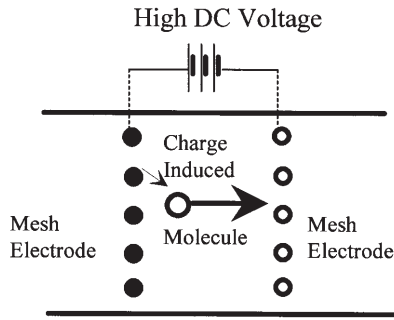


Fig.21. Schematic of the DC-charge injection electrohydrodynamic micropump [40, 41]

A typical structure of the traveling wave voltage driven micropump is shown in Fig. 22 [42]. The electrode array is formed on the glass surface and the flow channel is formed across the electrodes. Phase shifted rectangular voltages are applied along the channel direction. The principle is rather complicated. A practical requirement for the pumping is the induction of free electric charges that can interact with the traveling field due to the charge relaxation process in the volume of the fluid. This is possible under temperature induced conductivity gradients. The required conductivity is typically in the range between 10^{-14} and 10^{-9} S/cm. By using high frequency and low voltage wave form, a micropump which can drive conductive liquids from 10^{-4} to 10^{-1} S/cm has also been developed [43].

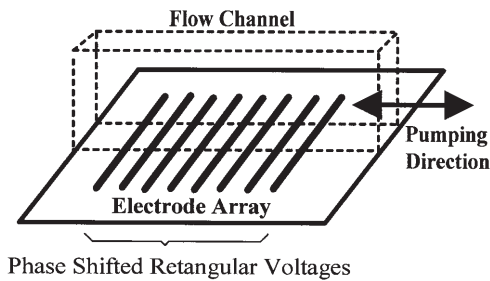


Fig.22. Schematic of the traveling wave electrohydrodynamic micropump [42]

- b) Traveling Flexural Wave (Ultrasonic). Fluidic motion induced by traveling flexural waves can also be used for the microtransport of liquids as an ultrasonically driven micropump [44, 45]. Liquid can move in the directions of wave propagation with the speed proportional to the square of the acoustic amplitude.
- c) Electroosmosis. Electrokinetic phenomena of electroosmosis can also be used in pumping electrolyte solutions [46]. This pumping is observed in capillaries with a diameter of less than 50 μm .

- d) Thermocapillary. Thermocapillary pumping uses changes in surface tension to induce a pressure-driven flow [47]. To move a liquid drop, surface tension at one drop end is decreased by heating. This method has been applied in planer DNA μ TAS.

4.4
Micro Flow Sensors

Many gas micro flow sensors have been developed [48]. The majority of them use thermotransfer for flow detection. Recently, several liquid micro flow sensors have also been developed. Three types of flow sensors are illustrated in Fig. 23:

- a) Thermotransfer. A typical thermotransfer type micro flow sensor consists of a micro heater and two micro temperature sensors located symmetrically upstream and downstream of the flow in the channel (Fig. 23 a) [10]. The heat distribution from the middle microheater is sensed by both temperature

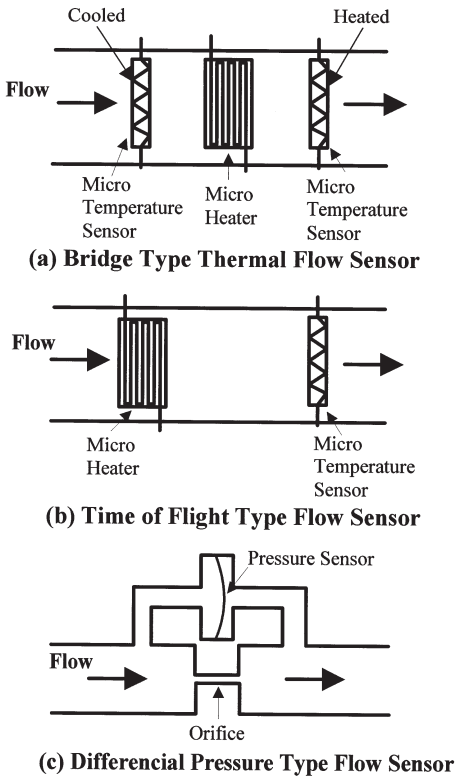


Fig. 23. Schematics of the liquid flow sensors [10, 49]

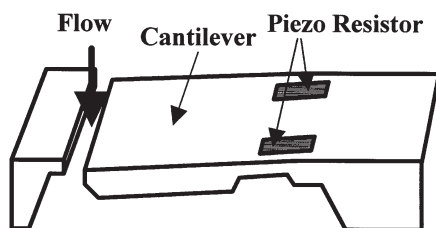


Fig. 24. Structure of the drag flow type micro liquid flow sensor [51]

sensors. The difference between the temperatures up- and down stream proportional to the mass flow is detected. Both the heater and two temperature sensors are simple resistors made of thin metal films or polysilicon. Another type of flow sensor using diodes or transistors as a heater and temperature sensor has also been developed [49].

- b) Thermal time-of-flight. The flow rate is measured by the transit-time of heat pulse generated by the micro heater and carried by the liquid (Fig. 23b). Diodes fabricated on the silicon wafer have been used as both the heating device and temperature sensor [49].
- c) Differential Pressure and Drag Force. In laminar flow conditions with a small Reynolds number, the pressure difference around an orifice is proportional to the flow rate [50]. Micro pressure sensor can be used for measuring pressure difference (Fig. 23c). Figure 24 shows the flow sensor consisting of a cantilever beam having piezoresistive strain gauges [51]. When liquid flows through the sensor, a drag force of the skin friction and pressure difference across the beam acts on the beam. Linear response can be expected for small deflection of the beam and laminar flow in the slit.

5 Conclusions

Flow in micro fabricated fluidic devices and systems is usually laminar because the Reynolds number of fluids in micro channels of μm dimensions is small (< 200). In miniaturization of the conventional chemical analysis systems, new design concepts considering the microfluidics are necessary. Micro mixers, micro flow switches and micro fluidic filters have been designed taking the microfluidics into consideration. Micro flow devices of microvalves, micro-pumps and micro flow sensors reviewed in this chapter have operation ranges depending on the structure, dimensions and actuators used. These devices are chosen according to their characteristics when used in μTAS . Hybrid micro systems including partly integrated devices are most realistic. Assembly techniques play an important role in fabricating μTAS .

Acknowledgements. The author would like to thank to Dr B. H. van der Shoot, Professor N. F. de Rooij in the University of Neuchatel, Dr A. van den Berg in the Twente University, Dr W. K. Schomburg in the Forschungszentrum Karlsruhe and M. Richter in the Fraunhofer Institute for Solid State Technology for their help in the preparation of this article.

6 References

1. Shoji S, Esashi M (1994) *J Micromech Microeng* 4:157
2. Lammerink TSJ, Elwenspoek M, Fluitman JHJ (1993) *Proc Micro Electro Mechan Syst Workshop*, p 254
3. Gass V, van der Schoot BH, de Rooij NF (1993) *Tech Dig Int Conf Solid-State Sens Actuators Transducers '93*, p 1048
4. Shoji S, Nakagawa S, Esashi M (1990) *Syst Sens Actuators* A21 – A23:189
5. Van der Schoot BH, Verpoorte EMJ, Jeanneret S, Manz A, de Rooij NF (1995) *Micro Total Analysis Systems*, Kluwer, The Netherlands, p 181
6. Van den Berg A, Bergveld P (1996) *Proc 2nd Int Symp on Miniaturized Total Analysis Systems μ TAS-96*, p 9
7. Shoji S, Esashi M (1995) *Bonding and Assembling Methods for Realizing a μ TAS*, Micro Total Analysis Systems, Kluwer, The Netherlands, p 165
8. Gravesen P, Branebjerg J, Jensen OS (1993) *J Micromech Microeng* 3:169
9. Manz A, Verpoorte E, Raymond DE, Effenhauser CS, Burggraf N, Widmer HM (1995) *Micro Total Analysis Systems*, Kluwer, The Netherlands, p 5
10. Ocvirk G, Verpoorte E, Manz A, Widmer HM (1995) *Analytical Methods and Instrumentation* 2:74
11. Harrison DJ, Fluri K, Chiem N, Tang T (1995) *Tech Dig Int Conf Solid-State Sensors and Actuators Transducers '95*, 1, p 752
12. Shoji S, Esashi M, Matsuo T (1988) *Sens Actuators* 14:101
13. Shoji S, Esashi M (1988) *Chemical Sensor Technology*, Kodansha, Tokyo, 1:179
14. Shoji S, van der Shoot BH, de Rooij NF, Esashi M (1991) *Tech Dig Int Conf Solid-State Sensors and Actuators Transducers '91*, p 1052
15. Ohori T, Shoji S, Miura K, Yotsumoto T (1997) *Proc Micro Electro Mechanical Systems Workshop*, to be presented.
16. Branebjerg J, Gravesen P, Krog JP, Nielsen R (1996) *Proc Micro Electro Mechanical Systems Workshop*, p 441
17. Branebjerg J, Fabius B, Gravesen P (1994) *Micro Total Analysis Systems*. Kluwer, The Netherlands, p 141
18. Miyake R, Lammerink TSJ, Elwenspoek M, Fluitman JHJ (1993) *Proc Micro Electro Mechanical Systems Workshop*, p 248
19. Mensinger H, Richter T, Hessel V, Dopfer J, Ehrfeld W (1994) *Micro Total Analysis Systems*, Kluwer, The Netherlands, p 237
20. Larsen UD, Branebjerg J, Blankenstein G (1996) *Proc 2nd Int Symp on Miniaturized Total Analysis Systems μ TAS-96*, p 228
21. Blankenstein G, Scampavia, Branebjerg J, Larsen UD, Ruzica J, (1996) *Proc 2nd Int Symp on Miniaturized Total Analysis Systems μ TAS-96*, p 82
22. Brody JP, Osborn TD, Forster FK, Yager P (1995) *Tech Dig Int Conf on Solid-State Sensors and Actuators Transducers '95*, p 779
23. Brody JP, Yager P (1996) *Tech Dig Solid-State Sens Actuator Workshop*, p 105
24. Terry SC, Jerman JH, Angell JB (1979) *IEEE Trans Electron Device*, ED-26:1880
25. Barth PW (1995) *Tech Dig Int Conf on Solid-State Sens Actuators Transducers '95*, p 276
26. Esashi M (1990) *Sens Actuators* A21 – A23:161
27. Zdeblick MJ, Anderson R, Jankowski J, Kline-Schoder B, Christel L, Miles R, Weber W (1994) *Tech Digest of Solid-State Sens Actuators Workshop*, p 251
28. Van Lintel HTG, van de Pol FCM and Bouwstra S (1988) *Sens Actuators* 15:153
29. Tiren J, Tenerz L, Hok B, (1989) *Sens Actuators* 18:389
30. Mobius H, Ehrfeld W, Hessel V, Richter T (1995) *Tech Dig Int Conf on Solid-State Sens Actuators Transducers '95* 1:775
31. Esashi M, Shoji S, Nakano A (1989) *Sens Actuators* 20:163
32. Smith L and Hok B (1991) *Tech Dig Int Conf on Solid-State Sensors and Actuators Transducers '91*:1049

33. Schomburg KW, Scherrer B (1992) *J Micromech Microeng* 2:184
34. Shoji S, van der Schoot BH, de Rooij NF, Esashi M (1992) *Sens Actuators A*, 32:335
35. Steme E, Steme G (1993) *Tech Dig Int Conf on Solid-State Sens Actuators Transducers '93*, p 110
36. Olsson A, Enoksson P, Steme G, Steme E (1996) *Proc Micro Electro Mechanical Systems Workshop*, p 479
37. Zengerle R, Geigel W, Richter A, Ulrich Y, Kliige S, Richter A (1994) *Proc Actuator '94*, p 25
38. Rapp R, Schomburg WK, Maas D, Schulz J, Stark W (1994) *Sens Actuators A*, 40: 57
39. Bustgens B, Bacher W, Menz W, Schomburg WK (1994) *Proc Micro Electro Mechanical Systems Workshop*, p 18
40. Richter A, Sandmaier H (1991) *Proc Micro Electro Mechanical Systems Workshop*, p 99
41. Furuya A, Shimokawa F, Matsuura T, Sawada R (1996) *J Micromech Microeng* 6:310
42. Bart SE, Travrow LS, Mehregany M, Lang JH (1990) *Sens Actuators*, A21 – A23:193
43. Fuhr G, Hagedorn R, Muller T, Benecke W, Wangner B (1992) *Proc Micro Electro Mechanical Systems Workshop*, p 25
44. Moroney RM, White RM, Howe RT (1991) *Proc Micro Electro Mechanical Systems Workshop*, p 277
45. Miyazaki S, Kawai T, Araragi M (1991) *Proc Micro Electro Mechanical Systems Workshop*, p 283
46. Harrison DJ, Seiler K, Manz A, Fan Z (1992) *Tech Digest of Solid-State Sensors and Actuator Workshop*, p 110
47. Sammarco TS, Fields YD, Johnson BN, Jones DK, Burke DT, Mastrangelo CH, Burns MA, *Proc 2nd Int Symp on Miniaturized Total Analysis Systems μ TAS-96*, p 150
48. Van Oudheusden BW (1992) *Sens Actuators A* 31:9
49. Yang C and Soeberg H (1992) *Sens Actuators A* 33:143
50. Boillat MA, van der Wiel AJ, Hoogerwerf AC, de Rooij NF (1995) *Proc Micro Electro Mechanical Systems Workshop*, p 350
51. Gass V, van der Schoot BH, de Rooij NF, (1993), *Proc Micro Electro Mechanical Systems Workshop*, p 167

Sensor Systems

G. A. Urban, G. Jobst

Albert-Ludwigs-Universität Freiburg, Institut für Mikrosystemtechnik, Am Flugplatz, D-79085 Freiburg, Germany. *E-mail: urban@INFORMATIK.UNI-FREIBURG.DE*

Recent developments in sensor technology allow to create different integrated and miniaturized sensor arrays. Using microsystemtechnology fluidics can be added creating whole micro-analytical devices on chip. However, there are drawbacks involving inappropriate sensor function in media and production. Using sophisticated sensor construction and microfluidics such drawbacks can be overcome. In this chapter different sensor systems and whole micro-analytical devices are presented with emphasis on their applications.

Keywords: Integrated miniaturized sensor arrays, microfluidics, biosensors, microelectronic, microsystemtechnology.

1	Introduction	189
2	Sensor Arrays	190
2.1	Mechanical Sensor Systems	190
2.2	Thermal Sensor Arrays	191
2.3	Integrated Optical Devices	193
2.4	Electrochemical Sensor Arrays	193
2.4.1	Conductometric Sensors	193
2.4.2	Potentiometric Sensors	194
2.4.3	Amperometric Sensors	196
3	Microanalytical Systems	200
3.1	Gas Sensor Systems	200
3.2	Separation Based Devices	201
3.3	Bioanalytical Sensor Systems	201
4	Conclusions and Outlook	209
5	References	209

1 Introduction

All biological systems which are inherently not in thermodynamic equilibrium require a variety of sensing components to maintain control and stability. Multiple sensor systems are essential for life processes and may serve as sampels for various technical systems.

Sensors have been used in industry for years, and the rise of microelectronic technology has caused an increased need for more and better sensor devices. The increasing complexity of technical systems requires development of complex sensor systems – a strategy as nature shows.

It is not surprising that the first integrated and miniaturized sensor systems were developed for investigating biological systems and especially the most complex system – the brain [1].

Since such pioneering times, the need for integrated sensor systems has increased in science and research for monitoring purposes in medicine. In addition, sensor systems are now also used in analytical science, environmental control and bioprocessing.

In contrast, rapid growth of integrated, “smart” sensor systems in real and industrial application has not been fulfilled till now. The industry used well-established mechanical and electromechanical sensors in the past, especially in aircraft and automotive industries which resisted changes to electronic systems mainly for reasons of safety.

In the 1980s microprocessor driven applications and sensor interfaces entered the market, and also a variety of conventional sensors were used to create sensor systems by simply adding different sensors and using sensor bus systems or smart distributed systems [2]. In process technology, aircraft and automotive applications distributed conventional sensor systems are now state-of-the-art.

On the other hand, integrated sensor systems were used only in CCD TV and photo-cameras [3] in large numbers and for special applications. The reasons for this include difficulties of production, yield and the risk of new markets despite the emerging needs in medicine, biology and environmental control.

In this chapter the state-of-the-art of different sensor systems with emphasis on integrated systems for microanalytical application will be given. The technology, mainly the so-called microsystem technology (MST), is able to create complex miniaturized and integrated analytical systems which have entered the field of chemical and medical research. Industrial application of such systems is rare and only marketed for physical application fields, but the impact for the future will be highlighted in the following chapter.

2 Sensor Arrays

2.1 Mechanical Sensor Systems

Miniaturized and integrated sensor systems were developed early for pressure and accelerometer sensors. The technology of silicon micromachining leads to sensitive pressure sensors which were marketed early [4]. Also accelerometers were developed mainly driven by the huge market of air bag application and crash sensors [5].

Integrated systems of pressure and temperature are also on the market [5]. For analytical purposes only SAW devices are used for antibody and gas detection which are in an early stage of research [6].

2.2

Thermal Sensor Arrays

Thermal sensor array systems for medical-analytical purposes were developed early [7]. Temperature distributions and blood perfusion in the brain were measured with thin film thermistors exhibiting a temperature resolution of 0.1 mK with a time constant of few milliseconds.

The principle of calorimetry is very interesting for biological applications. Calorimetric biosensors are based on the detection of the heat production of biological reactions which is caused by enthalpy changes. The micro calorimetric sensing principle is very versatile because of the exothermic nature of nearly all enzymatic reactions [8] and was introduced as a conventionally constructed device very early [9]:

If a reaction is occurring in an adiabatically isolated mass, defined as calorimeter, the temperature of the mass will change according to the expression (1)

$$\Delta T = \frac{\Delta Q}{MC_c} \quad (1)$$

where ΔT is the temperature change, ΔQ is the energy difference, M the total mass of the calorimeter and C_c is the total thermal capacity of the calorimeter.

Conventional calorimetric biosensors with thermistors as the transducer were invented early by proposing a thermal biosensor in a flow stream [10]. So far the design of enzyme thermistors does not entirely match the market demand well, but it seems well suited for special applications [10, 11]. A number of devices have utilized discrete pairs of thermistors for differential measurements with immobilized enzymes or with separate enzyme columns [9, 10, 11].

As a second transducer thermopile sensors are well suited for performing differential measurements because of their underlying physical principle. With conventional design there are some difficulties related to size, sensitivity and mechanical stability of thermocouples.

If silicon technology is involved all thermal sensors suffer from the high thermal conductivity of silicon, which dramatically decrease their sensitivity [12]. However, by use of micromachining and integrated silicon technology a powerful thermal biosensor can be realized. Using a thermopile integrated on a thin micromachined silicon membrane reduces thermal loss due to the substrate and so excellent performance can be accomplished [13].

The thermopile depends on basic physical principles with the inherent ability to measure temperature differences directly with high common-mode rejection [13]. Furthermore the compatibility with silicon technology enables size reduction and direct immobilization of the biochemical sensing part onto the chip.

Thermopiles made according to standard bipolar or CMOS process can be purchased from XENSOR Integration (Delft, The Netherlands). An array of p-type silicon/Al thermocouples is connected to form a thermopile and integrated

in an n-type silicon epitaxial layer. By standard micromachining techniques a membrane is etched onto which the sensing junctions are placed. Enzyme immobilization was performed simply by way dropping enzyme solution within the cavity formed on the reverse side of the thermophile during the micromachining process.

To realize glucose-, urea- and penicillin sensors in a flow injection mode (FIA) appropriate enzymes can be immobilized [13]. The measuring range is very limited in all reported cases due to enzyme kinetics and a more sophisticated set up is required.

To perform calorimetric measurements in a conventional way the lack of well matched thermistors are a draw-back. Recently a thin-film thermistor based on amorphous germanium has closed this gap [7, 14]. The temperature resolution is 0.1 mK and the time resolution is in the msec range. Placing such an integrated miniaturized thermistor into an enzyme column urea or glucose can be measured but of course with the same draw backs of a limited measuring range due to enzyme kinetics and oxygen deficiency problems.

For clinical applications the calorimetric method was extended for whole blood measurements of glucose [15]. Using microelectronic and micromachining tools an array of thermistors covered by different enzymes can be easily produced leading to a multi-analyte detection using the same transducing principle [16]. Using such technologies the sample volume can be reduced to 1 μ l and the response time is well below one minute. Lactate, glucose, urea and penicillin measurements were performed in a microflow arrangement [17] (Fig. 1). Even for an in vivo approach such a measurement method can be used [18].

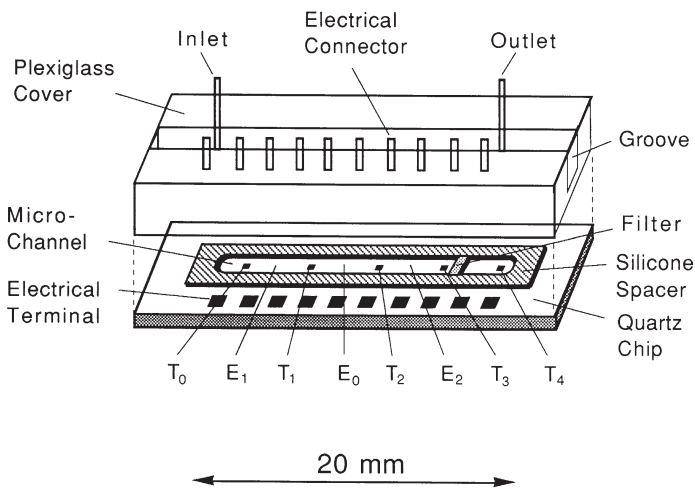


Fig. 1. Micro-thermistorarray with immobilized enzymes for calorimetric analysis
 T_i ... Thermistors, E_i ... Enzyme columns

2.3

Integrated Optical Devices

Optical sensors are interesting analytical tools capable of performing a variety of different measurements [19]. Most of the work has been done on measuring pH, O₂ and CO₂ but biosensing devices were also developed and marketed [19–22].

A conventional marketed sensor system uses optrodes for measuring blood gases in an clinical chemical analyzer based on fluorescence [23].

Integrated optical devices combine microelectronic production technology with the inherent advantages of optical sensing. Many of these developments are in an early state of research but a variety of optical biosensors can be realized in principle. Integrated optical device manufacturing is nowadays commercially available (IOT) and nearly all optical elements can be integrated and miniaturized on chip [24].

The biosensing devices focus mainly on affinity principles such as antibody – antigen reactions and are based on surface plasmon resonance [25], grating couplers [26] or interferometers [27]. It seems possible to get stable and highly sensitive devices based on these principles [28], and further investigations can lead to miniaturized sensor modules with reduced cost, size and complexity.

A combination of a highly sensitive transducer based on luminescence excitation in the evanescent field with fluidic systems gives detection limits of 100 femtomoles of analyte. Such systems are well suited for antigen-antibody detection and DNA analysis [29].

2.4

Electrochemical Sensor Arrays

Electrochemical biosensors based on well known and therefore most common transducing principles have been investigated intensively for the last 30 years.

Electrochemical transducers can be divided into conductometric, potentiometric and amperometric measuring principles.

2.4.1

Conductometric Sensors

A simple transducing principle is the measurement of impedance between planar electrodes which is changed by altering the ionic content of the measuring system.

If biological sensing elements are immobilized on such electrodes biosensors can be realized using changes of the conductivity in the electrolyte solution caused by biological reactions or changes of the double layer capacitance by binding or affinity reactions of the biological molecules immobilized on the electrode surface.

Planar interdigitated electrodes for impedimetric measurements can be produced by means of microelectronic technology [30]. Although this measuring

principle has been known for a long time more investigations are necessary to fully understand the transduction principle for biosensing [31]. One obstacle is the high concentration of the ionic background which is always present in biological samples [32], and a second problem is associated with electrode fouling.

One advantage of this general transducing principle is the simple possibility to create biosensing arrays sensitive to urea, L-asparaginase and creatinine [30]. Such arrays gives a fast response but are responding non-linear and are limited in the measuring range.

For gas sensing devices the conductimetric measuring principle is used in most cases with good success (see section on gas sensor systems). However, for practical applications and commercialization much more investigations are still needed.

2.4.2

Potentiometric Sensors

Potentiometric measurements involve the determination of the electrical potential between two electrodes at zero current flow. A reference electrode has to establish a constant potential independent of the electrolyte used. This is not easily performed even in a conventional measuring set-up and therefore various constructions have been investigated using different electrolyte chambers and porous plugs [33]. For microelectronic realization this problem becomes very severe [34].

The working electrode has to respond directly to the analyte to be measured. The most common potentiometric device is the pH-electrode and related ion-selective electrodes.

Such devices respond to changes in the analyte concentration by varying the electrical potential described by the Nernst equation (Eq. 2):

$$E = E_0 + RT/zF \ln a_1/a_2 \quad (2)$$

where E is the electromotoric force, E_0 the standard potential, R the gas constant, T the absolute temperature, z the exchanged electrons, F the Faraday constant and a_1 the activity of the species to be detected, a_2 is usually set = 1 mol^{-1} .

The first representative of a potentiometric sensor was the pH-glass electrode invented in 1906 [35]. Decades of development resulted in the invention of many more ion-selective electrodes including more recently those based on neutral carrier membranes [36] and of the microelectronic fabricated ion selective field effect transistor (ISFET) [37].

Such an ISFET was originally used for detecting pH changes but by casting with ion selective membranes a lot of different ion-selective sensors can be obtained in principle [38, 39]. Even a multi-parameter electrolyte sensitive chip for clinical applications was invented [39].

To obtain a microelectronic biosensor, a biological substance has to be immobilized onto the gate insulator of the ISFET.

The enzyme-containing FET, called ENFET, is fabricated from an ISFET by casting a thin membrane containing the enzyme over an ion-selective membrane

or an inorganic gate insulator. The underlying mechanism of ISFETs is described in reference [40] and the enzyme reactions in reference [41].

Local changes in the ion concentration as a result of substrate conversion by the immobilized enzymes have been measured using pH [41] or fluoride sensitive field effect transistors (pF-ISFET) [42] or ammonia-sensitive FETs [43].

Immunosensing with the FET gate by the direct detection of protein interaction has been described in the literature, but it seems that a direct detection of protein interaction with a pH-sensitive gate of a FET is limited by fundamental principles [44].

One of the great advantages of FET-type biosensors is the possibility of using a differential method which allows measurements with a pseudo-reference electrode [45] but with the drawback of weak stability. However, for a biosensor device one can circumvent the problem of non-specific responses for example to the changes of pH in the analyte using pH-ISFET devices as the reference electrode [42, 46]. Another advantage is the placing of a pre-amplifier in the near vicinity of the high resistive electrode in the case of ISFETs. However, some problems are associated with an ISFET device including drift, sensitivity to ambient light, dependence on buffer capacity in the sample, encapsulation problems and sensitivity against contamination [40].

The originally used gate materials for pH sensing, SiO_2 and Si_3N_4 exhibit a large drift and do not show the desired Nernstian response [37, 47]. Using special gate materials such as Al_2O_3 or Ta_2O_5 an enhancement of slope and better drift properties have been achieved [40, 48] although the reproducibility of results of different authors are not comparable.

Additionally the expected advantage in using a standard silicon technology is lessened by the fact that it is not possible to use the described special gate materials in a standard CMOS foundry.

For certain applications, solutions could be found which satisfy the special needs but up to now no general approach has been found that suits a wide range of applications with a single design. Therefore only a few ISFET- pH-sensors entered the market in the last years [49].

For biosensor devices these problems are aggravated because of the additional integration of a biological component on a planar device surface [50].

Different approaches have been reported for enzyme immobilization and membrane deposition including drop-on techniques [42, 51], ink-jet printing [52] and photolithographically patterned enzyme membranes [53, 54].

Integrated multi-biosensors based on ISFET can be produced by using a photosensitive polymer which incorporates the enzyme and is spun onto the gate [54]. The reported measuring range for glucose is 5 mM which is rather weak, and some cross sensitivities due to problems regarded with buffer type and capacity were also reported.

One method to extend linear range and to perform measurements in whole blood is to use a further diffusion limiting membrane [55]. Although such an approach slows down the sensor response, measurements in serum and biological fluid are possible.

Due to the fact that nearly all ENFET approaches lead to insufficient or unsatisfactory sensor performance, no ISFET based biosensor has been fully commercialized for wider applications to date.

Another approach is the use of the potentiometric principle with planar thin film electrodes on a separate chip but in close vicinity to a FET input amplifier. Glucose and urea chips are now on the market commercialized by the company i-stat. These sensors are based on ion selective electrodes. The problems of stability are circumvented by a simple on chip calibration procedure and by the use of such microelectronic electrodes as disposable single shot probes for measuring Na, K, Cl, BUN, Glucose, iCa, pH, pCO₂ and Hct [56, 57].

Such microelectronic biosensor systems are really microanalytical sensor systems which have already reached the clinical market.

2.4.3

Amperometric Sensors

Using the faradaic current derived from a redox reaction at an electrode a versatile chemical analytical method can be established. Applying a distinct potentiostatically controlled voltage between a working electrode and the electrolyte, with the redox species electrochemically converted only at the electrodes, results in a stationary current following Eq. 3. In this case, a diffusion controlled measurement of redox species can be obtained.

$$I = n F A D c_0 / d \quad (3)$$

where I is the diffusion limited current, n the exchanged electrons per reaction, F the faradaic equivalent, A the electrode area, D the diffusion constant of the analyte, c_0 the analyte concentration and d the thickness of the diffusion layer.

In contrast to the potentiometric principle where nearly no transport of analyte to the sensor occurs, the amperometric measurement requires the control of faradaic current at the electrodes and the diffusion of an analyte towards the electrode. One typical example for an electrochemical measuring device is the Clark electrode which uses the reduction of oxygen [58].

Microelectrode arrays can also be produced by thin film technology and silicon micromachining. Electrochemical analysis using planar thin film metal electrodes as transducer can be done with high performance in vitro [59].

Using chip-array electrodes even trace metals can be detected with high selectivity [60].

Due to the history of the principle it is not surprising that miniaturized enzymatic amperometric biosensors produced by means of thin and thick film technology were investigated extensively in recent years [61 – 66].

Amperometric biosensors combine the specificity and selectivity of biological sensing components with the analytical power of electrochemistry. Because of the use of metal electrodes which can be deposited on nearly all substrates, thin and thick film technology is the method of first choice. The limitation which occurs with silicon device technology is no longer decisive and biosensor production is not restricted to silicon production lines.

Placing an amperometric device in real samples, e.g. blood, a degradation of electrochemical performance over time occurs due to contamination of the electrode reducing electrochemically accessible reaction sites [67]. Therefore surface modifications or special electrode materials like e.g. carbon are needed and the electrodes have to be covered with functional membranes to ensure full faradaic current. This poses a problem in the production even using special technologies.

For microelectronic biosensors a further problem is the immobilization procedure of enzymes. Again different approaches were tried including drop-on techniques [61], ink-jet printing [68], spray techniques [62], electropolymerization [64], lift-off techniques [63, 66] and photolithographically patterned enzyme membranes [65].

At present nearly all of the cited amperometric microelectronic sensors intended for long term application are unable to work well in undiluted blood and even few conventional sensor systems are able to measure glucose and lactate concentration in undiluted media for a longer period [69, 70]. Transducer and biomembrane related difficulties have to be overcome with electrochemical transducers for measurements in undiluted biological media.

The best investigated systems use H_2O_2 producing oxidases. The subsequent oxidation of H_2O_2 on the working electrodes at a potential from +400 mV to 650 mV versus an Ag/AgCl reference electrode serves as the transducing mechanism.

The problem of interfering substances which are also oxidized at this potential can be overcome by differential methods using an enzyme covered electrode and a blank electrode and measuring the differential signal. Such systems are able to compensate for electrochemical interference but cannot hinder fouling of the electrodes [71].

A further method is the use of mediated devices allowing reduced working potentials down to +200 mV where the interfering substances are not oxidized [72]. The drawback of mediator based devices in long-term applications is the leakage of mediators [64].

However for short term measurements this means an excellent way to overcome the mentioned problems.

The first miniaturized electrochemical device for measuring glucose in whole blood was a mediated system produced in thick-film technology by screen printing [73]. This disposable, single-shot system is produced and actually marketed widely by the company Medisense. Several other companies are now following with similar approaches [74, 75].

For long term operation other approaches have to be used. To protect the Pt working electrodes against fouling and to prevent erroneous reading due to electrochemical interference, an electropolymerised semi-permeable membrane can be utilized [76].

The reported semi-permeable membrane consists of an electropolymerized di-amino-benzene in phosphate buffer (pH 7). Polymerization is achieved by cycling the potential between 200 mV and +800 mV for a certain period. In principle such an electrode modification hinders fouling in an excellent way [77].

To overcome immobilization of biological substances and to establish diffusion limitation a number of methods have been tried. For example in the mediated disposable glucose sensor screen printing of free enzymes and mediator have been used. Due to the solubility of both substances only single shot applications are possible. For long term applications more sophisticated methods are necessary.

A miniaturized planar amperometric glucose sensor has been created on Sapphire substrates. Thin film titanium-gold electrodes are covered with an enzyme layer which is patterned by a lift-off technique [66]. This sensor exhibits a fast response time of 30 seconds but the linear measuring range is poor.

The continuous in-vivo measurement of glucose by an implanted sensor in patients is of great importance. Such a monitoring can lead to a better control of normoglycaemia, a better quality of life and a hypoglycaemic alarm which is of outstanding importance [78].

Therefore, another type of planar glucose biosensor with Pt electrodes on a silicon substrate has therefore been developed for in vivo measurements [61]. The enzyme glucose oxidase was immobilized by the well known GDA-BSA method and the whole sensor was covered subsequently by a polyurethane membrane. This silicon chip has to be sawed and assembled on a flexible carrier for in vivo application, the assembled catheter was successfully evaluated in rats [79]. This sensor gives encouraging results in aqueous solutions and subcutaneous applications. Drawbacks of this include the complicated mounting and assembling procedures which are difficult and cumbersome.

An alternative approach places the Pt electrodes directly on a flexible polymer carrier [80]. Eli Lilly developed a three-electrode transducing system based on a polyimide carrier with electroadsorbed enzyme and a highly oxygen-permeable membrane covering the sensor. Such a system was tested in vivo and published results seem encouraging although the company cancelled the project.

For microelectronic production and for getting clinically reliable sensors the UV initiated free radical crosslinking of the polymer directly on the substrate is advantageous since it allows microfabrication and designing the physico-chemical properties of the membrane [65].

A combination of different technologies such as electropolymerization and photopatternable enzyme membranes can lead to reliable sensor systems. An easy to handle thin film process was developed for immobilizing different H_2O_2 producing enzymes [77]. The hydrogel layer, containing e.g. the enzyme GOD, was patterned by photolithography and could be placed selectively on the individual working electrode [71]. An uppermost photopatternable membrane was introduced containing the enzyme catalase which decomposes excess H_2O_2 into O_2 and H_2O in order to prevent the release of the cytotoxic agent H_2O_2 into the biological environment. This membrane also prevents sensor fouling by blood components because of the low protein deposition characteristics of pHEMA [81]. To increase the diffusion pathway and to separate the H_2O_2 source (GOD) and the H_2O_2 sink (catalase), an additional pHEMA membrane was placed between the GOD and catalase membrane.

The electropolymerization of the semipermeable membrane can be performed on the Pt electrodes on a wafer as well as the photopatterning of the enzyme mem-

branes. Subsequently the additional diffusion barrier and the catalase layer were placed over all working and counter electrodes in the same manner.

Multi-analyte chips can be produced in this way using microelectronic technology.

The sensors do not show any dependence on interferences [77]. They exhibit extended linear ranges with high sensitivities and low residual currents. Due to the wafer processing a high reproducibility can be obtained [77].

The thin hydrogel membranes exhibit a fast response time of 25 sec to 98% equilibrated signal and a fast hydration time of several minutes. The sensor chips can be stored dry for at least one year at 4 °C without changes in performance.

The long term operational stability in undiluted bovine serum spiked with analyte is more than one week at 37 °C.

This is an example where multi-enzyme sensor devices can be designed to obtain precise, reliable, integrated biosensors with extended measuring range for clinical use. They can be produced by means of microelectronic technology. Such multi-enzyme sensors were accomplished by immobilizing different enzymes into stacked membranes which were structured by photolithography. This is an important step towards commercialization, and an additional feature is the possibility to integrate additional electrochemical sensors for measuring O_2 , CO_2 and pH on one substrate. Such an integrated lab-on chip seems to be a realistic vision and can revolutionize both point of care testing and metabolic monitoring. In addition, the technology of photopatterned multi-enzyme sensors can be used for the creation of in vivo devices on a flexible polyimide strip [82] (Fig. 2).



Fig. 2. Photograph of a flexible polyimide-based in vivo sensor for glucose, lactate and pH measurements

3 Microanalytical Systems

Modified microelectronic technology has created integrated and miniaturized sensor arrays. Additionally, microsystem technology allows to form whole microanalytical systems with integrated fluidics.

3.1 Gas Sensor Systems

A good example for a microanalytical device is the gas sensor array. The conductometric approach for gas sensing was favored during the last years using metal oxides or conductive polymers. Unfortunately such sensors are quite unspecific and therefore sensor arrays with modified sensing layers have to be used. The selectivity derives from a sophisticated data processing using neural networks. Complete gas analysis systems with microfluidic and data acquisition are now under development.

Integrated array sensors produced by thin film technology and micromachining use integrated heaters and SnO_2 -semiconductors as well as conducting polymers [83, 84]. Another approach uses piezoelectric quartz crystals [85]. Such systems appear closer for industrial use in detecting complex odors from foodstuff or beverages.

For air monitoring a complete miniaturized system made by silicon micromachining has been proposed [86]. Valves, gas fluidics, filters, thin film sensors and pumps are integrated in silicon and mounted on a printed circuit board (Fig. 3). The application of such systems will become apparent in the future.

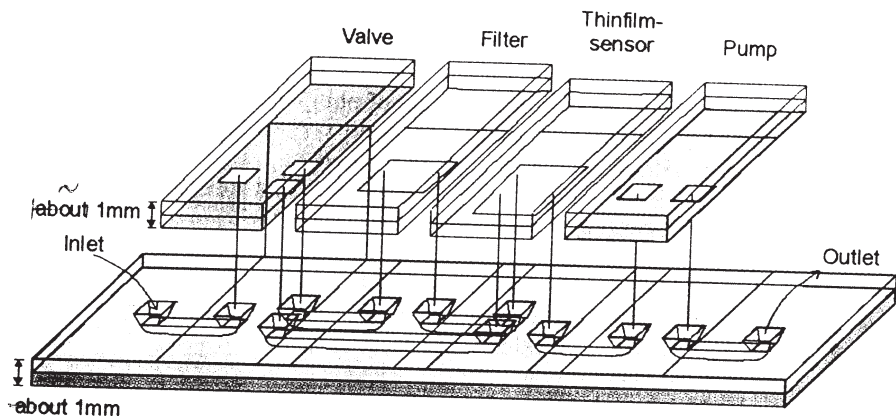


Fig. 3. Proposed microanalytical measuring system for gas analysis

3.2

Separation Based Devices

The concept of an total analysis system (TAS) was presented early by Widmer [87] and was extended to a μ TAS concept by Manz [88]. In contrast to sensor systems such systems are based on unspecific sensors gaining the selectivity by separation principles. Electrophoresis devices are good candidates for miniaturization saving time and reducing production costs. Further details are given in various chapters in this book.

3.3

Bioanalytical Sensor Systems

The technology for integrating different biosensors on a chip forms the basis for the lab on-chip which will require additional liquid handling and optionally active liquid treatment. Different approaches for a microanalytical system (μ TAS) have been published [89] and are now an emerging field of research.

For several reasons, most applications of chemo- and biosensors require flow through devices, for example in allowing analysis of samples from multiple sources, removing flow sensitivities, avoiding sterilization and biocompatibility problems, enabling recalibration or performing bioanalytical assays.

A classical approach for a flow-through device with sensors is the clinical-chemical analyzer already introduced in several hospitals. Such devices use standard miniaturized electrodes and a sophisticated fluid handling system which is bulky [90].

In order to minimize the assembling effort, to reduce system costs, and to allow miniaturization the classical build-up of enzymatic and ion selective electrodes is successively replaced by solid supported functional membranes, in this way integrating functional membrane and transducer. Integration of the liquid handling environment with the sensors further reduces assembling effort, minimizes internal volumes and increases reliability of the measuring system. Furthermore, by integrating fluidic functions which allow sample pretreatment and reagent addition, such devices open up new applications.

ISFET based systems have been developed at different laboratories [91–93] using a planar or three dimensional set up. Such systems which are equipped with micropumps and valves are able to detect ions and other interesting chemical parameters (Fig. 4). Different approaches have been made in the detection of ions and diluted gases. Microarrays for measuring pressure, temperature, pH, O_2 and CO_2 were realized using silicon technology and a hybrid set up of the different components [94]. Blood gas measurements with integrated pH, O_2 and CO_2 -electrodes have been tested in real samples [95].

Hybride micro-FIA systems produced in silicon technology using oxygen microelectrodes and microcavities have been developed for measuring phosphate concentrations [96]. Multiple analyte biosensor arrays can also be realized using thin film and silicon technology. The so-called containment technology has been applied to immobilize enzymes in three dimensional cavities formed in silicon wafers to get fully process compatible biosensor devices [97] (Fig. 5).

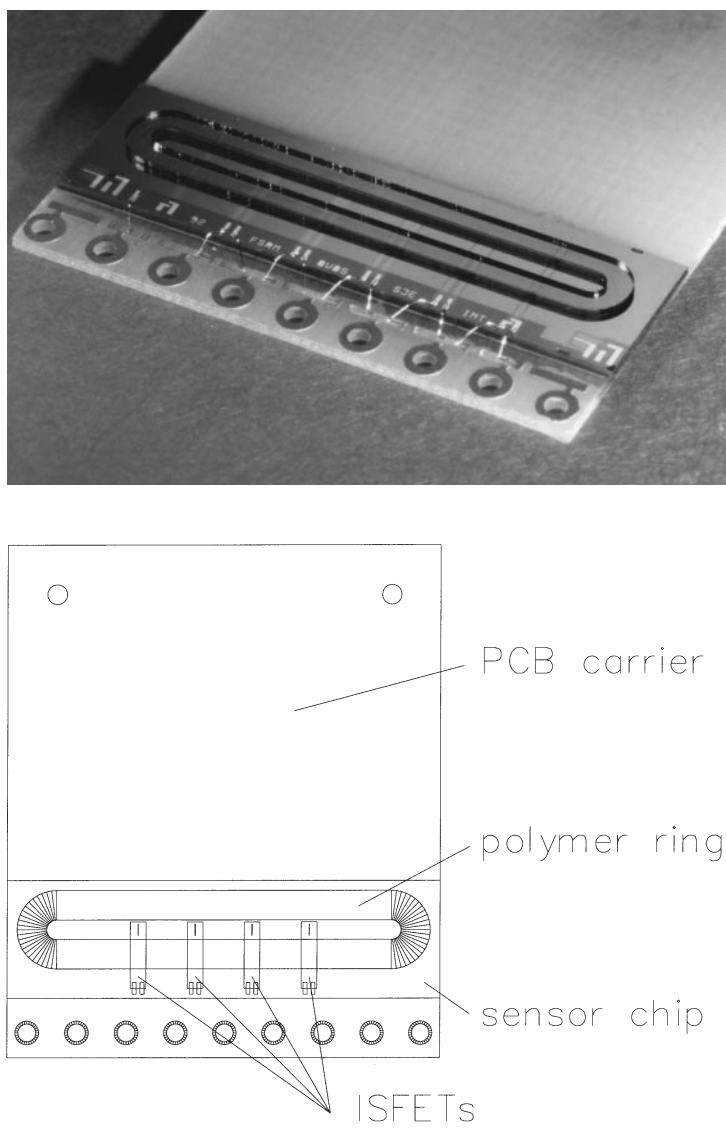


Fig.4. Layout and photograph of a ISFET array with polysiloxane ring

Such systems have been developed and used also for microdialysis sampling in human serum [98].

Another type of thin film device consists of four $0.5 \times 0.5 \text{ mm}^2$ platinum working electrodes and a Ag/AgCl reference electrode made on a 0.3 mm glass carrier. The enzymes were immobilized onto the working electrodes in a photo crosslinked pHEMA membrane and additionally covered by a diffusion limiting and a catalase containing top layer [77].

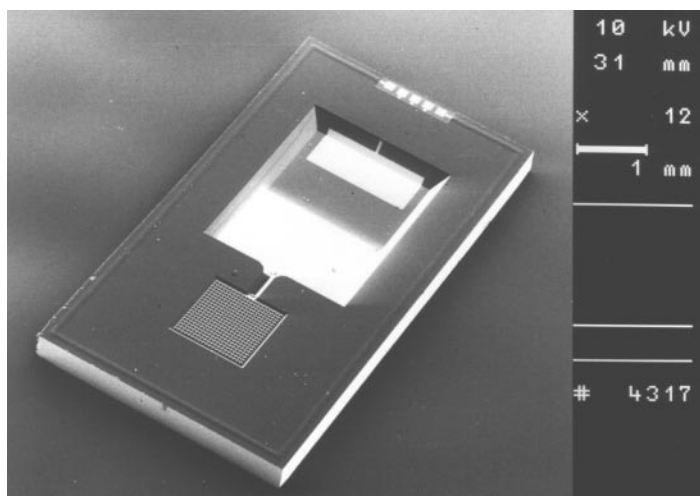


Fig. 5. Electron micrograph of a microcontainment oxygen sensor (source: ICB)

A low cost microfluidic device was realized by utilizing printed circuit board technology which is capable of producing microsystems [99, 100]. The printed circuit board (PCB) for the assembly of the thin film biosensor array comprises conducting pads for the thin film device and the plug connection to the potentiostat, a $5 \times 1 \text{ mm}^2$ gold counter electrode, drilled through holes for liquid inlet and outlet, and a photopatterned spacer made from the dry film resist used for insulation of the PCB (Fig. 6). In a second configuration, used for on line buffering and reagent addition, the PCB additionally comprises a mixing coil of $170 \times 0.6 \times 0.1 \text{ mm}^3$ dimension ($=10.2 \mu\text{l}$) together with a second inlet hole. The entire processing was done with conventional PCB technology equipment. Assembling of the thin film sensor array with this PCB (Fig. 6) gives the analytical micro flow system. The dimension of the flow chamber is $5 \times 1 \times 0.3 \text{ mm}^3$ ($=1.5 \mu\text{l}$) (Figs. 7 and 8).

Ex vivo blood monitoring experiments with human volunteers were performed by placing a device comprising two glucose and two lactate sensors into the sampling line of a double lumen catheter. Venous blood was continuously withdrawn and in line heparinized with a dilution of less than 5%.

These experiments are described in detail in reference [101]. The glucose/lactate device was first one point calibrated with a protein-free buffer solution. The measured sensitivities were applied to the sensor currents for calculation of glucose and lactate levels and the time course of glucose and lactate levels of a combined intravenous and oral glucose tolerance test together with reference values was determined (Figs. 9 and 10).

The good agreement between sensor and laboratory results proves the effectiveness of the pre-calibration procedure and sensor stability. The results suggest that these devices can be used for short term glucose-lactate monitoring in for example the intensive care unit, the operation theater, in sports, medicine, rehabilitation and in diabetology.

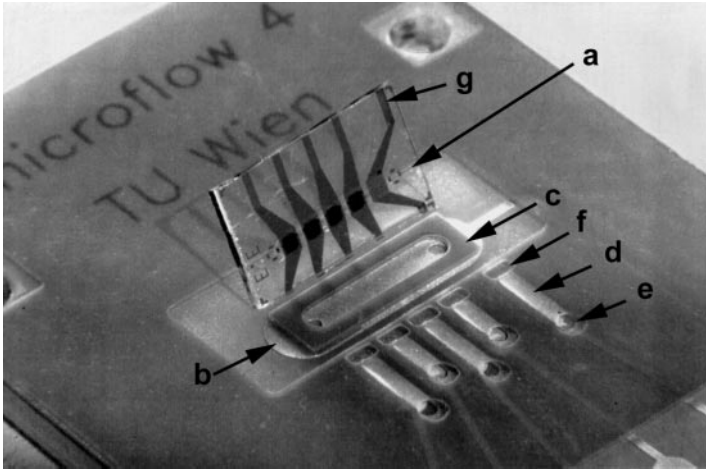


Fig. 6. Photomicrograph illustrating the assembling of the thin film sensor array with the printed circuit board. *a.* sensor array, *b.* counter electrode, *c.* pacer, *d.* channel for conductive adhesive with conducting pad of PCB, *e.* inlet hole for conductive adhesive, *f.* outlet hole for conductive adhesive, *g.* bonding pads

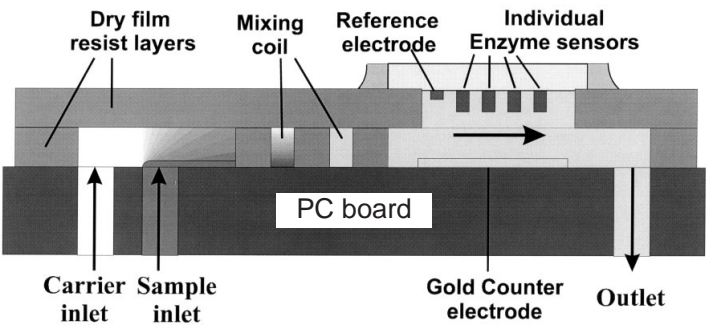


Fig. 7. Schematic cross section of the flow through device with integrated static mixer

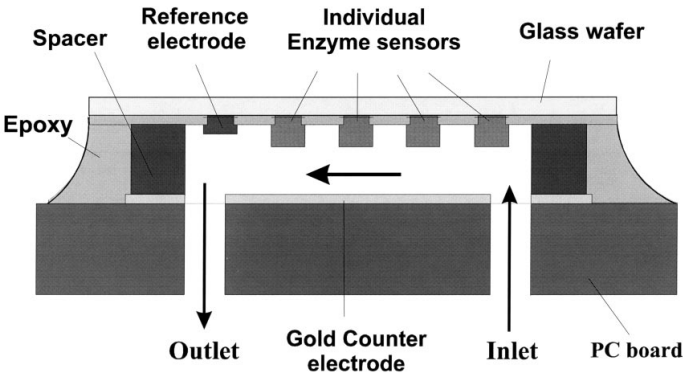


Fig. 8. Schematic cross section of the flow cell of the flow through device

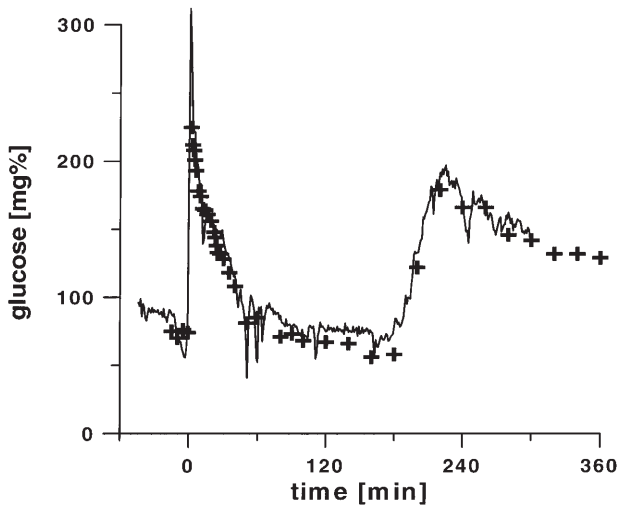


Fig. 9. Glucose sensor reading (*solid line*) and reference values (*crosses*) of an IVGTT/OGTT

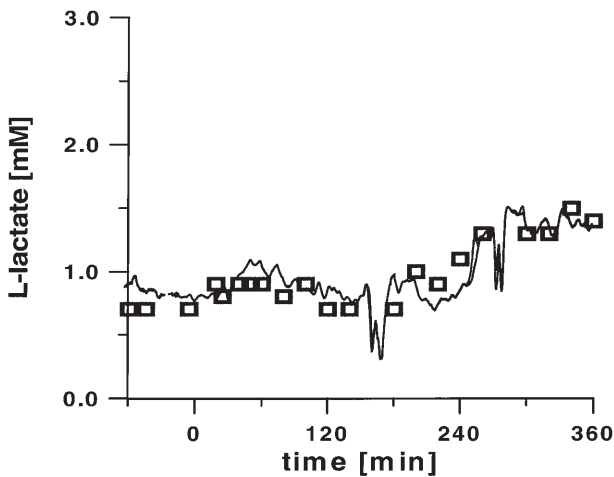


Fig. 10. L-Lactate sensor reading (*solid line*) and reference values (*boxes*) of an IVGTT/OGTT

To meet the demands for multianalyte monitoring in biotechnology, where closed loop control of metabolites is expected to increase fermentation reliability and yield, a glucose–lactate–glutamine–glutamate device which can monitor the concentrations of this four substances simultaneously, without any reagent, and with no need for sample pretreatment was realized by Moser and co-workers [102]. Figure 11 shows the calibration graphs of such a device which needs little effort for monitoring. A sensor array comprising two lactate and two lactose sensors was assembled with a PCB comprising a mixing coil (Fig. 7) for yoghurt fermentation monitoring.

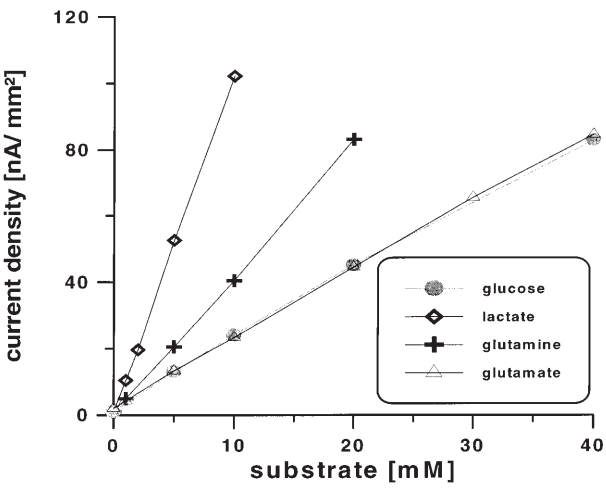


Fig. 11. Calibration graphs of a glucose–lactate–glutamine–glutamate monitoring device

The sample flow of 6 $\mu\text{l}/\text{min}$ was on line buffered and diluted with 100 $\mu\text{l}/\text{min}$ PBS pH 7.4 carrier solution. During yoghurt fermentation, the pH of the sample changes drastically by several pH units. Reliable measurements with biosensors are, due to the pH sensitivity of the enzymes used, not possible without sample pretreatment. Figure 12 shows that employing the on-line buffering strategy allows the monitoring with biosensors even in considerable changing matrices. Such changes in matrix composition occur during most bacterial and fungal fermentations.

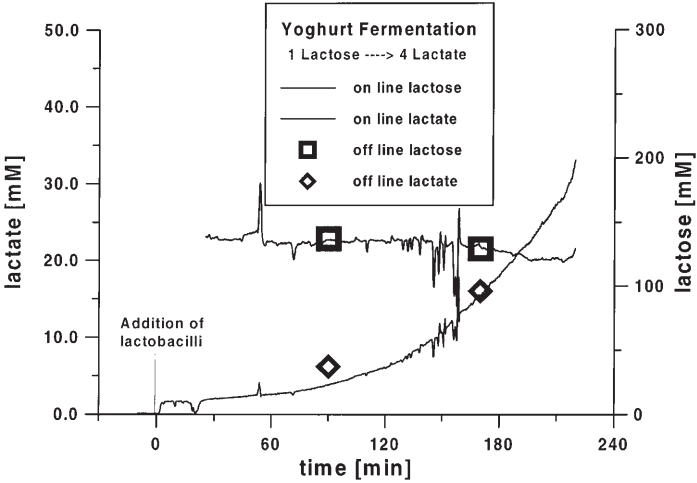


Fig. 12. Yoghurt fermentation monitoring

Another application of the device comprising a mixing coil is reagent addition, as demonstrated by assay for the glutamate producing enzymes glutamic oxaloacetic transaminase (GOT) and glutamic pyruvic transaminase (GPT) [103]. A thin film biosensor array comprising two glutamate and two blank sensors is assembled with a PCB comprising a mixing coil. The sample containing the enzyme to be assayed and a reagent with the respective enzyme substrates are mixed in the mixing coil. After stopped flow the increase in glutamate concentration is monitored by the difference signal from the glutamate and the blank sensors. The calibration graphs of such a device for the GOT and GPT assays are shown in Fig. 13. Compared to conventional spectrophotometric assays for these enzymes, this assay offers the advantage of not needing enzymes to be added to the reagent and of electrical readout which allows the assay working in whole blood. This assay scheme with a bioanalytical microsystem can be applied to a variety of diagnostically important enzymes. Attractive is also the possibility to directly combine metabolite analysis, e.g. lactate and glucose, with enzyme assays in one device, giving a more versatile lab-on chip.

Since these devices are made from two components produced by means of well-established mass production technologies (thin film and printed circuit board technology) and assembling of the parts is compatible to IC packaging techniques, cost effective mass fabrication of this device seems realistic.

Microphysiometry is the measurement of the metabolic activity of living cells in a miniaturized environment. Considerable interest in such devices from the industry arises from their use in drug screening.

Other applications are toxicity monitoring and cytotoxin response measurement of cancer cells [104]. Future applications may be strain prescreening in biotechnology, rapid sterility tests and preanalytical screening in combinatorial chemistry.

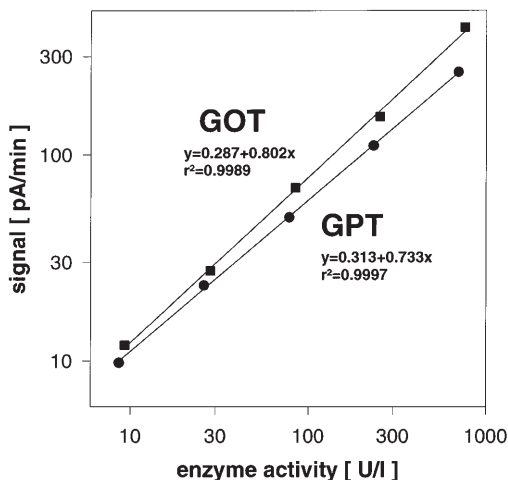


Fig. 13. Calibration graph of the GOT and the GPT assay

According to the different ways in which cells alter their environment, e.g. heat produced, acidification, oxygen consumption or metabolite production, to some extent reflecting metabolic pathways, various sensors can be used to measure metabolic activity. In order to get deeper insight into the cell metabolism, different sensors were integrated into one small test chamber [99]. Even an entire fermenter has been realized by means of silicon-micromachining [105].

For high throughput applications, such as drug screening, massive parallelization and therefore miniaturization is required. Different companies are now entering the market with microphysiometer arrays [106] based on light-addressable potentiometric sensors (LAPS) for pH sensing. There are several reasons why pH sensor based microphysiometers are the most advanced and used devices. Proton extrusion rates of mammalian cells are in the order of 10^8 protons/cell that is between two and three orders of magnitude higher than their oxygen consumption [99]. In contrast to oxygen and enzyme sensors, the sensing principle is usually based on an equilibrium measurement and therefore the measurement influences the composition of the test solution, which is altered by the cells, very little. LAPS devices are very attractive transducers for microphysiometer arrays since their production costs are low compared to CMOS and ISFET production, largely compatible with silicon-micromachining and their operation principle allows easy mapping of the pH dependent surface potential on the wafer surface. A drawback of all potentiometric measuring techniques suffer from the need of a reference electrode. Recently, Cheng [107] published an amperometric pH sensor with a pH responsive monolayer modified microelectrode. Monolayer protonation modulates the electron transfer rate of ferricyanide reduction. This method would have the drawback of the tolerance of the cells to the added redox species if applied to microphysiometry. But since an electrode arrangement for amperometry can be realized in sub-nanoliter containments [108], even single cell microphysiometry seems feasible with this method. Only 10^8 protons are required to protonate a $13\text{ }\mu\text{m}$ diameter modified electrode. In an approach with a low cost optical device, an ultrathin pH responsive membrane is placed on replicated chirped grating couplers [109, 110]. A resolution of 10^{-4} pH units was achieved but miniaturization is limited.

Probing oxygen consumption or metabolite production provides additional or complementary information about the cell metabolism. However, oxygen and enzyme sensors consume their substrates. With oxygen sensors it is possible to overcome this problem by using an inert anode, in this way balancing the oxygen consumption by the oxygen production on the anode [111]. With enzyme sensors, analyte depletion can be avoided by the application of substrate recycling. Monitoring glutamate can be done by adding or coimmobilizing the GOT and adding the substrate aspartate. But of course such recycling schemes are only applicable to a limited number of metabolites and may suffer from the influence of the cosubstrate on the cells metabolism. Furthermore, since the metabolite consumed by the enzyme sensor, due to the short diffusion distances, is rapidly drained from micropools, this offers the possibility of directly accessing absolute numbers of metabolite production rates. Cooper and co-workers

recently succeeded in measuring metabolic activity of single cells [112]. One neutrophil is placed in a sub-nanoliter pool comprising an electrode arrangement for amperometry [103] and superoxide release is monitored by means of a cytochrome-C modified electrode.

The challenge of establishing hundreds or thousands of electrical contacts if such amperometrically transduced microphysiometers are massive parallelized can be satisfied by multiplexing the individual sensors by CMOS components integrated on a silicon wafer [113].

Some even more exciting news can be expected from this combination of bio-sciences and micro system technology in the near future.

Microchip arrays for parallel binding and detection of DNA or proteins for drug discovery and different clinical microsystems are under development [114].

4

Conclusions and Outlook

It can be concluded that although extensive research work has been done on microanalytical devices the enthusiasm and high expectations in such systems have not been fulfilled to date. Further work and technological breakthroughs are still necessary in the long run. Up to now only niche markets can be covered by microanalytical sensor systems for remote locations.

Increasing production volumes resulting in lower prices of devices will push the whole market and open additional ones. The expectations of using small samples as well as small reagent volumes, minimization of time expenditure of skilled clinical people, minimization of calibration fluid consumption and waste are still key advantages of such a micro technology.

If it is possible to get highly reliable devices to process thousands of samples immediately with an appropriate production technology to obtain cheap and portable devices, a breakthrough of microanalytical sensor systems is still to be expected.

In addition on-line measurements are now possible for the first time. The technological route for realization of microanalytical sensors systems will now be evaluated and for market driven decentralized applications a distinct solution can still be expected in the near future.

5

References

1. Prohaska O, Kohl F, Goiser P, Olcaytug F, Urban G, Jachimowicz A, Pirker K, Chu W, Patil M, LaManna J, Vollmer R (1987) Multiple chamber-type probe for biomedical application. *Techn Digest Transd* 87: pp 1 – 4
2. Technical Digest Honeywell: Outline Sensorik and Automation, "Smart distributed systems" Jg 9: 9
3. Data sheet Eastman Kodak "KAF-6300 Image Sensor/Multi-Megapixel Full-Frame CCD" Rochester 1993
4. Technical Digest Lucas NovaSensor "Solid state pressure Sensor" 1997
5. Technical Digest SensoNor "Micromachined Sensors for a Global market" edn. 1/95

6. Amico A, Natale C, Verona E (1997) Acoustic devices. In: Kress Rogers (ed) Handbook of Biosensors and Electronic Noses, Medicine, Food, and the Environment. CRC, Boca Raton, p 197
7. Urban G, Jachimowicz A, Kohl F, Kuttner H, Olcaytug F, Goiser P, Prohaska O (1990) Sens Actuators A22:650
8. Spink CH (1980) Crit Rev Anal Chem May 1: pp 1–54
9. Mosbach K, Danielsson B (1974) Biochim Biophys Acta 364:140
10. Danielsson B, Mosbach K (1987) Theory and application of calorimetric sensors. In: Turner A, Karube F, Wilson IG (eds) Biosensors, Fundamentals and Applications. Oxford University Press, pp 575–595
11. Wehnert G, Sauerbrei A, Bayer Th, Scheper Th, Schügerl K, Herold Th (1987) Anal Chim Acta 200:73
12. Muramatsu H, Dicks JM, Karube I (1987) Anal Chim Acta 197:347
13. Bataillard P, Steffgen E, Haemmerli S, Manz A, Widmer H (1993) Bios Bioelectronic 8:89
14. Urban G, Kamper H, Jachimowicz A, Kohl F, Kuttner H, Olcaytug F, Goiser P, Pittner F, Schalkhammer T, Mann-Buxbaum E (1991) Bios Bioelectron 6:275
15. Xie B, Hedberg U, Mecklenburg M, Danielsson B (1993) Sens Actuators B15:141
16. Xie B, Danielsson B, Winquist F (1993) Sens Actuators B15:443
17. B Xie, M Mecklenburg, A Dzgoev, B Danielsson (1996) Proc 2nd Int Symp Miniaturized Total Analysis Systems TAS '96, Basel, 19–22 November, pp 95–99
18. Muehlbauer M, Guilbeau E, Towe B (1990) Sens Actuators B2: 223
19. Wolfbeis OS (ed.) (1991) Fiber optical chemical sensors and biosensors, CRC, Boca Raton, Florida vol 1 & 2
20. Gehrich J, Lübbers D, Opitz N, Hansmann D, Mikker W, Tusa J, Yafuso M (1986) Optical fluorescence and 1st application to an intravascular blood gas monitoring system, IEEE Trans Biomed Engin BME-33:117
21. Weigl B, Trettnak W, Holobar A, Klimant I, Gruber W, Hager R, Benes R, O Leary P (1993) Determination of pH, oxygen, and carbon dioxide in microgravity bioreactors with emphasis on application in BIOST (Bioprocessing space technology) Proc 5th Europ Symp On Life Sciences Research in Space. Arcachon, France ESA SP-366, August 1994
22. BIA gets set for the next century (1995) BIA J 2:15
23. Leiner M (1995) Sens Actuators B29:169
24. Roß L (1989) Integrated optical components in substrate glasses, Glastechn Ber 62, Nr 8, 285
25. Karlsson R, Michaelson A, Mattson L (1991) J Immunol Meth 145:229
26. Nellen Ph M, Lukosz W (1993) Bios Bioelectronic 8:129
27. Stamm Ch, Lukosz W (1994) Sens Actuators B18–19:183
28. Kunz RE, Duveneck G, Ehrat M (1994) Proc SPIE Vol 2331, pp 1–16
29. Duveneck G, Verpoorte E, Oroszlan P, Pawlak M, Erbacher C, Spielmann A, Neuschäfer D, Ehrat M (1996) Planar waveguide sensing systems: A combination of highly sensitive transducers with smart fluidic systems to a true TAS, Proc 2nd International Symposium on Miniaturized Total Analysis Systems TAS96, Basel, 19–22 November, pp 158–162
30. Cullen DC, Sethi RS, Lowe CR (1990) Anal Chim Acta 231:33
31. Jacobs P, Suls J, Sansen W (1994) Sens Actuators B20:193
32. Watson LD, Maynard P, Cullen DC, Sethi RS, Brettell J, Lowe CR (1987/88) Biosensors 3:101
33. Ives DJG, Janz GJ (eds) (1961) Reference electrodes—Theory and practice. Academic Press, New York
34. van den Berg A, Grisel A, van den Vlekkert HH, De Rooij NF (1990) Sens Actuators B1:425
35. Cremer M (1906) Z Biol 47:562
36. Ammann D, Morf WE, Anker P, Meier PC, Pretsch E, Simon W (1983) Ion-Selective Electrode Rev 5:3
37. Bergveld P (1972) IEEE Trans Biomed Eng BME-19:342
38. Thompson JM (1990) Med Biol Eng Comput 28:B29
39. Sibbald A, Covington AK, Carter RF (1984) Clin. Chem 30:135

40. Lundström I, van den Berg A, van der Schoot B, van den Vlekert H (1991) Field effect Chemical sensors. In: Göpel W, Hesse J, Zemel J (eds) *Sensors*. VCH Verlagsgesellschaft, Weinheim, Germany
41. Turner APF, Karube I, Wilson G (1987) *Biosensors fundamentals and applications*. Oxford University Press
42. Hintsche R, Dransfeld I, Scheller F, Pham M, Hoffmann W, Hueller J, Moritz W (1990) *Bios Bioelectronics* 5:327
43. Winquist F, Danielsson B (1990) Semiconducting field effect devices. In: Cass AEG (ed) *Biosensors-A practical approach*. IRL Press, p 171
44. Bergveld P (1991) *Biosens Bioelectronics* 6:55
45. Bergveld P, van den Berg A, van der Wal PD, Skowronska-Ptasinska M, Sudhölter EJR, Reinhoudt DN (1989) *Sens Actuators* 18:309
46. Kuriyama T, Kimura J, Kawana Y (1985) *NEC Res Dev* 78:1
47. Matsuo T, Esashi M (1981) *Sens Actuators* 1:77
48. Abe H, Esashi M, Matsuo M (1979) *IEEE Trans Electron Devices* ED-26:1939
49. *Technical Digest Sentron* (1995)
50. Hanazato Y, Inatomi K, Nakako M, Shiono S, Maeda M (1988) *Anal Chim Acta* 212:49
51. Anzai J, Tezuka S, Osa T, Nakajima H, Matsuo T (1987) *Chem Pharm Bull* 35:2, 693
52. Kimura J, Kawana Y, Kuriyama T (1988) *Biosensors* 4:41
53. Shiono S, Hanazato Y, Nakako M (1986) *Anal Sci* 2:517
54. Hanazato Y, Nakako M, Satorus S, Mitsuo M (1989) *IEEE Trans Electron Dev* 36:1303
55. Saito A, Ito N, Kumura J, Kuriyama T (1994) *Sens Actuators* B20:125
56. Erickson K, Wilding P (1993) *Clin Chem* 39/2:283
57. Jacobs E, Vadasdi E, Sarkozi L, Colman N (1993) *Clin Chem* 39/6:1069
58. Clark Jr LC (1956) *Trans Am Soc Artif Int Organs* 2:41
59. Pifl C, Jachimowicz A, Urban G, Kohl F, Goiser P, Theiner J, Nauer G (1990) *Sens Actuators* B1:468
60. Uhlig A, Paeschke M, Schnakenberg U, Hintsche R, Diedrich H, Scholz F (1995) *Sens Actuators* B24–25:899
61. Koudelka M, Gernet S, DeRoos NF (1989) *Sens Actuators* 18:157
62. Yokoyama K, Sode K, Tamiya E, Karube I (1989) *Anal Chim Acta* 218:137
63. Murakami T, Nakamoto S, Kimura J, Kuriyama T, Karube I (1986) *Anal Lett* 19:1973
64. Tamiya E, Karube I, Hattori S, Suzuki M, Yokoyama K (1989) *Micro Glucose Sensor using Electron Mediators Immobilized on a Polypyrrole-Modified Electrode, and Actuators* 18:297
65. Takatsu I, Moriizumi T (1987) *Sens Actuators* 11:309
66. Nakamoto S, Ito N, Kuriyama T, Kimura J (1988) *Sens Actuators* 13:165
67. Elbicki JM, Stephen WG (1989) *Biosensors* 4:251
68. Newman JD, Turner APF, Marazza G (1992) *Anal Chim Acta* 262:13
69. Pfeiffer D, Scheller F, Setz K (1993) *Anal Chim Acta* 281: (3) 489
70. Kost G, Wiese D, Bowen T (1991) *JIFCC* 3: (4) 160
71. Urban G, Jobst G, Keplinger F, Aschauer E, Tilado O, Fasching R, Kohl F (1992) *Biosens Bioelectron* 7:733
72. Matthews D, Holman R, Brown, Sreemson J, Watson A, Hughes S (1987) *Lancet* i:778
73. Cass AEG, Davis G, Francis GD, Hill HAO, Aston WJ, Higgins IJ, Plotkin EV, Scott LDL, Turner APF (1984) *Anal Chem* 56:667
74. Pollmann KH, Gerber MT, Kost KM, Ochs ML, Walling PD, Bateson JE, Kuhn LS, Han CA (1994) US Patent 5,288 636, *Enzyme electrode system*. Boehringer Mannheim
75. Yoshioka T (1993) US Patent 5,192 415, *Biosensor utilizing enzyme and a method for producing them*, Matsushita
76. Geise R, Adams JM, Barone NJ, Yacynych AM (1991) *Bios Bioelectron* 6:151
77. Urban G, Jobst G, Aschauer E, Tilado O, Svasek P, Varahram M (1994) *Sens Actuators* B19 (1–3):592
78. Fischer U, Rebrin K, Woedtke T, v Abel P (1994) *Horm Metab Res* 26:515

79. Bobbioni-Harsch E, Rohner-Jeanrenaud F, Koudelka M, deRoos N, Jeanrenaud B (1993) *J Biomed Eng* 15:457
80. Mastrototaro J, Johnson K, Morff R, Lipson D, Andrew C, Allen D (1991) *Sens Actuators B5* (1-4):139
81. Jeyanthi R, Rao PR (1990) *Biomaterials* 11:238
82. Urban G, Jobst G, Keplinger F, Aschauer E, Fasching R, Svasek P (1994) *Technol Health Care* 1: 215
83. Althainz P, Goschnik J, Ehrmann S, Ache H (1996) *Sens Actuators B33*:72
84. Gardner J, Pike A, deRoos N, Koudelka-Hep M, Clerc P, Hierlemann A, Göpel W (1995) *Sens Actuators B26-27*:135
85. Hierlemann A, Weimar U, Kraus G, Schweizer-Berberich M, Göpel W (1995) *Sens Actuators B26-27*:126
86. Meckes A, Behrens J, Hausner M, Gebhard M, Benecke W (1996) *Proc 2nd Intl Symp Miniaturized Total Analysis Systems TAS '96*, Basel, 19-22 November, pp 126-128
87. Widmer H (1983) *Trends Anal Chem* 2:VIII
88. Manz A, Graber N, Widmer H (1990) *Sens Actuators B1*:244
89. van den Berg A, Bergveld, P (eds) (1995) *Micrototal analysis systems*, Kluwer Academic Publishers
90. Sachs Ch, Finetti P, Mollard J, Ritter C (1996) *Proc 14th Intl Symp Electrolyte/blood gas AACC & Japan Soc Biomed* 18-21:2 Hawaii, p 428
91. Hoffmann W, Rapp R (1996) *Sens Actuators B34*:471
92. van der Schoot B, Jeanneret S, van den Berg A, deRoos N (1993) *Sens Actuators B15-16*:211
93. Drost S, Wörmann W, Ross B, Chemnitus G, Rospert M, Konz W, Hartmann Frimmel F, Schuhmann W, Ferretti R, Meixner L (1996) *Proc 2nd Intl Symp Miniaturized Total Analysis Systems TAS '96*, Basel, 19-22 November, p 199
94. Steenkiste F, Grünkorn H, Claesen L, Baert K, Hermans L, Debruyker D, Cooman M, Spiering V, van den Berg A, van der Schoot B, Arquint P, Born R, Schuhmann K (1996) *Proc 2nd Intl Symp Miniaturized Total Analysis Systems TAS '96*, Basel, 19-22 November, pp 138-140
95. Arquint Ph, van den Berg A, van der Schoot BH, Bühler H, Morf WE, Dürselen L, de Roos NF (1993) *Sens Actuators B13-14*:340
96. Hinkers H, Conrath N, Czupor N, Frebel H, Hüwel S, Köckemann K, Trau D, Wittkamp M, Chemnitus G, Haalck L, Meusel M, Cammann K, Knoll M, Spener F, Rospert M, Kakerow R, Köster O, Lerch T, Mokwa W, Woias P, Richter M, Abel T, Meixner L (1996) *Proc 2nd Intl Symp Miniaturized Total Analysis Systems TAS '96*, Basel, 19-22 November, pp 110-112
97. Knoll M German patent application DE 4115414 A1
98. Steinkuhl R, Sundermeier C, Hinkers H, Dumschat C, Cammann K, Knoll M (1996) *Sens Actuators B33*:19
99. Urban G, Jobst G, Svasek P, Varahram M, Moser I, Aschauer E (1994) *Univ Twente*:249
100. Jobst G, Svasek P, Moser I, Varahram M, Trajanoski Z, Wach P, Kotanko P, Skrabal F, Urban G (1997) *Sens Actuators* (in press)
101. Jobst G, Moser I, Varahram M, Svasek P, Aschauer E, Trajanoski Z, Wach P, Kotanko P, Skrabal F, Urban G (1996) *Anal Chem* 68:3173
102. Moser I, Jobst G, Aschauer E, Svasek P, Varahram M, Urban G, Zanin V, Tjoutrina G, Zharikova A, Berezov T (1995) *Biosens Bioelectron* 10:527
103. Moser I, Jobst G, Svasek P, Svasek E, Varahram M, Urban G (1997) *Sens Actuators* (in press)
104. Brischwein MW, Baumann R, Ehret A, Schwinde M, Kraus B, Wolf (1996) *Diagnostik Naturwissenschaften* 83:193
105. Walther I, van der Schoot BH, Jeanneret S, Arquint Ph, de Roos NF, Gass V, Bechler B, Lorenzi G, Cogoli A (1994) *J Biotechnol* 38:21
106. Bousse L, McReynolds RJ, Kirks G, Dawes T, Lam P, Bemiss WR, Parce JW (1994) *Sens Actuators B20* (2-3):145

107. Cheng Q, Brajter-Toth A (1996) *Anal Chem* 68:4180
108. Bratten CDT, Cobbold PH, Cooper JM (1997) *Anal Chem* 69:253
109. Jobst G, Moser I, Urban G, Dübendorfer J, Kunz R (1997) Optical grating coupler with ultrathin pH responsive membrane for microphysiometry (in preparation)
110. Kunz RE, Edlinger J, Sixt P, Gale MT (1995) *Sens Actuators A47*:482
111. Jobst G, Urban G, Jachimowicz A, Kohl F, Olcaytug F, Lettenbichler I, Nauer G (1993) *Bios Bioelectron* 8, 3/4:123
112. Cooper JM, Bratten CDT, Cobbold PH, Krause S, Jiang L (1997) Single cell measurements using micromachined electrochemical vessels (in preparation)
113. Hinkers H, Hermes T, Sundermeier C, Borchardt M, Dumschat C, Cammann K, Knoll M, Bucher S, Buhner M (1995) *Sens Actuators B24* (1/3):300
114. Microminiature tools affecting lab products, (1994) *Biomed Business Intl, Labmedica Intl* 11/12: pp 8–9

Sample Preparation In Microstructured Devices

Jing Cheng^{1*} · Larry J Kricka² · Edward L Sheldon¹ · Peter Wilding²

¹ Nanogen Inc, 10398 Pacific Center Court, San Diego, CA92121, USA.

E-mail: jcheng@nanogen.com

² Department of Pathology and Laboratory Medicine, School of Medicine,
University of Pennsylvania, 3400 Spruce Street, Philadelphia, PA19104, USA

Handling and processing of μl and sub- μl sized samples are challenging, and have a series of attendant problems, such as loss of sample on the walls of transfer devices, loss by evaporation, loss of components of the sample during manipulation and processing, and obtaining a representative sample from an nonhomogeneous specimen. A further difficulty is that the expected concentration of the analyte restricts the scale of miniaturization of the sample. Detection of rare cell types (e.g., cancerous cells, fetal cells in maternal circulation, assessment of minimal residual disease) and microorganisms is problematic, and the expected cell frequency or microbial load will determine a sample size compatible with detection. In such cases a specific selection or a preconcentration step is a more logical approach to ensure the presence of the desired cells or microorganisms. In this review the principles and applications of the current range of microfluidic (e.g., pumps, valves) and microfiltration systems (e.g., silicon microfilters) and electronically controlled microstructured devices relevant to the micro-sample preparation are critically discussed.

Keywords: Fluid handling, microfiltration, complexity reduction, microstructured device, sample preparation, DNA analysis.

1	Introduction	216
2	Particular Problems for Microsamples	218
3	Microfabrication	218
3.1	Micromachining and Microfabrication	218
3.2	Advantages of Microfabrication	219
4	Microfabricated Fluid Control Elements	220
4.1	Micropumping	220
4.1.1	Electroosmotic Pumping	220
4.1.2	Traveling-Wave Pumping	221
4.1.3	Thermal Capillary Pumping	222
4.1.4	Piezoelectric Pumping	222
4.2	Microvalving	223

* Corresponding author.

4.2.1 Freeze-Thaw Valving 223

4.2.2 Magnetic Valving 224

5 Sample Preparation in Microstructured Devices 224

5.1. Microfiltration 224

5.2 Electronic Sample Preparation 227

6 Conclusion 230

7 References 230

1

Introduction

A typical analytical reaction comprises the following three steps:

1. Sample preparation.
2. Chemical reaction.
3. Detection/quantitation of the signal.

In the past various approaches have been explored in the effort to integrate all three steps but with little success. The sample preparation step is often the most difficult step in an assay, particularly for complex mixtures such as biological fluids, and is therefore typically performed separately from the reaction and detection/quantitation steps. However, the long awaited, totally integrated analytical system may soon become a reality as a result of progress in the application of the microfabrication processes used in the microelectronics industry into the analytical arena [1–3]. Microfabrication has played a central role in the development and current mass production of microprocessor and memory chips for the computer industry. This miniaturization process has brought down the scale of the computer from a machine that typically occupied several rooms to the size of a small notebook. Now these microfabrication processes are being explored for the production of micromachined silicon or glass chips with diverse analytical functions for use in basic research, forensic science and clinical diagnostics. These devices are showing great promise for totally integrated analytical systems that could form the basis of smaller, more efficient benchtop or even palmtop analyzers that require only pl–nl sized samples as compared to the µl–ml sized samples required for most conventional assays.

A problem that has proved particularly difficult is the simplification of the sample preparation step for nucleic acid analyzes. Preparation of samples for DNA or RNA analysis is laborious. The traditional approaches for preparing nucleic acids can be classified into two categories: liquid-liquid extraction and liquid-solid extraction.

Liquid-liquid extraction of polynucleotides normally involves the use of an organic solvent (such as phenol or chloroform) or an aqueous solution (such as sodium perchlorate, guanidine hydrochloride or guanidine thiocyanate in high concentration) to remove the proteinaceous materials from the aqueous phase

that contains DNA or RNA. The extraction of DNA using proteinase K digestion followed by phenol/chloroform extraction is an established method [4]. There are, however, several disadvantages to this procedure. First, the method is time-consuming and the organic solvents used are hazardous. In addition, it is difficult to completely separate the DNA-containing aqueous phase from the organic phase which contains digested and/or denatured proteins and lipids. These form a small but appreciable intermediate layer. The presence of proteinase K also increases the level of proteinaceous contamination and may cause some degradation to DNA due to the presence of contaminating nuclease [5]. An alternative procedure to extract DNA from blood employs phenol/chloroform without proteinase K [6]. This procedure gives good yields of DNA in a relatively short period of time.

Buffone and Darlington used incubation with sodium perchlorate instead of proteinase K and phenol to extract DNA from human blood [7]. DNA has also been extracted by dehydrating and then precipitating the cellular proteins using a protein salting-out procedure [8]. This method requires vigorous shaking for deproteinization which may cause shearing of DNA. In addition, DNA can be lost as a result of co-precipitation with proteins. In another method, guanidine hydrochloride was used instead of sodium dodecyl sulfate (SDS) to lyse cells and salt-out the proteins [9]. DNA extracted this way is difficult to redissolve. In contrast, DNA extracted using guanidine hydrochloride and proteinase K can be redissolved quickly [10]. Also methods using pronase instead of proteinase K [11] or using proteinase K at 60 °C, instead of 37 °C [12], produced good quality DNA. Liquid-solid extraction, on the other hand, requires the use of a solid material such as polymerized silica gel or glass beads to remove the protein contents from the lysate containing polynucleotide. DNA has been extracted from cultured cells by a method reported by Thompson et al. using guanidine thiocyanate and glass particles [13]. Although the DNA was extracted in high yield relatively quickly, the time required to re-dissolve the DNA was long. In two separate reports, DNA has been isolated using proteinase K, silica gel and phenol/chloroform [14, 15]. Although proteinase K and phenol were still used, significant time saving was achieved. In a modification of the above method, sodium perchlorate, polymerized silica gel and chloroform were employed together with a specially designed plastic tube to extract DNA from micro-samples of human blood. The total time involved in the extraction and redissolution of DNA was approximately 2 h [16]. Extraction of DNA has also been achieved by means of a Sephadex G-25 column [17] and columns packed with insoluble particulate materials containing pendent groups which are chemically similar to phenol [18].

Most of these DNA isolation procedures are time-consuming or hazardous to the operators because toxic chemicals are used in the sample extraction procedure. They all require centrifugation, pipetting, vortexing or thermal incubation steps which are almost impossible to integrate with current instrumentation.

The isolation of polynucleotides in microstructured devices provides a promising new approach that may be compatible with total integration of subsequent analytical steps and its current status is examined in the following sections.

2

Particular Problems for Microsamples

Handling and processing of microsamples (e.g. μl and sub- μl sized samples) are difficult, and most of the current analytical methods used in the life sciences usually analyze samples at volumes of $> 2 \mu\text{l}$. Analysis of sub- μl volume samples has a series of attendant problems, including:

- i) Loss of sample on the walls of transfer devices (e.g. pipette tips).
- ii) Loss by evaporation.
- iii) Loss of components of the sample (e.g. the analyte to be detected) during manipulation and processing (e.g. loss by adsorption onto the walls of tubing, or containment vessels).
- iv) Obtaining a representative sample from a nonhomogeneous specimen.

A further difficulty is that the expected concentration of the analyte restricts the scale of miniaturization of the sample. For example, for an analyte present at a concentration of 1 zeptomol l^{-1} ($10^{-21} \text{ mol l}^{-1}$) there are only 602 molecules present in one liter of sample. Hence, in a $1 \mu\text{l}$ sample there is less than one molecule of the analyte, and thus this degree of miniaturization is impracticable.

In genetic analysis of genomic targets the prospects for sample miniaturization are excellent. Adult human blood contains between 4,400 and 11,000 white cells in a $1 \mu\text{l}$ sample. In theory a single white cell is sufficient as the sample for a polymerase chain reaction (PCR) to amplify a genomic DNA target, and for a blood specimen with a white blood cell count of $10,000 \mu\text{l}^{-1}$ this would be contained in a 100 pl sample. Miniaturization of samples for analyzes designed to detect rare cell types (e.g. detection of cancerous cells, fetal cells in maternal circulation, assessment of minimal residual disease) or for the detection of microorganisms is more problematic, and the expected cell frequency or microbial load will determine a sample size compatible with detection. In such cases a specific selection (e.g. magnetic immunobead technology) or a preconcentration step is a more logical approach to ensure the presence of the desired cells or microorganisms.

3

Microfabrication

3.1

Micromachining and Microfabrication

A range of techniques and materials are available for micromachining which rely upon the controlled removal or deposition of material at a μm scale (Table 1). Simple wet etching of silicon is the most extensively developed technology [19, 20], but there is increasing interest in micromachining of glass (soda glass and Pyrex) because of its optical and insulating properties. Generally, feature sizes of approximately $1 \mu\text{m}$ are possible using conventional photolithography and wet etching of silicon and other fabrication methods can produce structures with minimum feature sizes of $< 1 \mu\text{m}$ (e.g. $0.3 \mu\text{m}$, deep UV (230 – 260 nm); $0.1 \mu\text{m}$,

Table 1. Materials and methods for microfabrication

Materials	Methods
Metals and Elemental Materials	Etching
Aluminum, copper, diamond, gold, silicon	Anisotropic etching, isotropic etching
Glass	Microscopy-Based Techniques
Pyrex, soda	Atomic force microscopy, scanning probe microscope
Oxides	Ablation
Alumina, quartz, rubidium molybdenum oxide	Electron-beam, focused ion-beam, laser, reactive ion etching
Polymers	Miscellaneous
Fluorocarbon polymers	Embossing
Semiconductors	
Gallium-arsenide, indium phosphide	
Miscellaneous	
Silicon carbide	

X-ray and e-beam ; < 1 nm, scanning tunneling microscope) [20–23]. Moving parts can be fabricated in microdevices by sacrificial layer techniques, in which an intermediate sacrificial layer is selectively removed to release an overlying structure. This technique has been used to produce complex multicomponent devices with moving parts such as motors [24]. Complex microchip structure can also be manufactured by bonding together components to form multilayer structures and holes introduced by laser drilling [25].

3.2
Advantages of Microfabrication

An advantage of microfabrication is that it offers increased flexibility in design and ease of manufacture compared to the processes used to manufacture macroscale devices. In the case of devices made from silicon, the pre-existing microelectronics industry manufacturing processes are already in place for high volume, low-cost production (millions of wafers per year). Thousands of devices can be fitted onto a 4 or 6 inch wafer, and thus many different microchip designs can be simultaneously fabricated on a wafer. This facilitates more rapid design cycles and design iterations than would normally be possible for a macroscale device. Also, changing the design of a microfabricated device is easier and cheaper, because it would only involve relatively simple modifications to the photolithographic mask.

The low internal volume of a microchip analyzer (pl–µl) produces an economic benefit because reagent consumption per test is correspondingly low, and also a clinical benefit because the volume of sample for analysis is small (pl–nl) in comparison to the µl volumes used in macroscale analyzers. Small sample sizes are particularly beneficial in a clinical setting (finger stick versus venipuncture). It also minimizes exposure of health workers to potentially

hazardous specimens. Finally, the low capacity of microchip devices minimizes waste fluid volume, and there is also the possibility that the sample can be entombed in the device (unreacted sample, reagents and reaction mixture) for safe disposal.

Other advantages of microfabricated devices include faster response times, and the fabrication of multiple test sites for simultaneous replicate assays in one microfabricated device. This analytical redundancy provides a safeguard that is not easily attained in a conventional macroscale analyzer, where duplicate assays represent the usual extent of repetitive assay of a sample. Encapsulation technology used in the microelectronics industry may also be applicable to microscale devices and could be extended to operations over a wide range of environmental conditions of humidity, and temperature.

Finally the flexibility in the design of a microchip device does not lock the chip into a single assay design. Development of single-principle polynucleotide-assay devices suitable for assaying large or small targets (capillary electrophoresis or hybridization assay designs) has been fraught with difficulties – such limitations do not apply to microfabricated devices.

In the following discussion we examine microflow control elements useful for sample preparation such as valving and micropumping. We then examine the devices designed specifically for sample preparation, i. e. microfiltration devices and electrical sample preparation devices.

4

Microfabricated Fluid Control Elements

Control of a fluid within an integrated analytical microchip is an important task. Fluid control tasks include acquisition of the sample by the microchip from a specimen container or reservoir, movement of the sample to different regions of the microchip for processing and distribution of the sample to multiple processing or test sites. A range of microfabricated pump and valve technologies have been described and these may ultimately provide the fluid control elements anticipated to be required for integrated microchips.

4.1

Micropumping

4.1.1

Electroosmotic Pumping

Electroosmotic pumping in a fused capillary column was first reported by Jorgenson and Lukacs in 1981 [26]. Since then this type of pumping mechanism has been adopted by several groups to move solutions in microchannels in glass chips. Seller et al. reported the first example of fluid flow driven by electroosmotic pumping in a network of intersecting capillaries integrated on a glass chip [27]. Controlling the potentials applied to the capillaries allowed quantitative transport of reagents from different streams to an intersection of capillaries. Electrophoretic transportation of biomolecules such as DNA and proteins has

been accomplished in an integrated microchip to perform enzymatic digestion [28]. As a follow-up to the electroosmotic or electrophoretic pumping, an electrodynamic focusing unit composed of a two-dimensional sheath flow chamber fabricated in a glass chip was employed to accelerate the flow speed and also to confine spatially the flow of both fluids and ions [29]. In another report a combination of both mechanical pumping force and electrophoretic mobility discrimination was applied in a free flow chip electrophoresis device for selective sampling of one or several components from a complex sample [30].

4.1.2

Traveling-Wave Pumping

Flow movement of fluid and particles suspended in solution was achieved via traveling-wave pumping [31]. The driving force was generated by application of four square-wave voltages of 1 MHz frequency, with progressive phase differences of 90° to the appropriate electrodes. A typical pump has a planar array of 13 microfabricated electrodes on the glass chip which formed one side of a pump channel (Fig. 1). Each electrode was $0.5\ \mu\text{m}$ high, $35\ \mu\text{m}$ wide and the gap between adjacent electrodes was $35\ \mu\text{m}$. The pump channel was $50\ \mu\text{m}$ deep, $600\ \mu\text{m}$ wide and $4\ \text{mm}$ long. The high-frequency traveling wave generated inside the pump is able to drive the liquid forward but can also trap micro-particles present in the fluid. The latter feature of this type of pumping may be especially useful for “filtering” particles such as bacteria from a water sample.

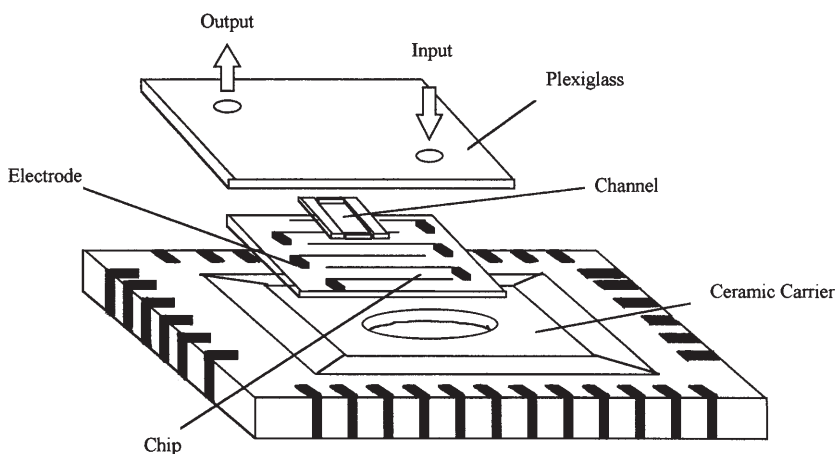


Fig. 1. The traveling-wave micropump assembly. The electrode array chip, with a channel cut in a glass cover mounted on it, is sandwiched between a ceramic carrier and a Plexiglass cover. The volume between the chip and Plexiglass cover forms the circulatory space, consisting of the pump channel itself as well as the two side-channels around the outside of the return flow [31]

4.1.3

Thermal Capillary Pumping

The transportation of discrete nanoliter sized drops of fluid through enclosed microchannels fabricated in a silicon chip has been achieved using addressable local heating [32]. Heating was achieved by a selective flow of D.C. current through the addressed electrode built inside the capillary channel. The electrodes were made by first depositing a $0.35\text{ }\mu\text{m}$ thick layer of aluminum on the silicon wafer using an electron beam coating technique, and then covering the metallic electrode sequentially with $1\text{ }\mu\text{m}$ SiO_2 , $0.25\text{ }\mu\text{m}$ Si_3N_4 , and $1\text{ }\mu\text{m}$ SiO_2 using plasma-enhanced chemical vapor deposition. The thermal capillary pump can accurately mix, measure, and divide drops by simple electronic control thereby providing a versatile pumping method with integrated functions. Figure 2 shows the transportation and mixing of two separate reagent streams in a Y-shaped channel device.

4.1.4

Piezoelectric Pumping

A piezoelectric pump is constructed with two glass plates and a silicon wafer [22]. A pressure chamber and a raised flat surface suspended with a thin diaphragm are formed on the upper glass plate (Fig. 3). The piezoelectric actuator is placed on the raised flat surface. In order to guide the flow of the pumped liquid, two check valves made of poly-silicon are fabricated on the silicon wafer

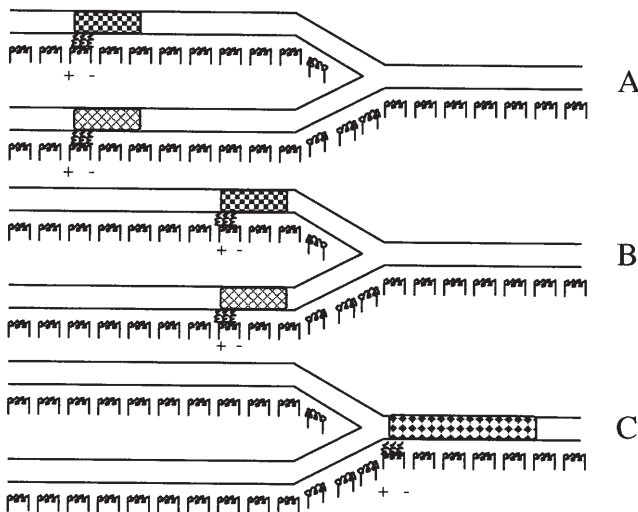


Fig. 2. Drop motion and mixing in a Y-channel device. The device was constructed by bonding the silicon heater elements and glass channels. (A) Initiation of movement by heating the left interface of two drops (nl level) at their starting locations in the branches of the Y-channel, (B) the movement in progress, and (C) the combined drop

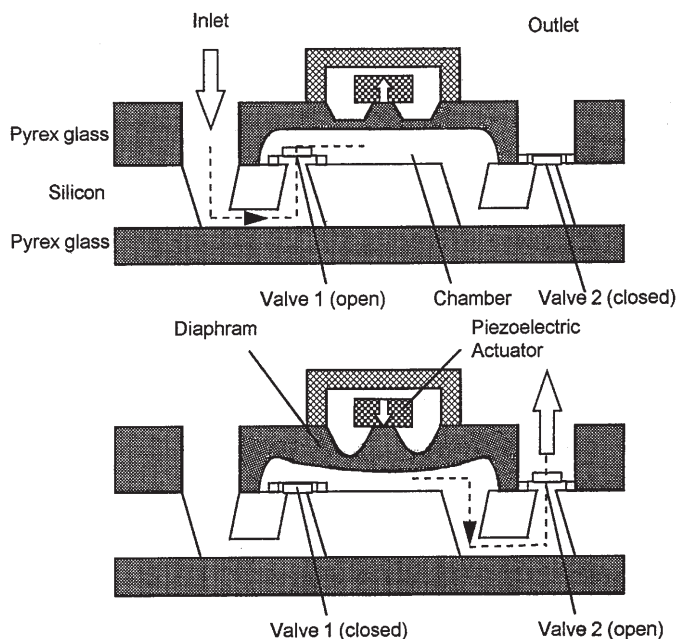


Fig. 3. Structure and principle of the piezoelectric micropump using poly-silicon check valves [22]

at the inlet and outlet of the pressure chamber respectively. The liquid is driven to the outlet when the piezoelectric actuator is switched on. When the actuator is switched off, liquid flows from the inlet into the pressure chamber. As a periodic voltage is applied to the actuator, pumping of fluid is achieved. An interesting recent development is the so called dynamic passive valves which have exceeded the performance of the traditional static passive valves. The static passive valves usually use a mechanical element such as a flap, a sphere or a membrane to stop the flow of the fluid. In contrast, the dynamic passive valve uses flow-channels which have a simple truncated pyramidal shape [25, 33].

4.2

Microvalving

4.2.1

Freeze-Thaw Valving

The freeze-thaw valve is a recently developed microvalving system [34, 35]. Unlike all other valving systems it does not require any moving parts in the capillary channel and has no dead volume. A small section of fluid inside the capillary is made to act as its own shut-off valve upon freezing. The freezing process was achieved by using a fine jet of a mixture of liquid and gaseous carbon dioxide at

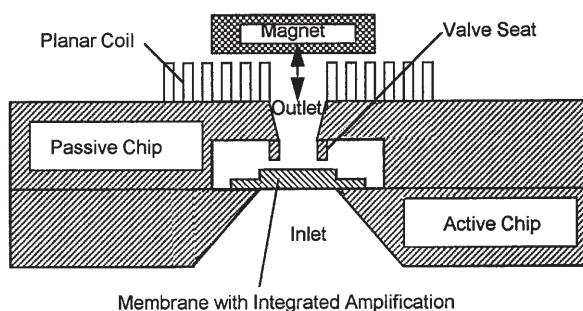


Fig. 4. Cross-section view of the magnetically driven valves, 2/2 ways [36]

approximately -65°C delivered from a cylinder of the compressed liquid. Flow of fluid driven by the electroosmotic pumping can be halted by localized freezing. This can be monitored by the instantaneous loss of current due to the formation of an insulating plug of ice. To make the cooling system compatible with the planar microstructures, a chip-based electrothermal cooling device such as a Peltier device may be fabricated.

4.2.2

Magnetic Valving

In the magnetic valving system reported by Löchel et al., a thin square shaped membrane structure ($2 \times 2 \text{ mm}$) of NiFe alloy was used as the flow-controlling element driven by the presence or absence of a magnet applied externally to the chip device [36]. The nickel-iron alloy was deposited by electroplating. In the middle of the membrane an integrated bar of the same ferromagnetic material amplifies the force for moving the membrane. The four edges of the membrane were sealed against the silicon substrate. Fig. 4 shows the cross section of this type of magnetically-driven valve. As shown in Fig. 4, the magnetic valve is normally open and flow occurs if a high pressure is applied from the upper side of the valve. The application of a magnetic field drives the ferromagnetic membrane toward the valve seat and closes the valve. If the fluid pressure increase is from the lower side of the valve, then the flow moves the membrane towards the seat and closes the valve. The valve can be opened again by re-applying the magnet field using an external magnet.

5

Sample Preparation in Microstructured Devices

5.1

Microfiltration

When designing filters to effect blood cell separation or isolation, it is soon apparent that the deformability of the cells plays a major role in the separation

efficiency. The reported sizes of blood cells are often based on morphological studies of the stained cells. However, filtration of the spherical and discoid white and red blood cells is influenced by the cell concentration, applied pressure, viscosity of the medium, and the size of the filter port. Red blood cells with relatively stable discoid architecture will readily align themselves to facilitate passage through a 3 μm gap while highly deformable white blood cells with spherical diameters in excess of 15 μm will pass through filter gaps of only 7 μm .

A fundamental consideration in the design of filter systems on microchips aimed at the isolation a white blood cell population with very low red cell contamination [i.e. to prevent inhibition of PCR by hemoglobin] is the level of tolerable efficiency. For genomic studies it is not essential to achieve high efficiency in white cell collection, but rather to achieve an adequate number of cells for successful amplification (e.g. PCR). Thus, a filter system that receives 1.0 μl whole blood containing approximate 5000 white blood cells would still be effective if the resulting white cell collection was only 10% (i.e., collected 500 cells) provided the red cell population remaining was less than 50,000 cells. Therefore, a system that isolates white blood cells with 10% efficiency and removes red blood cells with 99% efficiency will meet requirements. When filters are designed appropriately, they are capable of retaining white blood cells and allowing red cells to flow around them to the exit port.

One approach to microfiltration is to fabricate filters directly from silicon. A series of silicon microfilters have been fabricated using both conventional wet etching and reactive ion etching. Different designs were explored including simple arrays of posts, tortuous channels [37], comb-shape filter [3] and weir-type filters [38]. The general structure of a microfiltration chip is an etched channel (or chamber) that contains the filter element across the entire width of the channel. The structure is capped with a Pyrex glass top and this provides for convenient visual inspection of the filtration process. Sample is introduced into the channel and mechanically pumped through the filter by a syringe pump. Depending on the size of the filter, different particulate components are trapped at the front surface (Fig. 5) or within the filter bed (Fig. 6).

The main focus of the microfiltration development has been the efficient isolation of white blood cells from whole blood as part of sample preparation for nucleic acid amplification reactions such as PCR [39]. Weir-type filters have proved particularly effective in this regard. These are fabricated from a strip of silicon that lies across the entire length of a channel. This strip is selectively etched to a depth of between 3 and 5 μm and then the structure capped with glass. The gap between the top of the silicon strip and the glass is the active filter for cells (Fig. 7). Weir-type filters with gaps of approximately 3–4 μm effectively isolate white cells from whole human blood without retaining red blood cells. Microchips that integrate this type of filter and a PCR chamber have been designed and tested and shown to be effective for the isolation and direct PCR analysis of genomic DNA targets.

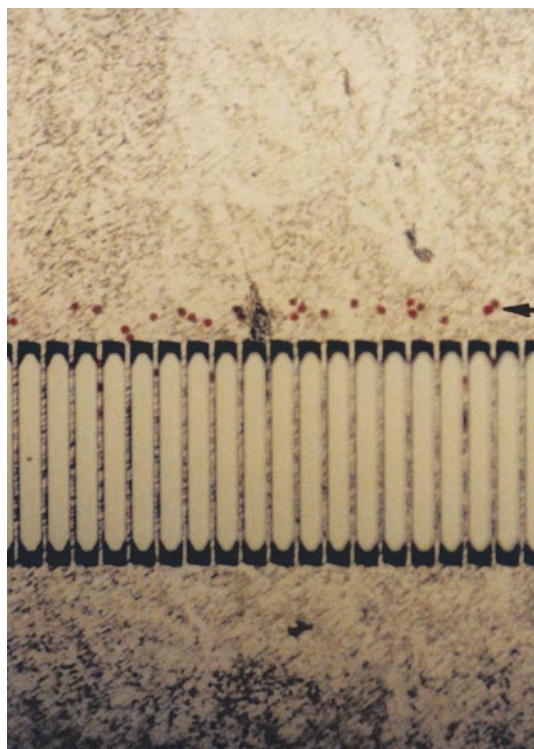


Fig. 5. Filtration of the white blood cells from diluted human whole blood using a comb-type filter chip. The white blood cells were stained with New Methylene Blue dye. The image was taken by reversing the applied pressure slightly to allow the trapped white cells be released from the front surface of the filters (*arrow*) and be seen clearly [3]

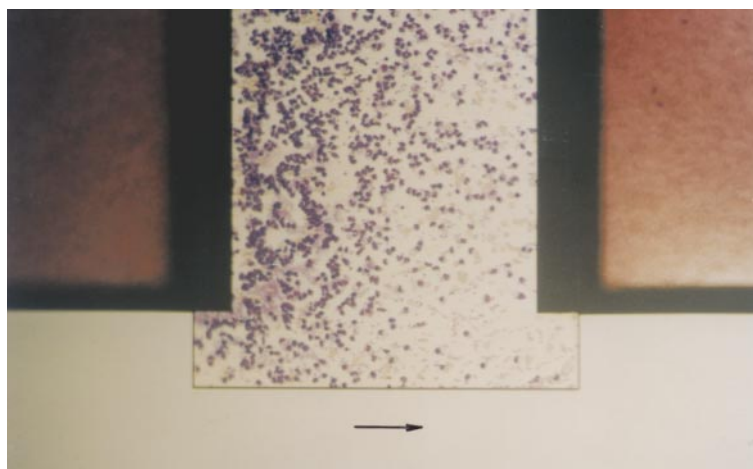


Fig. 6. Filtration of the white blood cells from New Methylene Blue dye stained undiluted human whole blood using a weir-type filter chip (flows direction is indicated by the *arrow*). The image was taken during the filtration process. The *purple-blue particles* seen in the middle of the chip were the stained white cells trapped on the surface of the weir filter

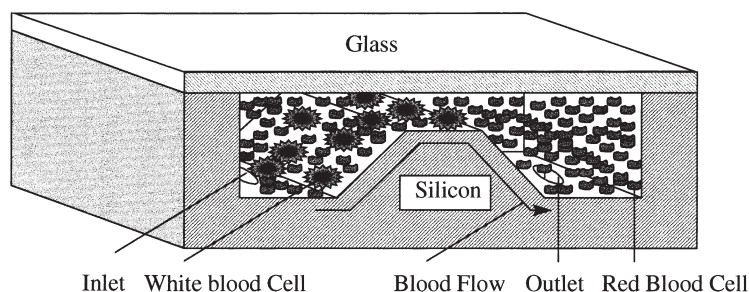


Fig. 7. A cross-section view of the weir-type filter to illustrate how the weir-type filter chip works

5.2

Electronic Sample Preparation

Microfabricated arrays of posts in a silicon chip were used to study the electrophoretic migration behavior of DNA several kilobases long [40]. The silicon chip was bonded with a glass cover to form a chamber containing a two-dimensional array of posts in SiO_2 . Each post is $0.15\ \mu\text{m}$ high, $1.0\ \mu\text{m}$ in diameter and has $2.0\ \text{m}$ center-to-center spacing. A device like this could be useful for the isolation of the large-sized chromosome DNA from crude lysate or human lymphocytes directly lysed within the device.

Devices have also been developed which separate nucleic acid sequences from complex biological specimens using proprietary methods based on differences in charge, size and sequence. For the initial stage of separation from the crude sample, a device which performs electrophoretically-driven purification of nucleic acids from samples (up to $1000\ \mu\text{l}$ in volume) has been fabricated. The subsequent stage employs a microdevice with feature sizes as small as $200\ \mu\text{m}$ for sequence enrichment or complexity reduction. The complexity reduction process allows target sequences in complex genomes to be enriched prior to a hybridization assay. In complex mixtures of sequences such as genomic DNA, the irrelevant sequences are so abundant that they cause interference with hybridization to single copy per genome sequences. In order to prevent interference in conventional assays for human genes, enrichment is accomplished by performing a sequence-specific amplification process, e.g. PCR. However, the use of amplification complicates quantitation of target sequences. Previous strategies include the Southern blot procedure [41], involving the digestion of genomic DNA, followed by size fractionation using gel electrophoresis and blotting to a membrane, to spread out the DNA according to size to allow hybridization without significant interference.

The complexity reduction device captures sequence specific sequences using an electrophoretically-driven hybridization process [42–44]. The process of using electrode bias to control a hybridization reaction is shown in Fig. 8. In the first step, a complex mixture of nucleic acids in solution is added to the complexity reduction device. In the second step, the electrode is positively biased to attract

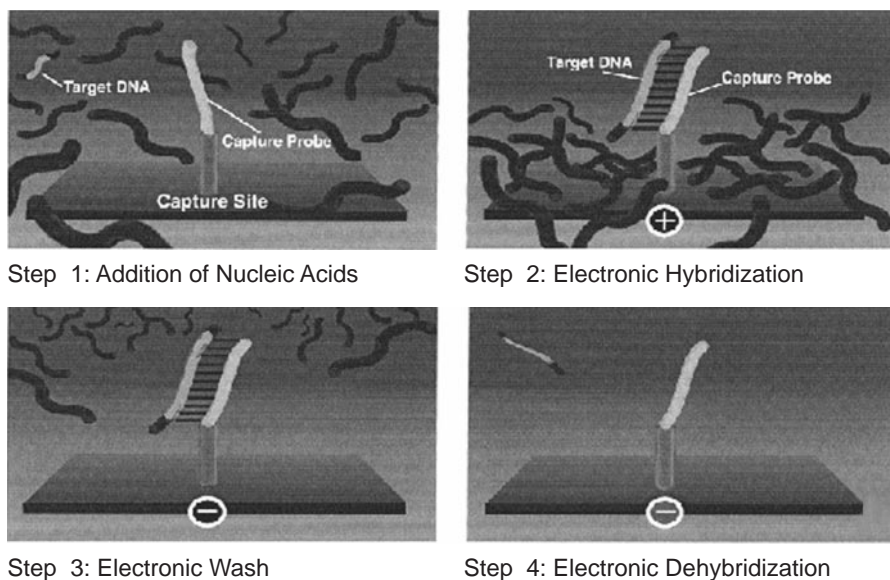


Fig. 8. Illustration of the complexity reduction process

the negatively charged polynucleotides in the sample. Capture probes immobilized in a permeation layer above the electrode hybridize to the sequence of interest. In the third step, the unhybridized sequences are driven away from the capture probes by reversing the bias of the electrode to negative. Next, the solution is replaced to remove the unhybridized material. In the fourth step, the field strength of the negatively biased electrode is raised by increasing the current level. At higher field strength the specific target is dehybridized from the capture probe and can be transported to an assay site where the signal associated with the target can be concentrated for more sensitive detection. Although the assay may also involve an electronically driven hybridization reaction [44], the hybridization sites used in complexity reduction are larger (200 to 500 μm vs 80 μm) to accommodate the crowding caused by the irrelevant nucleic acid sequences.

The complexity reduction device shown in Fig. 9 consists of a plastic sample chamber mounted on top of a printed circuit board (PCB) with holes through both the chamber and the PCB. The diameters of the holes at the top of the chamber range from 200 to 500 μm . To provide electrodes, the walls of the holes in the PCB are plated with gold and electrically connected to a standard electronic interface at one end of the PCB. To contain the aqueous sample in the chamber, the through holes are filled with a hydrogel, typically a polyacrylamide derivative. The polyacrylamide is derivatized or combined with streptavidin to permit attachment of oligonucleotide probes which protrude into the sample chamber. Another function served by the hydrogel is that gas bubbles caused by electrolysis at the electrodes are prevented from rising to the hybridization site in the chamber. Thus, current levels as high as 500 μA can be used without bubbles blocking hybridization.

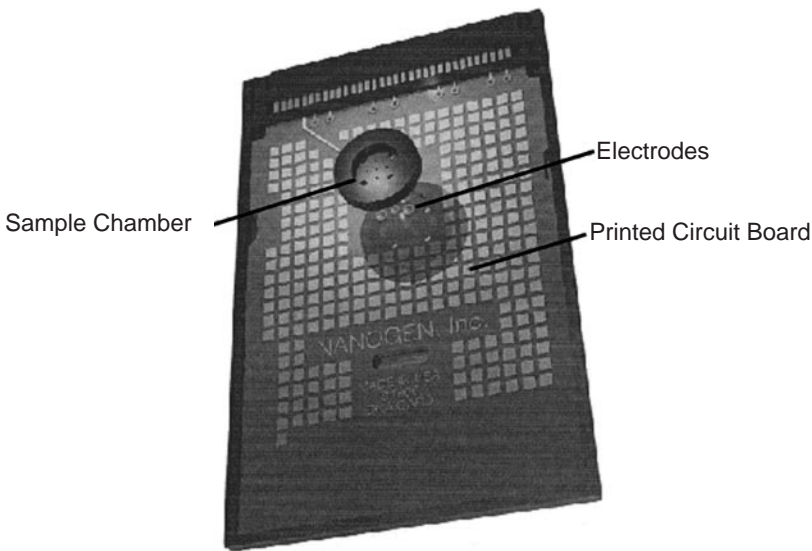


Fig. 9. Diagram of the complexity reduction device

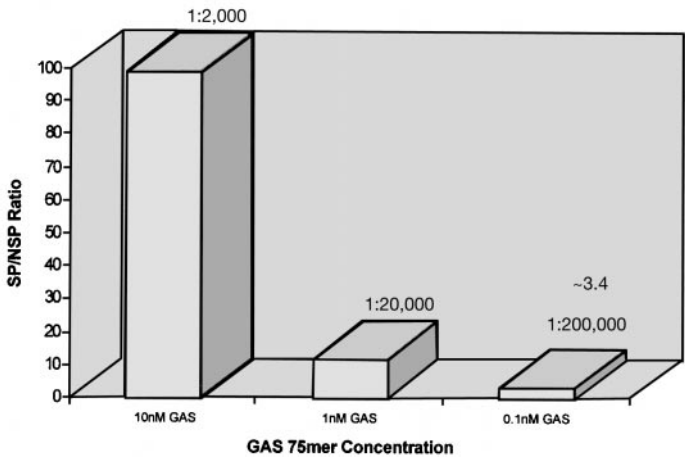


Fig. 10. Capture of a target sequence at different dilutions in human DNA

The device has been used to capture DNA sequences in very complex mixtures [45]. For the experiment shown in Fig. 10, a model target sequence consisting of a 75-mer based on a sequence from group A *Streptococcus pyogenes* (GAS) was synthesized and labeled with the fluorophore Bodipy Texas Red. In addition, the unlabeled complement to the 75-mer was synthesized. Equimolar amounts of the two oligonucleotides in amounts varying from 0.1 to 10 nM were combined with 2 μ g sheared and denatured human DNA with a final volume of

40 μl . Typically, we combined the target DNAs with a standard electrophoresis buffer such as $0.5 \times \text{TBE}$. A 48-mer complementary to the fluorophore-labeled 75-mer oligonucleotide was also attached to the derivatized polyacrylamide at some sites in the device to provide a specific capture probe. An unrelated oligonucleotide was attached to other sites to provide a control probe. Electronic hybridization was accomplished by adding the target solution and biasing the electrodes below the 200 μm diameter sites in a negative ramp mode from 50 to 5 μA for 90 s. After hybridization, the unhybridized DNA is driven from the hybridization sites by reversing the bias and then removed by replacing the hybridization solution with fresh buffer. It has also been shown that the signal from the hybridized target DNA may be released from the capture site by increasing the current level at the negatively biased electrode to 50 μA .

The signal at the hybridization site was detected by exciting the fluorophore with a 594-nm laser and collecting the emitted light through an objective lens and optical filters onto a cooled charge coupled device (CCD) camera connected to a personal computer with a frame grabber card. Signal levels were measured using an imaging program [43]. As can be seen from the graph in Fig. 10, the level of signal at the specific probe exceeded the signal at the nonspecific probe by over 3-fold when the weight ratio of human DNA to 75-mer was 200,000:1 [45]. At higher amounts of 75-mer, the signal strength at the specific probe was even greater relative to the signal at the nonspecific probe.

Electronic complexity reduction may provide an alternative method for sequence enrichment that is rapid, user-friendly and potentially quantitative. The device used in this experiment permits very high current densities and thus allows transport in buffers other than those typically used for electrophoresis. Beyond the use in complexity reduction, this device, with its ability to sustain high current densities, may have application in hybridization assays with a limited number of probes, immunoassays or other protein-binding reactions, and cell transport studies. Furthermore, the use of electrophoretic transport through all of the steps from sample processing through the assay should facilitate systems integration.

6 Conclusion

Progress in the development of on-chip sample preparation has been extensive and there are already devices that can isolate white cells from whole blood and isolate specific DNA sequences. In addition, the first step to integrating sample preparation with other analytical procedures, e.g. PCR, has been achieved, thus demonstrating the potential of totally integrated microfabricated analyzers.

7 References

1. Manz A, Graber N, Widmer HM (1990) *Sens Actuators B1*:244
2. Manz A, Harrison DJ, Verpoorte EMJ, Fettingner JC, Ludi H, Widmer HM (1991) *Chimia* 45:103
3. Cheng J, Fortina P, Sorrey S, Kricka, LJ, Wilding P (1996) *Molec Diagn* 1:183

4. Maniatis T, Fritsch EF, Sambrook J (1982) Molecular cloning: A laboratory manual. Cold Spring Harbour Laboratory, Cold Spring Harbor, New York, p 458
5. Johns MB Jr, Paulus-Thomas E (1989) *Anal Biochem* 180:276
6. John SWM, Weitzner G, Rozen R, Sriver CR (1991) *Nucleic Acids Res* 19:408
7. Buffone GJ, Darlington GJ (1985) *Clin Chem* 31:164
8. Miller SA, Dykes DD, Polesky HF (1988) *Nucleic Acids Res* 16:1215
9. Xu H-W, Jevnikar AM, Rubin-Kelley VE (1991) *Nucleic Acids Res* 18:4943
10. Jeanpierre M (1987) *Nucleic Acids Res* 15:9611
11. Kendall TL, Byerley DJ, Dean R (1991) *Anal Biochem* 195:74
12. Grimberg J, Nawoschik S, Belluscio L, McKee R, Truck A, Eisenberg A (1989) *Nucleic Acids Res* 17:8390
13. Thompson JD, Cuddy KK, Haines DS, Gillespie D (1991) *Nucleic Acids Res* 18:1074
14. Tilzer L, Thomas S, Moreno RF (1989) *Anal Biochem* 183:13
15. Thomas SM, Moreno RF, Tilzer LL (1989) *Nucleic Acids Res* 17:5411
16. Ma HW, Cheng, J, Caddy B (1994) *J Forensic Sci Soc* 34:231
17. Adeli K, Ogbonna G (1990) *Clin Chem* 36:261
18. McCormick RM (1989) *Anal Biochem* 181:66
19. Bard A (ed) (1994) Integrated chemical systems. Wiley, New York, p 324
20. Petersen KE (1982) *Proc IEEE* 70:420
21. Garfunkel E, Rudd G, Novak D, Wang S, Ebert G, Greenblatt M, Gustafsson T, Garofalini SH (1989) *Science* 246:99
22. Shoji S, Esashi M (1993) *Appl Biochem Biotechnol* 41:21
23. Sze SM (1988) VLSI technology, 2nd edn. McGraw Hill, New York
24. Fan L-S, Tai Y-C, Muller RS (1988) *IEEE Trans Electron Devices* 35:724
25. Shoji S, Esashi M (1995) In: van den Berg A, Bergveld P (eds) Micro total analytical systems. Kluwer Academic Publishers, Dordrecht, p 165
26. Jorgenson JW, Lukacs KD (1981) *Anal Chem* 53:1298
27. Seller K, Fan ZH, Fluri K, Harrison DJ (1994) *Anal Chem* 66:3485
28. Jacobson CS, Ramsey MJ (1996). *Anal Chem* 68:720
29. Jacobson CS, Ramsey MJ (1997) HPCE 97, January 26–30, Anaheim, California, USA
30. Raymond DE, Manz A, Widmer HM (1994) *Anal Chem* 66:2858
31. Müller T, Arnold WM, Schnelle T, Hagedorn R, Fuhr G, Zimmermann U (1993) *Electrophoresis* 14:764
32. Burns MA, Mastrangelo CH, Sammarco TS, Man FP, Webster JR, Johnson BN, Foerster B, Jones D, Fields Y, Kaiser, AR, Burke DT (1996) *Proc Natl Acad Sci USA* 93:5556
33. Olsson A, Stemme G, Stemme E (1995) *Sens Actuators A* 46–47:549
34. Bevan CD, Mutton IM (1995) *J Chromatogr A* 697:541
35. Bevan CD, Mutton IM (1995) *Anal Chem* 67:1470
36. Löchel B, Maciossek A, Quenzer HJ, Wagner B, Engelmann G (1995) *Sens Actuators A* 46–47:98
37. Wilding P, Pfahler J, Bau HH, Zemel JN, Kricka LJ (1994) *Clin Chem* 40:43
38. Kricka LJ, Wilding P, Cheng J (1997) HPCE 97, January 26–30, Anaheim, California, USA.
39. Cheng J, Shoffner MA, Hvizhia GE, Kricka, LJ, Wilding P (1996) *Nucleic Acids Res* 24:380
40. Volkmuth WD, Austin RH (1992) *Nature* 358:600
41. Southern E (1975) *J Mol Biol* 98:503
42. Heller MJ, Tu E (1995) International Patent Publication Numer: WO 95/12808
43. Heller MJ (1996) *IEEE Engineering in Medicine and Biology March/April*:100
44. Sosnowski RG, Tu E, Butler WF, O'Connell JP, Heller MJ (1997) *Proc Natl Acad Sci USA* 94:1119
45. Sheldon, EL (1996) NIST-ATP Workshop on Tools for DNA Diagnostics, September 9, Gaithersburg, Maryland, USA

Microreactors for Chemical Synthesis and Biotechnology – Current Developments and Future Applications

W. Ehrfeld · V. Hessel · H. Lehr

Institut für Mikrotechnik Mainz GmbH, Carl-Zeiss-Str. 18–20, D-55129 Mainz-Hechtsheim, Germany

The modern methods of three dimensional microfabrication have lead to the development of extremely miniaturized chemical and biotechnological systems. These so called microreactors represent novel approaches in respect of production flexibility and chemical reactions not yet applied in chemical processing. This has stimulated world-wide research in this field so that the technical feasibility of such devices has been demonstrated in the laboratory scale.

Microreactor technology has developed to such an extent that a wide variety of microreactor components, e. g. micropumps, mixers, reaction chambers, heat exchangers, separators and complete integrated microreaction systems with process control units have been fabricated using the appropriate microfabrication process and materials that are suitable for specific applications.

Keywords: Microreactors, microsystems, LIGA technique, chemistry, biotechnology.

List of Abbreviations	234
1 Worldwide Activities in the Field of Microreactors	234
2 Definitions of Microreactors	235
3 Microreactor Components and Integrated Systems	238
3.1 Micropumps and -valves	238
3.2 Micro Heat Exchangers	238
3.3 Micromixers	240
3.4 Microseparators	243
3.5 Micro Reaction Units	244
3.6 Integrated Microreaction Systems	245
4 Major Applications of Microreaction Systems	245
4.1 Microreactors for Chemical Production	246
4.2 Microreactors for Mass Screening	247
5 Fabrication Techniques and Materials for Microreaction Systems	248
6 Conclusions	248
7 References	250

List of Abbreviations

ACHEMA	Ausstellungstagung für Chemisches Apparatewesen, Frankfurt, Germany
AGIE	AGIE, Losone, Suisse
AIChE	American Institute of Chemical Engineers
BASF	Badische Anilin und Soda Fabrik, Ludwigshafen, Germany
DECHEMA	Deutsche Gesellschaft für Chemisches Apparatewesen, Chemische Technik und Biotechnologie e.V., Frankfurt, Germany
DMST	Abteilung Mikrosystemtechnik (Department of Microsystem Technology), Technische Universität Ilmenau, Germany
DUPONT	DuPont de Nemours, Wilmington, USA
IMM	Institut für Mikrotechnik Mainz GmbH, Germany
ISFET	Ion Sensitive Field Effect Transistor
KFK	former Kernforschungszentrum Karlsruhe, present: Forschungszentrum Karlsruhe (FZK), Germany
LIGA	Lithographie, Galvanoformung, Abformung
μTAS	Micro Total Analysis Systems
PNNL	Pacific Northwest National Laboratory, USA

1

Worldwide Activities in the Field of Microreactors

In the last two decades powerful tools have been developed for the fabrication of microdevices [1–3]. This led to the miniaturization of mechanical, optical, thermal and fluidic components. Recently, micromachine technologies are also being applied for synthetic and screening purposes in the field of microreactors [4–13]. Main achievements of this vivid development have been made in Europe and the United States [8]. In Europe research groups and industry are especially active in Great Britain, Denmark, France, Belgium and Germany [14]. In the United States most of the developments have been made by institutes, e.g. Redwood Microsystems or the Pacific Northwest National Laboratory (PNNL), to mention only two. In the Far East, especially in Japan, founding programs for microsystem technology of large financial volume have been started [8]. However, these activities are more related to fields different from microfluidic applications.

Although some components of microreactors, e.g. micropumps [15] and miniaturized analytical systems [16, 17] have been described much earlier, a systematic development and fabrication of components and integrated systems for chemical synthesis started only 3 or 4 years ago [18]. While the development was mainly initiated by research institutes [18], considerable interest is meanwhile found in the chemical and pharmaceutical industry [19]. This is not only manifested by joined projects between institutes and industry, but, moreover, by first microreaction systems which are currently under commercial investigation in industry [19]. A first national conference (with many international contributions) which dealt with microreactors for chemical and biological applications was jointly organized by IMM and DECHEMA (the German equivalent of AIChE) already in 1995 [18]. In 1996 a session of the Spring National Meeting of

the AIChE was related to microreaction systems [8]. The first international conference about microreactors was held in 1997, again under the leadership of IMM and DECHEMA. Microreactors were selected as a separate topic on the AIChE (June 1997), the German exhibition of chemical technology.

2

Definitions of Microreactors

The term microreactor has actually been used a long time before microtechniques were applied for microfluidic purposes [20]. Small fixed bed reactors with typical dimensions in the centimeter range were termed microreactors and used to probe reactions under process conditions similar to those in macroscopic reactors. These reactors were fabricated by conventional mechanical engineering techniques and are still a powerful tool in chemical engineering, e.g. in fluid catalytic cracking. Thus, from the very beginning, investigations of miniaturized reactors were believed to give important data for the control of large-scale processes [21].

Miniaturization of chemical and biological systems started in the last decade with the development of a number of microanalytical systems. These devices combine sensors, actuators and microfluidic elements to create micro total analysis systems (μ TAS). The subject has been treated in a series of conferences held every two years [16, 17]. Main goals were the fabrication of systems which needed reduced amounts of expensive chemicals due to miniaturization and integration of several subunits. Further interest concentrated on the favorable use of surface phenomena for an increase in sensitivity and gain in analysis time per sample due to parallelization or use of different process regimes. Only two among a huge number of these devices are mentioned here: the group of N. Rooij developed biological reactors which were applied in outer space [16]. Miniaturized micro electrophoresis chips were built by several groups, e.g. by Widmer, Manz and colleagues [22] and by Mathies [23, 24]. One main effect of chip miniaturization is the decrease of heat release, the so-called Joule effect, by enhanced heat flow which led to much shorter analysis times still at a high resolution due to higher voltages achievable [24].

While a big scientific community has been established for analysis systems (such as μ TAS), the interest in research on synthesis and screening systems is relatively new and only identified around three years ago [17]. It is still a very vivid and open circle whose industrial part has significantly increased during the last two years [19]. Nearly all chemical companies are at present more or less involved in this development.

Microstructures which are used in this context will be termed microreactors in the following (a more precise definition is given below and in the next chapters). It should be emphasized that microreactors are not constrained to microscopic sizes (nor to minuscule processing rates) as first outlined by Wegeng [8]. His precise definition of microreactors is repeated here:

“Components and systems that exploit engineered structures, surface features or dimensions that are typically measured in terms of microns (one millionth of a meter) to hundreds or thousands of microns, and that may include microelectronic components as an integral part of the system”.

The most remarkable point of this definition is the conclusion that, in contrast to many analytical systems, not all lateral dimensions along the axis of flow have to be in the μm range, but only some of them as much as it is demanded by the application desired. Actually, in today's microreactors a number of small microchannels are often connected to a common large feed stream (principle of manifolding or partitioning [7]). This combination of very small and large units requires a high technological flexibility which needs the application of both microfabrication and precision engineering techniques. The parallelization of microchannels leads to a high throughput which is needed in synthetical rather than in analytical applications [8, 25]. Parallelization is often accompanied by a shortening of the flow axis in order to keep the pressure drop as low as possible, if this is allowed by the kinetics of the process [8]. Indeed, a micromixer array developed at IMM utilizes both effects and can be operated at a flow rate of up to 3 l/h while still maintaining good mixing quality [26]. However, reactions running at this high speed have to be necessarily fast, otherwise the length of the miniaturized part has to be increased with the consequence of reduced flow rates. Having this in mind, three categories of process regimes can be defined which correspond to different types of microreactors:

1. In the regime of fast single reactions continuous flow systems with relatively short miniaturized paths will be used.
2. In the regime of slow single reactions semi-batch systems including valves will be adequate.
3. In the regime of multiple parallel reactions, either fast or slow, semi-batch systems similar to titer plates have to be developed which are connected to microdispensing systems and separation/analysis units (Fig. 1).

Microreactor components of types 1 and 3 have been developed in a number of cases [8]. Those of type 2 have not been realized to our best knowledge. However, future developments will certainly move into this field, since the majority of reactions, in particular those in liquid media, are of that type.

Microreactors can not only be characterized by the types of reactions and process regimes they address. In addition, a task definition should be given which determines the complexity of the systems and, therefore, what kind of functions are provided (see Fig. 1). The simplest subsystems are microreaction components which correspond to a single operation. Most often these are unit operations which e.g. perform mixing, heat exchange, reaction, separation and others. The majority of present microfluidic structures actually belong to this group [5]. Since usually more than one (unit) operation is necessary to result in a net effect, individual microreactor components are mainly used to serve as demonstration units. Heat transfer coefficients and heat fluxes have been determined for this purpose, e.g. by temperature measurements of hot and cold solvent streams passing through micro heat exchangers [5]. The quality of mixing has been analyzed in micromixers by standard reactions which have originally been developed for the characterization of macroscopic vessels, e.g. neutralization reactions yielding a change of color [9, 27] or, much more elaborated, concurrent reactions which are affected by local changes of mixing quality [26].

Phenomenological Definition of Microreactors

- | | |
|---|---|
| 1) Microreactors for fast single reactions | Continuous flow systems with relatively short miniaturized paths |
| 2) Microreactors for long single reactions | Semi-batch systems including valves |
| 3) Microreactors for multiple parallel reactions, either fast or long | Semi-batch systems similar to titer-plates connected to microdispensing systems and separation/analysis units |

Functional definition of microreactors

- | | |
|--|--|
| 1) Microreaction components | Single (unit) operation, e.g. mixing, heat exchange, reaction, separation |
| 2) Integrated microreaction systems for single reactions | Single reaction with several (unit) operations → System with several components in fixed sheets |
| 3) Integrated microreaction automats for multiple-step reactions | Multiple reaction with several (unit) operations → System with several components in flexible sheets |

Fig. 1. Different types of microreactors: Functional definition of microreactors

However, some of these microreaction components may be successfully applied for specific purposes, e.g. for the production of colloidal particles whose precipitation process is sensitive to mixing or for the preparation of emulsions for cosmetic industry.

In the majority of applications, more complex systems have to be constructed which will be termed integrated microreaction systems [8, 29]. Here, components are assembled to form a complete and complex unit so that macroscopic channels are only found at the end and beginning of the whole system, while fluidic channels in the system show diameters in the μm -range. These devices can be regarded as microscopic analogues of typical laboratory equipment such as three-necked flasks connected to coolers, distillers and drop funnels. First integrated systems have been realized by PNNL, IMM and DuPont by a sandwich-type arrangement of microstructured sheets [7, 8, 28]. Each of these integrated systems is especially designed for one single reaction so that the microstructured units are fixed. Although structural details may be varied by the exchange of sheets, the reactors are still confined to one purpose. Designs different from sheet architecture have also been realized, mainly for μTAS applications. Fiehn proposed a fluidic ISFET microsystem (FIM) based on a planar integrated system [29]. Also, alternatives with reversibly mounted components perpendicular to the substrate have been presented [30]. Finally, van den Berg developed a so-called mixed circuit board (MCB) containing the fluid channels as well as the electronic circuitry in combination with the silicon-based fluidic components (modules) [31].

Even more complex systems will be given by integrated microreaction systems for multiple-step reactions. They will be composed of flexible sheets which may be divided into classes each representing a homologous series of components. Thus, similar to the series of flasks with variable sizes of 25, 50,

100 and 250 ml, micromixer sheets with variable dimensions of lamella and lengths of mixing zone may be part of such systems. However, this demands a standardization for interconnection (similar to that for laboratory equipment).

If microreactors, either as components or integrated systems, will run in parallel as an array, new solutions for feeding or dispensing systems have to be developed. This is also true for the process control of a large number of product streams which will be a challenge for realization. Tomorrow's answers to these questions will determine which type of microreactor will be favored and will specify the major applications, either simulation of processes, synthetic production or mass screening.

3

Microreactor Components and Integrated Systems

In order to introduce the basic microreactor components this chapter gives an overview of some important developments which have been achieved in the last five years, instead of presenting a comprehensive survey of the whole field of microreactor technology. Different components and their applications are discussed, also leading to a characterization of their efficiency for synthetic applications.

3.1

Micropumps and -valves

Micropumps and -valves were the first components to be explored on a large scale. They were fabricated with or without moving mechanical parts [8]. Active pumps contain a diaphragm which is actuated by electrostatic, piezoelectric, electromagnetic or electro-thermopneumatic forces resulting in a constant volume displacement with each stroke. Although many of these pumps have been designed for purposes different from those discussed here, e.g. for medical applications, some of them may be applied as components in microreactors depending on their flow rate, cycle time and pressure accessible. Wegeng attributes electro-thermopneumatic actuators with the highest force output and the capability of extremely short cycle times (from 10^{-3} to 10^{-5} s) [8, 32]. Typical flow rates published for a number of micropumps are in the range of 10–500 $\mu\text{l}/\text{min}$ [33–39]. Higher pump rates were reported for a bi-directional pump (about 800 $\mu\text{l}/\text{min}$) [40, 41]. Still higher rates of 14,000 $\mu\text{l}/\text{min}$ were found for a valveless diffusor-nozzle micropump [42] and an electro-hydrodynamic (EHD) micropump with 16,000 $\mu\text{l}/\text{min}$ [43]. A microvalve delivered by Redwood Microsystems even withstands a backpressure of 67 bar [8] (Fig. 2).

3.2

Micro Heat Exchangers

Micro heat exchangers were expected to give enhanced heat transfer in chemical reactions, e.g. in order to control undesired reactions. Wegeng and Ehrfeld attribute the main potential of miniaturized heat exchangers to the minimization of

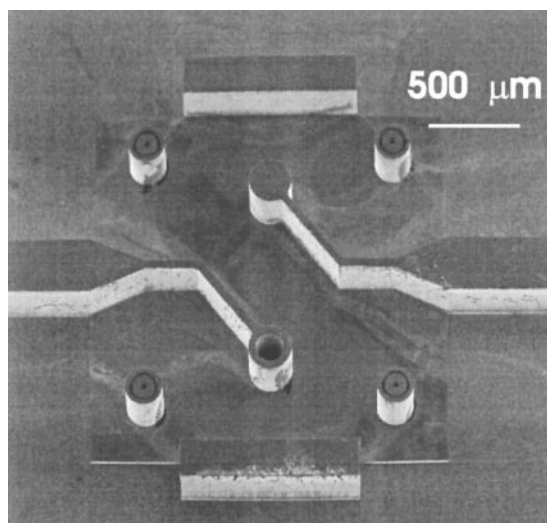


Fig. 2. Mold insert in nickel for membrane micropump made by LIGA technique using multiple irradiation

local temperature changes in case of exo- and endothermic reactions, thus yielding essentially isothermal conditions [8, 25]. While tube-like micro heat exchangers have been reported to be applied as components in integrated systems by IMM [44], planar sheet architectures have been favored in other cases [8, 45].

For the design of micro heat exchangers, it has to be considered that both heat and mass transport time-scales are strongly correlated with the characteristic dimensions of the exchanger according to diffusion theory [8, 9]:

Heat transport: $t \sim d^2/\alpha$

Mass transport: $t \sim d^2/D$

(t : time-scale, d : channel width,

α : thermal diffusivity of fluid, D : mass diffusivity)

Taking into account typical numbers for α and D , this underlines that the channel width should be considerably smaller than 1 mm (1000 μm) in order to achieve short residence times. Actually, heat exchangers of such small dimensions are not completely new, because liquid cooled microchannel heat sinks for electronic applications allowing heat fluxes of 790 watts/cm^2 were already known in 1981 [46]. About 9 years later a 1 cm^3 cross flow heat exchanger with a high aspect ratio and channel widths between 80 and 100 μm was fabricated by KFK [10, 47]. The overall heat transport for this system was reported to be 20 kW. This concept of multiple, parallel channels of short length to obtain small pressure drops has also been realized by other workers, e.g. by PNNL and IMM. IMM has reported a counter-current flow heat exchanger with heat transfer coefficients of up to 2.4 $\text{kW}/\text{m}^2 \text{ K}$ [45] (see Fig. 3).

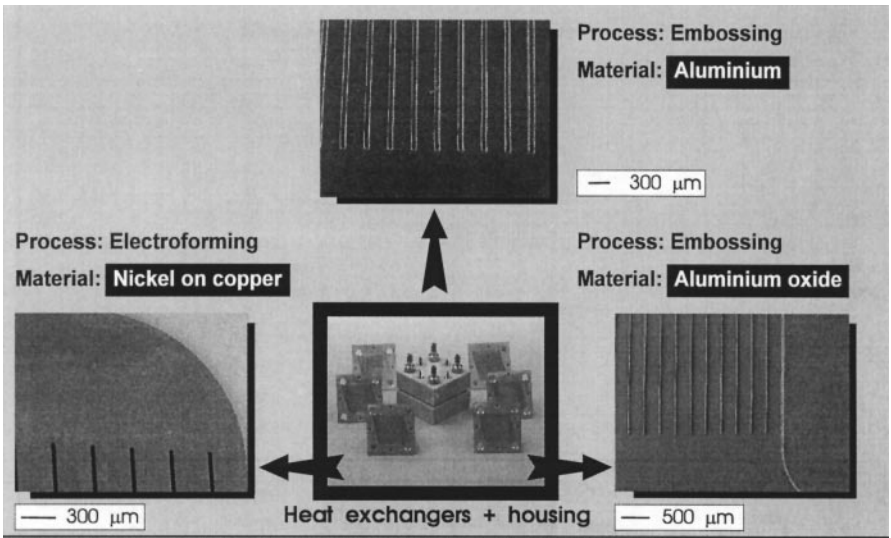


Fig. 3. Miniaturized plate-type heat exchanger fabricated by LIGA technique and housing. Structural height: 300 µm, Materials: Nickel on copper, aluminum oxide and aluminum. The aluminum oxide and aluminum heat exchangers were realized by embossing with embossing tools. In the first case an embossing tool in nickel on copper was used which was realized by electroforming. In the second case the embossing tool in stainless steel was fabricated by die sinking with LIGA electrodes

This number is comparable to that of macroscopic heat exchangers with fins. PNNL designed similar structures and different ones with pins resulting in a heat transport of up to 100 W/cm² and heat transfer coefficients of 10–35 kW/m² K at low pressure drops of about 0,13–0,20 bar [8, 48]. The channel widths and depths were varied in a relatively huge range from 50 to 1000 µm and the lengths were in the order of several centimeters. Not only single-phase flow experiments were performed, but also evaporative and condensing flow cases have been realized. The high performance of evaporative micro heat exchangers has also been demonstrated by other authors [49].

3.3 Micromixers

Different types of static mixers have been reported which nearly all use the principle of multi lamination to achieve fast mixing via diffusion [5, 8, 9, 27, 28, 44, 45]. The flow regime in microreactors is laminar in almost all cases due to small channel dimensions so that diffusion is the only mechanism which contributes to mixing, while convective segmentation mechanisms as found in the turbulent regime are absent. An intermediate region with Reynolds numbers between 2 and 100 exists where inertia forces assist segmentation [9]. Apart from that, the subdivision of laminar sheets by means of geometric constraints

(=changes in the dimensions of the microchannels) is the only solution to achieve mixing in microreactors. This is to be compared with stirring and creation of turbulent flow which are the most prominent ways to achieve good mixing in macroreactors. Different concepts have been reported for microreactors, including the direct subdivision of the channel size by splitting [2] the main stream into a large number of substreams or other indirect means, e.g. multiple splitting, drilling or bending which are based on a separation-reunification mechanism [5, 8, 9, 27, 28, 44, 45] (see Fig. 4).

Drilling and bending mechanisms regenerate the original channel geometry before reunification so that a multiple repetition of the separation step can be performed. Thereby, the widths of the lamellae are halved in each consecutive step. In the case of direct subdivision the width of the lamella depends on that of the channel, although repeating steps may be included, too.

It was pointed out by different authors that these mechanisms allow a mixing in a time interval considerably shorter than 1 s [4, 8, 9]. This mixing time t is proportional to d^2/D , d being the width of the channel and D the mass diffusivity [9]. Thus, the reduction of the channel width strongly influences the quality of

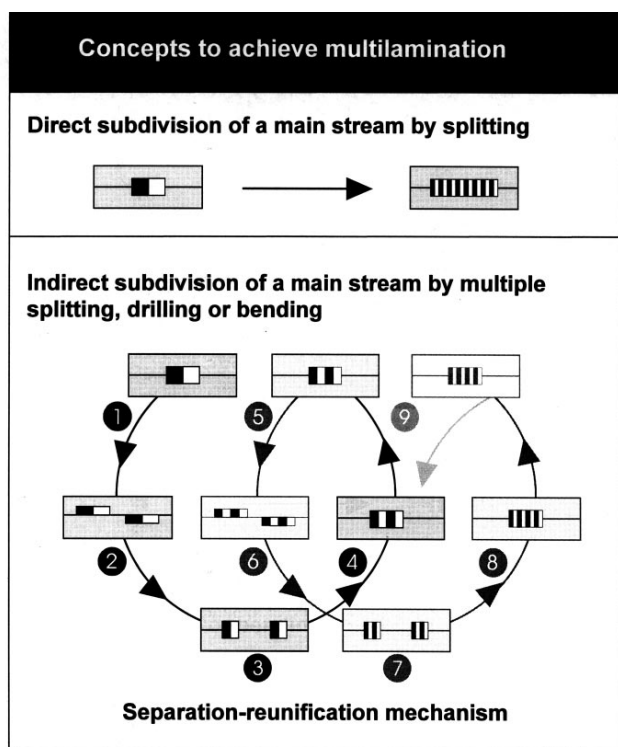


Fig. 4. Concepts to achieve multilamination: Direct subdivision by splitting of a main stream and indirect methods by splitting, drilling or bending based on separation-reunification mechanisms

mixing. Channel widths reported for microstructures made by silicon micro-machining and LIGA technology were in the range of 20 to 50 μm which allow complete mixing in a time-scale of approximately 100–300 ms. Although this time-scale seems to be rather short, one has to consider that for velocities of about 0.1 m/s (which is high, but still typical for reactions in microreactors) an according channel length results of 10,000–30,000 μm for complete mixing! This also defines the minimal length of the passage through a heat exchanger in case of exothermic reactions with heat release after mixing.

These crude estimations determine the distance between mixer and heat exchanger (if not directly embedded) which should be smaller than about 1000–3000 μm corresponding to 10% of the overall mixing length. This simple calculation exhibits two important issues of future development work: The channel dimensions have to be minimized to achieve a better mixing condition. Mixer and heat exchanger have to be part of an integrated system for effective mixing in the subsequent heat exchange step. A negative effect of the reduction of the channel widths is certainly a decrease of the overall flow. This may be overcome by a parallel arrangement of mixing units in arrays and high aspect ratios to increase the depth of the channels. These requirements are easily met applying LIGA technology as well as micro spark erosion techniques. Another aspect of the so-called vertical lamination of LIGA technology is the lower pressure drop compared to that of mixers based on horizontal lamination such as silicon microstructures made by wet etching technologies [9]. The length of typical silicon mixers ranges between 3000 and 10,000 μm [9, 27], while the

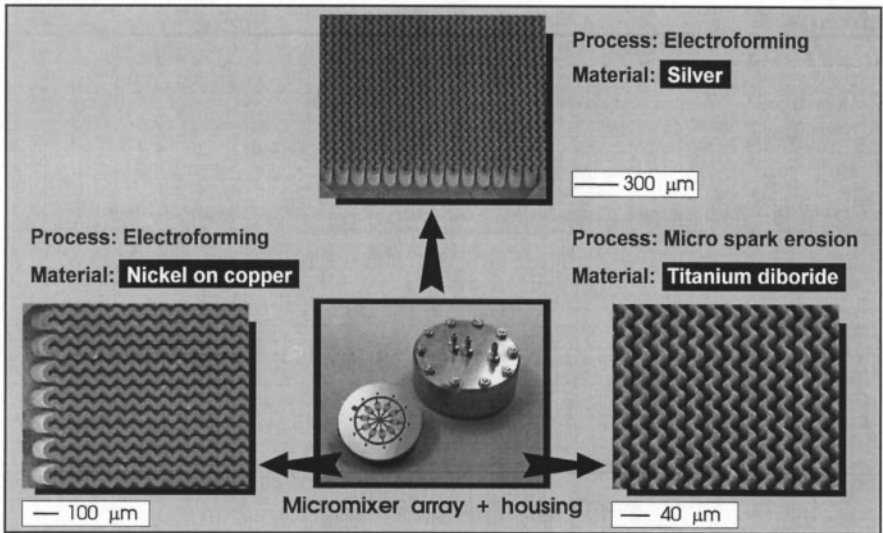


Fig. 5. Single mixer and micromixer array in nickel on copper fabricated by LIGA technique and housing. Channel width: 40 μm , Materials: Nickel on copper, silver and titanium diboride. The silver and nickel-on-copper micromixers were realized by electroforming, the titanium diboride micromixer was fabricated by die sinking with LIGA electrodes

length of LIGA type mixers can be less than 300 μm [45] resulting in a higher throughput (up to 3 l/h compared to 10–600 $\mu\text{l/h}$). Thus, the field of applications for LIGA mixers is at present completely different from that of silicon mixers. The latter were designed for μTAS applications, while the former meet the requirements of synthetic processes.

Silicon-type mixers using the separation-reunification principle have been reported by PNNL [8], Danfoss [9] and DMST [27]. Polymeric analogues made by LIGA technology have been reported by IMM [25] (see Fig. 5).

The quality of these mixers was characterized by ultrafast acid–base reactions which prove a certain degree of mixing by a change of colour indicating a change of pH [8, 9]. These experiments led to important information for the feasibility of the systems, but hardly resulted in any quantitative data. Since the concentration of acids and bases vary in each publication and are sometimes not reported in detail, the degree of mixing associated with the colour change is different for each system which limits the comparability of the results. Furthermore, first experiments to disperse gas and liquids as well as immiscible liquids have been reported [27].

A mixer based on the principle of direct subdivision was fabricated by IMM [5, 45]. This LIGA-type mixer is available as single units as well as mixer arrays

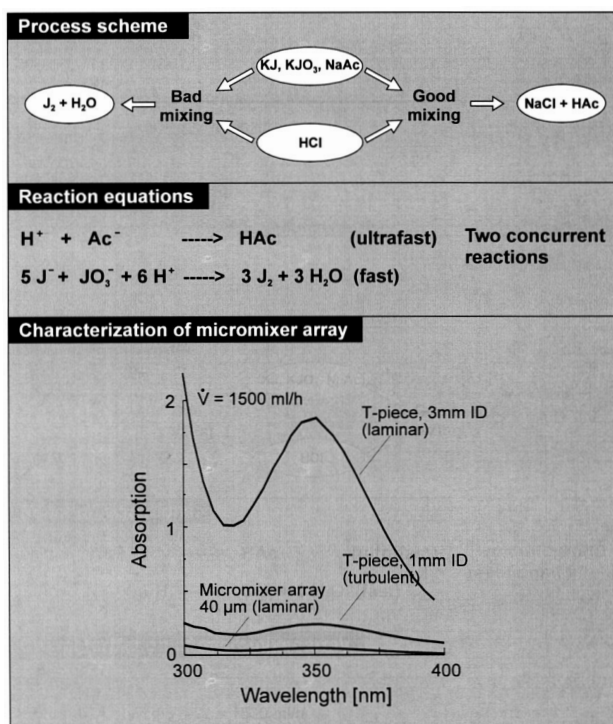


Fig. 6. Test reaction and characterization of mixing in the micromixer array

with 10 mixing units. The parallelization allows a flux of up to 3 l/h. The LIGA-type mixer was recently characterized by a modified reaction which was originally applied for the analysis of mixing in batch macroreactors [26]. Two concurrent reactions take place: An ultrafast acid-base reaction between an acid and sodium acetate and a fast redox reaction between iodide and iodate ions yielding iodine whose concentration can be determined by UV-vis spectroscopy. In the case of perfect mixing the ultrafast reaction dominates the fast one so that no iodine can be observed. Instead, incomplete mixing leads to local concentration changes of the solutions to be mixed, so that the fast reaction takes place parallel to the ultrafast one. The concentration of the iodine can hence be used as a quantitative indicator of the degree of mixing. Experiments with the micromixer array prove good mixing quality over a huge range of flux (250–3000 ml/h). The mixing is better than in reference systems, namely stirred and non-stirred batch macrosystems and T-pieces with a turbulent and laminar flow regime as analogues for continuous flow macrosystems. The authors expect for single mixing units even better results, since the reaction is not only sensitive to local concentration changes, but also to changes which result from distribution problems of the main stream to the single units which are only present in an array. (See Fig. 6)

3.4

Microseparators

Microseparation units make use of the enhancement of mass transport between different phases. PNNL workers reported a microchannel gas-liquid contactor

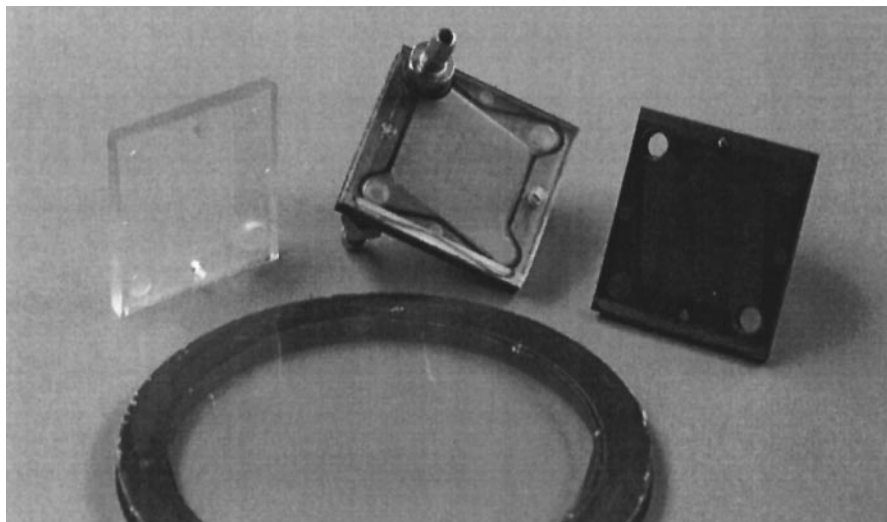


Fig. 7. Demonstration unit of a membrane module with a dense, thin polymeric membrane and polymeric microstructured support

and performed proof-of-principle measurements for the absorption of ammonia in water at high absorption rates [8]. This allows the integration of absorber and heat exchange units in integrated systems. The same group developed a miniaturized solvent extractor in which a large contact area between feed and solvent is created and rapid mass diffusion is achieved due to the reduction of channel width. Extractors have also been reported by CRL and IMM. In the first case the contact area between the two fluids is limited by a partial overlap of the channels, while in the latter case this area is defined by a separating wall with microstructured openings. First demonstration units for membrane modules with dense, thin polymeric membranes on microstructured polymeric supports have been fabricated by IMM. The individual parts have been interconnected by laser welding techniques. These parts and the assembled microsystem are shown in Fig. 7.

3.5

Micro Reaction Units

Examples of reactor components containing a catalyst are rare at present. Again, the PNNL group designed a microchannel combustor/evaporator [8]. In a prototype version the combustion of methane has been demonstrated. The thermal energy due to the reaction has been removed in the evaporator unit and heat flow rates of 25 W/cm² have been obtained. Glucose oxidase enzyme reactors with immobilized enzymes at the microchannel surfaces are another example of reactors containing heterogeneous catalysts [50], although the application field, namely biotechnology, is completely different from that of gas phase reactions.

3.6

Integrated Microreaction Systems

The development of integrated microreaction systems is only at its very beginning. The general goal so far was the integration of as many components as possible in a limited number of sheets which are assembled. First systems made of silicon have been reported by DuPont and were used for chemical processing of several reactions [7]. IMM fabricated an integrated system utilizing photoetchable glass whereby static mixers and heat exchangers have been realized [28]. Recently, an integrated system made from a special alloy has been fabricated in a close co-operation between BASF, AGIE and IMM [19] (see Fig. 8).

This system includes several mixing and heat exchange units. A concept for an integrated, microtechnology-based fuel processor was proposed by PNNL [8]. As examples for unit operations which may be included in future integrated systems the same publication mentions reactors for steam reforming and/or partial oxidation, water–gas shift reactors and preferential oxidation reactors for carbon monoxide conversions, heat exchangers, membranes or other separation components.

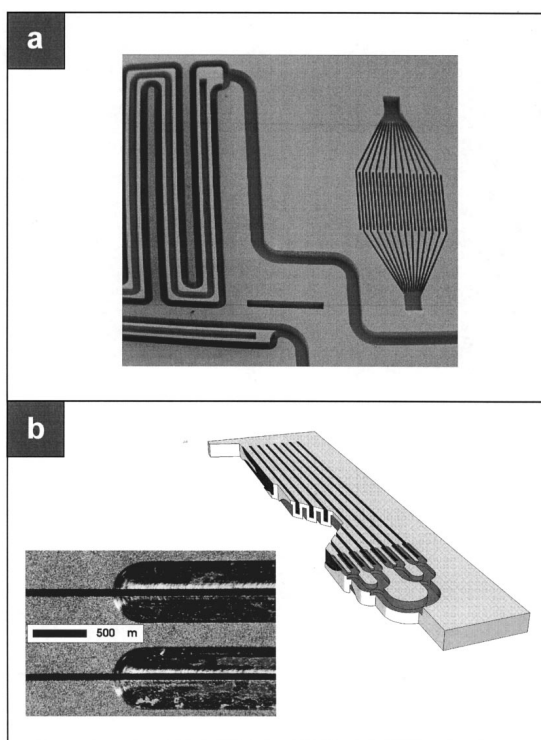


Fig. 8. Integrated microreaction system containing mixing units and heat exchangers: **a** Integrated system in photoetchable glass made by photolithography and wet etching. **b** Detail of an integrated system in a special alloy made by micro spark erosion (EDM-grinding)

4

Major Applications of Microreaction Systems

The activities are at present related to two major topics, namely chemical production and mass screening [3, 8, 25]. While miniaturization in the first field focuses on new process regimes due to enhanced heat and mass transfer, the second field of application results in an increase of reaction and detection units per reactor volume. Thus, miniaturization – the reduction of characteristic dimensions – directly influences the process performance in the first case, while in the last case this is only indirect by an increase in flexibility and multiplicity.

4.1

Microreactors for Chemical Production

Although there are only few examples of microreactors used for chemical production future developments may be subdivided into three classes: First, micro-

reactors which will be used to simulate large-scale processes, e.g. by providing new process regimes. Other applications will aim at production by parallelization of several units which may be used to realize new processes or the mobile and flexible production in the frame of existing processes. The latter aim has not been reached until now. However, first integrated systems have been built for simulation purposes and investigations of these systems are under way. These systems enable the investigation of completely new reaction regimes which are either unrealizable on a macroscopic scale or principally realizable, but not feasible (due to various technical restrictions in macroscopic reactors), e.g. safety problems due to strongly exothermic reactions. In addition to process performance, automation offers an additional advantage of microreactors. Miniaturized continuous flow systems allow the study of reactions on a very short time-scale. Thus, their range of accessible process variations will supplement or even exceed that of conventional equipment.

A second field of application may be in the on-site and on-demand production [3, 8, 25]. A number of chemicals, especially those which are explosive or toxic, can not be efficiently produced at present on a medium or small scale, although large-scale processes exist. A parallelization of several microreactor units could synthesize flexible amounts of chemicals and may even allow a transport of the reaction units if desired.

The exploration of new process regimes is tightly correlated to the task of chemical production [3, 8, 25]. Microreactors will then not only serve to investigate processes of macroreactors under “ideal” or otherwise not feasible conditions, but are expected to partially replace macroreactors for different applications. An example for a reaction which can hardly be achieved even on a laboratory scale is the direct fluorination of aromatics.

4.2

Microreactors for Mass Screening

Chemical activities in the field of mass screening are often related to combinatorial chemistry [51, 52]. One major goal, especially in the field of solid phase chemistry involving polymers like DNA or peptides, aims at the increase in the number of compounds per reactor volume and time. Commercially available microtiter plates are established as reactors in this case whereby robotic feed systems fit perfectly to their dimensions. A drastic reduction of reaction volume and increase in number of reaction vessels (“wells”) leads to the so-called nanotiter plates (e.g. with 3456 wells). Microfabrication methods such as the LIGA process are ideal means for the cost effective fabrication of nano-titer plates in polymeric materials by embossing or injection molding techniques so that inexpensive one-way tools are realized.

A further dramatic increase in the number of wells requires new types of feeding systems. While many robotic feed systems are still oriented on macroscopic analogues, new approaches which are adapted to the microdimensions of the overall system need to be developed. Further challenges are posed by the redistribution of volumes smaller than drops and the prevention of significant evaporation of the solvent. This will again lead to major changes of feed systems

and calls for wells with high depth, hence for microfabrication techniques with high aspect ratios. Furthermore, surface effects like adsorption may become more and more important in this regime.

In addition, fully automated systems have to be constructed which combine the synthesis of the molecules to be tested and the subsequent screening of these molecules. Still a few non-automated steps are established in industrial research due to the absence of suitable tools.

The reduction of sample size calls for an improvement of detection sensitivity. Optical detection methods have been most commonly applied in most cases. However, fluorescence detection will still gain more importance due to the higher sensitivity of this technique. An interesting approach is the combination of reaction vessels and testing cells. One solution is the incorporation of microlenses below the wells which allow a detection "on-site". Highly sensitive methods may be also obtained by the use of miniaturized electrochemical detection systems.

5 Fabrication Techniques and Materials for Microreaction Systems

None of the existing microfabrication techniques available cover the complete range of materials which might be of interest in the present case. The choice of the microfabrication method therefore selects the material to be applied and determines the range of temperature, pressure or solvents for the application. Material selection is therefore important when new applications of microreactors are envisaged.

State of the art materials for microreactors are silicon, glass and polymers. Metals, stainless steel, special alloys or ceramic materials for microfluidic applications have been recently introduced and will certainly gain much more attention in the future, if further improvements of the corresponding fabrication techniques occur. Although polymeric materials are ideal candidates for most biological applications, their potential for chemical processes will be strongly related to the finding of chemically inert and thermally stable polymers which can be injection molded and assembled by suitable techniques. Ceramic materials have, so far, not been largely used for microfluidic applications. The development of suitable structuring and assembly techniques, especially those which allow mass fabrication (e.g. injection molding), is still at its infancy. In particular, high temperature gas phase reactions will demand ceramic materials as the only choice for certain processes.

6 Conclusions

The process of wet-chemical etching of single-crystalline silicon was the first process suitable for the mass fabrication of micromechanical components [53]. Simple geometric structures like grooves, channels or membranes have been incorporated in microreactor components such as pumps, valves, static mixers and (most often) analytical devices. Bonding processes, either thermally or

anodically, allowed the build-up of microreactors with sheets of silicon connected to silicon or glass layers.

Silicon is undoubtedly the material which has been most often applied for microfluidic applications, especially in the field of analysis systems. Detailed information has also been obtained for a number of microreactor components and some of them are already commercially available. Even more striking, first experiments with integrated systems have been reported by DuPont [8]. However, silicon components did not find a broad use in industrial applications, especially in the field of synthetic chemistry. For this purpose, future developments have to address a broader variety of components than those mentioned above, including e.g. heat exchangers, extractors and others, and the feasibility of the fabrication of integrated systems has to be demonstrated in more detail.

Highly anisotropic removal of material is given by dry etching processes using directed ions from a low pressure plasma or an ion beam generated at high vacuum. The applicability of dry etching is much less hindered by geometrical and materials choice restrictions compared to wet chemical etching processes. In addition, high resolution and high aspect ratios are characteristic features of this process. The potential of dry etching for the fabrication of microreactors has not been largely exploited so far, but may gain more importance in the future.

LIGA and its related techniques are based on a sequence of process steps combining (deep) lithography [3, 54, 55], electroforming [56] and molding [57]. Characteristics of this process allow the possibility of fabricating microstructures with high precision, high surface quality and high aspect ratios using a wide variety of materials ranging from metals, metal alloys and ceramics to polymers.

Several polymeric or metallic microreactor components like pumps, static mixers and heat exchangers have been realized by LIGA- or laser-LIGA-techniques [58]. Feasibility experiments, either internally or in cooperation with industry, have been already performed or are under way. The fabrication of integrated systems has not been reported so far. Two major arguments for an ongoing development of LIGA-type microreactors are inexpensive mass fabrication of polymeric components by injection molding and improvements in the preparation of ceramic green tapes for tape casting and ceramic powders for injection molding which will allow to introduce this material for microreactor applications [59].

Microstructuring of glass can be performed by standard lithographic methods [23] or by a special variant of this process using wafers made of a special photosensitive glass (FOTURAN) [60]. Major advantages of glass for chemical and biochemical microreactors are its material properties such as chemical and temperature resistance and biocompatibility. Improvements of the microstructuring of glass have to deal with the modification of assembly techniques, as leakage problems have been reported for a number of cases. Glass soldering techniques seem to represent an interesting alternative to the thermal bonding method.

In addition, standard methods of precision mechanical engineering like micromilling [61] and micro spark erosion [62] can be applied for fabricating components of microreactors. In order to achieve low-cost mass fabrication

these methods can be favorably combined with suitable replication techniques which also extend the number of applicable materials.

By a combination of micro spark erosion and micromilling a first integrated microreaction system has been fabricated for BASF [19]. The special alloy used allows a high thermal and chemical resistance which is important for the process investigated. An extension to conductive ceramic materials seems to offer interesting perspectives for future applications of micro spark erosion techniques. Although precision engineering techniques will hardly allow the inexpensive mass fabrication as offered by injection molding (LIGA technique), they still attain a considerable attention for the fabrication of high-quality-low-number microreaction units.

7 References

- Peterson KE (1982) Proc. IEEE 70:420
- Muller RS (1990) Sens Actuators A21:1
- Ehrfeld W, Lehr H (1995) Rad Phys Chem 45 (3):349
- Ehrfeld W, Hessel V, Möbius H, Richter Th, Russow K (1996) Potentials and Realization of Micro Reactors. In: Microsystem Technology for Chemical and Biological Microreactors DECHEMA monograph Vol. 132. Verlag Chemie, Weinheim, p 1
- Ehrfeld W, Löwe H, Hessel V, Richter Th (1996) Chemie Ingenieur Technik 68 (9):1091
- Kämper K-P, Ehrfeld W, Döppler J, Hessel V, Lehr H, Löwe H, Richter Th, Wolf A (1997) Proc IEEE MEMS, Jan. 26 – 30, Nagoya, Japan
- Lerou JJ, Harold MP, Ryley J, Ashmead J, O'Brien TC, Johnson M, Perrotto J, Blaisdell CT, Rensi TA, Nyquist J (1996) Microfabricated minichemical systems: Technical feasibility. In: Microsystem Technology for Chemical and Biological Microreactors, DECHEMA Monographs Vol. 132, Verlag Chemie, Weinheim, p 51
- Wegeng RW, Call CJ, Drost MK (1996) Proc 1996 Spring National Meeting AIChE, Feb. 25 – 29 New Orleans, Seiten 1 – 13
- Branbjerg J, Gravesen P, Krog JP, Nielsen CR (1996), Proc IEEE MEMS '96, San Diego, USA
- Bier W, Keller W, Linder W, Seidel D, Schubert K (1990) ASME, DSC 19, New York, USA
- Shaw J, Miller B, Turner C, Harper M, Graham S (1996) Proc 2nd Int Symp Miniaturized Total Analysis Systems, TAS Basel, 19 – 22 Nov. 96, Widmer HM, Verpoorte E, Barnard S (eds), p 185
- van Steenkiste F, Grünkorn H, Claesen L, Baert K, Hermans L, Debruyker D, de Cooman M, Spiering V, van den Berg A, van der Schoot P, Arquint P, Born R, Schumann K (1996) Proc 2nd Int Symp Miniaturized Total Analysis Systems, TAS. Widmer HM, Verpoorte E, Barnard S (eds), p 138
- Hönicke D, Wießmeier G (1996) Heterogeneously catalyzed reactions in a microreactor. In: Microsystem Technology for Chemical and Biological Microreactors DECHEMA monograph Vol.132, Verlag Chemie: Weinheim, p 93
- See list of participants of the "First international conference on microreaction technology", organized by Dechema and IMM, Frankfurt (1997)
- van Lintel HTG, van den Pol FCM, Bouwstra S (1988) Sens Actuators 15 (2):153
- TAS(1995) Miniaturized Total Chemical Analysis Systems, Kluwer, Amsterdam
- Verpoorte EMJ, van der Schoot BH, Jeanneret S, Manz A, Widmer HM, de Rooij NF (1994) J Micromech Microeng 4:246
- Workshop on Microsystem Technology for Chemical and Biological Microreactors, organized by DECHEMA and IMM, Mainz (1997)
- Wolf A, Ehrfeld W, Lehr H, Michel F, Richter Th, Gruber H, Wörz O (1997) F & M Feinwerktechnik, Mikrotechnik, Meßtechnik 6:436
- Kochloefl K (1975) Chemie-Technik 4:443

21. see also Benson RS, Ponton JW (1993) *Trans IChemE* 71, Part A:160
22. Effenhauser CS, Paulus A, Widmer HM, Manz A (1994) *Anal Chem* 66:2953
23. Woolley AT, Mathies RA (1994) *Proc Natl Acad Sci USA* 91:11348
24. Woolley AT, Mathies RA (1995) *Anal Chem* 67 (20):3676
25. Hessel V, Ehrfeld W, Möbius H, Richter Th, Russow K (1995) *Proc Int. Symp. Microsystems, Intelligent Materials Robots, Sendai, Japan*, 45
26. Recent internal results of IMM (1997) in press
27. Schwesinger N, Frank T, Wurmus H (1996) *J Micromech Microeng* 6:99
28. Mensinger H, Richter Th, Hessel V, Döpfer J, Ehrfeld W (1995) Microreactor with integrated static mixer and analysis system. In: *Micro Total Analysis Systems*, van den Berg A, Bergveld P (eds) Kluwer Academic Publishers, The Netherlands, p 237
29. Fiehn H, Howitz S, Pham MT, Vopel T, Bürger M, Wegener T (1994) In: van den Berg A, Bergveld P (eds) Kluwer, The Netherlands, p 289
30. Hintsche R, Paeschke M, Uhlig A, Kruse C, Dittrich F, Pham MT, Howitz S (1995) *Proc Transducers '95, Stockholm, Schweden*, p 772
31. an den Berg A, Lammerink TSJ, Spiering V, Olthuis W (1996) Modular concept for miniature chemical systems, In: *Microsystem Technology for Chemical and Biological Microreactors*, DECHEMA Monographs Vol. 132, Verlag Chemie, Weinheim, p 51
32. Muntz E, Shiflett G, Erwin D, Kunc J (1992) *J Microelectromech Syst*: September
33. Mehregany M (1993) *IEEE Circuits Devices*, July
34. Smits J (1990) *Sens Actuators*
35. Richter A, Sandmaier H (1990) *IEEE MEMS Conference Proceedings*
36. Lammerink T, Elfswenspoek M, Fluitman J (1993) *IEEE MEMS Conference Proceedings*
37. Ahn C, Allen M (1995) *IEEE MEMS Conference Proceedings*
38. Gerlach T, Wurmus H (1995) *IEEE MEMS Conference Proceedings*
39. Döpfer J, Clemens M; Ehrfeld W, Kämper K-P, Lehr H (1996) *Proceedings Actuator '96, Bremen*
40. Zengerle R, Kluge S, Richter M, Richter A (1995) *IEEE MEMS Conference Proceedings*
41. Stehr M, Messner S, Sandmaier H, Zengerle R: (1996) *IEEE MEMS Conference Proceedings*
42. Stemme E, Stemme G (1993) *Sens Actuators*
43. Richter A, Sandmaier H, Plettner A (1990) *Proc Micro System Technologies* 90
44. Möbius H, Ehrfeld W, Hessel V, Richter Th (1995) Sensor controlled processes in chemical micro reactors, In: *Transducers '95 – Eurosensors IX, Proc. of 8th Int. Conf. on Solid-State Sensors and Actuators/Eurosensors IX, Stockholm*, p 775
45. Ehrfeld W, Golbig K, Hessel V, Löwe H, Richter Th (1997) Anwendungspotentiale chemischer und biologischer Mikroreaktoren, In *The Annual Report of GVC, Gesellschaft Verfahrenstechnik und Chemieingenieurwesen* (in press)
46. Tuckerman D, Pease R (1981) *IEEE Electron Device Lett* 126
47. Bier W, Keller W, Linder G, Seidel D (1990) *Microstruct Sens Actuators*, 19
48. Cuta J, Bennett W, McDonald C (1995) *SPIE Micromachining Microfabrication '95, Conference Proceedings*
49. Bowers M, Mudawar I (1993) *Intl J Heat Mass Transfer* 3:321
50. Laurell T, Rosengren L, Drott J (1995) *DECHEMA Workshop: Microsystem Technology for Chemical and Biological Microreactors*
51. Früchtel JS, Jung G (1996) *Angew Chem* 108:19
52. Balkenhohl F, Bussche-Hünnefeld C v-d, Lansky A, Zechel C (1996) *Angew Chem* 108:2436
53. James JB, Terry SC, Barth PW (1993) *Sci Am* 4:248
54. Ehrfeld W, Abraham M, Ehrfeld U, Lacher M, Lehr H (1994) *Proc 7th IEEE Intl Workshop Micro Electro Mechanical Systems, Japan*
55. Ehrfeld W, Lehr H (1994) *Synchrotron Rad News* 7:9
56. Löwe H, Mensinger H, Ehrfeld W (1994) *Galvanoformung in der LIGA-Technik, Jahrbuch Oberflächentechnik*, Band 50, S: 11, Metall Verlag Heidelberg
57. Bauer H, Weber L, Ehrfeld W (1994) *Formeinsätze für die Massenfertigung von hochpräzisen Kunststoffteilen: Die LIGA-Technik, Werkzeug und Formenbau* 4/94, S:22

58. Arnold J, Dasbach U, Ehrfeld W, Hesch K, Löwe H (1995) Appl Surface Sci 86:251
59. Stadel M, Freimuth H, Hessel V, Lacher M (1996) *LIGA-Technik*, Keram Zeitschrift 48 (12): 1112
60. Dietrich TR, Ehrfeld W, Lacher M, Krämer M, Speit B (1996) Microelectronic Engineering 30:497
61. Friedrich C, Kikkeri B (1995) SPIE Micromachining Microfabrication '95, Conference Proceedings
62. Michel F, Ehrfeld W, Lehr H, Wolf A, Gruber H-P, Bertholds A (1996) *Mikrofunken-erodieren als Strukturierungsverfahren in der Mikrotechnik*, in: Tagungsband 41. Int. Wissenschaftl. Koll. "Wandel im Maschinenbau durch Feinwerktechnik und Mikrosystemtechnik", 23–26.09.96, TU Ilmenau, p 233

Author Index Volumes 151–194

Author Index Vols. 26–50 see Vol. 50

Author Index Vols. 51–100 see Vol. 100

Author Index Vols. 101–150 see Vol. 150

The volume numbers are printed in italics

- Adam W, Hadjirapoglou L (1993) Dioxiranes: Oxidation Chemistry Made Easy. *164*:45–62
- Alberto R (1996) High- and Low-Valency Organometallic Compounds of Technetium and Rhenium. *176*:149–188
- Albini A, Fasani E, Mella M (1993) PET-Reactions of Aromatic Compounds. *168*:143–173
- Allan NL, Cooper D (1995) Momentum-Space Electron Densities and Quantum Molecular Similarity. *173*:85–111
- Allamandola LJ (1990) Benzenoid Hydrocarbons in Space: The Evidence and Implications. *153*:1–26
- Alonso JA, Balbás LC (1996) Density Functional Theory of Clusters of Transition Metals Using Simple Models. *182*:119–171
- Améduri B, Boutevin B (1997) Telomerisation Reactions of Fluorinated Alkenes. *192*:165–233
- Anderson RC, McGill G, Lipshutz RJ (1998) Polynucleotide Arrays for Genetic Sequence Analysis. *194*:117–129
- Anwender R (1996) Lanthanide Amides. *179*:33–112
- Anwender R (1996) Routes to Monomeric Lanthanide Alkoxides. *179*:149–246
- Anwender R, Herrmann WA (1996) Features of Organolanthanide Complexes. *179*:1–32
- Artymiuk PJ, Poirette AR, Rice DW, Willett P (1995) The Use of Graph Theoretical Methods for the Comparison of the Structures of Biological Macromolecules. *174*:73–104
- Astruc D (1991) The Use of p-Organoirron Sandwiches in Aromatic Chemistry. *160*:47–96
- Azumi T, Miki H (1997) Spectroscopy of the Spin Sublevels of Transition Metal Complexes. *191*:1–40
- Baerends EJ, see van Leeuwen R (1996) *180*:107–168
- Baker BJ, Kerr RG (1993) Biosynthesis of Marine Sterols. *167*:1–32
- Balbás LC, see Alonso JA (1996) *182*:119–171
- Baldas J (1996) The Chemistry of Technetium Nitrido Complexes. *176*:37–76
- Balzani V, Barigelletti F, De Cola L (1990) Metal Complexes as Light Absorption and Light Emission Sensitizers. *158*:31–71
- Bardin VV, see Petrov VA (1997) *192*:39–95
- Barigelletti F, see Balzani V (1990) *158*:31–71
- Bassi R, see Jennings RC (1996) *177*:147–182
- Baumgarten M, Müllen K (1994) Radical Ions: Where Organic Chemistry Meets Materials Sciences. *169*:1–104
- Beau J-M and Gallagher T (1997) Nucleophilic C-Glycosyl Donors for C-Glycoside Synthesis. *187*:1–54
- Bechthold A F-W, see Kirschning A (1997) *188*:1–84
- Berces A, Ziegler T (1996) Application of Density Functional Theory to the Calculation of Force Fields and Vibrational Frequencies of Transition Metal Complexes. *182*:41–85
- Bersier J, see Bersier PM (1994) *170*:113–228
- Bersier PM, Carlsson L, Bersier J (1994) Electrochemistry for a Better Environment. *170*:113–228

- Besalú E, Carbó R, Mestres J, Solà M (1995) Foundations and Recent Developments on Molecular Quantum Similarity. *173*:31–62
- Bignozzi CA, see Scandola F (1990) *158*:73–149
- Billing R, Rehorek D, Hennig H (1990) Photoinduced Electron Transfer in Ion Pairs. *158*:151–199
- Bissell RA, de Silva AP, Gunaratne HQN, Lynch PLM, Maguire GEM, McCo, CP, Sandanayake KRAS (1993) Fluorescent PET (Photoinduced Electron Transfer) Sensors. *168*:223–264
- Blasse B (1994) Vibrational Structure in the Luminescence Spectra of Ions in Solids. *171*:1–26
- Bley K, Gruber B, Knauer M, Stein N, Ugi I (1993) New Elements in the Representation of the Logical Structure of Chemistry by Qualitative Mathematical Models and Corresponding Data Structures. *166*:199–233
- Boullanger P (1997) Amphiphilic Carbohydrates as a Tool for Molecular Recognition in Organized Systems. *187*:275–312
- Boutevin B, see Améduri B (1997) *192*:165–233
- Brandi A, see Goti A (1996) *178*:1–99
- Brunvoll J, see Chen RS (1990) *153*:227–254
- Brunvoll J, Cyvin BN, Cyvin SJ (1992) Benzenoid Chemical Isomers and Their Enumeration. *162*:181–221
- Brunvoll J, see Cyvin BN (1992) *162*:65–180
- Brunvoll J, see Cyvin SJ (1993) *166*:65–119
- Bundle DR (1990) Synthesis of Oligosaccharides Related to Bacterial O-Antigens. *154*:1–37
- Buot FA (1996) Generalized Functional Theory of Interacting Coupled Liouvillean Quantum Fields of Condensed Matter. *181*:173–210
- Burke K, see Ernzerhof M (1996) *180*:1–30
- Burrell AK, see Sessler JL (1991) *161*:177–274
- Burton DJ, Lu L (1997) Fluorinated Organometallic Compounds. *193*:45–89
- Caffrey M (1989) Structural, Mesomorphic and Time-Resolved Studies of Biological Liquid Crystals and Lipid Membranes Using Synchrotron X-Radiation. *151*:75–109
- Canceill J, see Collet A (1993) *165*:103–129
- Carbó R, see Besalú E (1995) *173*:31–62
- Carlson R, Nordhal A (1993) Exploring Organic Synthetic Experimental Procedures. *166*:1–64
- Carlsson L, see Bersier PM (1994) *170*:113–228
- Carreras CW, Pieper R, Khosla C (1997) The Chemistry and Biology of Fatty Acid, Polyketide, and Nonribosomal Peptide Biosynthesis. *188*:85–126
- Ceulemans A (1994) The Doublet States in Chromium (III) Complexes. A Shell-Theoretic View. *171*:27–68
- Chambers RD, Vaughan JFS (1995) Nucleophilic Reactions of Fluorinated Alkenes. *192*:1–38
- Chambron J-C, Dietrich-Buchecker Ch, Sauvage J-P (1993) From Classical Chirality to Topologically Chiral Catenands and Knots. *165*:131–162.
- Chan WH, see Lee AWM (1997) *190*:101–129
- Chang CWJ, Scheuer PJ (1993) Marine Isocyanate Compounds. *167*:33–76
- Chen RS, Cyvin SJ, Cyvin BN, Brunvoll J, Klein DJ (1990) Methods of Enumerating Kekulé Structures. Exemplified by Application of Applications of Rectangle-Shaped Benzenoids. *153*:227–254
- Chen RS, see Zhang FJ (1990) *153*:181–194
- Cheng J, Kricka LJ, Sheldon EL, Wilding P (1998) Sample Preparation in Microstructured Devices. *194*:215–231
- Chiorboli C, see Scandola F (1990) *158*:73–149
- Chiu P, Lautens M (1997) Using Ring-Opening Reactions of Oxabicyclic Compounds as a Strategy in Organic Synthesis. *190*:1–85
- Cimino G, Sodano G (1993) Biosynthesis of Secondary Metabolites in Marine Molluscs. *167*:77–116.
- Ciolkowski J (1990) Scaling Properties of Topological Invariants. *153*:85–100
- Clark T (1996) Ab Initio Calculations on Electron-Transfer Catalysis by Metal Ions. *177*:1–24
- Cohen MH (1996) Strengthening the Foundations of Chemical Reactivity Theory. *183*:143–173

- Collet A, Dutasta J-P, Lozach B, Canceill J (1993) Cyclotrimeratrylenes and Cryptophanes: Their Synthesis and Applications to Host-Guest Chemistry and to the Design of New Materials. *165*:103–129
- Colombo M G, Hauser A, Güdel HU (1994) Competition Between Ligand Centered and Charge Transfer Lowest Excited States in bis Cyclometalated Rh^{3+} and Ir^{3+} Complexes. *171*:143–172
- Cooper DL, Gerratt J, Raimondi M (1990) The Spin-Coupled Valence Bond Description of Benzenoid Aromatic Molecules. *153*:41–56
- Cooper DL, see Allan NL (1995) *173*:85–111
- Cordero FM, see Goti A (1996) *178*:1–99
- Cyvin BN, see Chen RS (1990) *153*:227–254
- Cyvin SJ, see Chen RS (1990) *153*:227–254
- Cyvin BN, Brunvoll J, Cyvin SJ (1992) Enumeration of Benzenoid Systems and Other Polyhexes. *162*:65–180
- Cyvin SJ, see Cyvin BN (1992) *162*:65–180
- Cyvin BN, see Cyvin SJ (1993) *166*:65–119
- Cyvin SJ, Cyvin BN, Brunvoll J (1993) Enumeration of Benzenoid Chemical Isomers with a Study of Constant-Isomer Series. *166*:65–119
- Dartyge E, see Fontaine A (1989) *151*:179–203
- De Cola L, see Balzani V (1990) *158*:31–71
- Dear K (1993) Cleaning-up Oxidations with Hydrogen Peroxide. *16*
- de Mendoza J, see Seel C (1995) *175*:101–132
- de Raadt A, Ekhardt CW, Ebner M, Stütz AE (1997) Chemical and Chemo-Enzymatic Approaches to Glycosidase Inhibitors with Basic Nitrogen in the Sugar Ring. *187*:157–186
- de Silva AP, see Bissell RA (1993) *168*:223–264
- Descotes G (1990) Synthetic Saccharide Photochemistry. *154*:39–76
- Dias JR (1990) A Periodic Table for Benzenoid Hydrocarbons. *153*:123–144
- Dietrich-Buchecker Ch, see Chambron J-C (1993) *165*:131–162
- Dobson JF (1996) Density Functional Theory of Time-Dependent Phenomena. *181*:81–172
- Dohm J, Vögtle, F (1991) Synthesis of (Strained) Macrocycles by Sulfone Pyrolysis. *161*:69–106
- Dolbier WR jr. (1997) Fluorinated Free Radicals. *192*:97–163
- Drakesmith FG (1997) Electrofluorination of Organic Compounds. *193*:197–242
- Dreizler RM (1996) Relativistic Density Functional Theory. *181*:1–80
- Driguez H (1997) Thiooligosaccharides in Glycobiology. *187*:85–116
- Dutasta J-P, see Collet A (1993) *165*:103–129
- Eaton DF (1990) Electron Transfer Processes in Imaging. *156*:199–226
- Ebner M, see de Raadt A (1997) *187*:157–186
- Edelmann FT (1996) Rare Earth Complexes with Heteroallylic Ligands. *179*:113–148
- Edelmann FT (1996) Lanthanide Metallocenes in Homogeneous Catalysis. *179*:247–276
- Effenhauser CS (1998) Integrated Chip-Based Microcolumn Separation Systems. *194*:51–82
- Ehrfeld W, Hessel V, Lehr H (1998) Microreactors for Chemical Synthesis and Biotechnology – Current Developments and Future Applications. *194*:233–252
- Ekhardt CW, see de Raadt A (1997) *187*:157–186
- El-Basil S (1990) Caterpillar (Gutman) Trees in Chemical Graph Theory. *153*:273–290
- Engel E (1996) Relativistic Density Functional Theory. *181*:1–80
- Ernzerhof M, Perdew JP, Burke K (1996) Density Functionals: Where Do They Come From, Why Do They Work? *190*:1–30
- Fasani A, see Albin A (1993) *168*:143–173
- Fernández-Mayoralas A (1997) Synthesis and Modification of Carbohydrates using Glycosidases and Lipases. *186*:1–20
- Fessner W-D, Walter C (1997) Enzymatic C–C Bond Formation in Asymmetric Synthesis. *184*:97–194
- Fessner W-D, see Petersen M (1997) *186*:87–117
- Fontaine A, Dartyge E, Itie JP, Juchs A, Polian A, Tolentino H, Tourillon G (1989) Time-Resolved X-Ray Absorption Spectroscopy Using an Energy Dispersive Optics: Strengths and Limitations. *151*:179–203

- Foote CS (1994) Photophysical and Photochemical Properties of Fullerenes. *169*:347–364
- Fossey J, Sorba J, Lefort D (1993) Peracide and Free Radicals: A Theoretical and Experimental Approach. *164*:99–113
- Fox MA (1991) Photoinduced Electron Transfer in Arranged Media. *159*:67–102
- Freeman PK, Hatlevig SA (1993) The Photochemistry of Polyhalocompounds, Dehalogenation by Photoinduced Electron Transfer, New Methods of Toxic Waste Disposal. *168*:47–91
- Fuchigami T (1994) Electrochemical Reactions of Fluoro Organic Compounds. *170*:1–38
- Fuhr G, Shirley SG (1998) Biological Application of Microstructures. *194*:83–116
- Fuller W, see Grenall R (1989) *151*:31–59
- Galán A, see Seel C (1995) *175*:101–132
- Gallagher T, see Beau J-M (1997) *187*:1–54
- Gambert U, Thiem J (1997) Chemical Transformations Employing Glycosyltransferases. *186*:21–43
- Gehrke R (1989) Research on Synthetic Polymers by Means of Experimental Techniques Employing Synchrotron Radiation. *151*:111–159
- Geldart DJW (1996) Nonlocal Energy Functionals: Gradient Expansions and Beyond. *190*:31–56
- Gerratt J, see Cooper DL (1990) *153*:41–56
- Gerwick WH, Nagle DG, Proteau, PJ (1993) Oxylipins from Marine Invertebrates. *167*:117–180
- Gigg J, Gigg R (1990) Synthesis of Glycolipids. *154*:77–139
- Gislason EA, see Guyon P-M (1989) *151*:161–178
- Goti A, Cordero FM, Brandi A (1996) Cycloadditions Onto Methylene- and Alkylidene-cyclopropane Derivatives. *178*:1–99
- Gray HB, see Miskowski VM (1997) *191*:41–57
- Greenall R, Fuller W (1989) High Angle Fibre Diffraction Studies on Conformational Transitions DNA Using Synchrotron Radiation. *151*:31–59
- Gritsenko OV, see van Leeuwen R (1996) *180*:107–168
- Gross EKV (1996) Density Functional Theory of Time-Dependent Phenomena. *181*:81–172
- Gruber B, see Bley K (1993) *166*:199–233
- Güdel HU, see Colombo MG (1994) *171*:143–172
- Gunaratne HQN, see Bissell RA (1993) *168*:223–264
- Guo XF, see Zhang FJ (1990) *153*:181–194
- Gust D, Moore TA (1991) Photosynthetic Model Systems. *159*:103–152
- Gutman I (1992) Topological Properties of Benzenoid Systems. *162*:1–28
- Gutman I (1992) Total π -Electron Energy of Benzenoid Hydrocarbons. *162*:29–64
- Guyon P-M, Gislason EA (1989) Use of Synchrotron Radiation to Study-Selected Ion-Molecule Reactions. *151*:161–178
- Hashimoto K, Yoshihara K (1996) Rhenium Complexes Labeled with $^{186/188}\text{Re}$ for Nuclear Medicine. *176*:275–292
- Hadjarapoglou L, see Adam W (1993) *164*:45–62
- Hart H, see Vinod TK (1994) *172*:119–178
- Harbottle G (1990) Neutron Activation Analysis in Archaeological Chemistry. *157*:57–92
- Hatlevig SA, see Freeman PK (1993) *168*:47–91
- Hauser A, see Colombo MG (1994) *171*:143–172
- Hayashida O, see Murakami Y (1995) *175*:133–156
- He WC, He WJ (1990) Peak-Valley Path Method on Benzenoid and Coronoid Systems. *153*:195–210
- He WJ, see He WC (1990) *153*:195–210
- Heaney H (1993) Novel Organic Peroxygen Reagents for Use in Organic Synthesis. *164*:1–19
- Heidbreder A, see Hintz S (1996) *177*:77–124
- Heinze J (1989) Electronically Conducting Polymers. *152*:1–19
- Helliwell J, see Moffat JK (1989) *151*:61–74
- Hennig H, see Billing R (1990) *158*:151–199
- Herrmann WA, see Anwender R (1996) *179*:1–32
- Hesse M, see Meng Q (1991) *161*:107–176

- Hessel V, see Ehrfeld W (1998) 194:233–252
- Hiberty PC (1990) The Distortive Tendencies of Delocalized π Electronic Systems. Benzene, Cyclobutadiene and Related Heteroannulenes. 153:27–40
- Hintz S, Heidbreder A, Mattay J (1996) Radical Ion Cyclizations. 177:77–124
- Hirao T (1996) Selective Transformations of Small Ring Compounds in Redox Reactions. 178:99–148
- Hladka E, Koca J, Kratochvil M, Kvasnicka V, Matyska L, Pospichal J, Potucek V (1993) The Synthon Model and the Program PEGAS for Computer Assisted Organic Synthesis. 166:121–197
- Ho TL (1990) Trough-Bond Modulation of Reaction Centers by Remote Substituents. 155:81–158
- Holas A, March NH (1996) Exchange and Correlation in Density Functional Theory of Atoms and Molecules. 180:57–106
- Höft E (1993) Enantioselective Epoxidation with Peroxidic Oxygen. 164:63–77
- Hoggard PE (1994) Sharp-Line Electronic Spectra and Metal-Ligand Geometry. 171:113–142
- Holmes KC (1989) Synchrotron Radiation as a source for X-Ray Diffraction – The Beginning. 151:1–7
- Hopf H, see Kostikov RR (1990) 155:41–80
- Houk KN, see Wiest O (1996) 183:1–24
- Humbs W, see Yersin H (1997) 191:153–249
- Hutchinson J, Sandford G (1997) Elemental Fluorine in Organic Chemistry. 193:1–43
- Indelli MT, see Scandola F (1990) 158:73–149
- Inokuma S, Sakai S, Nishimura J (1994) Synthesis and Inophoric Properties of Crownophanes. 172:87–118
- Itie JP, see Fontaine A (1989) 151:179–203
- Ito Y (1990) Chemical Reactions Induced and Probed by Positive Muons. 157:93–128
- Itzstein von M, Thomson RS (1997) The Synthesis of Novel Sialic Acids as Biological Probes. 186:119–170
- Jackman RJ, see Qin D (1998) 194:1–20
- Jennings RC, Zucchelli G, Bassi R (1996) Antenna Structure and Energy Transfer in Higher Plant Photosystems. 177:147–182
- Jobst G, see Urban GA (1998) 194:189–213
- Johannsen B, Spiess H (1996) Technetium(V) Chemistry as Relevant to Nuclear Medicine. 176:77–122
- John P, Sachs H (1990) Calculating the Numbers of Perfect Matchings and of Spanning Trees, Pauling's Bond Orders, the Characteristic Polynomial, and the Eigenvectors of a Benzenoid System. 153:145–180
- Jones RO (1996) Structure and Spectroscopy of Small Atomic Clusters. 182:87–118
- Jucha A, see Fontaine A (1989) 151:179–203
- Jurisson S, see Volkert WA (1996) 176:77–122
- Kaim W (1994) Thermal and Light Induced Electron Transfer Reactions of Main Group Metal Hydrides and Organometallics. 169:231–252
- Kappes T, see Sauerbrey B (1997) 186:65–86
- Kavarnos GJ (1990) Fundamental Concepts of Photoinduced Electron Transfer. 156:21–58
- Kelly JM, see Kirsch-De-Mesmaeker A (1996) 177:25–76
- Kerr RG, see Baker BJ (1993) 167:1–32
- Khairutdinov RF, see Zamaraev KI (1992) 163:1–94
- Khosla C, see Carreras CW (1997); 188:85–126
- Kim JJ, Stumpe R, Klenze R (1990) Laser-induced Photoacoustic Spectroscopy for the Speciation of Transuranic Elements in Natural Aquatic Systems. 157:129–180
- Kikuchi J, see Murakami Y (1995) 175:133–156
- Kirsch-De-Mesmaeker A, Lecomte J-P, Kelly JM (1996) Photoreactions of Metal Complexes with DNA, Especially Those Involving a Primary Photo-Electron Transfer. 177:25–76
- Kirschning A, Bechthold A F-W, Rohr J (1997) Chemical and Biochemical Aspects of Deoxysugars and Deoxysugar Oligosaccharides. 188:1–84

- Kitazume T, Yamazaki T (1997) Enzymatically Controlled Reactions of Organofluorine Compounds. *193*:91–130
- Klaffke W, see Thiem J (1990) *154*:285–332
- Klein DJ (1990) Semiempirical Valence Bond Views for Benzenoid Hydrocarbons. *153*:57–84
- Klein DJ, see Chen RS (1990) *153*:227–254
- Klenze R, see Kim JI (1990) *157*:129–180
- Knauer M, see Bley K (1993) *166*:199–233
- Knops P, Sendhoff N, Mekelburger H-B, Vögtle F (1991) High Dilution Reactions – New Synthetic Applications. *161*:1–36
- Koca J, see Hladka E (1993) *166*:121–197
- Koepp E, see Ostrowicky A (1991) *161*:37–68
- Kohnke FH, Mathias JP, Stoddart JF (1993) Substrate-Directed Synthesis: The Rapid Assembly of Novel Macropolycyclic Structures via Stereoregular Diels-Alder Oligomerizations. *165*:1–69
- Korchowiec J, see Nalewajski RF (1996) *183*:25–142
- Kostikov RR, Molchanov AP, Hopf H (1990) Gem-Dihalocyclopropanes in Organic Synthesis. *155*:41–80
- Kratochvil M, see Hladka E (1993) *166*:121–197
- Křen V (1997) Enzymatic and Chemical Glycosylations of Ergot Alkaloids and Biological Aspects of New Compounds. *186*:45–64
- Kricka LJ, see Cheng J (1998) *194*:215–231
- Krogh E, Wan P (1990) Photoinduced Electron Transfer of Carbanions and Carbocations. *156*:93–116
- Krohn K, Rohr J (1997) Angucyclines: Total Syntheses, New Structures, and Biosynthetic Studies of an Emerging New Class of Antibiotics. *188*:127–195
- Kryutchkov SV (1996) Chemistry of Technetium Cluster Compounds. *176*:189–252
- Kumar A, see Mishra PC (1995) *174*:27–44
- Kunkeley H, see Vogler A (1990) *158*:1–30
- Kuwajima I, Nakamura E (1990) Metal Homo-enolates from Siloxycyclopropanes. *155*:1–39
- Kvasnicka V, see Hladka E (1993) *166*:121–197
- Lammerink TS, see van den Berg A (1998) *194*:21–49
- Lange F, see Mandelkow E (1989) *151*:9–29
- Lautens M, see Chiu P (1997) *190*:1–85
- Lecomte J-P, see Kirsch-De-Mesmaeker A (1996) *177*:25–76
- van Leeuwen R, Gritsenko OV, Baerends EJ (1996) Analysis and Modelling of Atomic and Molecular Kohn-Sham Potentials. *180*:107–168
- Lee AWM, Chan WH (1997) Chiral Acetylenic Sulfoxides and Related Compounds in Organic Synthesis. *190*:103–129
- Lefort D, see Fossey J (1993) *164*:99–113
- Lehr H, see Ehrfeld W (1998) *194*:233–252
- Lipshutz RJ, see Anderson RC (1998) *194*:117–129
- Little RD, Schwaabe MK (1997) Reductive Cyclizations at the Cathode. *185*:1–48
- Lopez L (1990) Photoinduced Electron Transfer Oxygenations. *156*:117–166
- López-Boada R, see Ludena EV (1996) *180*:169–224
- Lozach B, see Collet A (1993) *165*:103–129
- Lu L, see Burton DJ (1997) *193*:45–89
- Ludena EV, López-Boada (1996) Local-Scaling Transformation Version of Density Functional Theory: Generation of Density Functionals. *180*:169–224
- Lüning U (1995) Concave Acids and Bases. *175*:57–100
- Lundt I (1997) Aldonolactones as Chiral Synthons *187*:117–156
- Lymar SV, Parmon VN, Zamarev KI (1991) Photoinduced Electron Transfer Across Membranes. *159*:1–66
- Lynch PLM, see Bissell RA (1993) *168*:223–264
- Maguire GEM, see Bissell RA (1993) *168*:223–264

- Mandelkow E, Lange G, Mandelkow E-M (1989) Applications of Synchrotron Radiation to the Study of Biopolymers in Solution: Time-Resolved X-Ray Scattering of Microtubule Self-Assembly and Oscillations. *151*:9–29
- Mandelkow E-M, see Mandelkow E (1989) *151*:9–29
- March NH, see Holas A (1996) *180*:57–106
- Maslak P (1993) Fragmentations by Photoinduced Electron Transfer. Fundamentals and Practical Aspects. *168*:1–46
- Mathias JP, see Kohnke FH (1993) *165*:1–69
- Mattay J, Vondenhof M (1991) Contact and Solvent-Separated Radical Ion Pairs in Organic Photochemistry. *159*:219–255
- Mattay J, see Hintz S (1996) *177*:77–124
- Matyska L, see Hladka E (1993) *166*:121–197
- McCoy CP, see Bissell RA (1993) *168*:223–264
- McGall G, see Anderson RC (1998) *194*:117–129
- Mekelburger H-B, see Knops P (1991) *161*:1–36
- Mekelburger H-B, see Schröder A (1994) *172*:179–201
- Mella M, see Albini A (1993) *168*:143–173
- Memming R (1994) Photoinduced Charge Transfer Processes at Semiconductor Electrodes and Particles. *169*:105–182
- Meng Q, Hesse M (1991) Ring Closure Methods in the Synthesis of Macrocyclic Natural Products. *161*:107–176
- Merz A (1989) Chemically Modified Electrodes. *152*:49–90
- Mestres J, see Besalú, E (1995) *173*:31–62
- Meyer B (1990) Conformational Aspects of Oligosaccharides. *154*:141–208
- Meyer J-U, see Stieglitz T (1998) *194*:131–162
- Mezey PG (1995) Density Domain Bonding Topology and Molecular Similarity Measures. *173*:63–83
- Michalak A, see Nalewajski RF (1996) *183*:25–142
- Miki H, see Azumi T (1997) *191*:1–40
- Mishra PC, Kumar A (1995) Mapping of Molecular Electric Potentials and Fields. *174*:27–44
- Miskowski VM, Gray HB (1997) Magnetic and Spectroscopic Properties of $\text{Os}_2(\text{O}_2\text{CR})_4\text{Cl}_2$. Evidence for a $^3(\delta^*\pi^*)$ Ground State. *191*:41–57
- Misumi S (1993) Recognitory Coloration of Cations with Chromoacerands. *165*:163–192
- Mizuno K, Otsuji Y (1994) Addition and Cycloaddition Reactions via Photoinduced Electron Transfer. *169*:301–346
- Mock WL (1995) Cucurbituril. *175*:1–24
- Moeller KD (1997) Intramolecular Carbon – Carbon Bond Forming Reactions at the Anode. *185*:49–86
- Moffat JK, Helliwell J (1989) The Laue Method and its Use in Time-Resolved Crystallography. *151*:61–74
- Molchanov AP, see Kostikov RR (1990) *155*:41–80
- Moore TA, see Gust D (1991) *159*:103–152
- Müllen K, see Baumgarten M (1994) *169*:1–104
- Murakami Y, Kikuchi J, Hayashida O (1995) Molecular Recognition by Large Hydrophobic Cavities Embedded in Synthetic Bilayer Membranes. *175*:133–156
- Nagle DG, see Gerwick WH (1993) *167*:117–180
- Nakamura E, see Kuwajima I (1990) *155*:1–39
- Nalewajski RF, Korchowiec J, Michalak A (1996) Reactivity Criteria in Charge Sensitivity Analysis. *183*:25–142
- Nédélec J-Y, Périchon J, Troupel M (1997) Organic Electroreductive Coupling Reactions Using Transition Metal Complexes as Catalysts. *185*:141–174
- Nicotra F (1997) Synthesis of C-Glycosides of Biological Interest. *187*:55–83
- Nishimura J, see Inokuma S (1994) *172*:87–118
- Nolte RJM, see Sijbesma RP (1995) *175*:25–56
- Nordahl A, see Carlson R (1993) *166*:1–64

- Okuda J (1991) Transition Metal Complexes of Sterically Demanding Cyclopentadienyl Ligands. *160*:97–146
- Omori T (1996) Substitution Reactions of Technetium Compounds. *176*:253–274
- Oscarson S (1997) Synthesis of Oligosaccharides of Bacterial Origin Containing Heptoses, Uronic Acids and Fructofuranoses as Synthetic Challengers. *186*:171–202
- Ostrowicky A, Koeppe E, Vögtle F (1991) The “Vesium Effect”: Synthesis of Medio- and Macrocyclic Compounds. *161*:37–68
- Otsuji Y, see Mizuno K (1994) *169*:301–346
- Pálinkó I, see Tasi G (1995) *174*:45–72
- Pandey G (1993) Photoinduced Electron Transfer (PET) in Organic Synthesis. *168*:175–221
- Parmon VN, see Lymar SV (1991) *159*:1–66
- Patterson HH (1997) Luminescence and Absorption Studies of Transition Metal Ions in Host Crystals, Pure Crystals and Surface Environments. *191*:59–86
- Perdew JP, see Ernzerhof M (1996) *180*:1–30
- Périchon J, see Nédélec J-Y (1997) *185*:141–174
- Percy JM (1997) Building Block Approaches to Aliphatic Organofluorine Compounds. *193*:131–195
- Perlmutter P (1997) The Nucleophilic Addition/Ring Closure (NARC) Sequence for the Stereocontrolled Synthesis of Heterocycles. *190*:87–101
- Petersen M, Zannetti MT, Fessner W-D (1997) Tandem Asymmetric C–C Bond Formations by Enzyme Catalysis. *186*:87–117
- Petersilka M (1996) Density Functional Theory of Time-Dependent Phenomena. *181*:81–172
- Petrov VA, Bardin VV (1997) Reactions of Electrophiles with Polyfluorinated Olefins. *192*:39–95
- Pieper R, see Carreras CW (1997) *188*:85–126
- Poirette AR, see Artymiuk PJ (1995) *174*:73–104
- Polian A, see Fontaine A (1989) *151*:179–203
- Ponec R (1995) Similarity Models in the Theory of Pericyclic Macromolecules. *174*:1–26
- Pospichal J, see Hladka E (1993) *166*:121–197
- Potucek V, see Hladka E (1993) *166*:121–197
- Proteau PJ, see Gerwick WH (1993) *167*:117–180
- Qin D, Xia Y, Rogers JA, Jackman RJ, Zhao X-M, Whitesides GM (1998) Microfabrication, Microstructures and Microsystems. *194*:1–20
- Raimondi M, see Copper DL (1990) *153*:41–56
- Rajagopal AK (1996) Generalized Functional Theory of Interacting Coupled Liouvillean Quantum Fields of Condensed Matter. *181*:173–210
- Reber C, see Wexler D (1994) *171*:173–204
- Rettig W (1994) Photoinduced Charge Separation via Twisted Intramolecular Charge Transfer States. *169*:253–300
- Rice DW, see Artymiuk PJ (1995) *174*:73–104
- Riekel C (1989) Experimental Possibilities in Small Angle Scattering at the European Synchrotron Radiation Facility. *151*:205–229
- Rogers JA, see Qin D (1998) *194*:1–20
- Rohr J, see Kirschning A (1997) *188*:1–83
- Rohr J, see Krohn K (1997) *188*:127–195
- Roth HD (1990) A Brief History of Photoinduced Electron Transfer and Related Reactions. *156*:1–20
- Roth HD (1992) Structure and Reactivity of Organic Radical Cations. *163*:131–245
- Rouvray DH (1995) Similarity in Chemistry: Past, Present and Future. *173*:1–30
- Roy R (1997) Recent Developments in the Rational Design of Multivalent Glycoconjugates. *187*:241–274
- Rüsch M, see Warwel S (1993) *164*:79–98
- Sachs H, see John P (1990) *153*:145–180
- Saeva FD (1990) Photoinduced Electron Transfer (PET) Bond Cleavage Reactions. *156*:59–92
- Sahni V (1996) Quantum-Mechanical Interpretation of Density Functional Theory. *182*:1–39

- Sakai S, see Inokuma S (1994) 172:87–118
- Sandanayake KRAS, see Bissel RA (1993) 168:223–264
- Sandford G, see Hutchinson J (1997) 193:1–43
- Sauerbrei B, Kappes T, Waldmann H (1997) Enzymatic Synthesis of Peptide Conjugates – Tools for the Study of Biological Signal Transduction. 186:65–86
- Sauvage J-P, see Chambron J-C (1993) 165:131–162
- Schäfer H-J (1989) Recent Contributions of Kolbe Electrolysis to Organic Synthesis. 152:91–151
- Scheuer PJ, see Chang CWJ (1993) 167:33–76
- Schmidtke H-H (1994) Vibrational Progressions in Electronic Spectra of Complex Compounds Indicating Strong Vibronic Coupling. 171:69–112
- Schmitt M (1994) Umpolung of Ketones via Enol Radical Cations. 169:183–230
- Schönherr T (1997) Angular Overlap Model Applied to Transition Metal Complexes and d^N -Ions in Oxide Host Lattices. 191:87–152
- Schröder A, Mekelburger H-B, Vögtle F (1994) Belt-, Ball-, and Tube-shaped Molecules. 172:179–201
- Schulz J, Vögtle F (1994) Transition Metal Complexes of (Strained) Cyclophanes. 172:41–86
- Schwaebel MK, see Little RD (1997) 185:1–48
- Seel C, Galán A, de Mendoza J (1995) Molecular Recognition of Organic Acids and Anions – Receptor Models for Carboxylates, Amino Acids, and Nucleotides. 175:101–132
- Sendhoff N, see Knops P (1991) 161:1–36
- Sessler JL, Burrell AK (1991) Expanded Porphyrins. 161:177–274
- Sheldon EJ, see Cheng J (1998) 194:215–231
- Sheldon R (1993) Homogeneous and Heterogeneous Catalytic Oxidations with Peroxide Reagents. 164:21–43
- Sheng R (1990) Rapid Ways of Recognize Kekuléan Benzenoid Systems. 153:211–226
- Shirley SG, see Fuhr G (1998) 194:83–116
- Shoji S (1998) Fluids for Sensor Systems. 194:163–188
- Sijbesma RP, Nolte RJM (1995) Molecular Clips and Cages Derived from Glycoluril. 175:57–100
- Sodano G, see Cimino G (1993) 167:77–116
- Sojka M, see Warwel S (1993) 164:79–98
- Solà M, see Besalú E (1995) 173:31–62
- Sorba J, see Fossey J (1993) 164:99–113
- Soumillion J-P (1993) Photoinduced Electron Transfer Employing Organic Anions. 168:93–141
- Spiess H, see Johannsen B (1996) 176:77–122
- Stanek Jr J (1990) Preparation of Selectively Alkylated Saccharides as Synthetic Intermediates. 154:209–256
- Steckhan E (1994) Electroenzymatic Synthesis. 170:83–112
- Steenken S (1996) One Electron Redox Reactions between Radicals and Organic Molecules. An Addition/Elimination (Inner-Sphere) Path. 177:125–146
- Stein N, see Bley K (1993) 166:199–233
- Stick RV (1997) The Synthesis of Novel Enzyme Inhibitors and Their Use in Defining the Active Sites of Glycan Hydrolases. 187:187–213
- Stieglitz T, Meyer J-U (1998) Microtechnical Interfaces to Neurons. 194:131–162
- Stoddart JF, see Kohnke FH (1993) 165:1–69
- Strasser J, see Yersin H (1997) 191:153–249
- Stütz AE, see de Raadt A (1997) 187:157–186
- Stumpe R, see Kim JI (1990) 157:129–180
- Suami T (1990) Chemistry of Pseudo-sugars. 154:257–283
- Suppan P (1992) The Marcus Inverted Region. 163:95–130
- Suzuki N (1990) Radiometric Determination of Trace Elements. 157:35–56
- Tabakovic I (1997) Anodic Synthesis of Heterocyclic Compounds. 185:87–140
- Takahashi Y (1995) Identification of Structural Similarity of Organic Molecules. 174:105–134

- Tasi G, Pálinkó I (1995) Using Molecular Electrostatic Potential Maps for Similarity Studies. *174*:45–72
- Thiem J, Klaffke W (1990) Synthesis of Deoxy Oligosaccharides. *154*:285–332
- Thiem J, see Gambert U (1997) *186*:21–43
- Thomson RS, see Itzstein von M (1997) *186*:119–170
- Timpe H-J (1990) Photoinduced Electron Transfer Polymerization. *156*:167–198
- Tobe Y (1994) Strained [n]Cyclophanes. *172*:1–40
- Tolentino H, see Fontaine A (1989) *151*:179–203
- Tomalia DA (1993) Genealogically Directed Synthesis: Starburst/Cascade Dendrimers and Hyperbranched Structures. *165*
- Tourillon G, see Fontaine A (1989) *151*:179–203
- Troupel M, see Nédélec J-Y (1997) *185*:141–174
- Ugi I, see Bley K (1993) *166*:199–233
- Urban GA, Jobst G (1998) Sensor Systems. *194*:189–213
- van den Berg A, Lammerink TSJ (1998) Micro Total Analysis Systems: Microfluidic Aspects, Integration Concept and Applications. *194*:21–49
- Vaughan JFS, see Chambers RD (1997) *192*:1–38
- Vinod TK, Hart H (1994) Cuppedo- and Cappedophanes. *172*:119–178
- Vögtle F, see Dohm J (1991) *161*:69–106
- Vögtle F, see Knops P (1991) *161*:1–36
- Vögtle F, see Ostrowicky A (1991) *161*:37–68
- Vögtle F, see Schulz J (1994) *172*:41–86
- Vögtle F, see Schröder A (1994) *172*:179–201
- Vogler A, Kunkel H (1990) Photochemistry of Transition Metal Complexes Induced by Outer-Sphere Charge Transfer Excitation. *158*:1–30
- Volkert WA, Jurisson S (1996) Technetium-99m Chelates as Radiopharmaceuticals. *176*:123–148
- Vondenhof M, see Mattay J (1991) *159*:219–255
- Voyer N (1997) The Development of Peptide Nanostructures. *184*:1–38
- Waldmann H, see Sauerbrei B (1997) *186*:65–86
- Walter C, see Fessner W-D (1997) *184*:97–194
- Wan P, see Krogh E (1990) *156*:93–116
- Warwel S, Sojka M, Rösch M (1993) Synthesis of Dicarboxylic Acids by Transition-Metal Catalyzed Oxidative Cleavage of Terminal-Unsaturated Fatty Acids. *164*:79–98
- Weinreb SM (1997) *N*-Sulfonyl Imines – Useful Synthons in Stereoselective Organic Synthesis. *190*:131–184
- Wessel HP (1997) Heparinoid Mimetics. *187*:215–239
- Wexler D, Zink JL, Reber C (1994) Spectroscopic Manifestations of Potential Surface Coupling Along Normal Coordinates in Transition Metal Complexes. *171*:173–204
- Whitesides GM, see Qin D (1998) *194*:1–20
- Wiest O, Houk KN (1996) Density Functional Theory Calculations of Pericyclic Reaction Transition Structures. *183*:1–24
- Wilding P, see Cheng J (1998) *194*:215–231
- Willett P, see Artymiuk PJ (1995) *174*:73–104
- Willner I, Willner B (1991) Artificial Photosynthetic Model Systems Using Light-Induced Electron Transfer Reactions in Catalytic and Biocatalytic Assemblies. *159*:153–218
- Woggon W-D (1997) Cytochrome P450: Significance, Reaction Mechanisms and Active Site Analogues. *184*:39–96
- Xia Y, see Qin D (1998) *194*:1–20
- Yamazaki T, see Kitazume T (1997) *193*:91–130
- Yersin H, Humbs W, Strasser J (1997) Characterization of Excited Electronic and Vibronic States of Platinum Metal Compounds with Chelate Ligands by Highly Frequency-Resolved and Time-Resolved Spectra. *191*:153–249
- Yoshida J (1994) Electrochemical Reactions of Organosilicon Compounds. *170*:39–82
- Yoshihara K (1990) Chemical Nuclear Probes Using Photon Intensity Ratios. *157*:1–34
- Yoshihara K (1996) Recent Studies on the Nuclear Chemistry of Technetium. *176*:1–16

- Yoshihara K (1996) Technetium in the Environment. *176*:17–36
- Yoshihara K, see Hashimoto K (1996) *176*:275–192
- Zamaraev KI, see Lymar SV (1991) *159*:1–66
- Zamaraev KI, Kairutdinov RF (1992) Photoinduced Electron Tunneling Reactions in Chemistry and Biology. *163*:1–94
- Zander M (1990) Molecular Topology and Chemical Reactivity of Polynuclear Benzenoid Hydrocarbons. *153*:101–122
- Zannetti MT, see Petersen M (1997) *186*:87–117
- Zhang FJ, Guo XF, Chen RS (1990) The Existence of Kekulé Structures in a Benzenoid System. *153*:181–194
- Zhao X-M, see Qin D (1998) *194*:1–20
- Ziegler T, see Berces A (1996) *182*:41–85
- Ziegler T (1997) Pyruvated Saccharides – Novel Strategies for Oligosaccharide Synthesis. *186*:203–229
- Zimmermann SC (1993) Rigid Molecular Tweezers as Hosts for the Complexation of Neutral Guests. *165*:71–102
- Zink JI, see Wexler D (1994) *171*:173–204
- Zucchelli G, see Jennings RC (1996) *177*:147–182
- Zybill Ch (1991) The Coordination Chemistry of Low Valent Silicon. *160*:1–46